U.S. Department
of Commerce

Volume 102
Number 2
April 2004

Fishery Bulletin

U.S. Department of Commerce
Donald L. Evans
Secretary

National Oceanic and Atmospheric Administration
Vice Admiral
Conrad C. Lautenbacher Jr., USN (ret.)
Under Secretary for Oceans and Atmosphere

National Marine Fisheries Service
William T. Hogarth
Assistant Administrator for Fisheries

The *Fishery Bulletin* (ISSN 0090-0656) is published quarterly by the Scientific Publications Office, National Marine Fisheries Service, NOAA, 7600 Sand Point Way NE, BIN C15700, Seattle, WA 98115-0070. Periodicals postage is paid at Seattle, WA, and at additional mailing offices. POSTMASTER: Send address changes for subscriptions to Fishery Bulletin, Superintendent of Documents, Attn.: Chief, Mail List Branch, Mail Stop SSOM, Washington, DC 20402-9373.

Although the contents of this publication have not been copyrighted and may be reprinted entirely, reference to source is appreciated.

The Secretary of Commerce has determined that the publication of this periodical is necessary according to law for the transaction of public business of this Department. Use of funds for printing of this periodical has been approved by the Director of the Office of Management and Budget.

For sale by the Superintendent of Documents, U.S. Government Printing Office, Washington, DC 20402. Subscription price per year: $55.00 domestic and $68.75 foreign. Cost per single issue: $28.00 domestic and $35.00 foreign. **See back for order form.**

Fishery Bulletin

Scientific Editor
Dr. Norman Bartoo

Associate Editor
Sarah Shoffler

National Marine Fisheries Service, NOAA
8604 La Jolla Shores Drive
La Jolla, California 92037

Managing Editor
Sharyn Matriotti

National Marine Fisheries Service
Scientific Publications Office
7600 Sand Point Way NE, BIN C15700
Seattle, Washington 98115-0070

Editorial Committee

Dr. Harlyn O. Halvorson	University of Massachusetts, Boston
Dr. Ronald W. Hardy	University of Idaho, Hagerman
Dr. Richard D. Methot	National Marine Fisheries Service
Dr. Theodore W. Pietsch	University of Washington, Seattle
Dr. Joseph E. Powers	National Marine Fisheries Service
Dr. Harald Rosenthal	Universität Kiel, Germany
Dr. Fredric M. Serchuk	National Marine Fisheries Service
Dr. George Watters	National Marine Fisheries Service

***Fishery Bulletin* web site: www.fishbull.noaa.gov**

The *Fishery Bulletin* carries original research reports and technical notes on investigations in fishery science, engineering, and economics. It began as the Bulletin of the United States Fish Commission in 1881; it became the Bulletin of the Bureau of Fisheries in 1904 and the *Fishery Bulletin* of the Fish and Wildlife Service in 1941. Separates were issued as documents through volume 46; the last document was No. 1103. Beginning with volume 47 in 1931 and continuing through volume 62 in 1963, each separate appeared as a numbered bulletin. A new system began in 1963 with volume 63 in which papers are bound together in a single issue of the bulletin. Beginning with volume 70, number 1, January 1972, the *Fishery Bulletin* became a periodical, issued quarterly. In this form, it is available by subscription from the Superintendent of Documents, U.S. Government Printing Office, Washington, DC 20402. It is also available free in limited numbers to libraries, research institutions, State and Federal agencies, and in exchange for other scientific publications.

U.S. Department of Commerce
Seattle, Washington

Volume 102
Number 2
April 2004

Fishery Bulletin

Contents

Articles

233–244 **Archer, Frederick, Tim Gerrodette, Susan Chivers, and Alan Jackson**
Annual estimates of the unobserved incidental kill of pantropical spotted dolphin (*Stenella attenuata attenuata*) calves in the tuna purse-seine fishery of the eastern tropical Pacific

245–250 **Chernova, Natalia V., and David L. Stein**
A remarkable new species of *Psednos* (Teleostei: Liparidae) from the western North Atlantic Ocean

251–263 **Chiang, Wei-Chuan, Chi-Lu Sun, Su-Zan Yeh, and Wei-Cheng Su**
Age and growth of sailfish (*Istiophorus platypterus*) in waters off eastern Taiwan

264–277 **Clark, Randall D., John D. Christensen, and Mark E. Monaco, Philip A. Caldwell, Geoffrey A. Matthews, and Thomas J. Minello**
A habitat-use model to determine essential fish habitat for juvenile brown shrimp (*Farfantepenaeus aztecus*) in Galveston Bay, Texas

278–288 **Delgado, Gabriel A., Claudine T. Bartels, Robert A. Glazer, Nancy J. Brown-Peterson, and Kevin J. McCarthy**
Translocation as a strategy to rehabilitate the queen conch (*Strombus gigas*) population in the Florida Keys

289–297 **Lage, Christopher, Kristen Kuhn, and Irv Kornfield**
Genetic differentiation among Atlantic cod (*Gadus morhua*) from Browns Bank, Georges Bank, and Nantucket Shoals

298–305 **Lenihan, Hunter S., and Charles H. Peterson**
Conserving oyster reef habitat by switching from dredging and tonging to diver-harvesting

The conclusions and opinions expressed in *Fishery Bulletin* are solely those of the authors and do not represent the official position of the National Marine Fisheries Service (NOAA) or any other agency or institution.

The National Marine Fisheries Service (NMFS) does not approve, recommend, or endorse any proprietary product or proprietary material mentioned in this publication. No reference shall be made to NMFS, or to this publication furnished by NMFS, in any advertising or sales promotion which would indicate or imply that NMFS approves, recommends, or endorses any proprietary product or proprietary material mentioned herein, or which has as its purpose an intent to cause directly or indirectly the advertised product to be used or purchased because of this NMFS publication.

306–327 **Macewicz, Beverly J., John R. Hunter, Nancy C. H. Lo, and Erin L. LaCasella**
Fecundity, egg deposition, and mortality of market squid (*Lolilgo opalescens*)

328–348 **Orr, James W., and James E. Blackburn**
The dusky rockfishes (Teleostei: Socrpaeniformes) of the North Pacific Ocean: resurrection of *Sebastes variabilis* (Pallas, 1814) and a redescription of *Sebastes ciliatus* (Tilesius, 1813)

349–365 **Powers, Joseph E.**
Recruitment as an evolving random process of aggregation and mortality

366–375 **Szedlmayer, Stephen T., and Jason D. Lee**
Diet shifts of juvenile red snapper (*Lutjanus campechanus*) with changes in habitat and fish size

376–388 **Webb, Stacey, and Ronald T. Kneib**
Individual growth rates and movement of juvenile white shrimp (*Litopenaeus setiferus*) in a tidal marsh nursery

Notes

389–392 **Forsythe, John, Nuutti Kangas, and Roger T. Hanlon**
Does the California market squid (*Loligo opalescens*) spawn naturally during the day or at night? A note on the successful use of ROVs to obtain basic fisheries biology data

393–399 **Kotas, Jorge E., Silvio dos Santos, Venâncio G. de Azevedo, Berenice M. G. Gallo, and Paulo C. R. Barata**
Incidental capture of loggerhead (*Caretta caretta*) and leatherback (*Dermochelys coriacea*) sea turtles by the pelagic longline fishery off southern Brazil

400–405 **Yang, Mei-Sun**
Diet changes of Pacific cod (*Gadus macrocephalus*) in Pavlof Bay associated with climate changes in the Gulf of Alaska between 1980 and 1995

406 *Subscription form*

Annual estimates of the unobserved incidental kill of pantropical spotted dolphin (*Stenella attenuata attenuata*) calves in the tuna purse-seine fishery of the eastern tropical Pacific

Frederick Archer
Tim Gerrodette
Susan Chivers
Alan Jackson

Southwest Fisheries Science Center
National Marine Fisheries Service
8604 La Jolla Shores Dr.
La Jolla, California 92037
E-mail address (for F. Archer): eric.archer@noaa.gov

Abstract—We estimated the total number of pantropical spotted dolphin (*Stenella attenuata*) mothers killed without their calves ("calf deficit") in all tuna purse-seine sets from 1973–90 and 1996–2000 in the eastern tropical Pacific. Estimates were based on a tally of the mothers killed as reported by color pattern and gender, several color-pattern-based frequency tables, and a weaning model. Over the time series, there was a decrease in the calf deficit from approximately 2800 for the western-southern stock and 5000 in the northeastern stock to about 60 missing calves per year. The mean deficit per set decreased from approximately 1.5 missing calves per set in the mid-1970s to 0.01 per set in the late-1990s. Over the time series examined, from 75% to 95% of the lactating females killed were killed without a calf. Under the assumption that these orphaned calves did not survive without their mothers, this calf deficit represents an approximately 14% increase in the reported kill of calves, which is relatively constant across the years examined. Because the calf deficit as we have defined it is based on the kill of mothers, the total number of missing calves that we estimate is potentially an underestimate of the actual number killed. Further research on the mechanism by which separation of mother and calf occurs is required to obtain better estimates of the unobserved kill of dolphin calves in this fishery.

Manuscript approved for publication 7 January 2004 by Scientific Editor.
Manuscript received 20 January 2004 at NMFS Sceintific Publications Office.
Fish. Bull. 102:233–244 (2004).

In the eastern tropical Pacific (ETP), yellowfin tuna (*Thunnus albacares*) are frequently found swimming under schools of pantropical spotted (*Stenella attenuata*) and spinner (*S. longirostris*) dolphins. For the past four decades, the ETP yellowfin tuna fishery has made use of this association by chasing the more visible dolphins at the surface and using purse-seines to encircle the schools "carrying" the tuna (NRC, 1992). The large bycatch of dolphins in this fishery has become widely known as the "tuna-dolphin issue" (Gerrodette, 2002). During the 1960s, the number of dolphins killed by the fishery was estimated to be 200,000–500,000 per year (Wade, 1995), and two stocks of spotted and spinner dolphins were reduced to fractions of their previous sizes (Smith, 1983; Wade et al.[1]). A long history of technological innovations by fishermen, laws and fishing regulations, dolphin quotas, eco-labeling of "dolphin-safe" tuna, and a comprehensive international observer program (Gosliner, 1999; Hall et al., 2000; Gerrodette, 2002) has reduced the dolphin bycatch to less than 1% of its former level. The reported bycatch in recent years is less than 2000 dolphins per year for all species combined (IATTC, 2002).

Although the reported kill has dramatically decreased, recent studies suggest that there is little evidence that the stocks are growing close to expected rates (Wade et al.[1]). One hypothesis for this lack of recovery has been that there are unobserved kills of dolphins during tuna purse-seine sets. Archer et al. (2001) presented evidence of an under-representation of suckling spotted and spinner dolphin calves in a sample of tuna purse-seine sets in the eastern tropical Pacific. Given that some of these missing calves are still dependent on their mothers for nutrition, it is likely that once separated they would die and this under-representation represents some degree of unobserved kill.

In Archer et al. (2001), the sample of sets examined was limited to those sets in which all of the animals killed had biological data collected by technicians aboard the tuna vessel. Calves still dependent on their mothers in the kill were identified by five intervals of body length, chosen to cover a range of

[1] Wade, P. R., S. B. Reilly, and T. Gerrodette. 2002. Assessment of the population dynamics of the northeastern offshore spotted and the eastern spinner dolphin populations through 2002. National Oceanographic and Atmospheric Administration Administrative Report LJ-02-13, 58 p. Southwest Fisheries Science Center, 8604 La Jolla Shores Dr., La Jolla, CA 92037.

calf sizes. Because of this approach, it was not possible to derive a single estimate of the number of missing calves or to extrapolate their estimate to sets not used in this analysis.

In the current study, we present a different method of estimating the number of missing calves in each set where offshore spotted dolphins (*S. attenuata attenuata*) were killed. For brevity, we call the shortage of calves in the kill in relation to the number of lactating females in the kill the "calf deficit." We examined the western-southern and northeastern offshore stocks separately according to the geographic boundaries described by Dizon et al. (1994). As they age, spotted dolphins change color through five color phases (Perrin, 1970). We used the color-phase frequency distribution of the kill in conjunction with age- and color-based frequency distributions from a sample of the kill to estimate the total number of missing calves in each stock, along with confidence intervals derived from bootstrap replications. This method also allowed us to examine the calf deficit from sets in recent years from which we did not have biological samples and to examine the time series of available years for evidence of a trend in the calf deficit.

Methods

Since 1973, observers have been randomly placed on tuna purse-seine vessels. For each spotted dolphin killed during an observed set, observers attempted to record the sex and the color phase of the dolphin (neonate, two-tone, speckled, mottled, and fused, see Perrin, 1970). From the National Marine Fisheries Service (NMFS) set log database, we obtained the number of northeastern and western-southern offshore spotted dolphins (by gender and color phase) killed in every observed set from 1973 to 1990. The Inter-American Tropical Tuna Commission (IATTC) provided the same data from 1996 to 2000.

Proration

In each set, color phase or gender (or both) may not have been recorded for some dolphins. Assuming that the distribution of the demographic composition of this missing data is equivalent to the overall demographic composition of the kill, we allocated the number of dolphins of unknown color phase (nu) to unknown gender in each color phase (ngu_c) according to the following formula,

$$ngu'_c = ngu_c + \left(nu \cdot \frac{N_c}{\sum_c N_c} \right), \quad (1)$$

where c = one of the five color phases (neonate to fused);
N_c = the total number of dolphins in each color phase in the entire data set; and
ngu'_c = the new number of dolphins in each color phase where gender is unknown, including the individuals of prorated unknown color phase

The number of male (nm'_c) or female (nf'_c) dolphins in a color phase was calculated as

$$nm'_c = nm_c + \left(ngu'_c \cdot \frac{Nm_c}{Nm_c + Nf_c} \right), \quad (2)$$

$$nf'_c = nf_c + \left(ngu'_c \cdot \frac{Nf_c}{Nm_c + Nf_c} \right), \quad (3)$$

where Nm_c and Nf_c are the total number of males and females, respectively, observed in that color phase in the entire data. Table 1 gives the sample size of sets for both stocks by year, as well as the fraction of the kill of unknown gender and color phase that were prorated as described above.

Number of suckling calves

As time permitted, NMFS observers would also collect biological data from a subset of the kill. For this study, we used ages estimated from teeth collected for a study of spotted dolphin growth and reproduction (Myrick et al., 1986). The specimens used were a random sample of all male and female spotted dolphins collected between 1973 and 1978 for which total body length was recorded and teeth were collected. However, additional specimens with lengths less than 150 cm were selected in order to match as closely as possible the length distribution of the aged sample to the underlying length distribution of the spotted dolphins in the kill. This was necessary because observers did not generally collect teeth from smaller, younger animals. Later, another sample of female spotted dolphins was selected from specimens collected in 1981. Specimens were aged as described in Myrick et al. (1986).

The final data set used in our analyses included age estimates for 1094 female spotted dolphin specimens and 798 male specimens. Of these, 649 females and 457 males belonged to the northeastern stock and had color phase recorded. These 1106 dolphins were used to generate the age frequency distribution for each color phase (F_{ac}, Table 2),

$$F_{ac} = \frac{S_{ac}}{\sum_a S_{ac}}, \quad (4)$$

where S_{ac} = the number of samples of age a in color phase c.

The oldest age recorded was 36 years.

To derive an age distribution for the dolphins killed in each tuna set, we estimated the number of dolphins in each age class (n_a) as

$$n_a = \sum_c (F_{ac} \cdot n'_c), \quad (5)$$

where n'_c = the sum of nm'_c and nf'_c (the number of males and females in each color phase after proration from Equations 2 and 3).

Table 1

Sample sizes of NMFS (1973–1990) and IATTC (1996–2000) observed sets with spotted dolphin kill made on two stocks of pantropical spotted dolphins (*Stenella attenuata*) by year.

	Northeastern stock				Western-southern stock			
Year	Number of sets with kill	Observed kill	Fraction of kill of unknown color phase	Fraction of kill of unknown gender	Number of sets with kill	Observed kill	Fraction of kill of unknown color phase	Fraction of kill of unknown gender
1973	332	5242	0.09	0.31	75	1199	0.17	0.34
1974	515	5864	0.16	0.23	92	1715	0.10	0.31
1975	554	8073	0.31	0.19	75	1702	0.30	0.20
1976	239	2376	0.24	0.25	356	6293	0.27	0.23
1977	467	2146	0.23	0.26	528	3358	0.18	0.32
1978	224	1016	0.18	0.41	329	3998	0.37	0.34
1979	218	1045	0.38	0.27	168	1262	0.40	0.14
1980	165	1132	0.45	0.28	106	1206	0.73	0.13
1981	121	815	0.46	0.13	112	1346	0.48	0.12
1982	171	1696	0.51	0.22	159	1966	0.37	0.38
1983	12	177	0.80	0.08	35	148	0.32	0.35
1984	43	294	0.37	0.25	71	961	0.48	0.15
1985	186	2625	0.39	0.40	54	381	0.49	0.13
1986	150	1816	0.48	0.28	132	1818	0.60	0.22
1987	630	3327	0.25	0.31	175	1768	0.62	0.14
1988	207	1142	0.18	0.27	107	479	0.36	0.34
1989	293	1096	0.29	0.25	323	2793	0.48	0.14
1990	157	515	0.16	0.31	121	829	0.35	0.13
1996	273	724	0.27	0.44	161	374	0.18	0.54
1997	163	393	0.15	0.42	274	738	0.24	0.48
1998	161	260	0.21	0.51	125	236	0.19	0.46
1999	189	317	0.18	0.58	88	159	0.11	0.56
2000	146	291	0.23	0.47	115	250	0.20	0.61

In Equation 4, an age distribution was generated for each color phase, and then the number of dolphins in each age class was summed across all color phases.

To estimate the number of calves in each set, we used this age distribution in conjunction with a weaning model developed from a study of the stomach contents and ages of calves (Archer and Robertson, in press). The model predicts the probability that an animal of a given age (a) will be suckling:

$$P(milk)_a = \frac{1}{1+e^{1.90-2.6a}}. \quad (6)$$

The estimated number of calves (N_{calf}) in a set is then

$$N_{calf} = \sum_{a=0}^{3} \left(n_a \cdot P(milk)_a\right). \quad (7)$$

In our estimate of N_{calf} we chose to use only the first four age classes (0 to 3) because $P(milk)_4$ was extremely small (2×10^{-4}). These age classes allowed us to decrease computational time without significantly affecting the estimates.

Number of lactating females

Observers visually examined the mammaries of the 649 females used in the age distribution above (Eq. 4) for the presence of milk as part of the suite of biological data collected. Using these data in conjunction with the color phase of these females, we calculated the fraction of lactating females in each color phase ($Flac_c$),

$$Flac_c = \frac{Slac_c}{Sfem_c}, \quad (8)$$

where $Slac_c$ and $Sfem_c$ = the number of females that were lactating and the total number of females in color phase c of the samples examined.

$Flac_c$ was 0.00, 0.01, 0.04, 0.22, and 0.50 for neonate, two-tone, speckled, mottled, and fused specimens, respectively. The estimated number of lactating females (N_{lac}) in a set was then

$$N_{lac} = \sum_c (nf_c' \cdot Flac_c). \quad (9)$$

Calf deficit

As described in Archer et al. (2001), the calf deficit (D) in each set was calculated by subtracting the number of calves (N_{calf}) from the number of lactating females (N_{lac}). If this value was zero or less, then D was set to zero to indicate that there were enough calves to account for all lactating females killed (Fig. 1),

$$D = \begin{cases} N_{lac} - N_{calf} & \text{if } N_{lac} > N_{calf} \\ 0 & \text{if } N_{lac} \leq N_{calf} \end{cases}. \quad (10)$$

We calculated three deficit-based fractions: 1) the mean deficit per set (D_s); 2) the mean deficit per dolphin killed (D_k); and 3), the mean deficit per lactating female killed (D_l):

$$D_s = \frac{\sum D}{ObsSets}, \quad (11)$$

$$D_k = \frac{\sum D}{ObsKill}, \quad (12)$$

$$D_l = \frac{\sum D}{EstLacKill}, \quad (13)$$

where ΣD = the total observed calf deficit in each year;
$ObsSets$ = the number of observed sets used in the analysis, including those sets without a dolphin kill;
$ObsKill$ = the number of dolphins killed in the observed sets; and
$EstLacKill$ = the total estimated number of lactating females killed.

The above analysis was conducted each year. Estimation error was evaluated with 20,000 bootstrap replicates for each year. For each replicate, the sets within that year were randomly resampled. The frequency tables F_{ac} and $Flac_c$ were also recalculated by resampling the list of biological specimens. The parameters for the weaning model, $P(milk)_a$, were estimated again by resampling the 29 calves and by fitting the logistic model to the new data set as described in Archer and Robertson (in press). All resampling was done with replacement. N_{calf}, N_{lac}, and D were estimated as described above for each set, and D_s, D_k, and D_l were calculated for the replicate. The 95% confidence intervals for N_{calf}, N_{lac}, D, D_s, D_k, and D_l were estimated from the 2.5% and 97.5% quantiles of the distributions of the bootstrap replicate values.

The total calf deficit (D_{total}) was estimated as the deficit per dolphin killed (D_k) multiplied by the total number of dolphins killed (N_{killed}) by stock each year,

$$D_{total} = D_k \times N_{killed}. \quad (14)$$

Table 2

Age-class frequency distribution for each color phase (F_{ac}).

Age (yr)	Neonate	Two-tone	Speckled	Mottled	Fused
0	0.80	0.12	0	0	0
1	0.20	0.32	0	0	0
2	0	0.31	0.04	0	0
3	0	0.16	0.18	0.01	0
4	0	0.05	0.14	0.02	0
5	0	0.02	0.13	0.03	0
6	0	0	0.13	0.04	0.01
7	0	0	0.06	0.05	0
8	0	0	0.10	0.06	0
9	0	0	0.06	0.07	0.01
10	0	0	0.01	0.10	0.01
11	0	0	0.01	0.14	0.03
12	0	0	0.01	0.08	0.02
13	0	0	0.04	0.07	0.03
14	0	0	0.03	0.07	0.03
15	0	0	0	0.06	0.06
16	0	0.01	0.01	0.06	0.07
17	0	0	0.01	0.03	0.07
18	0	0	0	0.01	0.07
19	0	0	0	0.03	0.09
20	0	0	0	0.03	0.07
21	0	0	0	0.01	0.08
22	0	0	0	0	0.06
23	0	0	0.01	0	0.07
24	0	0	0	0.01	0.04
25	0	0	0	0.01	0.04
26	0	0	0	0	0.04
27	0	0	0	0.01	0.03
28	0	0	0	0.01	0.02
29	0	0	0	0	0.01
30	0	0	0	0.01	0.02
31	0	0	0	0	0.01
32	0	0	0	0	0
33	0	0	0	0	0.01
34	0	0	0	0	0
35	0	0	0	0	0
36	0	0	0	0	0.01

For the period 1973–84, annual values of N_{killed} for each stock were provided by the IATTC (Joseph[2]). For 1984–90 and 1996–2000, values were published by IATTC (2002). In the bootstrap estimation of the 95% CI around D_{total}, for the 1973–90 period, each replicate was randomly sampled from a normal distribution by using the estimated total kill standard error. For 1996–2000, the total kill was reported to be exact; therefore the total kill was used without variance in all replicates.

[2] Joseph, J. 1994. Letter of September 6 to Michael Tillman, 2 p. Southwest Fisheries Science Center, 8604 La Jolla Shores Dr., La Jolla, CA 92037.

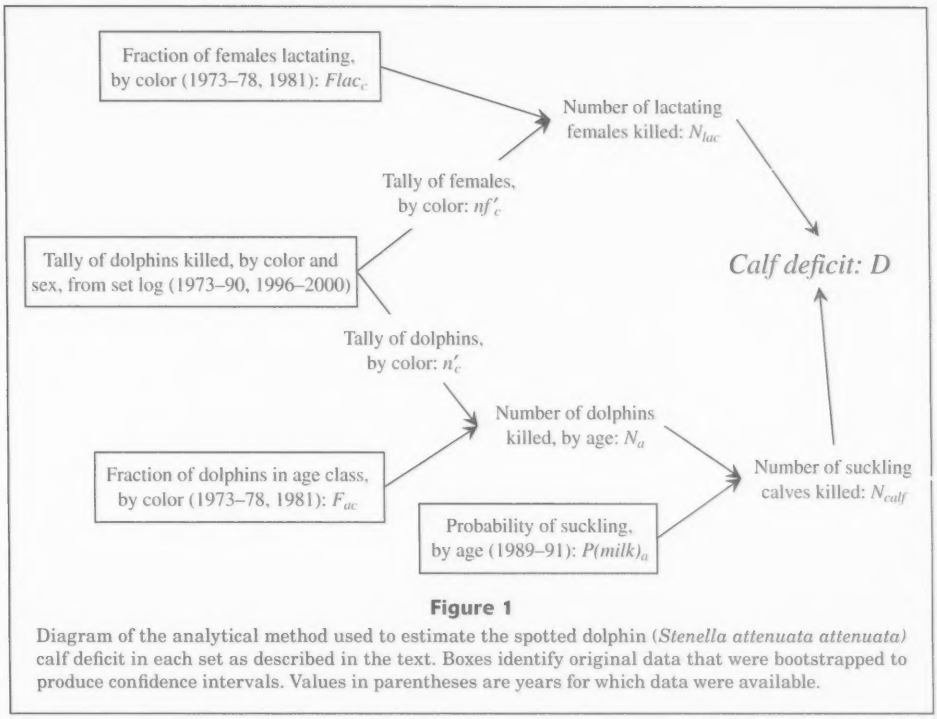
Fraction of females lactating, by color (1973–78, 1981): $Flac_c$
Number of lactating females killed: N_{lac}
Tally of females, by color: nf'_c
Tally of dolphins killed, by color and sex, from set log (1973–90, 1996–2000)
Calf deficit: D
Tally of dolphins, by color: n'_c
Number of dolphins killed, by age: N_a
Fraction of dolphins in age class, by color (1973–78, 1981): F_{ac}
Number of suckling calves killed: N_{calf}
Probability of suckling, by age (1989–91): $P(milk)_a$

Figure 1

Diagram of the analytical method used to estimate the spotted dolphin (*Stenella attenuata attenuata*) calf deficit in each set as described in the text. Boxes identify original data that were bootstrapped to produce confidence intervals. Values in parentheses are years for which data were available.

In a subset of the sets that we examined, every individual killed had been examined and biological samples had been collected from it; therefore, we knew the actual number of lactating females killed. There were 1108 of these "100% sampled" sets on the northeastern stock, and 697 on the western-southern stock from 1973 to 1990. We evaluated the accuracy of our frequency-based method by conducting a paired *t*-test between our estimate of the number of lactating females and the number observed in each of these sets.

Stomach-content data were not available for every animal in these 100%-sampled sets; therefore, we did not know the actual number of suckling calves. However, we also used paired *t*-tests to compare our estimate of the number of suckling calves in each set with the number of animals smaller than 122 cm, which was the estimated length at which the probability of milk in the stomach was 0.5, given the weaning model of Archer and Robertson (in press). Likewise, our estimate of the calf deficit was compared with the deficit as estimated by using a cutoff length of 122 cm. These tests were done to determine if the method in the present study would produce significantly different results from the method used in the previous study. Paired *t*-tests were conducted for each year separately, as well as for all years combined. A power analysis was also performed for these paired *t*-tests to determine the minimum detectable difference at which we could reject the null hypothesis of no difference between methods given observed sample sizes and variability.

Results

The calf deficit as a fraction of the number of dolphins killed (D_k) increased slightly during the mid-1970s but remained relatively constant throughout the rest of the time series at approximately 0.14 missing calves per dolphin killed for both stocks (Fig. 2). The total calf deficit (D_{total}) as estimated from the annual kill decreased from highs of approximately 5000 in the mid-1970s down to 2000–3000 by the early 1980s (Fig. 3). In the late 1980s, this value increased to approximately 5000 in northeastern spotted dolphins (Table 3A) and approximately 2800 in the western-southern stock (Table 3B), reflecting an increase in the reported kills. In the last five years of the time series (1996–2000), the estimated total deficit was approximately 60 missing calves.

The mean deficit per set (D_s) for northeastern spotters over all years was 1.03 missing calves per set, and the median was 0.30 (Fig. 4). For western-southern spotted dolphins, the mean was 1.28 missing calves per set, and the median was 0.33. The estimated mean deficit per set was approximately 1.5 in the mid-1970s and decreased over time to 0.01–0.02 at the end of the time series (Fig. 4). For both stocks, 75– 95% of lactating females killed were not killed with their calf (Fig. 5).

In the sets that were 100%-sampled, for all years combined, there was no significant difference between the observed and the estimated number of lactating females killed in either stock (Table 4). The results of paired *t*-tests

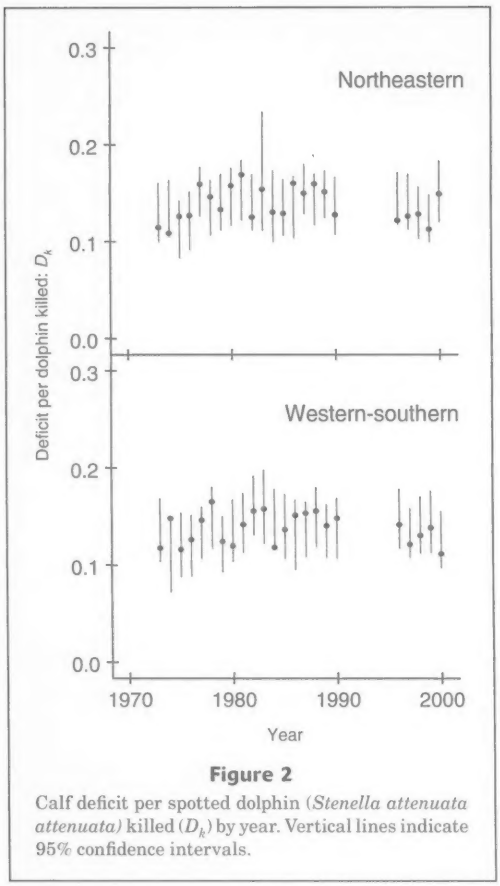

Figure 2

Calf deficit per spotted dolphin (*Stenella attenuata attenuata)* killed (D_k) by year. Vertical lines indicate 95% confidence intervals.

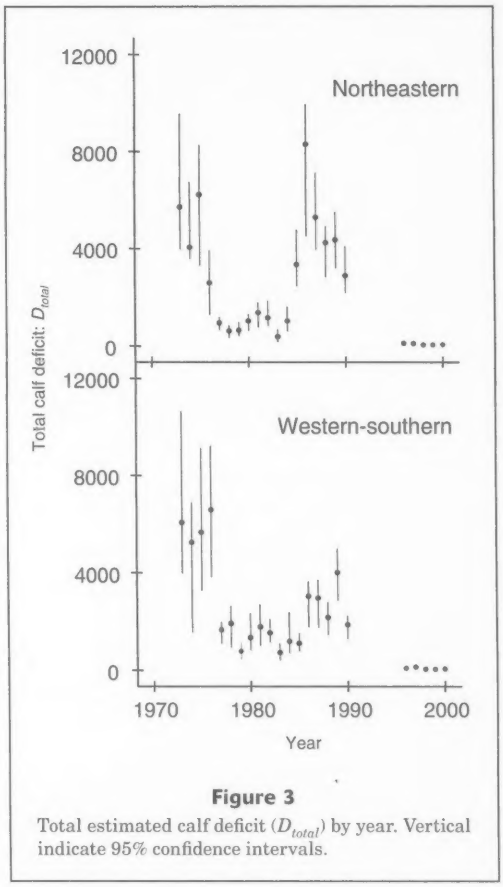

Figure 3

Total estimated calf deficit (D_{total}) by year. Vertical indicate 95% confidence intervals.

by year indicated that the observed number of lactating females in each set was significantly greater ($P \leq 0.05$) than the estimated number in 1977 for the northeastern and the western-southern stocks and in 1979 for the western-southern stock. The difference was significantly less in 1984 for the western-southern stock. Using 0.1 as our type-2 error level, we determined through power analysis that the minimum detectable difference ($\alpha=0.05$) between the mean observed and estimated number of lactating females per set across all years was approximately 0.08 and 0.09 in the northeastern and western-southern stocks respectively.

The observed number of calves per set, defined as the number of dolphins less than 122 cm, was significantly greater for both stocks, for all years combined, than the values estimated in this paper (Table 5). The overall mean difference was 0.17 calves per set for the northeastern stock and 0.12 for the western-southern stock. About half of the years showed a significant difference for each stock. In the comparison of the calf deficit by year, only a few years showed significant differences in either stock (Table 5). However, the estimated deficit tended to be larger than the observed deficit. The paired t-test for all years combined was significant for the northeastern stock, although the mean difference was only −0.06 missing calves per set. The minimum detectable difference from the power analysis for the mean number of calves per set and mean calf deficit per set across all years was 0.06 and 0.08 respectively for both stocks.

Discussion

In the present study, we present an estimate of the number of missing dependent northeastern and western-southern offshore spotted dolphin calves in the tuna purse-seine kill from 1973 to 1990 and from 1996 to 2000. The total number of missing calves decreased through the time series, which, because we estimated the calf deficit as a function of the size of the kill, was a direct result of the large reduction in the annual dolphin kill by the fishery. Between 1973 and 2000, the shortage of calves in the kill remained at a relatively constant fraction of the kill, about 14%, for both stocks of pantropical spotted dolphins (Fig. 2). On the assumption that suckling calves do not survive separation from their mother (Archer et al., 2001;

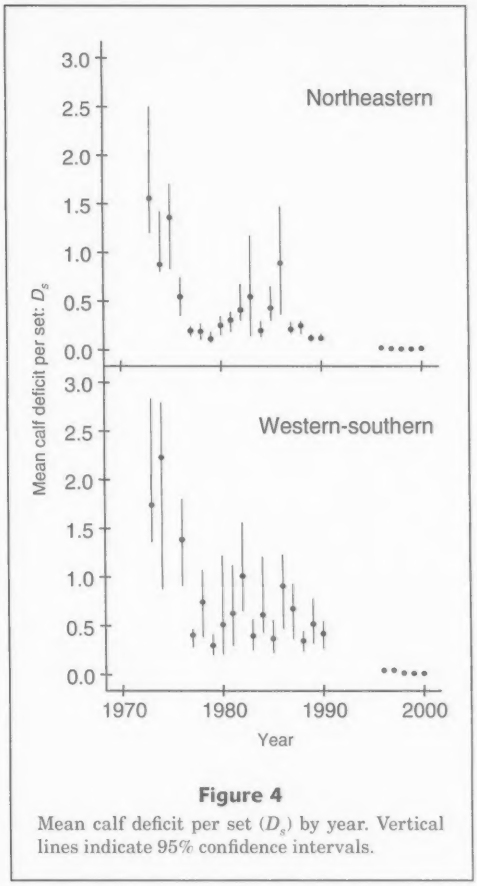

Figure 4

Mean calf deficit per set (D_s) by year. Vertical lines indicate 95% confidence intervals.

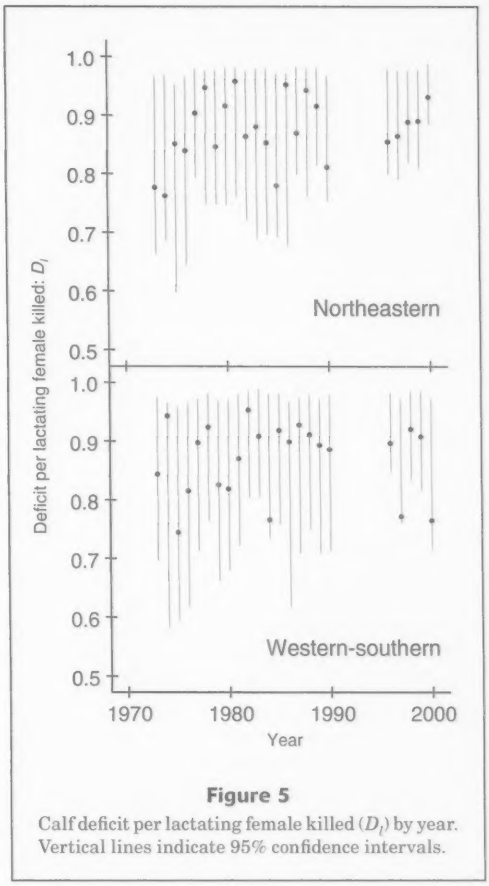

Figure 5

Calf deficit per lactating female killed (D_l) by year. Vertical lines indicate 95% confidence intervals.

Edwards[3]), the estimated calf deficit represents an approximately 14% underestimate of the reported kill.

The calf deficit in the present study was estimated from the number of dependent calves and lactating females killed by using age-color frequency tables and data on the stomach contents of weaning calves. Specimens used to derive the age and color table were collected from 1973 to 1978 and 1981, and specimens used for the weaning model were collected between 1989 and 1991. If the distributions of these samples were not representative of all years that we examined, then our results may be biased. However, the results of a study to construct the annual age distribution of the kill (Archer and Chivers[4]) indicated that there is no significant difference in the age-color frequency table across years. The sample size for the stomach data (29 calves) was too small to examine differences between years.

Our finding of no significant difference between our estimates of the number of lactating females and the observed tally of lactating females in sets where the entire kill was sampled validates this portion of our estimation procedure. However, because the number of suckling calves present in these 100%-sampled sets was not recorded, we were unable to validate the method used to generate these estimates in a similar manner.

The results of our paired *t*-tests indicated that the observed number of animals smaller than 122 cm tended to be greater than the number we estimated. This is most likely a result of the difference between how calves were counted in each method. Archer et al. (2001) considered all animals under a series of cutoff values to be calves that were dependent on suckling for survival. In the present study, the weaning model that we used (Archer and Rob-

[3] Edwards, E. F. 2002. Behavioral contributions to separation and subsequent mortality of dolphin calves chased by tuna purse-seiners in the eastern tropical Pacific Ocean. National Oceanographic and Atmospheric Administration Administrative Report LJ-02-28, 34 p. Southwest Fisheries Science Center, 8604 La Jolla Shores Dr., La Jolla, CA 92037.

[4] Archer, F., and S. J. Chivers. 2002. Age structure of the northeastern spotted dolphin incidental kill by year for 1971 to 1990 and 1996 to 2000. National Oceanographic and Atmospheric Administration Administrative Report LJ-02-12, 18 p. Southwest Fisheries Science Center, 8604 La Jolla Shores Dr., La Jolla, CA 92037.

Table 3

Estimated calf deficit per kill (D_k) and total calf deficit. Total number of spotted dolphins killed reported by the IATTC (2002) and Joseph (footnote 2 in the general text). Values in parentheses are 95% lower and upper confidence intervals.

Stock and year	Estimated calf deficit in observed sets	Observed dolphin kill	Mean calf deficit per kill (D_k)	Total number of NE spotted dolphins killed (±SE)	Estimated total calf deficit
A Northeastern (NE) stock					
1973	599 (464,964)	5242 (3947,6820)	0.11 (0.10,0.16)	49928 ±8899	5709 (3972,9532)
1974	634 (583,1027)	5864 (4943,6916)	0.11 (0.10,0.16)	37410 ±4222	4046 (3573,6708)
1975	1014 (618,1269)	8073 (6578,9965)	0.13 (0.08,0.14)	49399 ±8809	6206 (3297,8254)
1976	300 (196,408)	2376 (1786,3079)	0.13 (0.09,0.15)	20443 ±4721	2583 (1284,3903)
1977	341 (249,416)	2146 (1743,2622)	0.16 (0.13,0.18)	5937 ±690	943 (656,1167)
1978	148 (83,209)	1016 (684,1431)	0.15 (0.11,0.16)	4226 ±827	616 (336,836)
1979	138 (96,226)	1045 (680,1629)	0.13 (0.11,0.17)	4828 ±817	640 (428,963)
1980	178 (107,239)	1132 (724,1637)	0.16 (0.12,0.18)	6468 ±962	1016 (622,1300)
1981	137 (84,173)	815 (560,1122)	0.17 (0.12,0.18)	8096 ±1508	1366 (753,1774)
1982	212 (155,347)	1696 (1126,2395)	0.12 (0.11,0.17)	9254 ±1529	1155 (833,1840)
1983	27 (7,59)	177 (35,410)	0.15 (0.11,0.23)	2460 ±659	377 (169,678)
1984	38 (26,57)	294 (191,417)	0.13 (0.10,0.17)	7836 ±1493	1017 (608,1602)
1985	337 (235,508)	2625 (1839,3529)	0.13 (0.11,0.16)	25975 ±3210	3338 (2447,4748)
1986	290 (119,478)	1816 (859,3440)	0.16 (0.10,0.17)	52035 ±8134	8297 (4496,9935)
1987	497 (397,667)	3327 (2777,4002)	0.15 (0.13,0.18)	35366 ±4272	5280 (3949,7106)
1988	182 (122,215)	1142 (880,1462)	0.16 (0.12,0.17)	26625 ±2744	4234 (2825,4907)
1989	165 (120,217)	1096 (871,1371)	0.15 (0.12,0.17)	28898 ±3108	4357 (3186,5492)
1990	65 (53,90)	515 (421,632)	0.13 (0.11,0.17)	22616 ±2575	2875 (2176,4085)
1996	88 (76,142)	724 (568,926)	0.12 (0.12,0.17)	818	99 (96,139)
1997	49 (42,69)	393 (331,461)	0.13 (0.11,0.17)	721	91 (81,121)
1998	33 (26,41)	260 (230,296)	0.13 (0.10,0.16)	298	38 (30,46)
1999	36 (30,48)	317 (282,357)	0.11 (0.10,0.15)	358	40 (35,53)
2000	43 (32,58)	291 (247,342)	0.15 (0.12,0.18)	295	44 (35,54)

continued

Table 3 (continued)

Stock and year	Estimated calf deficit in observed sets	Observed dolphin kill	Mean calf deficit per kill (D_k)	Total number of NE spotted dolphins killed (±SE)	Estimated total calf deficit
B Western-southern (WS) stock					
1973	141 (110,229)	1199 (836,1638)	0.12 (0.10,0.17)	51,712 ±10,721	6076 (3993–10,633)
1974	254 (100,318)	1715 (939,2733)	0.15 (0.07,0.15)	35,499 ±10,309	5254 (1554,6890)
1975	197 (123,322)	1702 (1104,2434)	0.12 (0.09,0.15)	48,837 ±10,055	5664 (3285,9121)
1976	795 (524,1036)	6293 (4925,7860)	0.13 (0.09,0.15)	52,206 ±8883	6595 (3833,9223)
1977	491 (345,563)	3358 (2860,3906)	0.15 (0.11,0.16)	11,260 ±1186	1647 (1098,1959)
1978	660 (342,949)	3998 (2508,5922)	0.17 (0.12,0.18)	11,610 ±2553	1917 (932,2614)
1979	157 (104,216)	1262 (939,1643)	0.12 (0.09,0.15)	6,254 ±1229	776 (438,1138)
1980	144 (59,344)	1206 (411,2542)	0.12 (0.10,0.17)	11,200 ±2430	1339 (831,2320)
1981	191 (90,340)	1346 (577,2416)	0.14 (0.11,0.17)	12,512 ±2629	1775 (1010,2682)
1982	306 (198,474)	1966 (1337,2734)	0.16 (0.13,0.19)	9869 ±1146	1536 (1156,2088)
1983	23 (15,33)	148 (99,206)	0.16 (0.12,0.20)	4587 ±928	724 (418,1087)
1984	114 (80,224)	961 (526,1513)	0.12 (0.12,0.18)	10,018 ±2614	1183 (712,2352)
1985	52 (32,79)	381 (225,570)	0.14 (0.11,0.17)	8089 ±951	1105 (781,1524)
1986	275 (143,373)	1818 (1065,2784)	0.15 (0.10,0.17)	20,074 ±2187	3037 (1776,3617)
1987	271 (147,374)	1768 (1068,2661)	0.15 (0.11,0.16)	19,298 ±2899	2959 (1754,3695)
1988	75 (51,96)	479 (368,605)	0.16 (0.12,0.18)	13,916 ±1741	2166 (1453,2785)
1989	392 (242,589)	2793 (1819,4277)	0.14 (0.11,0.16)	28,560 ±2675	4011 (2861,4977)
1990	123 (78,160)	829 (582,1128)	0.15 (0.11,0.17)	12,578 ±1015	1864 (1283,2236)
1996	53 (42,71)	374 (308,448)	0.14 (0.12,0.18)	545	77 (64,97)
1997	89 (72,132)	738 (598,931)	0.12 (0.11,0.16)	1044	126 (112,165)
1998	31 (25,42)	236 (192,288)	341 (0.11,0.17)	44	0.13 (38,58)
1999	22 (16,32)	159 (123,209)	0.14 (0.11,0.18)	253	35 (28,44)
2000	28 (22,44)	250 (189,330)	0.11 (0.10,0.15)	435	48 (42,67)

Table 4

Annual mean observed and mean estimated number of lactating females per set in 100% sampled sets. Values in parentheses are 95% lower and upper confidence intervals assuming a normal distribution of differences. Bold type indicates significant difference from zero ($P \leq 0.05$) in the paired t-tests.

	Northeastern stock				Western-southern stock			
Year	No. of sets	Observed	Estimated	Difference (95% CI)	No. of sets	Observed	Estimated	Difference (95% CI)
1973	116	0.55	0.61	−0.06 (−0.17,0.05)	21	1.19	1.30	−0.11 (−0.63,0.42)
1974	98	0.51	0.54	−0.03 (−0.13,0.07)	16	0.75	0.81	−0.06 (−0.36,0.24)
1975	99	0.57	0.48	0.09 (−0.05,0.22)	14	1.07	0.92	0.15 (−0.46,0.77)
1976	51	0.28	0.35	−0.08 (−0.18,0.02)	90	0.500	0.502	−0.002 (−0.119,0.115)
1977	167	0.55	0.46	**0.09 (0.01,0.15)**	163	0.49	0.37	**0.12 (0.03,0.21)**
1978	82	0.37	0.40	−0.03 (−0.14,0.08)	93	0.50	0.52	−0.02 (−0.19,0.13)
1979	75	0.47	0.46	0.01 (−0.13,0.14)	61	0.64	0.47	**0.17 (0.01,0.33)**
1980	54	0.39	0.38	0.01 (−0.11,0.13)	34	0.50	0.44	0.06 (−0.09,0.20)
1981	41	0.53	0.74	−0.21 (−0.81,0.38)	38	0.66	0.64	0.02 (−0.16,0.19)
1982	36	0.62	1.18	−0.56 (−1.40,0.27)	33	0.30	0.44	−0.14 (−0.37,0.10)
1983	33	1.33	2.14	−0.81 (−7.89,6.28)	6	0.17	0.57	−0.40 (−1.57,0.77)
1984	4	0.25	0.49	−0.24 (−0.67,0.18)	29	0.48	1.08	**−0.60 (−0.96, −0.23)**
1985	70	0.34	0.50	−0.16 (−0.36,0.06)	17	0.35	0.50	−0.15 (−0.49,0.20)
1986	45	0.71	0.47	0.24 (−0.04,0.51)	28	0.61	0.42	0.19 (−0.01,0.38)
1987	121	0.43	0.46	−0.03 (−0.18,0.11)	30	0.27	0.46	−0.19 (−0.44,0.06)
1988	6	0.44	0.57	−0.13 (−0.59,0.35)	—	—	—	—
1989	24	0.96	1.03	−0.07 (−0.59,0.44)	15	0.93	0.96	−0.03 (−0.68,0.64)
1990	16	0.56	0.47	0.09 (−0.25,0.44)	9	0.67	0.93	−0.26 (−0.94,0.42)
All	1108	0.50	0.53	−0.03 (−0.08,0.02)	697	0.545	0.546	−0.001 (−0.053,0.051)

ertson, in press) estimated the probability that a calf of a given age class was still suckling. Given that body length has a near linear relationship with age in these young age classes (Perrin, 1976), this meant that for any chosen length of independence, each individual smaller than that cutoff value would only be counted fractionally, in effect correcting for the probability that an animal of a given age is not suckling. This procedure caused the method in this paper to tally fewer "calves" in each set than in the previous study. A secondary result of this effect was that the mean deficit per set estimated in the present study tended to be slightly higher than that presented by Archer et al. in 2001.

We estimated the total number of missing calves as a function of the number of dolphins killed in each stock (Table 3). Prior to 1995, only a fraction of the purse-seine trips carried scientific observers. To estimate the number killed in each stock, kill rates from the observed trips were applied to unobserved trips, stratified by area and stock (IATTC, 2002; Joseph, 1994[2]). Since 1995 it has been reported that all dolphin sets have been observed, and that the number of dolphins killed is therefore known without error (IATTC, 2002).

The total calf deficit could also be estimated as a function of the number of sets by multiplying the total number of sets made on each stock by D_s (Fig. 4). In the only study to estimate the number of sets made on each stock annually, Archer et al.[5] used a relatively simple proration scheme of unobserved sets derived from ratios of the number of sets made on each stock in observed sets. However, because Archer et al.[5] did not stratify unobserved sets by area, basing the total calf deficit on these estimates would produce a different result from that presented in Table 3. Because the estimates of the kill by stock included stratification by area, estimates of the total calf deficit calculated by multiplying the kill estimates by D_k are likely to be more accurate. It is important to realize that the deficit that we present is directly related to the kill observed in the sets that we used. In other words, if proration schemes for unobserved sets were the same for the number of sets made and the number of dolphins killed, estimates of the total calf deficit with either D_s or D_k would be equivalent.

Wade et al.[1] explored the effects of 50% and 100% additional fisheries-related mortality on the assessment of the northeastern spotted dolphin stock. The assumption of additional mortality led to higher estimates of maximum

[5] Archer, F., T. Gerrodette, and A. Jackson. 2002. Preliminary estimates of the annual number of sets, number of dolphins chased, and number of dolphins captured by stock in the tuna purse-seine fishery in the eastern tropical Pacific, 1971–2000. National Oceanographic and Atmospheric Administration Administrative Report LJ-02-10, 26 p. Southwest Fisheries Science Center, 8604 La Jolla Shores Dr., La Jolla, CA 92037.

Table 5

Annual mean number of dolphins killed ≤122 cm (calves killed based on length) and estimated number of suckling calves (calves based on weaning model) per set in 100% sampled sets (first line for each year). Mean deficit per set using 122 cm as cutoff length (calf deficit based on length) and calf deficit as estimated in this article (calf deficit based on weaning model) on second line for each year. Values in parentheses are 95% lower and upper confidence intervals assuming a normal distribution of differences. Differences in bold indicate significant difference from zero ($P \leq 0.05$) in the paired t-test.

	Northeastern stock				Western-southern stock			
		Calves killed based on length	Calves killed based on weaning model			Calves killed based on length	Calves killed based on weaning model	
Year	No. of sets	Calf deficit based on length	Calf deficit based on weaning model	Difference (95% CI)	No. of sets	Calf deficit based on length	Calf deficit based on weaning model	Difference (95% CI)
1973	116	0.54	0.21	**0.33 (0.18,0.50)**	21	0.33	0.06	**0.27 (0.01,0.55)**
		0.35	0.48	**−0.13 (−0.26,−0.03)**		1.00	1.25	−0.25 (−0.79,0.29)
1974	98	0.39	0.05	**0.34 (0.20,0.47)**	16	0.56	0.09	0.47 (−0.53,1.47)
		0.36	0.50	**−0.14 (−0.26,−0.03)**		0.56	0.74	−0.18 (−0.61,0.25)
1975	99	0.57	0.15	**0.42 (0.20,0.64)**	14	0.29	0.11	0.18 (−0.03,0.39)
		0.46	0.40	0.04 (−0.05,0.16)		0.93	0.83	0.10 (−0.45,0.66)
1976	51	0.18	0.11	0.07 (−0.01,0.15)	90	0.13	0.07	**0.06 (0.001,0.13)**
		0.28	0.31	−0.03 (−0.14,0.06)		0.49	0.47	0.02 (−0.10,0.15)
1977	167	0.10	0.03	**0.07 (0.02,0.12)**	163	0.17	0.06	**0.11 (0.06,0.16)**
		0.51	0.45	0.06 (−0.01,0.14)		0.46	0.35	0.11 (0.03,0.20)
1978	82	0.17	0.03	**0.14 (0.05,0.23)**	93	0.18	0.05	**0.13 (0.04,0.23)**
		0.35	0.39	−0.04 (−0.14,0.07)		0.43	0.50	−0.07 (−0.22,0.09)
1979	75	0.09	0.04	0.05 (−0.02,0.13)	61	0.31	0.13	**0.18 (0.04,0.32)**
		0.44	0.43	0.01 (−0.11,0.13)		0.51	0.37	0.14 (−0.03,0.31)
1980	54	0.16	0.03	**0.13 (0.02,0.25)**	34	0.00	0.01	**−0.01 (−0.02,−0.003)**
		0.373	0.371	0.002 −0.115,0.119)		0.50	0.44	0.06 (−0.08,0.21)
1981	41	0.105	0.110	−0.005 (−0.194,0.185)	38	0.05	0.04	0.01 (−0.04,0.07)
		0.53	0.65	−0.12 (−0.57,0.31)		0.63	0.62	0.01 (−0.17,0.20)
1982	36	0.44	0.21	0.23 (−0.10,0.55)	33	0.06	0.02	0.04 (−0.04,0.12)
		0.44	1.00	−0.56 (−1.27,0.14)		0.27	0.42	−0.15 (−0.37,0.08)
1983	33	0.00	0.14	0.14 (−0.64,0.36)	6	0.17	0.04	0.13 (−0.31,0.57)
		1.33	2.00	−0.67 (−7.25,5.91)		0.17	0.56	−0.39 (−1.56,0.76)
1984	4	0.00	0.02	−0.02 (−0.08,0.04)	29	0.14	0.04	0.10 (−0.01,0.21)
		0.25	0.49	−0.24 (−0.67,0.18)		0.35	1.04	−0.69 (−1.13,−0.26)
1985	70	0.13	0.04	**0.09 (0.02,0.15)**	17	0.06	0.04	0.02 (−0.06,0.10)
		0.29	0.47	−0.18 (−0.39,0.03)		0.35	0.49	−0.14 (−0.48,0.21)
1986	45	0.13	0.04	**0.09 (0.01,0.17)**	28	0.04	0.03	0.01 (−0.04,0.06)
		0.64	0.44	0.20 (−0.04,0.44)		0.57	0.39	0.18 (−0.02,0.38)
1987	121	0.14	0.02	**0.12 (0.05,0.20)**	30	0.23	0.08	**0.15 (0.02,0.30)**
		0.38	0.45	−0.07 (−0.22,0.07)		0.27	0.43	−0.16 (−0.41,0.09)
1988	6	0.11	0.12	−0.01 (−0.23,0.22)	—	—	—	—
		0.33	0.50	−0.17 (−0.62,0.28)				
1989	24	0.22	0.13	0.09 (−0.11,0.29)	15	0.47	0.20	**0.27 (0.05,0.49)**
		0.87	0.95	−0.08 (−0.60,0.43)		0.73	0.82	−0.09 (−0.66,0.48)
1990	16	0.31	0.21	0.10 (−0.18,0.38)	9	0.89	0.17	0.72 (−0.18,1.62)
		0.56	0.41	0.15 (−0.20,0.51)		0.33	0.77	−0.44 (−1.15,0.27)
All	1108	0.25	0.08	**0.17 (0.13,0.20)**	697	0.18	0.06	**0.12 (0.09,0.16)**
		0.42	0.48	**−0.06 (−0.10,−0.01)**		0.49	0.51	−0.02 (−0.08,0.03)

growth rates and lower estimates of the current size of the population in relation to carrying capacity. Wade et al.[1] did not model the calf deficit estimated in our present study, but the effect of 14% additional mortality would probably be less than the 50% additional mortality that was modeled. The 50% mortality was spread over all age classes, and additional mortality due to missing calves should be assigned to the first two year classes only. The important question is whether the calf deficit in the kill represents the main effect of mother-calf separation by the fishing process. As outlined in Archer et al. (2001), the mechanism by which suckling calves are separated from their mothers is unknown. If separation is simply a function of the number of lactating females killed, then the deficit presented here is an accurate representation of the number of "missing" calves.

However, there is some evidence that separation can occur without the mother being killed. In the early days of the backdown procedure, purse-seine skippers reported that "Babies swim around the outside of the net pushing to get back in probably because their mothers are still inside" (Gehres[6]). It is unclear whether these calves were separated prior to encirclement or were released early during backdown, prior to their mothers. Regardless, given that dolphins exhibit some of their fastest swimming during a set immediately upon release from the net (Chivers and Scott[7]), separated calves waiting immediately outside the net may risk separation if their mothers join the rest of the school rapidly swimming away from the net. If this, or any of the other scenarios regarding the manner in which permanent separation can occur without the mother being killed (Archer et al., 2001), then the calf deficit underestimates the actual number of orphaned calves. Future research should focus on the mechanism of calf separation because a better understanding of this process is the only way we will be able to estimate the magnitude of the unobserved calf mortality and its subsequent effects on the population.

Acknowledgments

The authors wish to thank Michael Scott and Nick Vogel of the IATTC for providing data as well as Jay Barlow and Bill Perrin for helpful reviews and analytical suggestions.

[6] Gehres, L. E. 1971. Letter of July 2 to Alan R. Longhurst, 2 p. Southwest Fisheries Science Center, 8604 La Jolla Shores Dr., La Jolla, CA 92037.

[7] Chivers, S. J., and M. D. Scott. 2002. Tagging and tracking of *Stenella* spp. during the 2001 Chase Encirclement Stress Studies cruise. National Oceanographic and Atmospheric Administration Administrative Report LJ-02-33, 21 p. Southwest Fisheries Science Center, 8604 La Jolla Shores Dr., La Jolla, CA 92037.

Literature cited

Archer, F., T. Gerrodette, A. Dizon, K. Abella and S. Southern.
2001. Unobserved kill of nursing dolphin calves in a tuna purse-seine fishery. Mar. Mamm. Sci. 17:540–554.

Archer, F., and K. M. Robertson.
In press. Age and length at weaning and development of prey preferences of pantropical spotted dolphins, *Stenella attenuata*, from the eastern tropical Pacific. Mar. Mamm. Sci.

Dizon, A. E., W. F. Perrin, and P. A. Akin.
1994. Stocks of dolphins (*Stenella* spp. and *Delphinus delphis*) in the eastern tropical Pacific: a phylogeographic classification. NOAA Tech. Rep. NMFS-119, 20 p.

Gerrodette, T.
2002. Tuna-dolphin issue. *In* Encyclopedia of marine mammals (W. F. Perrin, B. Wursig, and J. G. M. Thewissen, eds.), p. 1269–1273. Academic Press, San Diego, CA.

Hall, M. A., L. A. Dayton, and K. I. Metuzals.
2000. Bycatch: problems and solutions. Mar. Poll. Bull. 41:204–19.

IATTC (Inter-American Tropical Tuna Commission).
2002. Annual report of the Inter-American Tropical Tuna Commission 2000, 171 p. IATTC, La Jolla, CA.

Gosliner, M. L.
1999. The tuna-dolphin controversy. *In* Conservation and management of marine mammals (J. R. Twiss Jr., and R. R. Reeves, eds.), p. 120–155. Smithsonian Institution Press, Washington and London.

Myrick, Jr., A. C., A. A. Hohn, J., Barlow, and P. A. Sloan.
1986. Reproductive biology of female spotted dolphins, *Stenella attenuata*, from the eastern tropical Pacific. Fish. Bull. 84:247–259.

NRC (National Research Council).
1992. Dolphins and the tuna industry, 176 p. National Academy Press, Washington, D.C.

Perrin, W. F.
1970. Color patterns of the eastern Pacific spotted porpoise *Stenella graffmani* Lönnbeg (Cetacea, Delphinidae). Zoologica (NY) 54:135–149.

Perrin, W. F., J. M. Coe, and J. R. Zweifel.
1976. Growth and reproduction of the spotted porpoise, *Stenella attenuata*, in the offshore eastern tropical Pacific. Fish. Bull. 74:229–269.

Smith, T.
1983. Changes in size of three dolphin (*Stenella* spp.) populations in the eastern tropical Pacific. Fish. Bull. 81:1–13.

Wade, P. R.
1995. Revised estimates of incidental kill of dolphins (Delphinidae) by the purse-seine tuna fishery in the eastern tropical Pacific, 1959–1972. Fish. Bull. 93:345–354.

A remarkable new species of *Psednos* (Teleostei: Liparidae) from the western North Atlantic Ocean

Natalia V. Chernova

Zoological Institute
Russian Academy of Sciences
Universitetskaya nab. 1
St. Petersburg 199034, Russia

David L. Stein

NOAA/NMFS Systematics Laboratory
Smithsonian Institution
P.O. Box 37012
National Museum of Natural History, MRC-0153
Washington, D.C. 20013-7012
E-mail address (for D. L. Stein, contact author): david.stein@noaa.gov

Abstract—*Psednos rossi* new species (Teleostei: Liparidae) is described from two specimens collected in the North Atlantic Ocean off Cape Hatteras, North Carolina, at depths of 500–674 m. *Psednos rossi* belongs to the *P. christinae* group, which includes six other species and is characterized by 46–47 vertebrae and the absence of a coronal pore. *Psednos rossi* differs from those six species by having characters unique within the genus: straight spine, body not humpbacked at the occiput, and a very large mouth with a vertical oral cleft. Other distinguishing characters include a notched pectoral fin with 15–16 rays, eye 17–19% SL, and color in life orange-rose. With *P. rossi*, the genus *Psednos* as currently known includes 26 described and five undescribed species of small meso- or bathypelagic liparids from the Atlantic, Pacific, and Indian Oceans.

Manuscript approved for publication 7 January 2004 by Scientific Editor.

Manuscript received 20 January 2004 at NMFS Scientific Publications Office.

Fish. Bull. 102:245–250 (2004).

The liparid genus *Psednos* Barnard 1927 is a group of meso- and bathypelagic snailfishes distinguished from the genus *Paraliparis* by having the infraorbital canal of the cephalosensory system interrupted behind the eye and usually having a pronounced dorsal curvature of the spine, producing a "humpbacked" body. *Psednos* are small, easily damaged, and often misidentified as juvenile *Paraliparis*. Until 1978, the genus was known only from two specimens of a single species (*Psednos micrurus* Barnard 1927) collected off Cape Point, South Africa. Two additional specimens were collected in the southern Indian Ocean and reported by Stein (1978). No further specimens or species were described until Andriashev (1992) described another new species. Since then, active searches for material from collections around the world have yielded many specimens from the Atlantic, Pacific, and Indian Oceans. To date, 25 species have been described (Andriashev, 1992, 1993; Chernova, 2001; Stein et al., 2001; Chernova and Stein, 2002) and an additional five are undescribed (one in Stein et al., 2001, three in Chernova and Stein, 2002, all in poor condition; and another that is currently being described by Stein). In this article, we describe an especially noteworthy species of the genus from two specimens collected from the North Atlantic off Cape Hatteras, North Carolina.

Materials and methods

All characters available for both specimens were studied. Characters and terms used were described by Andriashev (1992), Chernova (2001), Stein et al. (2001), and Chernova and Stein (2002). Counts were made from a radiograph of the holotype and from each specimen where possible; vertebral counts include the urostyle. The first caudal vertebra is that with the haemal spine supporting the first anal-fin ray. The posterior tip of the lower jaw in *Psednos* forms a distinct and prominent ventrally directed angle, the retroarticular process (Chernova, 2001). Counts and proportions are given as a percentage of standard length (SL) and head length (HL). Nonstandard measurements are the following: distance from mandible to anus (from anterior tip of mandible to center of anus); distance from anus to anal-fin origin (from center of anus to anal-fin origin); interorbital width (measured between upper margins of eyes); postocular head length (distance from posterior margin of eye to tip of opercular flap).

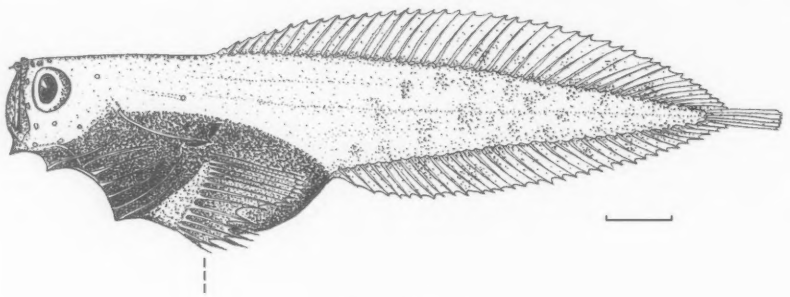

Figure 1

Psednos rossi n.sp., paratype, USNM 372727. Adult, 51.8 mm SL, 57.2 mm TL. Sta. CH-01-047, off Cape Hatteras. Scale 5 mm. Infraorbital pore 6 not shown owing to damage.

We selected the smaller specimen to serve as the holotype owing to its better condition (skin, pores, shape of head) and the availability of more characters. Unfortunately, it is distorted and does not look natural; therefore the undistorted larger (adult) specimen, the paratype, is illustrated. It is also more useful to have a drawing of an adult for comparison with other *Psednos* specimens.

In these small fishes, precise counts of number of tooth rows are possible only in disarticulated cleared and stained specimens; thus, we provide approximate counts. Similarly, the drawing of the gill arch of the paratype was made without dissection by viewing through an opening in the branchiostegal membrane.

Although Andriashev (1986) and Andriashev and Stein (1998) demonstrated the importance of the pectoral girdle in distinguishing among species and in explaining liparid relationships, we did not dissect, clear, and stain a pectoral girdle from these specimens owing to the high probability of damaging them and destroying other characters (Chernova, 2001; Chernova and Stein, 2002). The new species is so easily distinguished from congeners that it is not necessary for a diagnosis of the species to look at additional characters that the pectoral girdle can provide. Future specimens should be used to study these characters.

The holotype and paratype are permanently deposited in the Division of Fishes, Smithsonian Institution, National Museum of Natural History (USNM collection).

Results

Psednos rossi, n.sp.

Holotype

USNM 372726, juvenile, 37.2 mm SL, TL?, Sta. EL-00-033, off Cape Hatteras (The Point), 35°30.036′N, 74°46.497′W, 500–674 m over about 900 m depth, 23 July 2000, Tucker trawl. Good condition but distorted.

Paratype

USNM 372727, adult (sex not identified), 51.8 mm SL, 57.2 mm TL, Sta. CH-01-047, off Cape Hatteras (The Point), 35°28.93′N, 74°45.93′W, 628–658 m over 1090–704 m depth, 24 Aug. 2001, Tucker trawl. Throat slightly damaged, head slightly compressed, skin on head partly missing.

Diagnosis

Vertebrae 47, dorsal-fin rays 42–44, coronal pore absent. Mouth vertical, symphysis of upper jaw above level of eye. Body not humpbacked, vertebral column not curved behind cranium. Gill cavity enlarged. Anus on vertical behind head. Pectoral fin notched, rays 8+2+5–6. Eye 17–19% HL.

Description

Counts and proportions are given in Table 1. Head large, about one-third SL, its depth less than, and its width equal to or a little greater than, its length (Fig. 1). Head depth slightly greater than its width. Mouth very large, distinctly superior. Jaws almost vertical, at angle of about 90° to horizontal. Symphysis of upper jaw above level of eye. Ascending process of premaxilla horizontal, its distal end almost above center of eye. Posterior tip of lower jaw exactly below symphysis of upper jaw. Posterior (lower) end of mouth cleft well below level of lower margin of eye. When mouth closed, ventral surface of lower jaw forms entire frontal surface of head. Lower jaw included. Symphyseal process present at lower jaw symphysis, projecting forward prominently; retroarticular processes of lower jaw large, acute, directed anteroventrally (Fig. 2A). Teeth large, sharp, spear-shaped, strongly curved inward (Fig. 2B), in (smaller) holotype in approximately 22 and 24 (32 and 35) rows on upper and lower jaw; 5 (8–9) teeth in first full row near symphyses of both jaws. Snout short, 1.5 (1.0) times eye diameter. Olfactory rosette (7 lobes) and nostril above anterior third of eye. Eyes not large, close to upper

Table 1

Counts and proportions for the holotype and paratype of *Psednos rossi* new species. Proportions are in % of standard length (SL) followed by % head length (HL, in parentheses).

	USNM 372726 Holotype 37.2 mm SL	USNM 372727 Paratype 51.8 mm SL
Vertebrae	47	—
Dorsal-fin rays	44	42
Anal-fin rays	35	33
Pectoral-fin rays	16 [L] 15 [R]	15 [L, R]
Caudal-fin rays	6	6
Gill rakers	—	10
Head length	32.3	29.9
Head width	22.0 (68.1)	13.5 (45.2)
Head depth	23.7 (73.4)	17.4 (58.2)
Body depth	21.5 (66.6)	25.1 (83.9)
Body depth at anal-fin origin	13.4 (41.5)	17.0 (56.8)
Predorsal-fin length	29.6 (91.6)	26.6 (89.0)
Preanal-fin length	47.8 (148.0)	48.3 (161.5)
Mandible to anus	34.9 (108.0)	36.7 (122.7)
Anus to anal fin origin	23.7 (73.4)	21.2 (70.9)
Upper pectoral-fin lobe length	13.4 (41.5)	13.5 (45.2)
Pectoral-fin notch ray length	8.1 (25.1)	—
Lower pectoral-fin lobe length	9.4 (29.1)	—
Eye diameter	5.4 (16.7)	5.8 (19.4)
Snout length	8.1 (25.0)	7.7 (25.8)
Interorbital width	13.4 (42.0)	11.2 (37.4)
Postocular head length	18.8 (58.0)	19.3 (64.5)
Upper jaw length	16.1 (49.8)	12.5 (41.8)
Lower jaw length	16.1 (49.8)	13.5 (45.2)
Gill opening length	5.4 (16.7)	5.4 (18.1)
Opercle length	13.4 (41.5)	12.5 (41.8)

contour of head. Interorbital space flat, 2.5 (1.9) times eye diameter. Gill opening short, 1.0 (0.9) times eye diameter, at 45° angle, entirely above pectoral-fin base and slightly anterior to it (distance between ventral end of gill opening and base of upper pectoral ray about equal to length of gill opening). Opercular flap small, acute. Opercle very long, directed ventrally and posteriorly, its tip below level of posterior end of lower jaw. Interopercle of similar length, visible externally, its anterior tip projecting anteriorly from ventral contour of head (Fig. 1). Long opercle, interopercle and elongated branchiostegal rays support membranes of enlarged branchial cavity that appears externally as a black posterior part of head. Branchial cavity length slightly more than half head length. Branchiostegal rays (4+2) long and distinctly visible externally. Gill rakers modified, closely but irregularly set, mostly alternating (especially on gill arch one), often paired on the outer and inner sides of each gill arch (central part of arches two and three); plates flattened, triangular, similar in shape to those in *P. pallidus* or *Psednos* sp.1 of Chernova and Stein (2002, Figs. 9 and 13), spinule-bearing surface directed internally, flat and longitudinally oval. Spinules closely set, usually in two longitudinal rows, each of five to eight spinules, often with a few additional spinules in between (Fig. 2C).

Sensory pores difficult to see because of thin transparent skin (damaged in paratype). Nasal pores 2, the posterior on a vertical through center of eye. Paired nasal bones (through which the nasal canals run) long, tubular, and visible externally. Coronal pore absent. Lacrimal bones (bearing anterior portion of infraorbital canal) large, visible externally, slightly prominent anteriorly. Infraorbital canal (better preserved in holotype) interrupted behind eye, infraorbital pores 6 (5+1), posteriormost above posterior margin of eye (Fig. 2A). In paratype, skin behind eye missing. Preoperculomandibular pores 6 (3 on lower jaw + 3 on preopercular area). Two temporal pores present: t_1 a short distance behind posterior margin of eye, and t_{sb}, the suprabranchial pore, above and in front of gill opening (Fig. 2A).

Pectoral fin notched, of 16 (15) rays. Upper lobe of 8 (8) rays, the 2 (2) notch rays more widely spaced and placed exactly at middle of fin base. In holotype, left lower pectoral lobe with 6, on right 5, rays. In paratype, 5 rays on each side. Bases of lower-lobe rays stronger and thicker than those of upper-lobe rays. Level of uppermost pectoral ray below horizontal through lower end of upper jaw. Base of pectoral fin close to vertical, lowest ray almost directly below uppermost. Upper-lobe rays not reaching anal fin origin, lower-lobe rays not reaching vertical through ends of upper lobe rays. In holotype, length of notch rays 1.7 times in upper pectoral-fin lobe length, lower pectoral-fin lobe 1.4 times in it.

Body not humpbacked, dorsal contour of back almost straight; spine horizontal, its anterior end not dorsally curved (Fig. 3). Neural spines of vertebrae 1–4 neither longer nor broader than those posterior, unlike other species (see Fig. 5 in Chernova, 2001). Maximum body depth 4.2 (4.0) times in standard length and 1.6 (1.5) times depth at anal-fin origin. In holotype, occiput slightly swollen (Fig. 3); in paratype, dorsal outline of head and back in front of dorsal fin origin almost perfectly flat (Fig. 1), possibly an age-related difference. Abdominal part of body long, preanal length almost half of standard length. Interneural of first dorsal-fin ray between neural spines 3 and 4. Dorsal and anal fins moderately deep, maximum depth of erect dorsal fin in paratype 8.9 times in SL, 2.7 times in head length (damaged in holotype). Dorsal and anal fins overlapping about one-third of caudal-fin length. Anus on vertical behind head, slightly behind base of uppermost pectoral ray. Skin transparent. Gelatinous subcutaneous tissue weakly developed. In holotype (smaller specimen) body not as deep and jaws longer than in the paratype (larger specimen). Differences in head width and interorbital width are great because head of paratype was slightly compressed during fixation. Other proportions similar to those of holotype.

Body color in alcohol pale; under magnification, slightly dusky blotches of dots present caudally in paratype and absent in holotype. Head musculature pale. Black peritoneum visible through body wall. Mouth and gill cavities, gill arches, tongue, and both jaws black; gill rakers pale. Musculature of pectoral girdle appears pale on lateral surface of belly. Color in life orange-rose.

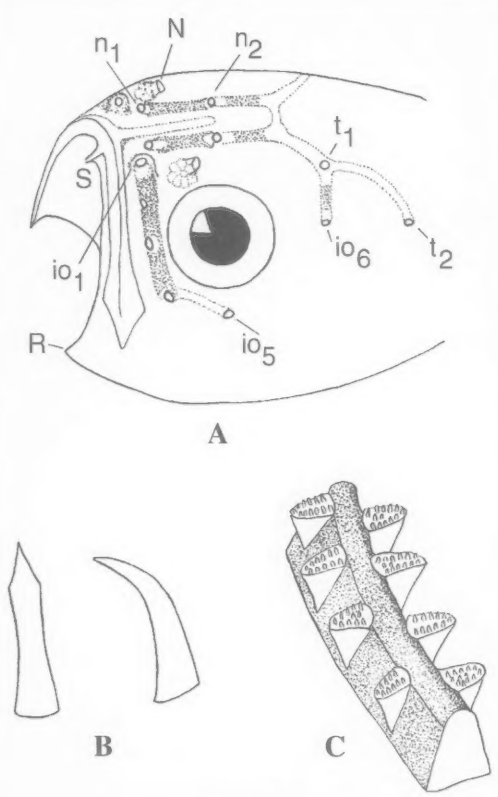

Figure 2

Details of anatomy of *Psednos rossi*. (**A**) Cephalic pores and prominent features of head. Portions of sensory canals passing through bones are stippled. N = nostril and olfactory rosette; io = infraorbital pores, n = nasal pores, t = temporal pores; S = symphyseal knob; R = retroarticular process. (**B**) Teeth of paratype: (left) frontal view; (right) lateral view. Tooth length about 0.25 mm. (**C**) First gill arch of paratype, USNM 372727, right side; view from inside of gill cavity. Raker height about 0.3 mm.

Distribution

Western North Atlantic off Cape Hatteras, mesopelagic at depths of 500–674 m.

Etymology

The patronym "rossi" after Steve W. Ross, who initially notified us of the captures and furnished the specimens to us for examination.

Comparative notes

Psednos rossi seems to belong to the *P. christinae* group (see Chernova, 2001; Chernova and Stein, 2002), including *P. andriashevi, P. barnardi, P. christinae, P. dentatus, P. groenlandicus,* and *P. harteli*. Species of this group are characterized by vertebrae 46–47, dorsal-fin rays 38–42, anal-fin rays 33–35, and coronal pore absent (versus the *P. micrurus* group having vertebrae 40–44, dorsal-fin rays 34–38, anal-fin rays 28–33, and coronal pore present) (Chernova, 2001). *Psednos rossi* distinctly differs from the other species of the *christinae* group in at least having occiput not swollen (vs. greatly swollen), not humpbacked because the vertebral column is straight (vs. humpbacked owing to the greatly curved anterior part of the spine), mouth vertical with jaws at 90° to horizontal, symphysis of upper jaw above level of eye (vs. a more or less oblique mouth at an angle of 30–45° and the upper jaw, symphysis on a horizontal with the lower half of the eye); and anus

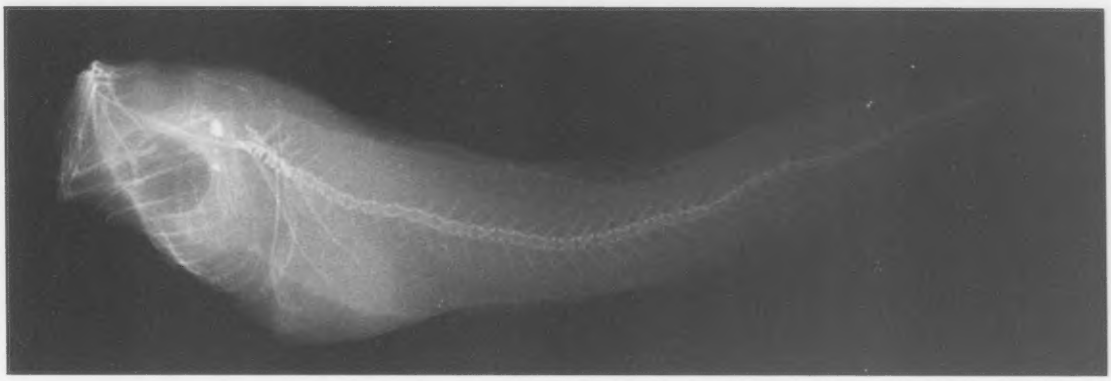

Figure 3

Radiograph of *Psednos rossi* n.sp., holotype, USNM 372726. Juvenile, 37.2 mm SL. Sta. EL-00-033, off Cape Hatteras.

behind the head (vs. anus below the posterior third of the head). The very oblique, almost vertical mouth occurs often in species of the *P. micrurus* group, five of which have the mouth at 75–85° to the horizontal (*P. anoderkes, P. cathetostomus, P. microps, P. mirabilis, P. sargassicus*). However, they all differ as described above.

Discussion

The physical features of *Psednos rossi* are unique in the genus. The straight vertebral column and body are outside the previous diagnosis of the genus, because all previously known species are humpbacked owing to the curved spinal column. Nevertheless, *P. rossi* clearly belongs in *Psednos* rather than *Paraliparis* because it has the other generic characters of *Psednos* (Chernova, 2001); particularly, its sensory canal system and pores are of *Psednos* type, having an interrupted infraorbital canal behind the eye. We suggest that its remarkable body shape is an extreme transformation of the usual *Psednos* body shape and is associated with the change of the mouth from oblique and of normal size to vertical and very large. In this process the anterior movement of the bony elements of the jaws greatly enlarges the branchial cavity.

The morphology of *Psednos rossi* invites speculation about its ecology. The very large superior mouth with vertical jaws, eyes located close to the dorsal contour of the head and oriented to look forward and up, and straight body suggest adaptation to feeding on detritus and animals (such as copepods) above it in the water column. These adaptations, similar to those of hatchetfishes (family Sternoptychidae), are highly advantageous for a mesopelagic mode of life. Sudden opening of the very large vertical lower jaw could produce a strong orobranchial suction, simultaneously bringing food into the mouth and thus saving energy for this fish, which is probably a poor swimmer.

Work over the last several years has made it clear that *Psednos* species exist at mesopelagic depths in the North Atlantic, Indian, North Pacific, and South Pacific Oceans. We confidently expect discovery of additional species from meso- and bathypelagic waters.

Acknowledgments

We wish to thank S. W. Ross, K. J. Sulak, and J. V. Gartner Jr. for collecting the specimens, bringing them to our attention, and loaning them to us for description. Collections were supported by the U.S. Geological Survey, State of North Carolina, North Carolina Coastal Reserve Program, and the Duke/UNCW Oceanographic Consortium. The figures are drawn by the senior author, who was supported by the Russian Science Foundation Grants 02-04-48669 and 00-15-07794.

Literature cited

Andriashev, A. P.

1986. Review of the snailfish genus *Paraliparis* (Scorpaeniformes: Liparididae) of the Southern Ocean, 204 p. Theses Zoologicae 7, Koeltz Scientific Books, Koenigstein

1992. Morphological evidence for the validity of the antitropical genus *Psednos* Barnard (Scorpaeniformes, Liparidae) with a description of a new species from the eastern North Atlantic. UO, Tokyo 41:1–18.

1993. The validity of the genus *Psednos* Barnard (Scorpaeniformes, Liparidae) and its antitropical distribution area. Vopr. Ikhtiol. 33 (1):5–15 [in Russian.] J. Ichthyol. 33 (5):81–98. [English translation.]

Andriashev, A. P., and D. L. Stein.

1998. Review of the snailfish genus *Careproctus* (Liparidae, Scorpaeniformes) in Antarctic and adjacent waters. Contr. Sci. Nat. Hist Mus. Los Angeles Cty. 470:1–63.

Chernova, N. V.
2001. A review of the genus *Psednos* (Pisces, Liparidae) with description of ten new species from the North Atlantic and southwestern Indian Ocean. Bull. Mus. Comp. Zool. 155:477–507.

Chernova, N. V., and D. L. Stein.
2002. Ten new species of *Psednos* (Pisces, Scorpaeniformes: Liparidae) from the Pacific and North Atlantic Oceans. Copeia 2002 (3):755–778.

Stein, D. L.
1978. The genus *Psednos* a junior synonym of *Paraliparis*, with a redescription of *Paraliparis micrurus* (Barnard) (Scorpaeniformes: Liparidae). Matsya 4:5–10.

Stein, D. L., N. V. Chernova, and A. P. Andriashev.
2001. Snailfishes (Pisces: Liparidae) of Australia, including descriptions of 30 new species. Rec. Austr. Mus. 53:341–406.

Age and growth of sailfish (*Istiophorus platypterus*) in waters off eastern Taiwan

Wei-Chuan Chiang
Chi-Lu Sun
Su-Zan Yeh
Institute of Oceanography
National Taiwan University
No. 1, Sec. 4, Roosevelt Road
Taipei, Taiwan 106
E-mail address (for C. L. Sun, contact author): chilu@ntu.edu.tw

Wei-Cheng Su
Taiwan Fisheries Research Institute
No. 199, Ho-Ih Road
Keelung, Taiwan 202

Abstract—Age and growth of sailfish (*Istiophorus platypterus*) in waters off eastern Taiwan were examined from counts of growth rings on cross sections of the fourth spine of the first dorsal fin. Length and weight data and the dorsal fin spines were collected monthly at the fishing port of Shinkang (southeast of Taiwan) from July 1998 to August 1999. In total, 1166 dorsal fins were collected, of which 1135 (97%) (699 males and 436 females) were aged successfully. Trends in the monthly mean marginal increment ratio indicated that growth rings are formed once a year. Two methods were used to back-calculate the length of presumed ages, and growth was described by using the standard von Bertalanffy growth function and the Richards function. The most reasonable and conservative description of growth assumes that length-at-age follows the Richards function and that the relationship between spine radius and lower jaw fork length (LJFL) follows a power function. Growth differed significantly between the sexes; females grew faster and reached larger sizes than did males. The maximum sizes in our sample were 232 cm LJFL for female and 221 cm LJFL for male.

Manuscript approved for publication 22 December 2003 by Scientific Editor.
Manuscript received 20 January 2004 at NMFS Scientific Publications Office.
Fish. Bull. 102(2): 251–263 (2004).

The sailfish (*Istiophorus platypterus*) is distributed widely in the tropical and temperate waters of the world's oceans. According to data from longline catches, sailfish are usually distributed between 30°S and 50°N in the Pacific Ocean, and highest densities are found in the warm Kuroshio Current and its subsidiary currents. This species has a tendency to be found close to the coast and near islands (Nakamura, 1985). During the 1990s the annual landings of sailfish off Taiwan ranged between 600 and 2000 metric tons, of which approximately 54% came from waters off Taitung (eastern Taiwan). Sailfish are seasonally abundant from April to October (peak abundance from May to July) and contribute substantially to the economic importance of the eastern coast of Taiwan where this species is taken primarily by drift gill nets, although they are also caught by set nets, harpoons, and as incidental bycatch in inshore longline fisheries.

Age and growth of sailfish caught in recreational fisheries in the Atlantic Ocean have been studied by using various methods, including length-frequency analysis (de Sylva, 1957), analysis of release-recapture data (Farber[1]), and inferences from observed marks on hard parts, such as spines (Jolley, 1974, 1977; Hedgepeth and Jolley, 1983) and otoliths (Radtke and Dean, 1981; Radtke, 1983; Prince et al., 1986). In contrast, very few attempts have been made to age sailfish in the Pacific Ocean. Koto and Kodama (1962) estimated the growth of sailfish caught with longlines from 1952 to 1955 in the East China Sea using length-frequency analysis, and Alvarado-Castillo and Félix-Uraga (1996, 1998) used the fourth spine of the first dorsal fin to estimate age and growth of sailfish caught from 1989 to 1991 in the recreational fishery off Mexico. However, western Pacific sailfish have not been aged with calcified structures in any previous study.

The aging of fishes, and consequently the determination of their growth and mortality rates, is an integral component of modern fisheries science (Paul, 1992). Mortality and growth rates provide quantitative information on fish stocks and are needed for stock assessment methods such as yield-per-recruit and cohort analysis (Powers, 1983).

The objectives of this study were to estimate age and growth of sailfish by counting growth rings on cross sections of the fourth spine of the first dorsal fin and to determine which of the Richards function and the standard von Bertalanffy growth function best represents growth of sailfish in waters off eastern

[1] Farber, M. I. 1981. Analysis of Atlantic billfish tagging data: 1954–1980 Unpubl. manuscr. ICCAT workshop on billfish, June 1981. Southeast Fisheries Center Miami Laboratory, National Marine Fisheries Service, NOAA, 75 Virginia Beach Drive, Miami, FL 33149.

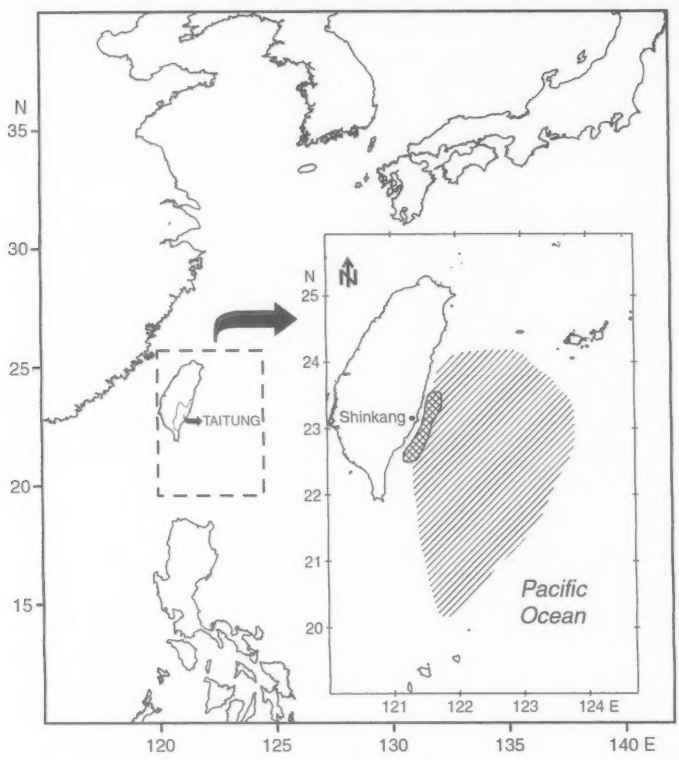

Figure 1

Fishing grounds of the gillnet (cross lines) and longline (oblique lines) fishing boats based at Shinkang fishing port.

Taiwan. This information could be used to determine the age composition of the catch and to assess the status of sailfish in these waters by using yield-per-recruit or sequential population analysis techniques.

Materials and methods

Materials

Data on total length (TL), eye fork length (EFL), lower jaw fork length (LJFL) (in cm), round weight (RW) (in kg) and the first dorsal fins of male and female sailfish were collected monthly at the fishing port of Shinkang (Fig. 1) from July 1998 to August 1999. In total, 304 TLs, 1166 LJFLs, 1166 RWs, and 1166 dorsal fins were collected. The dorsal fins were kept in cold storage before being boiled to remove surrounding tissue and to separate the fourth spines. Three cross sections (thickness 0.75 mm) were taken successively along the length of each spine with a low-speed "ISOMET" saw (model no. 11-1280) and diamond wafering blades, at a location equivalent to 1/2 of the maximum width of the condyle base measured above the line of maximum condyle width (Fig. 2A) (Ehrhardt et al., 1996; Sun et al., 2001, 2002). The sections were immersed in 95% ethanol for several minutes for cleaning, placed on disposable paper to air dry, and then stored in a labeled plastic case for later reading. Spine sections were examined with a binocular dissecting microscope (model: Leica-MZ6) under transmitted light at zoom magnifications of 10–20× depending on the sizes of the sections. The most visible one of these three sections was read twice, approximately one month apart. If the two ring counts differed, the section was read again, and if the third ring count differed from the previous two ring counts, the spine was considered unreadable and discarded. The precision of reading was evaluated by using average percent error (APE) (Beamish and Fournier, 1981; Campana, 2001) and coefficient of variation (CV) (Campana, 2001) statistics.

Images of the cross sections were captured by using the Image-Pro Image analysis software package (Media Cybernetics, Silver Spring MD, 1997) in combination with a dissecting microscope equipped with a charged coupled device (CCD) camera (model: Toshiba IK-630) and a Pentium II computer equipped with a 640×480 pixel frame grab card and a high-resolution (800×600 pixel) monitor.

The distance from the center of the spine section to the outer edge of each growth ring was measured in microns with the Image-Pro software package after calibration against an optical micrometer. The center of the spine

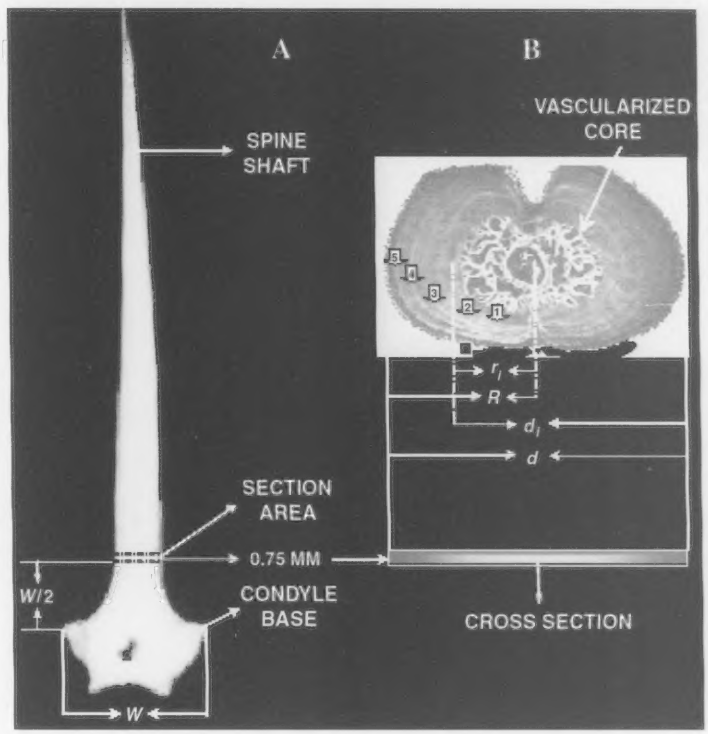

Figure 2

Schematic diagram of the fourth dorsal spine of sailfish (*I. platypterus*) and the location of the cross section (**A**), and a cross section showing the measurements taken for age determination of sailfish (**B**). W = maximum width of condyle base, R = radius of spine, r_i = radius of ring i, d = diameter of spine, d_i = diameter of ring i. The vascularized core and growth rings (1, 2, 3, 4, 5) are also shown.

section was estimated according to the methods of Cayré and Diouf (1983) (Fig. 2B). The distances (d_i) were then converted into radii (r_i) by using the equation (Megalofonou, 2000; Sun et al., 2001):

$$r_i = d_i - (d/2),$$

where r_i = radius of the ring i;
d_i = distance from the outside edge of ring i to the opposite edge of the cross section; and
d = diameter of the spine.

False growth rings were defined according to criteria of Berkeley and Houde (1983), Tserpes and Tsimenides (1995), and Ehrhardt et al. (1996).

Accounting for missing early rings

The first several growth rings of the larger specimens may be obscured because of the large size of the vascularized core of the spine. The number of early but missing growth rings was therefore estimated by the replacement method applied to Pacific blue marlin (*Makaira nigricans*) by Hill et al. (1989). This method involved first compiling ring radii statistics from younger specimens that had at least the first or second ring visible. Radii of the first four visible rings from samples that had missing early rings were then compared with the radii for these younger specimens. When the radii of at least two successive rings of the first four visible rings each fitted well within one standard deviation from the mean radii of each of two or more rings from the data compiled from the younger specimens, the number of missing rings was computed as the difference between the ring counts for the matched radii compiled from younger specimens and those for the specimen of interest.

Validation

The marginal increment ratio (MIR), which was used to validate the rings as annuli, was estimated for each

specimen by using the following equation (Hayashi, 1976, Prince et al., 1988; Sun et al., 2002):

$$MIR = (R - r_n)/(r_n - r_{n-1}),$$

where R = spine radius; and
r_n and r_{n-1} = radius of rings n and $n-1$.

The mean MIR and its standard error were computed for each month by sex for all ages combined, and also for the ages 1–5 and 6–11 for males and 1–5 and 6–12 for females.

Growth estimation

Growth for males and females was estimated by back-calculation of lengths at presumed ages. Two methods were used. Method 1 was based on the assumption that the relationship between spine radius (R) and LJFL (L) is linear, i.e., $L=a_1+b_1R$ (Berkeley and Houde, 1983; Sun et al., 2002), whereas method 2 was based on the assumption that this relationship is a power function, i.e., $L=a_2R^{b_2}$ (Ehrhardt, 1992; Sun et al., 2002). The parameters of the relationships were estimated by maximum likelihood, assuming log-normally distributed errors. Akaike's information criterion (AIC, Akaike, 1969) was used to select which of the linear and power functions best represented the data:

$$AIC = -2\ln L + 2p,$$

where $\ln L$ = logarithm of likelihood function evaluated at the maximum likelihood estimates for the model parameters, and
p = number of model parameters.

The equations used to back-calculate the lengths at presumed ages were

$$L_n = \begin{cases} a_1 + \left(\frac{r_n}{R}\right)(L - a_1) & \text{linear relationship} \\ \left(\frac{r_n}{R}\right)^{b_2} L & \text{power relationship} \end{cases},$$

where L_n = LJFL when ring n was formed;
L = LJFL at time of capture; and
r_n = radius of ring n.

The standard von Bertalanffy growth function (standard VB) (von Bertalanffy, 1938) and the Richards function (Richards, 1959) were then fitted to the mean back-calculated male and female lengths-at-age from methods 1 and 2, assuming additive error.

Standard VB:

$$L_t = L_\infty\left(1 - e^{-k(t-t_0)}\right),$$

Richards function:

$$L_t = L_\infty\left(1 - e^{-K(1-m)(t-t_0)}\right)^{\frac{1}{1-m}},$$

where L_t = the mean LJFL at age t;
L_∞ = the asymptotic length;
t_0 = the hypothetical age at length zero;
k and K = the growth coefficients; and
m = the fourth growth-equation parameter.

An analysis of residual sum of squares (ARSS) was used to test whether the growth curves for the two sexes were different (Chen et al., 1992; Tserpes and Tsimenides, 1995; Sun et al., 2001), and the log-likelihood ratio test was used to determine whether the Richards function provided a statistically superior fit to the data than the length-at-age standard VB growth function.

Results

Of the 1166 dorsal spines sampled, 1135 (97%) (699 males and 436 females) were read successfully. The average percent error (APE) was 6.31% (5.91% for males and 6.93% for females) and the coefficient of variation (CV) was 8.93% (8.36% for males and 9.81% for females). Of the 31 spines that could not be read, 22 were considered unreadable because the existence of multiple rings made the identification of annuli difficult or resulted in aging discrepancies between readings, and the remaining nine spines were unreadable because of abnormal growth.

The length-frequency and weight-frequency distributions for the 1166 individuals are shown in Figure 3. These individuals ranged from 78 to 221 cm LJFL (mean=177.62, SD=16.13, n=720) or 1 to 49 kg RW (mean=22.13, SD=5.68) for the males and from 80 to 232 cm LJFL (mean=179.96, SD=17.90, n=446) or 2 to 58 kg RW (mean=23.65, SD=7.34) for the females. The females were significantly larger than the males (t-test, $P<0.05$). Table 1 summarizes the relationships between EFL and LJFL and TL, and that between LJFL and weight. The latter relationship differed significantly between males and females (analysis of covariance; $P<0.05$).

At least the first or second ring in 417 (60%) of male spines and 300 (69%) of female spines was visible. The ring radii statistics by sex is summarized in Figure 4. All other specimens were assigned inner rings and final age estimates based upon these data. The mean ring radii by age group, for males and females, after correction for missing early rings, are listed in Table 2. The maximum age of the sampled sailfish, after correction for missing early rings, was 11 years for males and 12 years for females. The maximum ages before correction were 8 years for both sexes.

The monthly means of the marginal increment ratio (MIR) for males of all ages during May–August were high (~0.72) but declined markedly thereafter and reached a minimum of 0.46 in November (Fig. 5). Similarly, the MIR for females dropped from 0.71 in September to a minimum of 0.47 in November (Fig. 6). The monthly means of MIR did not differ significantly from each other over the period December–March (ANOVA, $P_{\sigma}=0.86$, $P_{\varphi}=0.96$). However, the monthly means of MIR from April through August for males and from April through September for females were

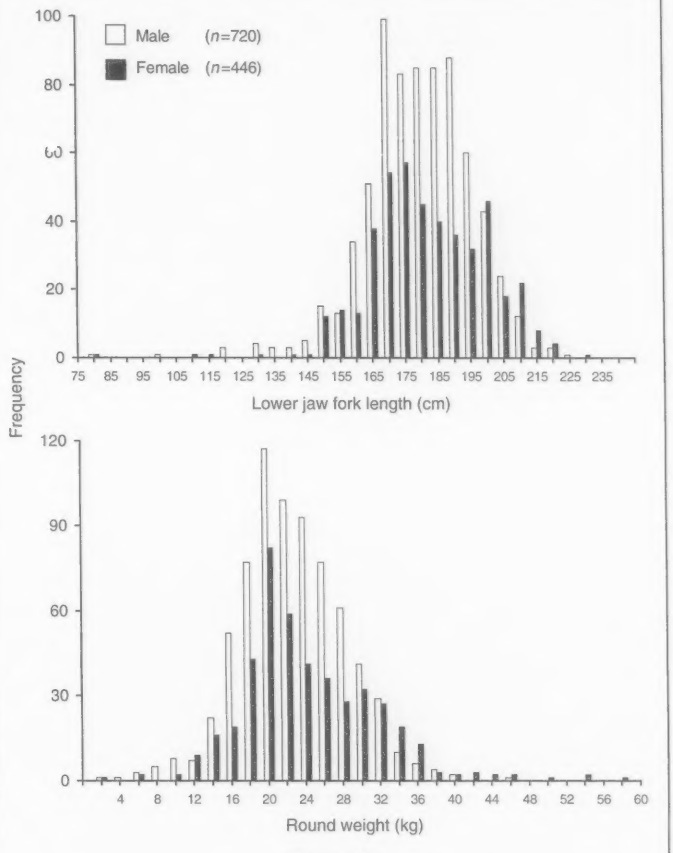

Figure 3

The size-frequency distributions by 5-cm intervals (upper figure) and by 2-kg intervals (lower figure) for male and female sailfish (*I. platypterus*) collected from the waters off eastern Taiwan.

significantly higher than those from September through November for males (t-test, $P<0.001$) and from October through November for females (t-test, $P<0.001$). Also, the mean MIR in November was significantly lower than that in December (t-tests, $P_{♂}<0.05$, $P_{♀}<0.05$). The trends in the monthly means of MIR when the data were split into ages 1–5 and 6+ were similar to those for all ages combined. The results in Figures 5 and 6 indicate that one growth ring is formed each year, most likely from September to November for males and from October to November for females.

Figure 7 shows the sex-specific relationships between LJFL and spine radius based on method 1 (linear regression) and method 2 (power function). The relationships for males and females are significantly different (method 1: $F_{698,435}=56.07$, $P<0.01$; method 2: $F_{698,435}=59.93$, $P<0.01$). According to AIC, the power function provides a better fit to the data (ΔAIC=38.57 and 30.96 for males and females, respectively). Therefore, the most parsimonious representation of the data is the power function with separate parameters for males and females.

The mean back-calculated lengths-at-age obtained from methods 1 and 2 are listed in Table 3. After the first year of life, the growth rates of both sexes slow appreciably. However, females still grow faster and consequently reach larger sizes than males. The standard VB and the Richards function for males and females are shown in Figure 8 and the corresponding parameter estimates are listed in Table 4. The growth curves for males differ significantly from those for females ($F=99.86$ $P<0.05$ and $F=107.38$ $P<0.05$ for the standard VB curve [methods 1 and 2], and $F=144.01$ $P<0.05$ and $F=48.43$ $P<0.05$ for the Richards function [methods 1 and 2]). The Richards function provides a statistically superior fit to the data (log-likelihood ratio test; $P<0.001$) when method 2 is used to back-calculate length-at-age but not when method 1 is used.

Table 1

Linear relationships ($Y=a+bX$) among total length (TL, cm), lower jaw fork length (LJFL, cm) and eye fork length (EFL, cm), and the log-linear length-weight (round weight, RW, kg) relationships for sailfish in the waters off eastern Taiwan. Values in parentheses are standard errors.

Y	X	a	b	n	LJFL range (cm)	RW range (kg)	r^2
Male							
TL	LJFL	19.660 (6.334)	1.205 (0.037)	184	78–211		0.854
TL	EFL	24.782 (6.176)	1.364 (0.042)	184	78–211		0.854
EFL	LJFL	–5.196 (0.772)	0.893 (0.004)	720	78–221		0.983
$\log_{10}$RW	$\log_{10}$LJFL	–5.381 (0.080)	2.985 (0.036)	720	78–221	1–46	0.906
Female							
TL	LJFL	6.728 (9.351)	1.286 (0.055)	120	109–210		0.824
TL	EFL	6.754 (9.505)	1.489 (0.064)	120	109–210		0.820
EFL	LJFL	–2.209 (0.802)	0.876 (0.004	446	80–232		0.989
$\log_{10}$RW	$\log_{10}$LJFL	–5.338 (0.103)	2.970 (0.046)	446	80–232	2–58	0.905

Discussion

Age estimate determined from dorsal-fin spines

Dorsal-fin spines appear to be useful for aging sailfish. They are easily sampled without reducing the economic value of the fish and can also be read easily (the growth rings stand out clearly). In contrast, scales cannot be used to age sailfish because scale deposition patterns change as sailfish age (Nakumura, 1985), and otoliths are extremely small and fragile and are often difficult to locate (Radtke, 1983). Reading otoliths is more time consuming and expensive than reading spines and spines can also be easily stored for future re-examination (Compeán-Jimenez and Bard, 1983; Sun et al., 2001, 2002).

The problems associated with the fin-spine aging method used in this study were the possible existence of false rings and the presence of the vascularized core which can obscure early growth rings in larger fish. These problems were also noted by Berkeley and Houde (1983), Hedgepeth and Jolley (1983), Tserpes and Tsimenides (1995), Megalofonou (2000), and Sun et al. (2001, 2002). However, Tserpes and Tsimenides (1995) and Megalofonou (2000) noted that experienced readers can overcome the problem of multiple rings by determining whether the rings are continuous around the circumference of the entire spine section and by judging their distance from the preceding and following rings. We observed false rings in spines for all age classes larger than age two, which we read without problem by using these guidelines. The missing early growth rings in larger specimens were accounted for by compiling ring radii statistics for younger specimens for which at least the first or second ring was visible and by comparing the radii of the first several visible rings of the specimens that had missing early rings to the mean radii and standard deviations of the compiled data. Similar approaches for solving the problem of missing rings have also been used for Pacific blue marlin (Hill et al., 1989).

Marginal increment ratio (MIR) analysis is the most commonly applied method for age validation (Campana, 2001). The MIR analysis conducted for sailfish suggested that one growth ring is formed each year from September to November for males and from October to November for females. Spawning for sailfish in the waters east of Taiwan lasts from April through September (Chiang and Sun[2]). This is exactly the period when growth is low, as indicated by the narrow and translucent rings. Similar findings have been reported for skipjack tuna (Antoine et al., 1983), swordfish (Ehrhardt, 1992; Tserpes and Tsimenides, 1995), and bigeye tuna (Sun et al., 2001). Although the timing of annulus formation coincides with spawning season for sailfish in the eastern Taiwan, annulus deposition

[2] Chiang, W. C., and C. L. Sun. 2000. Sexual maturity and sex ratio of sailfish (*Istiophorus platypterus*) in the eastern Taiwan waters. Abstracts of contributions presented at the 2000 annual meeting of the Fisheries Society of Taiwan, Keelung, Taiwan, 16–17 December 2000, 15 p. The Fisheries Society of Taiwan, 199 Hou-Ih Road, Keelung, 202 Taiwan.

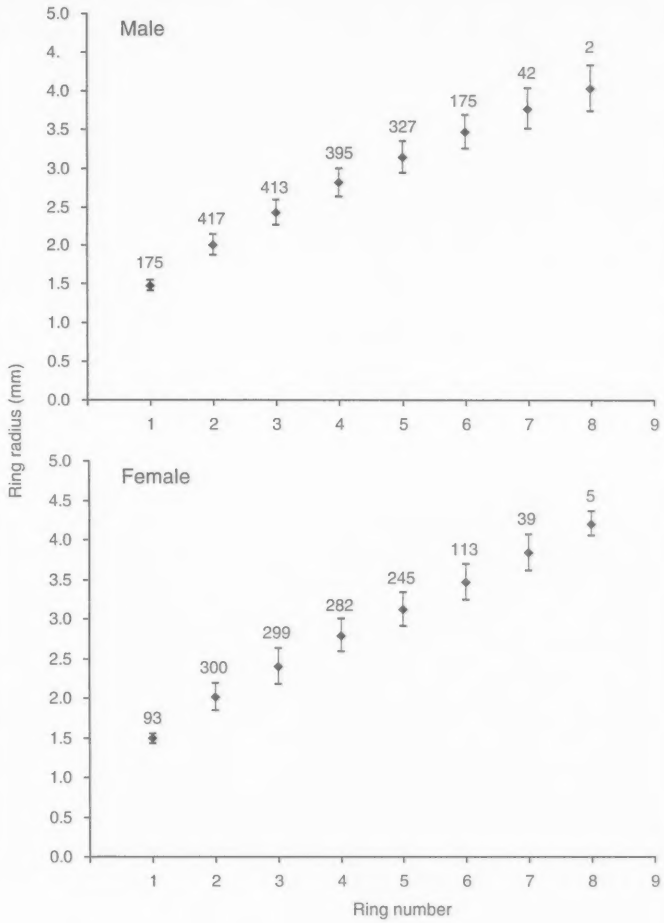

Figure 4

Mean (±1 SD) ring radius for male and female sailfish (*I. platypterus*) collected from the waters off eastern Taiwan that had at least the first or second ring present. The numbers above the vertical bars are the sample sizes.

may also be related to sailfish migration and environmental factors, as suggested by Sun et al. (2002) for swordfish. The MIR analysis provides only a partial age validation; complete validation requires either mark-recapture data or the study of known-age fish (Beamish and McFarlane, 1983; Prince et al., 1995; Tserpes and Tsimenides, 1995; Sun et al., 2001, 2002).

Selection of a growth curve

Female sailfish are typically larger for similar ages in males and grow faster than males, and the length-weight relationship differs significantly between the sexes. Similar results have been reported for east Pacific Ocean sailfish (Hernández-Herrera and Ramírez-Rodríguez, 1998), Indian Ocean sailfish (Williams, 1970) and Atlantic Ocean sailfish (Beardsley et al., 1975; Jolley, 1974, 1977; Hedgepeth and Jolley, 1983).

The Richards function appears to fit the data better than the standard VB curve (Fig. 8) and provides a more realistic description of growth for animals of age 0. The standard VB curve is commonly used to describe asymptotic growth in fish but did not fit the back-calculated lengths for fish younger than three (Table 4, Fig. 8).

Further discussion of growth curves will likely focus on method 2 (i.e., a power function relationship between spine radius and LJFL) because it provides a better fit to the data than method 1. Ehrhardt (1992), Ehrhardt et al.

Table 2

Mean radius of each ring for male and female sailfish in the waters off eastern Taiwan. Roman numerals indicate the number of rings. Numbers in parentheses are the number of specimens for which the specified ring was readable. "—"means no data owing to vascularization at core area.

Age class	Sample size	Mean radius (mm) of each ring											
		I	II	III	IV	V	VI	VII	VIII	IX	X	XI	XII
Male													
1	1	1.54 (1)											
2	4	1.53 (4)	2.08 (4)										
3	18	1.45 (12)	2.02 (18)	2.51 (18)									
4	68	1.49 (45)	2.02 (68)	2.48 (68)	2.91 (68)								
5	171	1.48 (62)	2.00 (152)	2.40 (171)	2.79 (171)	3.14 (171)							
6	198	1.46 (41)	2.02 (133)	2.44 (188)	2.83 (198)	3.17 (198)	3.49 (198)						
7	130	1.42 (10)	1.96 (38)	2.42 (94)	2.80 (123)	3.18 (128)	3.50 (130)	3.82 (130)					
8	74	1.44 (1)	1.96 (4)	2.44 (36)	2.79 (62)	3.14 (72)	3.48 (74)	3.81 (74)	4.09 (74)				
9	22	—	—	—	2.69(11)	3.02 (16)	3.37 (22)	3.70 (22)	4.02 (22)	4.29 (22)			
10	9	—	—	—	—	—	3.09 (5)	3.55 (8)	3.39 (8)	4.23 (9)	4.48 (9)		
11	3	—	—	—	—	—	2.90 (2)	3.28 (2)	3.74 (3)	4.04 (3)	4.33 (3)	4.50 (3)	
Mean		1.47	2.00	2.43	2.81	3.16	3.48	3.79	4.05	4.25	4.45	4.50	
SD		0.07	0.14	0.16	0.18	0.20	0.22	0.23	0.23	0.21	0.15	0.15	
Growth increase			0.53	0.43	0.38	0.34	0.32	0.31	0.26	0.20	0.20	0.05	
Female													
1	1	1.51 (1)											
2	1	1.58 (1)	2.23 (1)										
3	17	1.44 (15)	2.00 (17)	2.47 (17)									
4	38	1.48 (17)	2.00 (37)	2.39 (38)	2.80 (38)								
5	146	1.49 (46)	1.98 (132)	2.39 (146)	2.80 (146)	3.12 (146)							
6	107	1.52 (11)	2.05 (74)	2.45 (102)	2.84 (107)	3.17 (107)	3.48 (107)						
7	64	1.52 (2)	2.08 (34)	2.55 (59)	2.95 (64)	3.29 (64)	3.60 (64)	3.89 (64)					
8	35	1.53 (1)	2.02 (4)	2.40 (10)	2.76 (29)	3.17 (33)	3.53 (34)	3.86 (35)	4.16 (35)				
9	17	—	1.91 (1)	2.36 (4)	2.79 (10)	3.07 (16)	3.40 (17)	3.76 (17)	4.07 (17)	4.38 (17)			
10	7	—	—	—	—	2.81 (4)	3.10 (7)	3.46 (7)	3.84 (7)	4.23 (7)	4.55 (7)		
11	1	—	—	—	—	—	3.31 (1)	3.82 (1)	4.25 (1)	4.44 (1)	4.74 (1)	4.95 (1)	
12	1	—	—	—	—	—	—	3.88 (1)	4.12 (1)	4.49 (1)	4.81 (1)	5.14 (1)	5.32 (1)
Mean		1.49	2.01	2.44	2.83	3.16	3.50	3.84	4.10	4.35	4.60	5.04	5.32
SD		0.06	0.17	0.25	0.23	0.24	0.27	0.27	0.29	0.32	0.41	0.13	
Growth increase			0.52	0.43	0.39	0.33	0.34	0.34	0.26	0.25	0.25	0.44	0.28

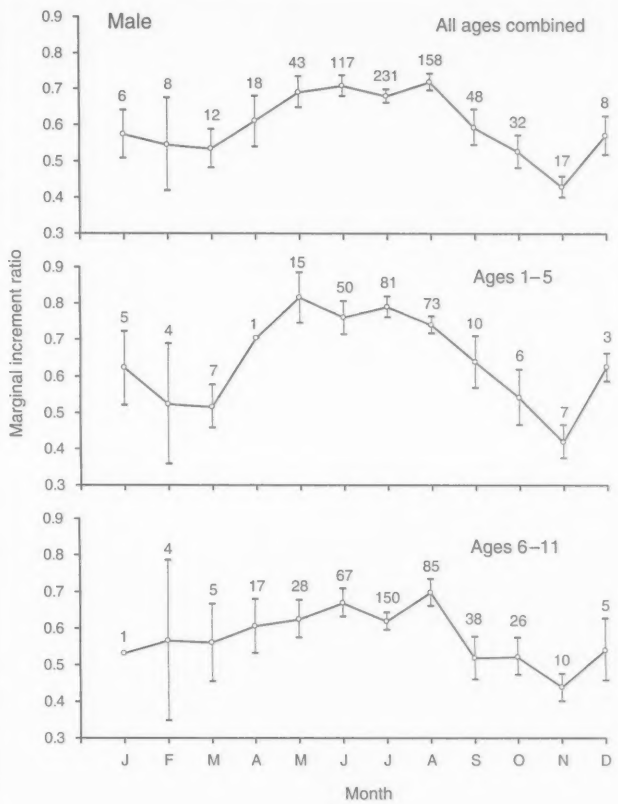

Figure 5

Monthly means of marginal increment ratio for male sailfish (*I. platypterus*) in the waters off eastern Taiwan for all ages combined and for age classes 1–5 and 6–11, respectively. Vertical bars are ±1 SE; numbers above the vertical bars are sample sizes.

Table 3

Mean back-calculated lower jaw fork lengths at age for sailfish in the waters off eastern Taiwan.

	Back-calculated length (cm)								
	Method 1		Method 2			Method 1		Method 2	
Age (yr)	Male	Female	Male	Female	Age (yr)	Male	Female	Male	Female
1	108.53	113.41	99.90	103.51	7	181.11	185.36	181.86	186.09
2	125.70	130.79	121.79	126.32	8	188.99	192.82	189.84	193.67
3	138.82	143.90	137.27	141.96	9	194.98	200.60	196.59	201.47
4	150.80	156.02	150.56	155.54	10	200.78	207.85	201.74	208.81
5	161.78	166.22	162.12	166.38	11	208.05	213.29	209.14	214.66
6	171.63	176.60	172.18	177.12	12		217.15		219.05

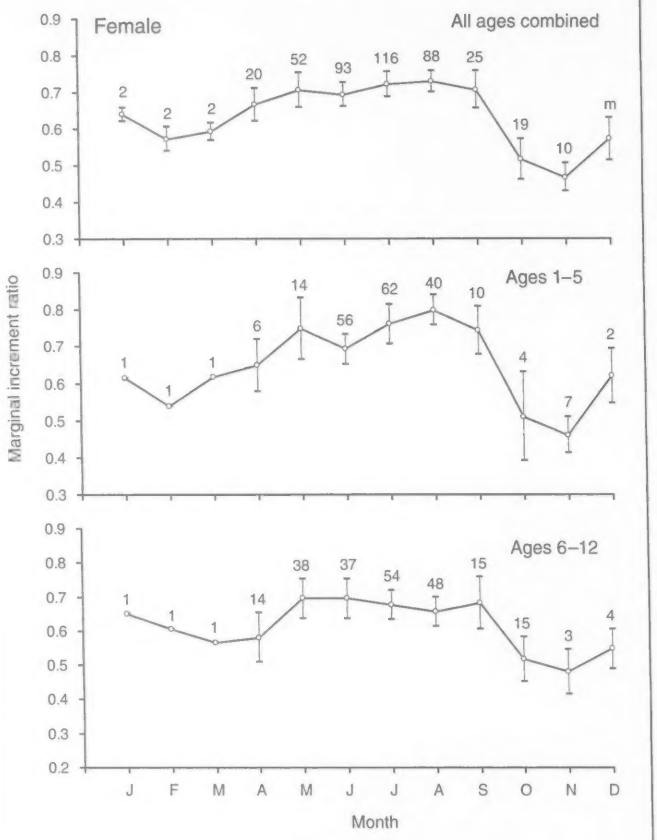

Figure 6

Monthly means of marginal increment ratio for the female sailfish (*I. platypterus*) in the waters off eastern Taiwan for all ages combined and for age classes 1–5 and 6–12, respectively. Vertical bars are ±1 SE; numbers above the vertical bars are sample sizes.

(1996), and Sun et al. (2002) favored method 2 because they believed it to be more biologically realistic. When the back-calculated lengths-at-age are generated with this method the Richards function provides a statistically superior fit to the length-at-age data. Therefore, the parameter estimates for the Richards function with method 2 listed in Table 4 are recommended as the most appropriate for calculating the age composition of sailfish in the waters to the east of Taiwan. It is perhaps worth noting that the t_0 values estimated for the Richards function with method 2 are much closer to zero than those estimated for the Richards function with method 1.

Comparison with previous studies

Figure 9 compares the age-length relationships of this paper with those for Atlantic (de Sylva, 1957; Hedgepeth and Jolley, 1983; Farber[1]) and Pacific sailfish (Koto and Kodama, 1962; Alvarado-Castillo and Félix-Uraga, 1998). De Sylva (1957) and Koto and Kodama (1962) used length-frequency analysis and concluded that sailfish are a very fast growing and short-lived species. However, they likely underestimated age and overestimated growth rate when their results are compared with those of other more recent studies.

The maximum ages found in this study (11 years for males and 12 years for females) are close to the maximum longevity of at least 13 years proposed by Prince et al. (1986) based on tagging data. Farber[1] analyzed Atlantic billfish tagging data and suggested that the asymptotic size was essentially reached by age 3 (Hedgepeth and Jolley, 1983), whereas the present study found a more gradual increase in length with age, in common with the results of Hedgepeth and Jolley (1983).

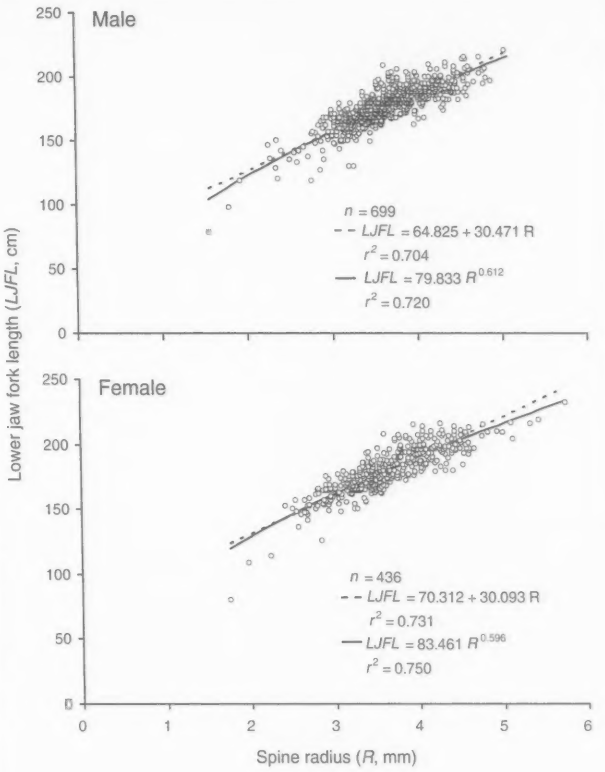

Figure 7

Relationship between lower jaw fork length and spine radius for male and female sailfish (*I. platypterus*) in the waters off eastern Taiwan.

Table 4

Parameter estimates and standard errors (in parenthesis) for the standard von Bertalanffy growth function and the Richards function for sailfish in the waters off eastern Taiwan.

	Standard von Bertalanffy growth function				Richards function			
	Method 1		Method 2		Method 1		Method 2	
Parameter	Male	Female	Male	Female	Male	Female	Male	Female
L_∞	252.6	261.4	240.4	250.3	271.8	280.4	294.0	343.8
	(3.652)	(3.397)	(3.794)	(4.278)	(22.713)	(19.882)	(29.607)	(47.921)
k	0.115	0.110	0.145	0.138				
	(0.005)	(0.004)	(0.008)	(0.008)				
t_0	−3.916	−4.207	−2.781	−2.990	−2.473	−2.608	−0.704	−0.468
	(0.143)	(0.147)	(0.154)	(0.186)	(0.931)	(0.896)	(0.279)	(0.186)
K					0.051	0.049	0.023	0.011
					(0.034)	(0.030)	(0.013)	(0.007)
m					−0.551	−0.578	−1.288	−1.639
					(0.472)	(0.436)	(0.308)	(0.243)

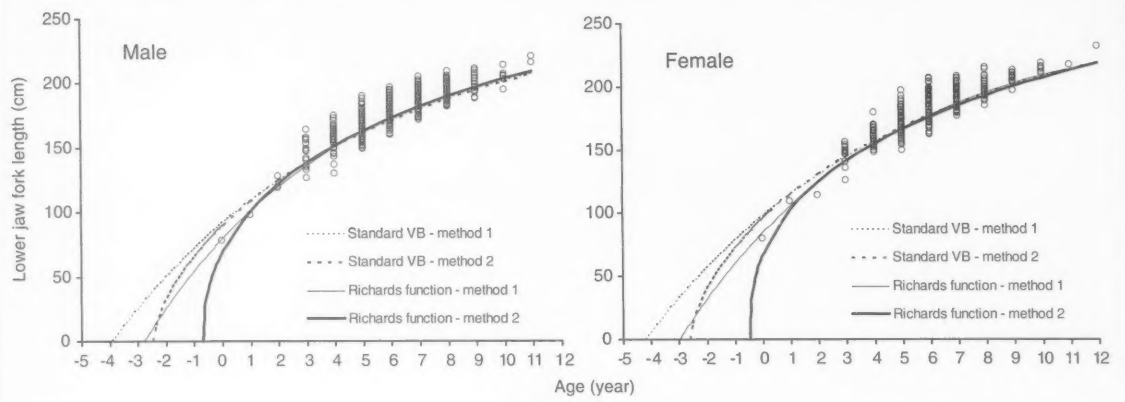

Figure 8

Observed and back-calculated length-at-age and standard von Bertalanffy and Richards function model-predicted growth curves for male and female sailfish (*I. platypterus*) in the waters off eastern Taiwan.

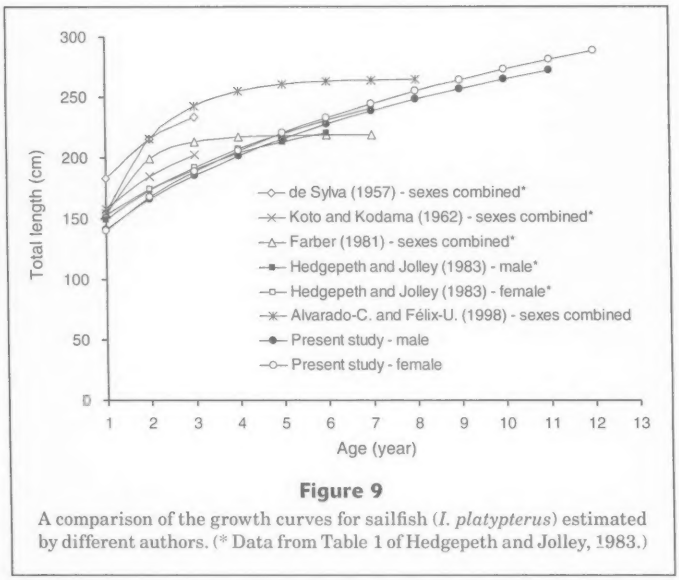
Total length (cm)
Age (year)
de Sylva (1957) - sexes combined*
Koto and Kodama (1962) - sexes combined*
Farber (1981) - sexes combined*
Hedgepeth and Jolley (1983) - male*
Hedgepeth and Jolley (1983) - female*
Alvarado-C. and Félix-U. (1998) - sexes combined
Present study - male
Present study - female

Figure 9

A comparison of the growth curves for sailfish (*I. platypterus*) estimated by different authors. (* Data from Table 1 of Hedgepeth and Jolley, 1983.)

Even though the aging method used in the present study is the same as that of Hedgepeth and Jolley (1983) and Alvarado-Castillo and Félix-Uraga (1998), there are nevertheless differences in the estimated length-at-age. This difference could be due to spatial differences in growth, the range of ages and sizes used in the analysis, or the form of the growth model applied. The size range in the present study is broader than those in previous studies and the growth curve is based on the Richards function rather than the standard VB function. Therefore, we believe that our growth parameter estimates are more appropriate for use in stock assessments of the sailfish population in the western Pacific Ocean.

Acknowledgments

The authors express sincere gratitude to André Punt, School of Aquatic and Fishery Sciences, University of Washington, for his valuable comments and comprehensive editing of the manuscript. This study was in part supported financially by the "Fisheries Agency, Council of Agriculture, Taiwan," through grant 91AS-2.5.1-F1(7) to Chi-Lu Sun.

Literature cited

Akaike, H.
1969. Fitting autoregressive models for prediction. Ann. Inst. Stat. Math. 21:243–247.

Alvarado-Castillo, R. M., and R. Félix-Uraga.
1996. Age determination in *Istiophorus platypterus* (Pisces: Istiophoridae) in the south of the Gulf of California, Mexico. Rev. Biol. Trop. 44:233–239.
1998. Growth of *Istiophorus platypterus* (Pisces: Istiophoridae) from the south of the Gulf of California. Rev. Biol. Trop. 46:115–118.

Antoine, L. M., J. J. Mendoza, and P. M. Cayré.
1983. Progress of age and growth assessment of Atlantic skipjack tuna, *Euthynnus pelamis*, from dorsal fin spines. NOAA Tech. Rep. NMFS 8:91–97.

Beamish, R. J., and D. A. Fournier.
1981. A method for comparing the precision of a set of age determinations. Can. J. Fish. Aquat. Sci. 38:982–983.

Beamish, R. J., and G. A. McFarlane.
1983. Validation of age determination estimates, the forgotten requirement. NOAA Tech. Rep. NMFS 8:29–33.
Beardsley, G. L., N. R. Merrett, and W. J. Richards.
1975. Synopsis of the biology of sailfish, *Istiophorus platypterus* (Shaw and Nodder, 1791). NOAA Tech. Rep. NMFS SSRF 675:95–120.
Berkeley, S. A., and E. D. Houde.
1983. Age determination of broadbill swordfish, *Xiphias gladius*, from the Straits of Florida, using anal fin spine sections. NOAA Tech. Rep. NMFS 8:137–146.
Campana, S. E.
2001. Accuracy, precision and quality control in age determination, including a review of the use and abuse of age validation methods. J. Fish. Biol. 59:197–242.
Cayré, P. M., and T. Diouf.
1983. Estimated age and growth of little tunny, *Euthynnus alletteratus*, off the coast of Senegal, using dorsal find spine sections. NOAA Tech. Rep. NMFS 8:105–110.
Chen, Y., D. A. Jackson, and H. H. Harvey.
1992. A comparison of von Bertalanffy and polynomial functions in modelling fish growth data. Can. J. Fish. Aquat. Sci. 49:1228–1235.
Compeán-Jimenez, G., and F. X. Bard.
1983. Growth of increments on dorsal spines of eastern Atlantic bluefin tuna, *Thunnus thynnus*, and their possible relation to migratory patterns. NOAA Tech. Rep. NMFS 8:77–86.
de Sylva, D. P.
1957. Studies on the age and growth of the Atlantic sailfish, *Istiophorus americanus* (Cuvier), using length-frequency curves. Bull. Mar. Sci. Gulf Caribb. 7:1–20.
Ehrhardt, N. M.
1992. Age and growth of swordfish, *Xiphias gladius*, in the northwestern Atlantic. Bull. Mar. Sci. 50:292–301.
Ehrhardt, N. M., R. J. Robbins, and F. Arocha.
1996. Age validation and estimation of growth of swordfish, *Xiphias gladius*, in the northwest Atlantic. ICCAT (International Commission for the Conservation of Tunas) Col. Vol. Sci. Pap. 45(2):358–367.
Hayashi, Y.
1976. Studies on the red tilefish in the east China sea—I. A fundamental consideration for age determination from otoliths. Bull. Jap. Soc. Sci. Fish. 42:1237–1242.
Hedgepeth, M. Y., and J. W. Jolley Jr.
1983. Age and growth of sailfish, *Istiophorus platypterus*, using cross section from the fourth dorsal spine. NOAA Tech. Rep. NMFS 8:131–135.
Hernández-Herrera, A., and M. Ramírez-Rodríguez.
1998. Spawning seasonality and length at maturity of sailfish (*Istiophorus platypterus*) off the Pacific coast of Mexico. Bull. Mar. Sci. 63:459–467.
Hill, K. T., G. M. Cailliet, and R. L. Radtke.
1989. A comparative analysis of growth zones in four calcified structures of Pacific blue marlin, *Makaira nigricans*. Fish. Bull. 87:829–843.
Jolley, J. W., Jr.
1974. On the biology of Florida east coast Atlantic sailfish, (*Istiophorus platypterus*). NOAA Tech. Rep. NMFS SSRF 675:81–88.
1977. The biology and fishery of Atlantic sailfish, *Istiophorus platypterus*, from southeast Florida. Fla. Mar. Res. Publ. 28, 31 p.
Koto, T., and K. Kodama.
1962. Some considerations on the growth of marlins, using size-frequencies in commercial catches. I. Attempts to estimate the growth of sailfish. Rep. Nankai. Reg. Fish. Res. Lab. 15:97–108.
Megalofonou, P.
2000. Age and growth of Mediterranean albacore. J. Fish. Biol. 57:700–715.
Nakamura, I.
1985. FAO species catalogue. Billfish of the world. An annotated and illustrated catalogue of marlins, sailfishes, spearfishes, and swordfishes known to date. FAO Fish. Synop. 125(5), 65 p
Paul, L. J.
1992. Age and growth studies of New Zealand marine fisheries, 1921–90: a review and bibliography. Aust. J. Mar. Freshw. Res. 43:879–912.
Powers, J. E.
1983. Some statistical characteristics of ageing data and their ramification in population analysis of oceanic pelagic fishes. NOAA Tech. Rep. NMFS 8:19–24.
Prince, E. D., D. W. Lee, C. A. Wilson, and S. A. Berkeley.
1988. Use of marginal increment analysis to validate the anal spine method for ageing Atlantic swordfish and other alternatives for age determination. ICCAT Col. Vol. Sci. Pap. 27:194–201.
Prince, E. D., D. W. Lee, C. A. Wilson, and J. M. Dean.
1986. Longevity and age validation of a tag-recaptured Atlantic sailfish, *Istiophorus platypterus*, using dorsal spines and otoliths. Fish. Bull. 84:493–502.
Prince, E. D., D. W. Lee, C. J. Cort, G. A. McFarlane, and A. Wild.
1995. Age validation evidence for two tag-recaptured Atlantic albacore, *Thunnus alalunga*, based on dorsal, anal, and pectoral finrays, vertebrae, and otoliths. *In* Recent developments in fish otolith research (D. H. Sector, J. M. Dean, and S. E. Campana, eds.), p. 375–396. Univ. South Carolina Press, Columbia, SC.
Radtke, R. L.
1983. Istiophorid otoliths: extraction, morphology, and possible use as ageing structures. NOAA Tech. Rep. NMFS 8:123–129.
Radtke, R. L., and J. M. Dean.
1981. Morphological features of the otoliths of the sailfish, *Istiophorus platypterus*, useful in age determination. Fish. Bull. 79:360–367.
Richards, F. J.
1959. A flexible growth function for empirical use. J. Exp. Bot. 10:290–300.
Sun, C. L., C. L. Huang, and S. Z. Yeh.
2001. Age and growth of the bigeye tuna, *Thunnus obesus*, in the western Pacific Ocean. Fish. Bull. 99:502–509.
Sun, C. L., S. P. Wang, and S. Z. Yeh.
2002. Age and growth of swordfish (*Xiphias gladius* L.,) in the waters around Taiwan determined from anal-fin rays. Fish. Bull. 100:822–835.
Tserpes, G., and N. Tsimenides.
1995. Determination of age and growth of swordfish, *Xiphias gladius* L., 1758, in the eastern Mediterranean using anal-fin spines. Fish. Bull. 93:549–602.
von Bertalanffy, L.
1938. A quantitative theory of organic growth (Inquiries on growth laws. II). Hum. Biol. 10:181–213.
Williams, F.
1970. The sport fishery for sailfish at Malindi, Kenya, 1958–1968, with some biological notes. Bull. Mar. Sci. 20(4):830–852.

A habitat-use model to determine essential fish habitat for juvenile brown shrimp (*Farfantepenaeus aztecus*) in Galveston Bay, Texas

Randall D. Clark
John D. Christensen
Mark E. Monaco
Biogeography Program
Center for Coastal Monitoring and Assessment
National Center for Coastal Ocean Science
National Ocean Service, NOAA
Silver Spring, Maryland 20910
E-mail address (For R. D. Clark): Randy.Clark@noaa.gov

Philip A. Caldwell
Geoffrey A. Matthews
Thomas J. Minello
Fishery Ecology Branch
Galveston Southeast Fisheries Science Center Laboratory
National Marine Fisheries Service, NOAA
Galveston, Texas 77550

Abstract—A density prediction model for juvenile brown shrimp (*Farfantepenaeus aztecus*) was developed by using three bottom types, five salinity zones, and four seasons to quantify patterns of habitat use in Galveston Bay, Texas. Sixteen years of quantitative density data were used. Bottom types were vegetated marsh edge, submerged aquatic vegetation, and shallow nonvegetated bottom. Multiple regression was used to develop density estimates, and the resultant formula was then coupled with a geographical information system (GIS) to provide a spatial mosaic (map) of predicted habitat use. Results indicated that juvenile brown shrimp (<100 mm) selected vegetated habitats in salinities of 15–25 ppt and that seagrasses were selected over marsh edge where they co-occurred. Our results provide a spatially resolved estimate of high-density areas that will help designate essential fish habitat (EFH) in Galveston Bay. In addition, using this modeling technique, we were able to provide an estimate of the overall population of juvenile brown shrimp (<100 mm) in shallow water habitats within the bay of approximately 1.3 billion. Furthermore, the geographic range of the model was assessed by plotting observed (actual) versus expected (model) brown shrimp densities in three other Texas bays. Similar habitat-use patterns were observed in all three bays—each having a coefficient of determination >0.50. These results indicate that this model may have a broader geographic application and is a plausible approach in refining current EFH designations for all Gulf of Mexico estuaries with similar geomorphological and hydrological characteristics.

Manuscript approved for publication 22 December 2003 by Scientific Editor.
Manuscript received 20 January 2004 at NMFS Scientific Publications Office.
Fish. Bull. 102:264–277 (2004).

Shallow estuarine habitats, whose complexity promotes survival and growth, are used by many young fish and macroinvertebrate species (Boesch and Turner, 1984). A complete understanding of how these habitats sustain species productivity is unknown and has become a focal point of federal fishery management programs. The National Marine Fisheries Service (NMFS) has developed guidelines to identify essential fish habitat (EFH) for all federally managed species based on four levels of available information that encompass the ecological linkages between habitats and fishery production. Examination of habitat-use patterns (habitat-related densities) are needed to determine which habitats are likely to be most essential. These patterns are measurable and can be reasonable indicators of habitat value. Relative habitat values have been estimated by comparing animal densities under the assumption that high densities reflect greater habitat quality and preferred habitat (Pearcy and Myers, 1974; USFWS, 1981; Zimmerman and Minello, 1984; Sogard and Able, 1991; Baltz et al., 1993).

Considerable bottom-type variation exists in northern Gulf of Mexico estuaries, including intertidal marsh, submerged aquatic vegetation, oyster reef, mangroves, tidal mudflats, and subtidal bay bottom. Within each of these habitats, environmental and structural gradients may affect the functional role or importance of these habitats for particular species. To understand these relationships, fisheries independent monitoring (FIM) data are needed to determine species-habitat affinities that provide evidence that not all habitats are of equal importance for the maintenance of a population (Monaco et al., 1998; Minello 1999; Beck et al., 2001). Habitat affinities may change with spatial and temporal fluctuations of environmental variables, such as salinity and temperature (Copeland and Bechtel, 1974; Baltz et al., 1998).

In this study we developed predictive models that estimate brown shrimp (*Farfantepenaeus aztecus*, formerly *Penaeus aztecus* [see Perez-Farfante and Kensley, 1997]) habitat-use patterns and interactions as a function of density-independent processes in Galveston Bay, Texas. Previous com-

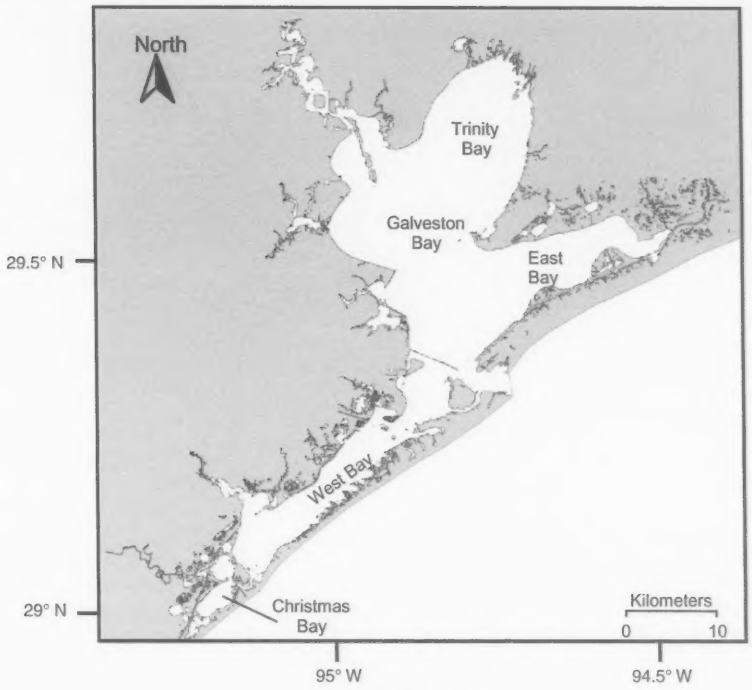

Figure 1
Map of Galveston Bay, Texas.

parisons of brown shrimp densities among different bottom types in Louisiana and Texas estuaries have been conducted within limited temporal and spatial scales (Peterson and Turner, 1994; Zimmerman et al., 1984; Zimmerman et al., 1990b; Rozas and Minello, 1998; Minello, 1999).

Our work expands upon these studies by developing a multivariate bottom-type use and environmental model incorporated into a geographic information system (GIS) that provides a spatial assessment of habitat use. In addition, the model is designed to be transferable to other northern Gulf of Mexico estuaries and thus would allow fishery managers to identify the relative importance of habitat types for population maintenance and recruitment into the fishery.

Materials and methods

Geographic setting

The Galveston Bay complex (Fig. 1) encompasses approximately 2020 km^2 and is one of the largest estuaries in the northern Gulf of Mexico (NOAA, 1989). Comprising several major embayments, including Trinity, Galveston, East, and West bays, the complex contains many smaller interconnecting subbays, rivers, streams, tidal creeks, wetlands, reefs, and tidal flats around its periphery. The bay bottom is mostly flat and shallow (mean depth is approximately 2 m) and has slightly elevated oyster reefs, elevated dredge material areas, river channels, and deeper dredged navigation channels.

Data collection

Sixteen years (1982–97) of brown shrimp density data were analyzed to quantify areas of potential EFH. A total of 46,080 brown shrimp were captured during this time period with a mean total length of 27.5 mm (Fig. 2). Data from published studies by Czapla (1991), Minello et al. (1991), Minello and Zimmerman (1992), Minello and Webb (1997), Rozas and Minello (1998), Zimmerman et al. (1984, 1989, 1990a, 1990b), Zimmerman and Minello (1984), and various unpublished sources from the Galveston Laboratory of the National Marine Fisheries Service were combined to comprise a comprehensive density database of associated bottom-type and environmental data that would support model development and GIS analyses. All samples were collected by using a drop trap sampler, described in Zimmerman et al. (1984), which employs large cylinders (1.0 or 2.6 m^2 area) released from a boom affixed to a boat to entrap organisms. This quantitative technique samples fishes and macro-invertebrates in highly structured shallow-water habitats such as salt marshes, seagrass beds, and oyster reefs where the efficiency of conventional trawl and bag-seine gear is diminished.

Habitat mapping

The underlying spatial framework for incorporating model predictions into the GIS consisted of six maps: four salinity periods, one bathymetric map, and one map defining bottom-type distribution. All GIS maps were developed in Universal Transverse Mercator projection, UTM, datum-1983, zone-15, using ArcView 3.1 (Redlands, CA) software. Each map consisted of 10 × 10 m grid cells where each cell contained pertinent salinity, depth, or bottom-type information.

Salinity maps were developed from depth-averaged salinity models by using historical Galveston Bay data collected during 1979–90 (Orlando et al., 1993). Four salinity periods were identified to represent typical salinity conditions under average seasonal freshwater inflow: low (March–June), increasing (July), high (August–October), and decreasing (November–February). Five isohalines were developed to display spatial salinity distribution (Christensen et al.[1]): 0–0.5, 0.51–5, 5.1–15, 15.1–25, and >25 parts per thousand (ppt) (Fig. 3).

Bottom types from the drop sample database were divided into three categories:

Marsh edge (ME)	intertidal marsh within 5 meters of open water habitat. This category consisted primarily of saltmarsh cord grass (*Spartina alterniflora*), and smaller proportions of salt meadow-grass (*Spartina patens*), black needle-rush (*Juncus roemerianus*), salt grass (*Distichlis spicata*), bullrushes (*Scirpus* spp.), and cattails (*Typha* spp.);
Submerged aquatic vegetation (SAV)	consisted primarily of shoalgrass (*Halodule wrightii*), wigeongrass (*Ruppia maritima*), and a sporadic distribution of wild celery (*Vallisneria americana*);
Shallow non-vegetated bottom (SNB)	generally restricted to waters less than 1 meter deep, including creeks, ponds, shoreline, and open bay habitat.

Density data for other bottom types were limited and were not used in the analysis.

Wetland maps, used in the creation of the bottom type map in the GIS, were obtained from the U.S. Fish and Wildlife Service's national wetland inventory (NWI). The NWI maps were obtained as vector files, created by digitizing boundaries between wetland types from 1989 aerial photographs and classified by using the classification scheme of Cowardin et al. (1979). Regularly flooded emergent vegetation and submerged aquatic vegetation distributions from the NWI maps of Galveston Bay were chosen to represent ME and SAV, respectively, from the drop sample database. Nonvegetated open water areas with depths greater than 1 m were eliminated throughout the bay to reflect depth range from the drop sample database. This elimination was done by plotting approximately 400,000 depth soundings obtained from the National Geophysical Data Center (NGDC), and a bathymetric grid map was developed in 1-m contours with ArcView 3.1 (6 nearest neighbors, power=2). The nonvegetated open water map from NWI was overlaid with the bathymetric map and only those areas within the 1-m contour were extracted and added to the bottom-type map (Fig. 4).

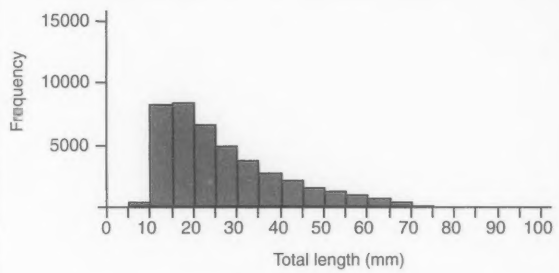

Figure 2

Total-length frequency distribution for juvenile brown shrimp captured in drop traps within Galveston Bay (1982–97).

Two maps were used to plot (map) seasonal model predictions, bottom type, and the respective salinity period. The salinity maps did not completely correspond temporally with seasons defined by cluster analysis of *in situ* temperature recordings from the density database. Salinity periods were chosen to correlate with temporal seasons based on maximum monthly overlap to develop the seasonal prediction maps: low salinity (spring); increasing salinity (summer); high salinity (fall); and decreasing salinity (winter).

The total area of Galveston Bay (2020 km^2) was determined by combining the total areas for regularly flooded emergent vegetation, irregularly flooded emergent vegetation, SAV, and open water classifications from NWI data. The bottom-type map reflects the study area and totaled 565.6 km^2 after excluding all areas >1 m in depth and with irregularly flooded emergent vegetation: SNB = 476.2 km^2, ME = 84.9 km^2, and SAV = 4.5 km^2. Initially, NWI's SAV classification totaled 5.7 km^2, but the final SAV coverage was reduced to 4.5 km^2 based on SAV mapping by White et al. (1993).

Regression modeling

ANOVA and Tukey-Kramer multiple means comparisons were used to determine if mean density varied significantly by bottom type, salinity zone, and season. Multiple regression with significant predictors was used to predict mean log density. The model was then applied to the GIS maps

[1] Christensen, J. D., T. A. Battista, M. E. Monaco, and C. J. Klein. 1997. Habitat suitability modeling and GIS technology to support habitat management: Pensacola Bay, Florida Case Study, 58 p. NOAA/NOS Strategic Environmental Assessments Division, Silver Spring, MD.

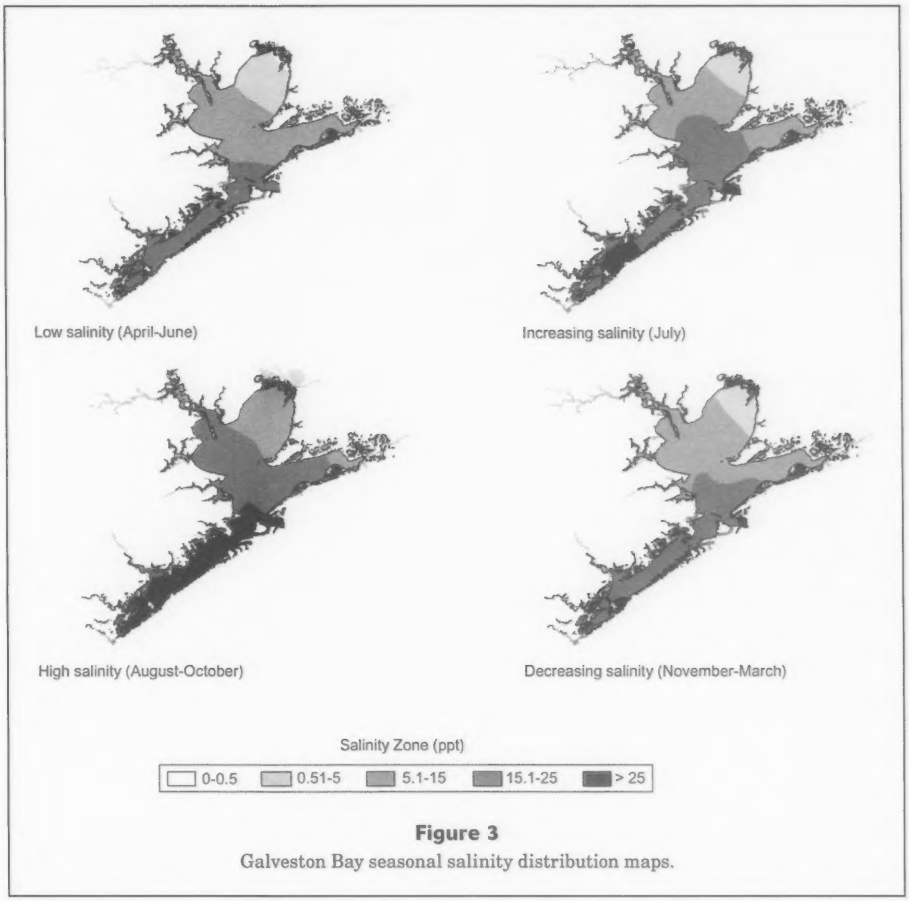

Figure 3
Galveston Bay seasonal salinity distribution maps.

to spatially display model predictions in each 10 × 10 m cell. The resulting values for each cell (predicted mean log density) were converted to numbers/m^2 and reclassified into 5 percentiles based on their resultant distribution: 0–20%, 21–40%, 41–60%, 61–80%, and 81–100%. All statistical analyses were conducted with JMP statistical software (SAS Institute, Cary, NC).

Due to difficulties in creating continuous salinity and temperature contour maps in GIS, these variables were classified as follows: salinity was classified by one of the five isohaline zones described previously and analyzed as such to determine its influence on brown shrimp distribution; and water temperature was classified by season determined by cluster analysis and analyzed to examine possible temporal effects of brown shrimp distribution.

Spatial patterns were evaluated by comparing the predicted mean log density values with the observed mean log density values from Galveston Bay drop samples. Additionally, the model's predictive performance was assessed by comparing the predicted mean log density values with observed mean log density values from samples collected in Matagorda, Aransas, and San Antonio bays using the same collection method. With this approach, the assumption was made that brown shrimp modeled in Galveston Bay respond similarly to the range of biotic and abiotic factors in the other bay systems.

Drop sample data collected during July–September 1984 (n=128), and April–June 1985 (n=144) from West Bay (ME, SNB) and Christmas Bay (ME, SAV, and SNB) were used to examine bottom-type preference or selectivity. Tukey-Kramer multiple comparisons test was used to compare log density patterns in areas where ME and SAV occurred together and in areas where SAV was not present.

Results

Brown shrimp model

ANOVA and Tukey-Kramer pair-wise comparisons showed significant differences in brown shrimp log density between the three bottom types, five salinity zones, and four seasons (Fig. 5). Multiple regression models were run with these discreet variables (Mahon and Smith, 1989;

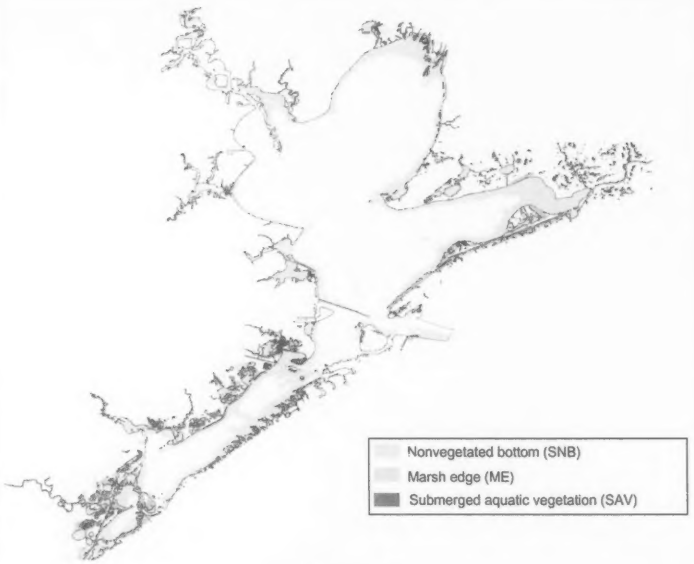

Figure 4

Spatial distribution of Galveston Bay bottom types used in the multivariate regression model.

Table 1

Results of the least squares multiple regression model for predicting seasonal brown shrimp density in Galveston Bay, Texas. * = significant at $P < 0.05$.

Model fit	r^2	Mean	Observations (n)	Mean square error	
	0.73	0.47	47	0.20	
			ANOVA		
Source	df	Sum of squares	Mean square	F ratio	Prob > F
Model	17	5.74	0.33	8.43	
Error	29	1.61	0.04		
Total	46	6.90			<0.0001*
			Effects		
Source	df	Sum of squares		F ratio	Prob > F
Season	3	1.85		15.43	<0.0001*
Bottom type	2	0.61		7.57	0.0023*
Salinity zone	4	3.15		19.68	<0.0001*
Bottom type × Salinity zone	8	0.86		2.69	0.0242*

Krumgalz et al., 1992; Garrison, 1999) and we tested for possible interactions between the variables. Only the interaction between bottom type and salinity zone yielded statistically significant results. ANOVA results for the model including the bottom-type and salinity-zone interaction term (Table 1) and variable coefficients (Table 2) fitted

Table 2

Variable coefficients (log +1) derived from brown shrimp multivariate regression model. ME = marsh edge; SAV = submerged aquatic vegetation; SNB = shallow nonvegetated bottom.

y–intercept	Bottom type	Season	Salinity zone	Bottom type×salinity zone
0.335	0.113 (ME)	0.239 (spring)	−0.525 (0–0.5)	−0.104 (ME/0–0.5)
	0.043 (SAV)	0.165 (summer)	−0.147 (0.5–5)	−0.055 (SAV/0–0.5)
	−0.156 (SNB)	−0.045 (fall)	0.079 (5–15)	0.159 (SNB/0–0.5
		−0.359 (winter)	0.286 (15–25)	0.273 (ME/0.5–5)
			0.307 (>25)	−0.396 (SAV/0.5–5)
				0.123 (SNB/0.5–5)
				−0.030 (ME/5–15)
				0.049 (SAV/5–15)
				−0.018 (SNB/5–15)
				−0.119 (ME/15–25)
				0.288 (SAV/15–25)
				−0.168 (SNB/15–25)
				−0.018 (ME/>25)
				0.114 (SAV/>25)
				−0.096 (SNB/>25)

the data well (r^2=0.73, n=47). Overall, density predictions were highest in the spring, declined through summer and fall, and reached the lowest values during winter (Fig. 6). SNB density predictions were highest in the >25 ppt salinity zone and declined as salinity declined in the estuary. ME density predictions exhibited similar density prediction trends; however, a smaller peak was observed in the 0.5–5 ppt salinity zone. This result may be an artifact of two fall samples that exhibited high density within this salinity zone. Density predictions within SAV were near zero in the lower two salinity zones, peaked in the 15–25 ppt salinity zone, and slightly decreased in the >25 ppt salinity zone.

Model prediction maps

For all seasons, highest density predictions corresponded with ME and SAV bottom types within the region of the bay with highest salinity—Christmas and West bays (Fig. 7). Density predictions decreased within all bottom types as salinity declined in the middle and upper regions of the bay. Spring density predictions were the highest; maximum values were predicted within ME (6.14/m^2) and SAV (14.49/m^2) located in Christmas and West bays (Fig. 7). Density predictions steadily declined through the middle bay and declined to 1/m^2 or less within SAV and SNB in the upper region of the bay (Trinity Bay) where salinities were less than 5 ppt. Density predictions during summer, fall, and winter were lower than those observed during the spring but exhibited similar spatial trends—higher predictions within the high salinity vegetated bottom types, and decreasing with decreasing salinity.

Model performance

Spatial patterns were assessed by plotting predicted mean density values from the model and observed mean density

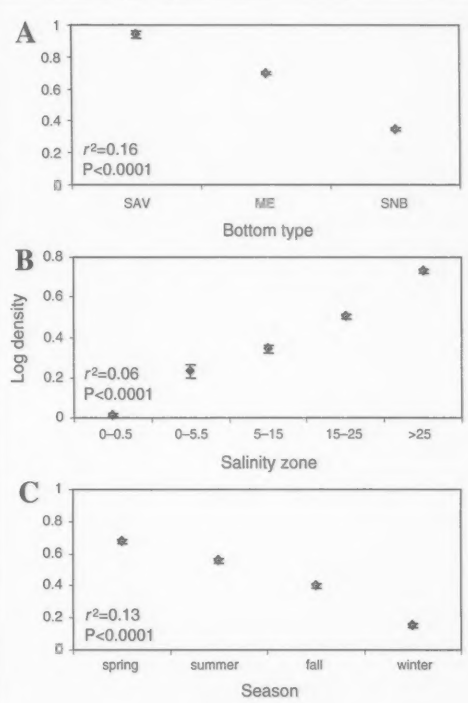

Figure 5

Analysis of variance and Tukey–Kramer pair-wise comparisons of brown shrimp density between (**A**) bottom type, (**B**) salinity zone and, (**C**) season. Mean densities are represented by solid diamonds and lines determine standard error. SAV = submerged aquatic vegetation; ME = marsh edge; SNB = shallow nonvegetated bottom.

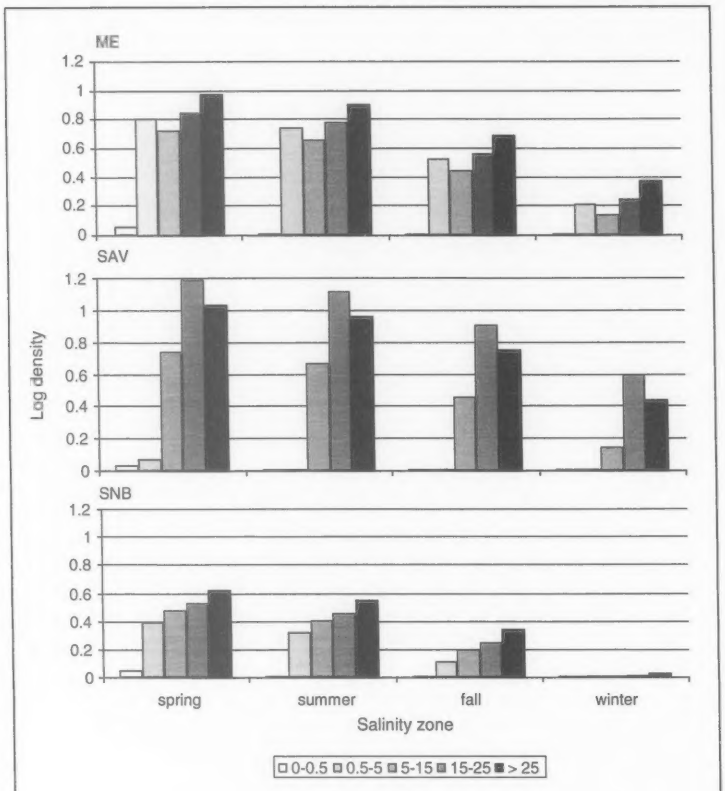

Figure 6

Seasonal density predictions for brown shrimp (*F. aztecus*) by bottom type and salinity zone. ME = marsh edge; SAV = submerged aquatic vegetation; SNB = shallow nonvegetated bottom.

values from drop sample data collected in Galveston Bay. Regression analysis from this plot exhibited a strong positive relationship (r^2=0.83, P<0.0001) between predicted and observed density data (Fig. 8). This analysis was performed to verify how the model represented the observed density data.

Model performance and transferability were assessed by regressing predicted mean density values from the Galveston Bay model on observed mean density values from drop sample data collected in Matagorda, San Antonio, and Aransas bays (Fig. 9). Regression analysis produced a positive relationship for the entire drop sample data from these bays combined (r^2=0.56) and individually: Matagorda—r^2=0.54; San Antonio—r^2=0.57; and Aransas—r^2=0.56. In Aransas and San Antonio bays, brown shrimp densities were greatest during the spring within the SAV bottom type and within salinities >15 ppt. In Matagorda Bay, brown shrimp densities were greatest in the spring within ME bottom types in waters >15 ppt. No SAV samples were taken in this estuarine system.

Use of bottom types

Results from spring (1985) and fall (1984) drop samples within Christmas and West Bay (in lower Galveston Bay) bottom types revealed significantly greater brown shrimp densities in Christmas Bay SAV than adjacent ME and SNB (P<0.0001). Brown shrimp densities in West Bay ME were not significantly different from Christmas Bay SAV but were significantly greater than densities within adjacent SNB and Christmas Bay ME and SNB bottom types (Fig. 10).

The model results were also used to roughly estimate an overall population of approximately 1.3 billion juvenile brown shrimp in Galveston Bay during the spring season, by multiplying predicted densities by bottom-type area (Table 3). Total area of bottom types in Galveston Bay were as follows: 4.5 km^2 (SAV); 84.9 km^2 of marsh edge (ME); and 1627.2 km^2 of nonvegetated bottom (29% [476.2 km^2] of the latter area was considered SNB). On the basis of predicted densities in different salinity regimes, we estimated that there would be 51.0 million shrimp

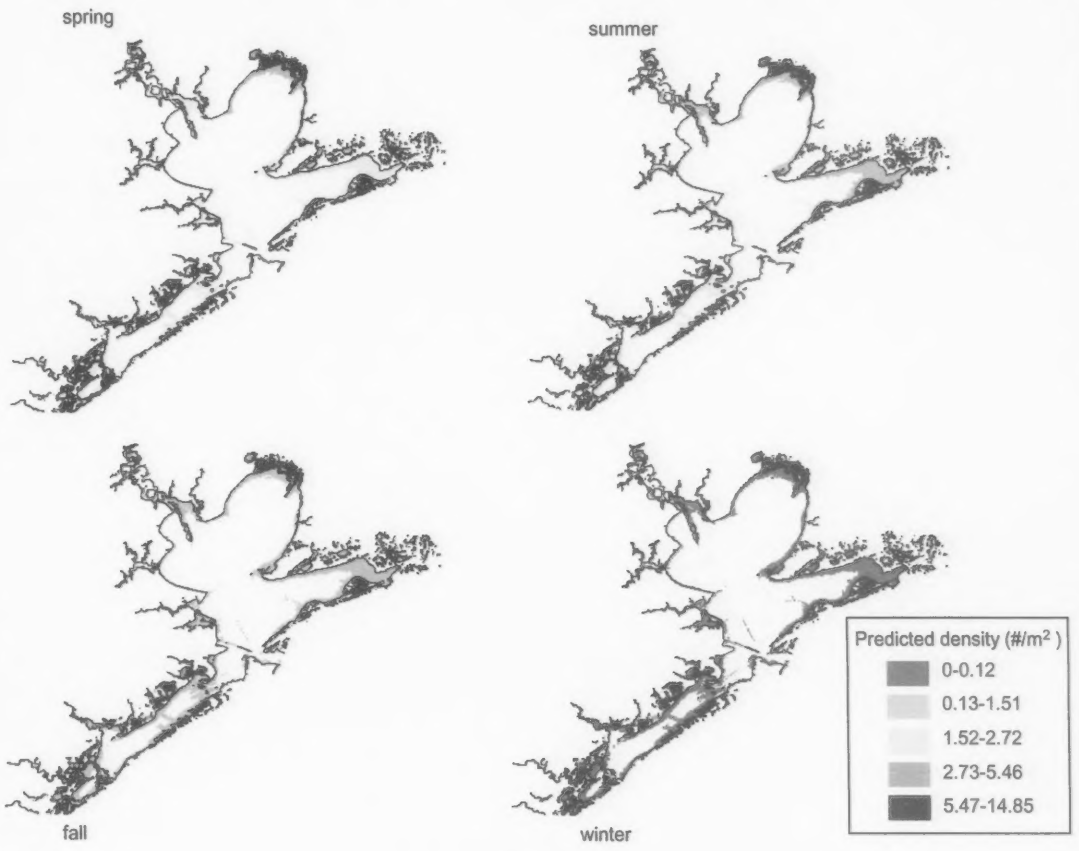

Figure 7
Seasonal spatial distribution maps of predicted densities for brown shrimp (*F. aztecus*).

in SAV and 858.7 million shrimp in SNB. We used marsh edge densities to estimate 473.5 million shrimp in regularly flooded vegetation or about 55,700 shrimp per hectare of this habitat type.

Discussion

Various factors are considered important in defining nursery areas for juvenile estuarine-dependent organisms; however, the specific contributions of these factors are poorly understood (Beck et al., 2001). Specific combinations of physiochemical conditions and cyclic primary production that are related to food availability, growth, and sanctuary from predation often define optimal environments (Miller and Dunn, 1980). Barry et al. (1999) considered prey availability to be a necessary component defining the nursery function of estuarine habitats. Shrimp and blue crab production has been correlated with the availability of wetland habitat in estuaries (Turner, 1977; Zimmerman et al., 2000). In the present study, brown shrimp were most abundant in the lower bay where vegetated habitats were most abundant. Zimmerman et al. (1990b) reported that benthic infauna are most abundant in vegetated habitats within lower Galveston Bay and are nutritionally important for penaeids (Zein-Eldin and Renaud, 1986; McTigue and Zimmerman, 1991, 1998). In addition, field and laboratory experiments have shown that brown shrimp growth is positively correlated with the abundance of marsh epiphytes and phytoplankton (Gleason and Zimmerman, 1984).

Most estuarine nekton are adaptable to the highly dynamic environmental conditions exhibited within estuaries (Gifford, 1962; Tagatz, 1971; Zimmerman et al., 1990b). These organisms are commonly found in a wide range of salinities and temperatures and are most affected by sudden changes in these environmental conditions

Table 3

Estimated area (km^2) of each bottom type and salinity zone combination sampled during spring (March–May), and estimated brown shrimp population based on spring density predictions from the model. ME = marsh edge; SAV = submerged aquatic vetetation; SNB = shallow nonvegetated bottom.

Bottom type	Salinity zone (ppt)	Bottom type area (km^2)	Density estimate (number/m^2)	Population estimate (millions)	Shrimp/ha. (thousands)
ME	0–0.5	1.4	0.14	0.2	1428
	0.5–5	1.6	5.50	8.8	55,000
	5–15	22.4	4.44	99.4	44,375
	15–25	59.5	6.14	365.3	61,394
	>25	0	8.46	0	0
	Total 84.9		473.5	55,771	
SAV	0–0.5	1.0	0.09	0.09	9000
	0.5–5	0.03	0.18	0.005	1667
	5–15	0.02	4.56	0.09	45,000
	15–25	3.5	14.52	50.8	145,142
	>25	0	9.91	0	0
	Total 4.5		51.0	114,680	
SNB	0–0.5	29.6	0	0	0
	0.5–5	54.2	1.01	54.7	10,092
	5–15	183.6	1.61	295.6	16,100
	15–25	203.3	2.41	489.9	24,097
	>25	5.5	3.37	18.5	33,636
	Total 476.2		858.7	18,032	
Total	565.6			1383.2	24,455

(Christensen et al., 1997). In laboratory experiments, Zein-Eldin and Aldrich (1965) concluded that higher salinities are more favorable for brown shrimp. Salinities of 20 ppt or greater were considered optimum in data from Louisiana (Barrett and Gillespie, 1973).

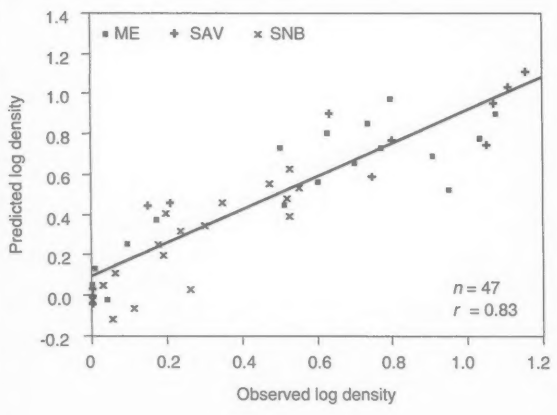

Figure 8

Relationship between predicted and observed densities of brown shrimp (*F. aztecus*) in Aransas, Matagorda and San Antonio bays and predicted densities from the Galveston Bay model. ME = marsh edge; SAV = submerged aquatic vegetation; SNB = shallow nonvegetated bottom.

In the present study, brown shrimp were captured throughout Galveston Bay, but highest densities were observed in the lower bay where salinities were greater than 15 ppt. This spatial trend was further strengthened by greater abundance of vegetated bottom types in the lower portions of the bay, where nearly half of the total marsh edge and 90% of seagrass beds are located (Fig. 4). These bottom types are regularly inundated and provide stable substrate for brown shrimp prey (epiphytic algae and infauna), whereas seasonal oligohaline marsh and SAV habitats in the upper bay may not promote favorable conditions for prey organisms (Zimmerman et al., 1990b). Therefore, salinity effects and the greater availability of vegetated habitats in the lower bay may work in a complementary manner to provide nursery areas for brown shrimp in Galveston Bay.

Previous attempts to examine spatial patterns of abundance and to determine linkages between organisms and habitat included the development of habitat suitability index (HSI) models. Early methods were derived by the U.S. Fish and Wildlife Service (USFWS) for freshwater species, where the HSI was defined as a numerical index that represented the capacity of a given habitat to support a selected species. The scale of HSI values (0–1.0) reflects a linear relationship between suitability and carrying capacity

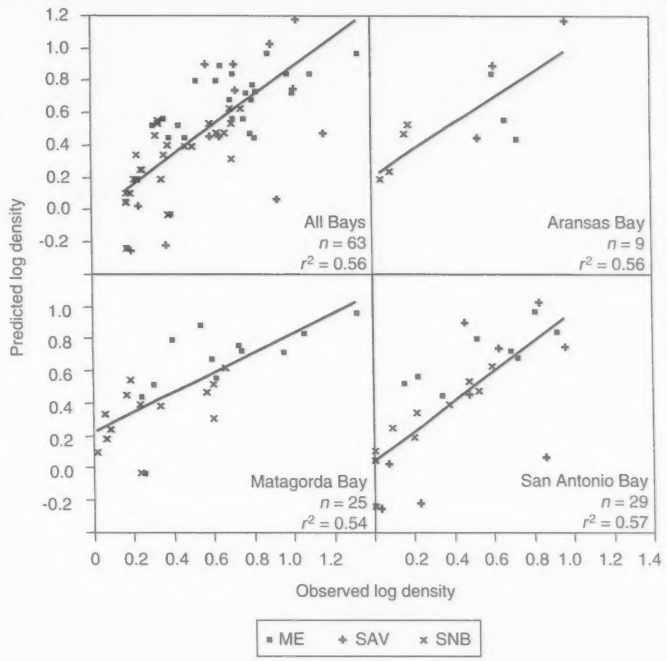

Figure 9

Relationships between observed densities of brown shrimp (*F. aztecus*) in Aransas, Matagorda, and San Antonio Bays and predicted densities from the Galveston Bay model. Relationships for all bays combined are shown in the upper left graph. For each relationship, the r^2 is shown for the least squares regression, and the number of observations (n) and the total number of samples in parentheses. ME = marsh edge; SAV = submerged aquatic vegetation; SNB = shallow nonvegetated bottom.

(USFWS, 1981). Recently, Christensen et al.[1] and Brown et al., 2000, developed suitability indices, based on literature reviews and expert opinion, and raster-based GIS models that produce a spatial view of relative suitability. The Florida Fish and Wildlife Conservation Commission-Marine Research Institute (FMRI) and the National Ocean Service's Center for Coastal Monitoring and Assessment (NOS/CCMA) collaborated to develop a suite of quantitative HSI modeling approaches, using fisheries-independent monitoring catch-per-unit-of-effort (CPUE) data (Rubec et al., 1998, 1999, 2001). These studies used an unweighted geometric mean formula as part of the HSI models to assess overall suitability. This approach assigns equal weight to all factors by using scaled suitability indices as inputs to the model. The regression approach used in this study more appropriately weights density according to the factors in the model and allows a more robust technique to elucidate spatial patterns of habitat use by using actual CPUE data. In addition, the method described in our study can support more complex analyses, such as interaction effects or trophic relationships (or both).

Our ANOVA (Table 1) revealed that season, bottom type, salinity, and the interaction between salinity and bottom type are significant factors that influence the distribution of juvenile brown shrimp in Galveston Bay. The addition of the interaction effect to the model increases the coefficient of determination from 0.63 to 0.73. Without this term in the model, predicted values for brown shrimp density are overestimated compared to the observed density data. Seagrass beds in salinities greater than 15 ppt supported significantly greater densities of brown shrimp than did marsh edge. However, in locations with salinities less than 15 ppt, brown shrimp densities were not significantly different between the two bottom types. These results indicate significantly lower use among all the bottom types analyzed in the fresher portion of the estuary. It is likely that salinity and a combination of other environmental factors directly or indirectly (or directly and indirectly) affect abundance on bottom types and habitat quality in this region. The results indicate that SAV supports greater brown shrimp density than do ME and SNB; however, SAV accounts for less than 1% of the total bottom type within

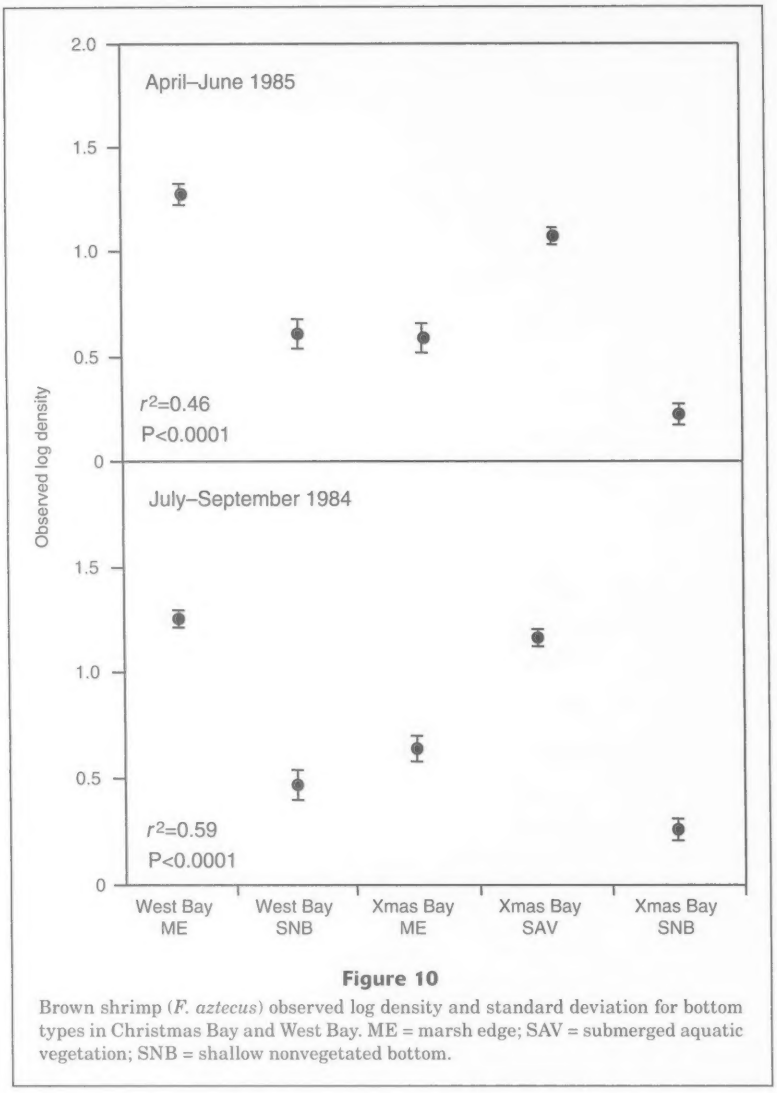

Figure 10

Brown shrimp (*F. aztecus*) observed log density and standard deviation for bottom types in Christmas Bay and West Bay. ME = marsh edge; SAV = submerged aquatic vegetation; SNB = shallow nonvegetated bottom.

Galveston Bay. Our data suggest that brown shrimp select SAV over ME when these habitats co-occur (Christmas Bay) and select ME when grassbeds are absent (West Bay) (Fig. 10). Habitat submergence time may explain high SAV use in Christmas Bay (Rozas and Minello, 1998). Subtidal grassbeds may provide more continuous refuge and food supply at both low and high tides than the marsh surface, which can be accessed only during high tides. Additionally, brown shrimp were significantly smaller in SAV ($\bar{x}$=17 mm) than in ME ($\bar{x}$=25 mm) (t-test, P<0.001), which may imply ontogenetic changes in habitat or trophic requirements (Conrow et al., 1990; Thomas et al., 1990; Rozas and Minello, 1999). Differences in the use of bottom types may correspond with the population's size distribution at the time of sampling. Additional research is needed to reveal ontogenetic habitat shifts and relationships among shallow estuarine bottom types (McIvor and Rozas, 1996).

Assessment of the model performance was based on FWS HSI theory where there is a positive relationship between HSI value and the carrying capacity of the available habitat. In the present study, the relationship equates high brown shrimp densities with optimal habitat conditions that promote high carrying capacity. Therefore, low densities would reflect a low suitability or a low capacity to support the population. Comparisons of predicted density with that of observed values from Galveston Bay, and other Texas bays (Figs. 7 and 8) agree with FWS theory by exhibiting a strong relationship between density and suitable habitat as determined from the model. Model performance and transferability were examined by applying

the Galveston Bay model (with interaction term) to brown shrimp density data from Aransas, Matagorda, and San Antonio bays. The results indicated similar habitat-use patterns in Aransas and San Antonio bays; there were higher densities in high-salinity seagrass beds and a declining density as salinity decreased in these bay systems. No SAV samples were taken in Matagorda Bay; however, the model performed well in predicting greater brown shrimp density in higher-salinity marsh-edge habitats. Our analysis suggests that although the empirical model is complex, it is general enough to be applicable across a broader range of habitat types. The model results may, however, have some geographic limitations. For instance, the model may not perform well within the Laguna Madre in south Texas, where freshwater inflow is diminished and hypersaline conditions exist. This conclusion is consistent with Rubec et al. (1999), who used similar methods to demonstrate that HSI models are applicable across estuaries in central Florida. Our results are promising in view of previous efforts where predictions of nekton abundance with empirical models have proven difficult.

Currently, estuarine EFH for most federally managed species in the Gulf of Mexico exists as mapped estimates of relative abundance from NOS's estuarine living marine resources (ELMR) database (GMFMC, 1998; Nelson and Monaco, 2000). The entire Galveston Bay complex was considered EFH for brown shrimp based on ELMR relative abundance data. Our model, generated by using brown shrimp density data, provides a more spatially resolved delineation of EFH (in waters <1 m depth) for brown shrimp <100 mm.

The analyses described in the present study focused on bottom types in waters less than 1 m which comprise about 25% of the available habitat in Galveston Bay. Trawl CPUE data from Texas Parks and Wildlife Department (TPWD) were analyzed to compare abundance and distribution patterns in waters >1 m. These trawls (3.8-cm stretched mesh) do not capture small size classes (<50 mm TL) of brown shrimp efficiently; thus the trawl analysis provides information only on larger size classes (mean=89 mm). However, few individuals in smaller size classes of shrimp (<50 mm TL) are likely to inhabit deeper bay waters; density estimates of small nekton, including shrimp, decline rapidly with depth (Mock, 1966; Baltz et al., 1993; Rozas, 1993; Rozas and Zimmerman, 2000). In addition, these CPUE values are likely underestimates of brown shrimp density; catch efficiency for shrimp in trawls can be roughly estimated at 20% (Zimmerman et al., 1984; Rozas and Minello, 1997). Despite these problems, shrimp abundance estimates in water >1 m appear low; abundance estimates from TPWD trawl data in deep open-bay waters were almost two orders of magnitude lower than densities in shallow water habitats.

Brown shrimp population estimates from the present study (Table 3) were highest in the lower bay (224,568 per ha.). Seagrass beds accounted for more than 60% of the estimate (145,142 per ha.) and marsh edge and nonvegetated bottom types combined were estimated at approximately 79,000 per ha. As noted earlier, the NWI regularly flooded emergent vegetation classification is not all marsh edge but is a complex of SNB, marsh edge, and inner marsh with different shrimp densities associated with each of these microhabitat types. Minello and Rozas (in press) modeled small-scale density patterns on the marsh surface in a 437-ha. salt marsh of lower Galveston Bay and applied these data to a GIS analysis of marsh landscape patterns. In this highly fragmented marsh complex that was 37% SNB and 63% marsh vegetation, they estimated brown shrimp populations at 37,000 per ha. We could not estimate brown shrimp populations in irregularly flooded emergent vegetation, although the areal coverage of this habitat type was large. Compared with the regularly flooded wetlands, overall densities of brown shrimp in these irregularly flooded systems should be relatively low because of higher marsh surface elevations (Rozas and Reed, 1993; Minello et al., 1994; Minello and Webb, 1997) and restricted tidal access (Rozas and Minello, 1999). We also were unable to assess the contribution of oyster reef as habitat for brown shrimp. Coen et al. (1999), however, reported brown shrimp on oyster reefs, and Powell (1993) estimated that there was 108 km^2 of this habitat in Galveston Bay.

Our modeling results provide evidence that estuarine habitat types are discriminately used by brown shrimp. The success of transferring our empirical model from Galveston Bay to adjacent bay systems in Texas suggests that the model has a broad application and can possibly be used to simulate patterns of habitat use in systems that lack sufficient density data. Continuing collections of density data in Gulf estuaries are necessary to make additional interestuary comparisons and to determine whether these habitat-use patterns differ throughout the distributional range of brown shrimp. The use of other habitat types also needs to be examined. For example, other available habitat types from Galveston Bay, such as oyster reef and inner marsh, and from other Gulf estuaries, such as mangrove, calcium carbonate rock formations, and sponge communities, may be important habitats for this federally managed species.

Acknowledgments

Funding and support for this work was provided by the Southeast Region of NOAA's National Marine Fisheries Service, The Southeast Fisheries Science Center, and the Biogeography Program of the National Ocean Service. We would like to thank Pete Sheridan, Lawrence Rozas, Ken Heck, and Roger Zimmerman for providing access to published and unpublished data sets. John Boyd helped with construction of the nekton density database.

Literature cited

Baltz, D. M., J. W. Fleeger, C.F. Rakocinski, and J. N. McCall. 1998. Food, density, and microhabitat: factors affecting growth and recruitment potential of juvenile saltmarsh fishes. Environ. Biol. Fish. 53:89–103.

Baltz, D. M., C. Rakocinski, and J. W. Fleeger. 1993. Microhabitat use by marsh-edge fishes in a Louisiana estuary. Environ. Biolog. Fish. 36:109–126.

Barret, B. B., and M. C. Gillespie.
1973. Primary factors which influence commercial shrimp production in coastal Louisiana. La. Wild Life Fish. Comm., Tech. Bull. 9, 28 p.

Barry, J. P., M. M. Yoklavich, G. M. Cailliet, D. A. Ambrose, and B. S. Antrim.
1999. Trophic ecology of the dominant fishes in Elkhorn Slough, California, 1974–1980. Estuaries 19:115–138.

Beck, M. W., K. L. Heck Jr., K. Able, D. Childers, D. Eggleston, B. M. Gillanders, B. Halpern, C. Hays, K. Hoshino, T. Minello, R. Orth, P. Sheridan, and M. Weinstein.
2001. The identification, conservation, and management of estuarine and marine nurseries for fish and invertebrates. Bioscience 51:633–641.

Boesch, D. F., and R. E. Turner.
1984. Dependence of fishery species on salt marshes: The role of food and refuge. Estuaries 7:460–468.

Brown, S. K., K. R. Buja, S. H. Jury, M. E. Monaco, and A. Banner.
2000. Habitat suitability index models for eight fish and invertebrate species in Casco and Sheepscot Bays, Maine. N. Am. J. Fish. Manag. 20:408–435.

Christensen, J. D., M. E. Monaco, and T. A. Lowery.
1997. An index to assess the sensitivity of Gulf of Mexico species to changes in estuarine salinity regimes. Gulf Res. Rep. 9(4):219–229.

Coen, L. D., M. W. Luckenbach, and D. L. Breitburg.
1999. The role of oyster reefs as essential fish habitat: a review of current knowledge and some new perspectives. *In* Fish habitat: essential fish habitat and rehabilitation (L. R. Benaka, ed.), p. 438–454. Am. Fish. Soc., Symposium 22, Bethesda, MD.

Conrow, R. A., V. Zale, and R. W. Gregory.
1990. Distributions and abundances of early life stages of fishes in a Florida lake dominated by aquatic macrophytes. Trans. Am. Fish. Soc. 119:521–528.

Copeland, B. J., and T. J. Bechtel.
1974. Some environmental limits of six gulf coast estuarine organisms. Contrib. Mar. Sci. 18:169–204.

Cowardin, L. J., V. Carter, F. C. Golet, and E. T. Laroe.
1979. Classification of wetlands and deepwater habitats of the United States. U.S. Fish Wildl. Serv. Biol. Serv. Program FWS/OBS-79/31, 131 p.

Czapla, T. E.
1991. Diets and prey selection of pinfish and southern flounder in a *Halodule wrightii* seagrass meadow. Ph.D. diss., 119 p. Texas A&M Univ., College Station, TX

Garrison, L. P.
1999. Vertical migration behavior and larval transport in brachyuran crabs. Mar. Ecol. Prog. Ser. 176:103–113.

Gifford, C. A.
1962. Some aspects of osmotic and ionic regulation in the blue crab, *Callinectes sapidus,* and the ghost crab, *Ocypode albicans.* Publ. Inst. Mar. Sci. 8:97–125.

Gleason, D. F., and R. J. Zimmerman.
1984. Herbivory potential of postlarval brown shrimp associated with salt marshes. J. Exp. Mar. Biol. Ecol. 84: 235–246.

GMFMC (Gulf of Mexico Fishery Management Council).
1998. Generic amendment for addressing essential fish habitat requirements. Prepared by the GMFMC, October 1998, 34 p.

Krumgalz, B. S., G. Fainshtein, and A. Cohen.
1992. Grain size effect on anthropogenic trace metal and organic matter distribution in marine sediments. Sci. Total Environ. 116(1–2):15–30.

Mahon, R. and R. W. Smith.
1989. Comparison of species composition in a bottom trawl calibration experiment. J. Northw. Atl. Fish. Sci. 9:73–79.

McIvor, C. C., and L. P. Rozas.
1996. Direct nekton use of intertidal saltmarsh habitat and linkage with adjacent habitats: a review from the southeastern United States. *In* Estuarine shores: evolution, environments and human alterations (K. F. Nordstrom and C. T. Roman, eds.), p. 311–334. John Wiley and Sons, Ltd., Chichester, England.

McTigue, T. A., and R. J. Zimmerman.
1991. Carnivory versus herbivory in juvenile *Penaeus setfierus* (Linnaeus) and *Penaeus aztecus* (Ives). J. Exp. Mar. Biol. Ecol. 15:1–16.
1998. The use of infauna by juvenile *Penaeus aztecus* (Ives) and *P. setiferus* (Linnaeus). Estuaries 21:160–175.

Miller, J. M., and M. L. Dunn.
1980. Feeding strategies and patterns of movement in juvenile estuarine fishes. *In* Estuarine perspectives (V. S. Kennedy, ed.), p. 437–448. Academic Press, New York, NY.

Minello, T. J.
1999. Nekton densities in shallow estuarine habitats of Texas and Louisiana and the identification of essential fish habitat. *In* Fish habitat: essential fish habitat and rehabilitation (L. Beneka, ed.), p. 43–75. Am. Fish. Soc., Bethesda, MD.

Minello, T. J., and L. P. Rozas.
In press. Nekton populations in Gulf Coast wetlands: fine-scale spatial distributions, landscape patterns, and restoration implications. Ecol. Appl.

Minello, T. J., and J. W. Webb Jr.
1997. Use of natural and created *Spartina alterniflora* salt marshes by fishery species and other aquatic fauna in Galveston Bay, Texas, USA. Mar. Ecol. Prog. Ser. 151:165–179.

Minello, T. J., J. W. Webb Jr., R. J. Zimmerman, R. B. Wooten, J. L. Martinez, T. J. Baumer, and M. C. Patillo.
1991. Habitat availability and utilization by benthos and nekton in Hall's Lake and West Galveston Bay. NOAA Tech. Memo. NMFS-SEFC-275, 37 p.

Minello, T. J., and R. J. Zimmerman.
1992. Utilization of natural and transplanted Texas salt marshes by fish and decapod crustaceans. Mar. Ecol. Prog. Ser. 90:273–285.

Minello, T. J., R. J. Zimmerman, and R. Medina.
1994. The importance of edge for natant macrofauna in a created salt marsh. Wetlands 14:184–198.

Mock, C. R.
1966. Natural and altered estuarine habitats of penaeid shrimp. Proceedings of the Gulf and Caribbean Fisheries Institute, 19th annual session, p. 86–98. Gulf and Caribbean Fish. Inst., Fort Pierce, FL.

Monaco, M. E., S. B. Weisberg, and T. A. Lowery.
1998. Summer habitat affinities of estuarine fish in US mid-Atlantic coastal systems. Fish. Manag. Ecol. 5:161–171.

NOAA (National Oceanic and Atmospheric Administration).
1989. Estuaries of the United States: vital statistics of a natural resource base, 79 p. Strategic Environmental Assessments Division, National Ocean Service (NOS), NOAA, Rockville, MD.

Nelson, D. M., and M. E. Monaco.
2000. National overview and evolution of NOAA's estuarine living marine resources (ELMR) Program. NOAA Tech. Memo. NOS NCCOS CCMA 144, 60 p. Center for

Coastal Monitoring and Assessment, NOS, NOAA, Silver Spring, MD.

Orlando, S. P. Jr., L. P. Rozas, G. H. Ward, and C. J. Klein.
1993. Salinity characteristics of Gulf of Mexico estuaries, 209 p. Office of Ocean Resources and Conservation and Assessment, NOAA, Silver Spring, MD.

Pearcy, W. G., and S. S. Myers.
1974. Larval fishes of Yaquina Bay, Oregon: a nursery ground for marine fishes? Fish. Bull. 72:201–213.

Perez-Farfante, I., and B. Kensley.
1997. Penaeoid and sergestoid shrimps and prawns of the world; keys and diagnoses for the families and genera. Memoires du Muséum National d'Histoire Naturelle, tome 175, 233 p.

Peterson, G. W., and R. E. Turner.
1994. The value of salt marsh edge vs. interior as a habitat for fish and decapod crustaceans in a Louisiana tidal marsh. Estuaries 17:235–262.

Powell, E. N.
1993. Status and trends analysis of oyster reef habitat in Galveston Bay. *In* Proceeding, second state of the bay symposium (R. W. Jensen et al., eds.), p. 207–209. Galveston Bay National Estuary Program, Houston, TX.

Rozas, L. P.
1993. Nekton use of salt marshes of the southeast region of the United States. *In* Proc. 8th symp. coastal and ocean management (O. T. Magoon, W. S. Wilson, H. Converse, and L. T. Tobin, eds.), p. 528–537. Coastal Zone '93 Conference, Am. Soc. Civil Eng., New Orleans, LA.

Rozas, L. P., and T. J. Minello.
1997. Estimating densities of small fishes and decapod crustaceans in shallow estuarine habitats: a review of sampling design with focus on gear selection. Estuaries 20: 199–213.
1998. Nekton use of salt marsh, seagrass, and nonvegetated habitats in a south Texas (USA) estuary. Bull. Mar. Sci. 63(3):481–501.
1999. Effects of structural marsh management on fishery species and other nekton before and during a spring drawdown. Wetl. Ecol. Manag. 7: 121–139.

Rozas, L. P., and D. J. Reed.
1993. Nekton use of marsh-surface habitats in Louisiana (USA) deltaic salt marshes undergoing submergence. Mar. Ecol. Prog. Ser. 96:147–157.

Rozas, L. P., and R. J. Zimmerman.
2000. Small-scale patterns of nekton use among marsh and adjacent shallow nonvegetated areas of the Galveston Bay estuary, Texas (USA). Mar. Ecol. Prog. Ser. 193:217–239.

Rubec, P. J., M. S. Coyne, R. H. McMichael Jr., and M. E. Monaco.
1998. Spatial methods being developed in Florida to determine essential fish habitat. Fisheries 23(7):21–25.

Rubec, P. J., J. C. W. Bexley, H. Norris, M. S. Coyne, M. E. Monaco, S. G. Smith, and J. S. Ault.
1999. Suitability modeling to delineate habitat essential to sustainable fisheries. Am. Fish. Soc. Symp. 22:108–133.

Rubec, P. J., S. G. Smith, M. S. Coyne, M. White, A. Sullivan, T. MacDonald, R. H. McMichael Jr., M. E. Monaco, and J. S. Ault.
2001. Spatial modeling of fish habitat suitability in Florida estuaries. *In* Spatial processes and management of marine populations (G. H. Kruse, N. Bez, A. Booth, M. W. Dorn, S. Hills, R. N. Lipcus, D. Pelltier, C. Roy, S. J. Smith, and D. Witherell, eds.), p. 1–18. Sea Grant report AK-SG-01-02. Univ. Alaska, Fairbanks, AK.

Sogard, S. M., and K. W. Able.
1991. A comparison of eelgrass, sea lettuce macroalgae, and marsh creeks as habitats for epibenthic fishes and decapods. Estuar. Coast. Shelf Sci. 33:501–519.

Tagatz, M. E.
1971. Osmoregulatory ability of blue crabs in different temperature-salinity combinations. Ches. Sci. 12:14–17.

Thomas, J. L., R. J. Zimmerman, and T. J. Minello.
1990. Abundance patterns of juvenile blue crabs (*Callinectes sapidus*) in nursery habitats of two Texas bays. Bull. Mar. Sci. 46:115–125.

Turner, R. E.
1977. Intertidal vegetation and commercial yields of penaeid shrimp. Trans. Am. Fish. Soc. 106:411–416.

USFWS (U.S. Fish and Wildlife Service).
1981. Standards for the development of habitat suitability index models for use with the habitat evaluation procedures. Report 103, ESM release 1-81, 66 p. Division of Ecological Services, USFWS, Washington, DC.

White, W. A., T. A. Tremblay, E. G. Wermund Jr., and L. R. Handley.
1993. Trends and status of wetland and aquatic habitats in the Galveston Bay System, Texas, 225 p. Galveston Bay National Estuary Program, Galveston, TX.

Zein-Eldin, Z. P., and D. V. Aldrich.
1965. Growth and survival of postlarval *Penaeus aztecus* under controlled conditions of temperature and salinity. Biol. Bull. (Woods Hole) 129:199–216.

Zein-Eldin, Z. P., and M. L. Renaud.
1986. Inshore environmental effects on brown shrimp, *Penaeus aztecus*, and white shrimp, *P. setiferus*, populations in coastal waters, particularly Texas. Mar. Fish. Rev. 48:9–19.

Zimmerman, R. J., and T. J. Minello.
1984. Densities of *Penaeus aztecus*, *P. setiferus* and other natant macrofauna in a Texas salt marsh. Estuaries 7: 421–433.

Zimmerman, R. J., T. J. Minello, T. J. Baumer, and M. C. Castiglione.
1989. Oyster reef as habitat for estuarine macrofauna. NOAA Tech. Memo., NMFS-SEFC-249, 16 p.

Zimmerman, R. J., T. J. Minello, M. C. Castiglione, and D. L. Smith.
1990a. The use of *Juncus* and *Spartina* marshes by fisheries species in Lavaca Bay, Texas, with reference to effects of floods. NOAA Tech. Memo., NMFS-SEFC-251, 40 p.
1990b. Utilization of marsh and associated habitats along a salinity gradient in Galveston Bay. NOAA Tech. Memo., NMFS-SEFC-250, 68 p.

Zimmerman, R. J., T. J. Minello, and L. P. Rozas.
2000. Salt marsh linkages to productivity of penaeid shrimps and blue crabs in the northern Gulf of Mexico. *In* Concepts and controversies in tidal marsh ecology (M. P. Weinstein and D.A. Kreeger, eds.), p. 293–314. Kluwer Academic Publ., Dordrecht, The Netherlands.

Zimmerman, R. J., T. J. Minello, and G. Zamora.
1984. Selection of vegetated habitat by *Penaeus aztecus* in a Galveston Bay salt marsh. Fish. Bull. 82:325–336.

Translocation as a strategy to rehabilitate the queen conch (*Strombus gigas*) population in the Florida Keys

Gabriel A. Delgado
Claudine T. Bartels
Robert A. Glazer
Florida Fish and Wildlife Conservation Commission
Florida Marine Research Institute
2796 Overseas Highway, Suite 119
Marathon, Florida 33050
E-mail address (for G. A Delgado): gabriel.delgado@fwc.state.fl.us

Nancy J. Brown-Peterson
Department of Coastal Sciences
College of Science and Technology
The University of Southern Mississippi
P.O. Box 7000
Ocean Springs, Mississippi 39566

Kevin J. McCarthy
National Marine Fisheries Service, NOAA
75 Virginia Beach Drive
Miami, Florida 33149

Abstract—Queen conch (*Strombus gigas*) stocks in the Florida Keys once supported commercial and recreational fisheries, but overharvesting has decimated this once abundant snail. Despite a ban on harvesting this species since 1985, the local conch population has not recovered. In addition, previous work has reported that conch located in nearshore Keys waters are incapable of spawning because of poor gonadal condition, although reproduction does occur offshore. Queen conch in other areas undergo ontogenetic migrations from shallow, nearshore sites to offshore habitats, but conch in the Florida Keys are prevented from doing so by Hawk Channel. The present study was initiated to determine the potential of translocating nonspawning nearshore conch to offshore sites in order to augment the spawning stock. We translocated adult conch from two nearshore sites to two offshore sites. Histological examinations at the initiation of this study confirmed that nearshore conch were incapable of reproduction, whereas offshore conch had normal gonads and thus were able to reproduce. The gonads of nearshore females were in worse condition than those of nearshore males. However, the gonadal condition of the translocated nearshore conch improved, and these animals began spawning after three months offshore. This finding suggests that some component of the nearshore environment (e.g., pollutants, temperature extremes, poor food or habitat quality) disrupts reproduction in conch, but that removal of nearshore animals to suitable offshore habitat can restore reproductive viability. These results indicate that translocations are preferable to releasing hatchery-reared juveniles because they are more cost-effective, result in a more rapid increase in reproductive output, and maintain the genetic integrity of the wild stock. Therefore, translocating nearshore conch to offshore spawning aggregations may be the key to expediting the recovery of queen conch stocks in the Florida Keys.

Manuscript approved for publication
24 November 2003 by Scientific Editor.
Manuscript received 20 January 2004
at NMFS Scientitific Publications Office.
Fish. Bull. 102:278–288 (2004).

The queen conch (*Strombus gigas*) is a large marine gastropod harvested intensively throughout the Caribbean for its meat and shell. In the Florida Keys, conch once supported commercial and recreational fisheries, but overharvesting severely depleted the population. The harvesting of conch has been banned in Florida since 1985, but the population has not recovered to levels that can support exploitation (Glazer and Berg, 1994; Berg and Glazer, 1995; Glazer and Delgado, 2003). Intensive fishing may invoke depensatory mechanisms as densities are reduced, limiting the ability of conch to locate mates and increasing the chance of recruitment failure (Appeldoorn, 1995). This seems to be the case in Florida because the lack of recovery has been attributed to diminished recruitment due in part to small spawning aggregations (Stoner et al., 1997; Stoner and Ray-Culp, 2000).

Queen conch occur in the various oceanside habitats of the Florida Keys archipelago with the exception of Hawk Channel (Glazer and Berg, 1994). This naturally occurring deep-water channel runs parallel to the Florida Keys, between the island chain and the offshore reef tract. The substrate on the bottom of Hawk Channel is predominantly soft sediment, which is poor conch habitat; consequently, Hawk Channel serves as a barrier to migration and isolates nearshore from offshore conch aggregations (Glazer and Berg, 1994). We have been monitoring queen conch stocks throughout the Florida Keys since 1987, and despite extensive surveys, we have never observed reproductive activity among conch in nearshore aggregations (Glazer and Berg, 1994). Conversely, reproductive behavior has been commonly observed among conch in offshore aggregations (Glazer and Berg, 1994). Moreover, a preliminary histological examination of conch from these two regions indicated that the gonads of offshore conch were capable of undergoing gametogenesis, whereas the gonads of nearshore conch were nonfunctional (Glazer and Quintero,

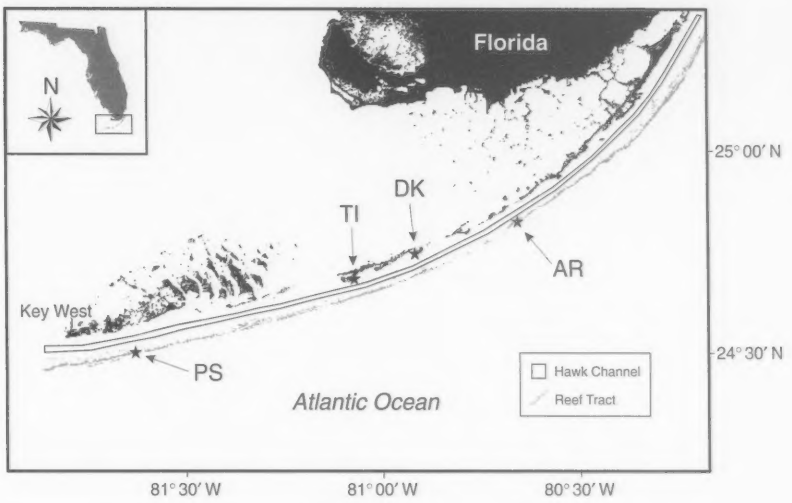

Figure 1

Queen conch (*Strombus gigas*) translocation sites in the Florida Keys (adapted from McCarthy et al. 2002). The nearshore region is the stretch of water on the landward side of Hawk Channel; the offshore region is the stretch of water on the other side of the channel, contiguous with the Atlantic Ocean. Nearshore conch were translocated from Tinglers Island (TI) to Alligator Reef (AR) and from Duck Key (DK) to Pelican Shoal (PS).

1998; McCarthy et al., 2002). In a metapopulation context, the nearshore region in the Florida Keys can be considered a "blackhole sink" for larval recruitment because conch that settle there do not spawn and thus do not contribute to the reproductive output of the stock (*sensu* Morgan and Botsford, 2001).

In 1990, the Florida Fish and Wildlife Conservation Commission's (FWC) Florida Marine Research Institute constructed an experimental hatchery to test the feasibility of rehabilitating queen conch stocks in the Florida Keys by releasing hatchery-reared juveniles. A series of experiments to determine the best size of juveniles, time of release, and area to release hatchery-reared juvenile conch were conducted, and a cost-benefit analysis was performed. Unfortunately, the high mortality of conch after release, coupled with high production costs, caused us to examine alternate strategies (Glazer and Delgado, 2003).

Translocation is defined as the intentional introduction or reintroduction of animals in an attempt to establish, reestablish, or augment a population in order to aid in the recovery of a native species whose numbers have been reduced by overharvesting or habitat loss (or both) (Griffith et al., 1989). This method of population recovery has been used to facilitate the recovery of numerous species of birds and mammals (Griffith et al., 1989) and several aquatic species, including cutthroat trout (Harig et al., 2000) and corals (Edwards and Clark, 1999; Rinkevich, 1995; van Treeck and Schuhmacher, 1997). Nest translocations have also proven effective in efforts to recover sea turtles (Garcia et al., 1996).

The present study was initiated to determine the potential of translocating nonspawning nearshore conch to offshore sites as a method to augment spawning aggregations and as an aid in the recovery of the queen conch population in the Florida Keys. However, this strategy will be beneficial only if the translocated conch regain their reproductive capacity. To test this approach, we translocated adult conch from the nearshore region into existing offshore breeding aggregations and examined changes in reproductive behavior (i.e., mating and spawning) and gonadal development.

Materials and methods

Translocations and reproductive behavior

During March 1999, we translocated adult conch from nearshore aggregations to aggregations offshore. Nearshore aggregations were located at Tinglers Island (24°41′N, 81°05′W; water depth <1–2 m) and Duck Key (24°45′N, 80°55′W; water depth <1–2 m) (Fig. 1). The habitat at the two nearshore sites was characterized as a matrix of hard-bottom and *Thalassia testudinum* patches. Offshore aggregations were located at Alligator Reef (24°51′N, 80°37′W; water depth 9–11 m) and Pelican Shoal (24°30′N, 81°37′W; water depth 5–7 m) (Fig. 1). The habitat at the offshore sites consisted of back-reef rubble, sandy plains, and patches of *Thalassia testudinum*.

We tagged 44 adult conch at Tinglers Island; 23 were translocated to Alligator Reef, and 21 were rereleased at

Table 1

The number of gonadal tissue samples taken from resident nearshore, resident offshore, and translocated nearshore queen conch, by sex and season.

	Spring		Summer		Fall	
	Females	Males	Females	Males	Females	Males
Resident nearshore	13	12	14	12	10	6
Resident offshore	22	20	19	20	25	15
Translocated nearshore	—	—	12	12	13	4

Table 2

Index and definitions used to quantify gonadal maturity in queen conch. This index is patterned after the maturity scale developed by Egan (1985). The dashed line separates the scores 1–5 from 6–8 that were combined for statistical analyses.

Gonadal condition	Score	Definition
Early development	1	primary and cortical alveolar oocytes in females; spermatogonia and spermatocytes in males
Mid development	2	vitellogenesis beginning in females; spermatozoa present in males
Late development	3	fully developed oocytes in females, none in oviduct; all stages of spermatogenesis, no spermatozoa in vas deferens
Ripe	4	oocytes in oviduct for females; spermatozoa in vas deferens for males
Spent	5	reabsorption of vitellogenic oocytes in females; empty lobules, residual spermatozoa in males
Atresia	6	reabsorption of oocytes and no vitellogenesis in females; reabsorption of spermatozoa in males
Regressed	7	only primary oocytes in females; only primary spermatogonia in males
No tissue	8	no gonadal tissue development and no germ cells present; this is an abnormal condition in adult females and males

Tinglers Island. We also tagged 132 adult conch at Duck Key; 73 were translocated to Pelican Shoal, and 59 were re-released at Duck Key. In addition, 100 resident offshore conch were tagged *in situ* at both Alligator Reef and Pelican Shoal. Conch were tagged with individually numbered tags that were secured to the shell spires by Monel wire; in addition, colored flagging tape was similarly attached to facilitate recapture.

Reproductive behavior of tagged queen conch was monitored at each of the four sites on a weekly basis, weather permitting, from March 1999 through November 1999. Offshore sites were surveyed by using SCUBA; nearshore sites were surveyed by snorkeling. Mating activity was quantified by counting the number of tagged individuals (both males and females) copulating; spawning activity was quantified by counting the number of tagged females laying egg masses. Data from the two nearshore sites were pooled and data from the two offshore sites were pooled. Data were also pooled by season: spring consisted of March, April, and May; summer consisted of June, July, and August; and fall consisted of September, October, and November.

Histological examinations

Gonadal tissue samples from adult conch were collected for histological examination at the initiation of the study (spring; the start of the breeding season), during July–August (summer; breeding season), and during October (fall; the end of the breeding season) in order to assess gonadal development in relation to time after translocation. We collected approximately 40 resident offshore conch during each season (Table 1). However, because of the small size of the nearshore aggregations and the small number of nearshore conch translocated offshore, we collected about 20 individuals from these two groups each season (Table 1). We did not determine the sex of the animals before sample collection; therefore the breakdown by sex is not exactly even (Table 1).

A one-cm^3 piece of tissue from the middle of the gonad of each animal was placed in a labeled plastic cassette and preserved in 10% neutral buffered formalin. After 7 to 14 days in fixative, the tissue samples were rinsed overnight in freshwater. The samples were then dehydrated in a se-

ries of graded ethanols (one change of 60% ethanol and two changes of 70% ethanol for two hours each) and loaded into an automatic tissue processor (Shandon Hypercenter XP, Shandon Scientific Ltd., Pittsburgh, PA) for dehydration, clearing, and paraffin infiltration. Tissues were embedded in Paraplast Plus (Fisher Scientific, Pittsburgh, PA) and sectioned at 4 μm with a rotary microtome. Two serial sections from each tissue sample were mounted on glass slides, allowed to dry overnight, and stained with hematoxylin 1 and eosin Y (Richard Allen Inc., Richland, MI). All laboratory procedures followed approved standard operating procedures developed under the Good Laboratory Practices guidelines (EPA and FDA guidelines).

A detailed histological inspection of each sample was made to assess the stage of gonadal maturity and the percentage of gametogenic tissue. Each animal was given a score from 1 to 8 to quantify gonadal maturity (Table 2). This index was derived from a maturity scale developed by Egan (1985). Because of the small number of animals collected, gonadal maturity scores from 1 to 5 were combined to group animals that would be capable of spawning or had recently spawned (Table 2). Scores from 6 to 8 were combined to group animals that would not spawn again in a season or were not capable of spawning (Table 2). In addition, the percentage of gametogenic tissue present (i.e., the percentage of ovarian or testicular tissue occupying the available space of the section) was visually estimated by using the following index: <25%, 25–50%, 51–75%, and >75%. For statistical analyses, this index was reduced to two categories: <50% and >50%.

Statistical analyses

We evaluated differences in reproductive behavior (mating and spawning) between resident nearshore and translocated nearshore conch for each season by using Fisher's exact test because it is not sensitive to small sample sizes (Zar, 1996). We also examined differences in gonadal condition (i.e., gonadal maturity and the percentage of gametogenic tissue) between resident nearshore and resident offshore conch for each season by using Fisher's exact test. Males and females were analyzed separately. In order to assess the effectiveness of the translocations to the offshore region, we used Fisher's exact test to compare the gonadal condition of translocated nearshore conch with the gonadal condition of resident nearshore conch in summer and in fall. Again, the sexes were analyzed separately. All tests were run on SPSS 9.0 (SPSS Inc., Chicago, IL) for Windows. Results were considered significant if $P<0.05$.

Results

Reproductive behavior: mating

Approximately 84% of the tagged resident nearshore conch, 69% of the tagged translocated nearshore conch, and 88% of the tagged resident offshore conch were observed at least once during monitoring. Resident nearshore conch and translocated nearshore conch were not observed mating during any of the field surveys; conversely, resident offshore conch were observed mating throughout the study (Table 3). The mating frequency of resident offshore conch was highest during the spring (5.3%) and decreased during subsequent seasons to 0.9% in the fall (Table 3). All observed mating occurred between resident offshore animals.

Table 3

Percentage of mating (the number of males and females mating divided by the total number of conch observed during that season) and spawning (the number of females spawning divided by the total number of females observed during that season) in nearshore conch and offshore conch by season (adapted from McCarthy et al., 2002). Numbers in parentheses represent the number of observations; *P* represents the probabilities from Fisher's exact test of differences in reproductive behavior between resident nearshore and translocated nearshore conch. The asterisk (*) indicates that the test was statistically significant. N/A indicates that statistical analyses were not conducted because no mating or spawning was observed among either resident nearshore or translocated nearshore animals.

	Offshore conch	Nearshore conch		
	Resident	Resident	Translocated	*P*
Mating				
Spring	5.3 (95)	0.0 (37)	0.0 (19)	N/A
Summer	2.4 (467)	0.0 (106)	0.0 (81)	N/A
Fall	0.9 (232)	0.0 (20)	0.0 (51)	N/A
Spawning				
Spring	46.2 (39)	0.0 (6)	0.0 (10)	N/A
Summer	16.8 (191)	0.0 (34)	12.2 (41)	0.041*
Fall	5.2 (97)	0.0 (9)	18.5 (27)	0.214

Reproductive behavior: spawning

Neither resident nearshore females nor translocated nearshore females were observed spawning during the spring (Table 3). However, by summer, translocated nearshore females had attained the capacity to spawn and had a significantly higher spawning frequency than resident nearshore females (12.2% vs. 0.0%, respectively) (Table 3). During the fall, spawning frequency of translocated nearshore females peaked at 18.5%, whereas resident nearshore females had still not exhibited any spawning behavior (Table 3). However, this difference was not statistically significant because of the small number of resident nearshore conch observed (Table 3). Looking at individual performance instead of spawning frequency, seven (or about 14%) of the approximately 50 nearshore females translocated offshore were observed spawning at least once during the study period.

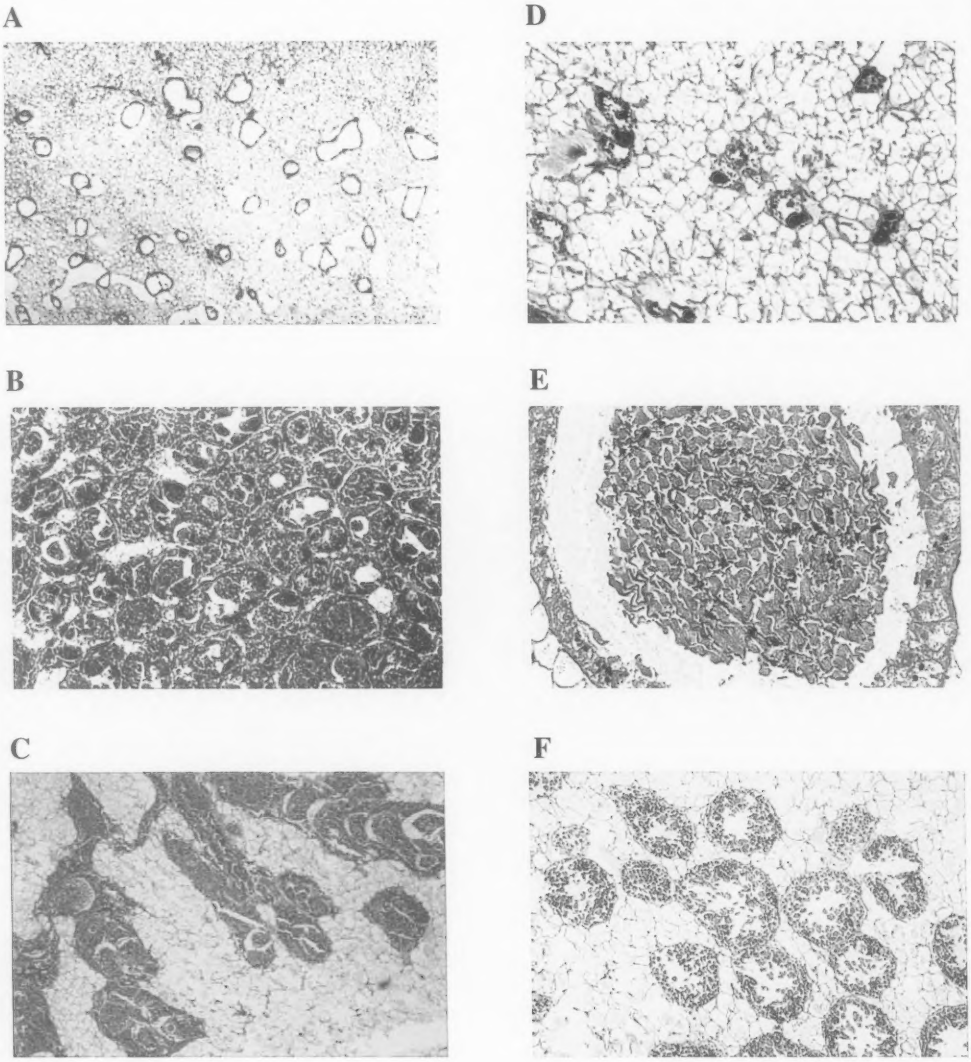

Figure 2

Photomicrographs of the gonadal condition of resident nearshore, resident offshore, and translocated nearshore queen conch (*Strombus gigas*). (**A**) Resident nearshore female during spring, no tissue and <25% gametogenic tissue. (**B**) Resident offshore female during spring, ripe and >75% gametogenic tissue. (**C**) Translocated nearshore female during summer, late development and 25–50% gametogenic tissue. (**D**) Resident nearshore male during spring, early development and <25% gametogenic tissue. (**E**) Resident offshore male during spring, ripe and >75% gametogenic tissue. (**F**) Translocated nearshore male during summer, ripe and 25–50% gametogenic tissue.

Resident offshore females were observed spawning throughout the study (Table 3). Their spawning frequency peaked during the spring at 46.2% and decreased during subsequent seasons to 5.2% in the fall (Table 3).

Histology: females

Histological examinations revealed that the gonadal condition of resident nearshore and resident offshore female

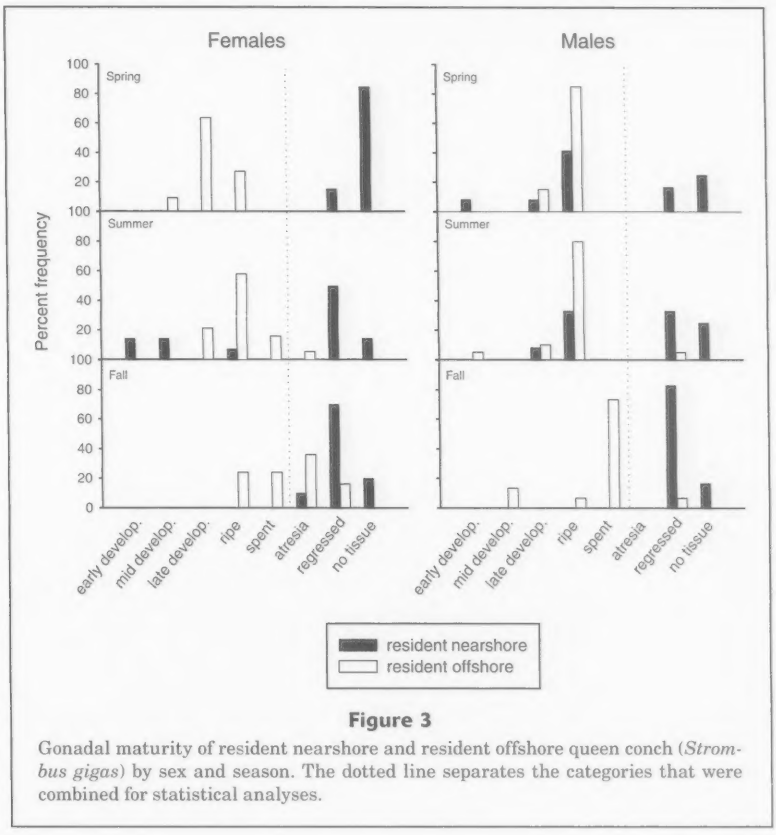

Figure 3

Gonadal maturity of resident nearshore and resident offshore queen conch (*Strombus gigas*) by sex and season. The dotted line separates the categories that were combined for statistical analyses.

conch were markedly different at the beginning of the study (Fig. 2, A and B). There were significant differences in gonadal maturity between resident offshore and resident nearshore female conch during the spring, summer, and fall (Table 4). During the spring, the gonads of most resident offshore females were categorized as being in late development; by summer most were ripe and by fall most were either spent, in atresia, or regressed (Fig. 3). In contrast, the gonads of most resident nearshore females contained no germ cells during the spring (Fig. 3). By summer, the gonads of some resident nearshore females were found to be in the early stages of development, but most females were still incapable of spawning, and by fall, all the resident nearshore females sampled were incapable of spawning (Fig. 3). There were also significant differences in the percentage of gametogenic tissue between resident offshore and resident nearshore females during the spring, summer, and fall (Table 4). The gonads of most resident offshore females contained >75% gametogenic tissue throughout the study period, whereas those of most resident nearshore females had <25% (Fig. 4).

The gonadal condition of translocated nearshore females (Fig. 2C) improved when compared with the gonadal condition of resident nearshore females (Fig. 2A). There were significant differences in gonadal maturity between translocated nearshore and resident nearshore females during both the summer and fall (Table 5). There was

Table 4

Probabilities from Fisher's exact test of differences in gonadal maturity and the percentage of gametogenic tissue between resident nearshore and resident offshore conch by sex and season. *n* represents the total number of observations. Asterisks (*) indicate that the test was statistically significant.

	Females		Males	
	n	*P*	*n*	*P*
Gonadal maturity				
Spring	35	<0.001*	32	0.004*
Summer	33	<0.001*	32	0.002*
Fall	35	0.006*	21	<0.001*
% gametogenic tissue				
Spring	35	<0.001*	32	<0.001*
Summer	33	<0.001*	32	<0.001*
Fall	35	0.002*	21	<0.001*

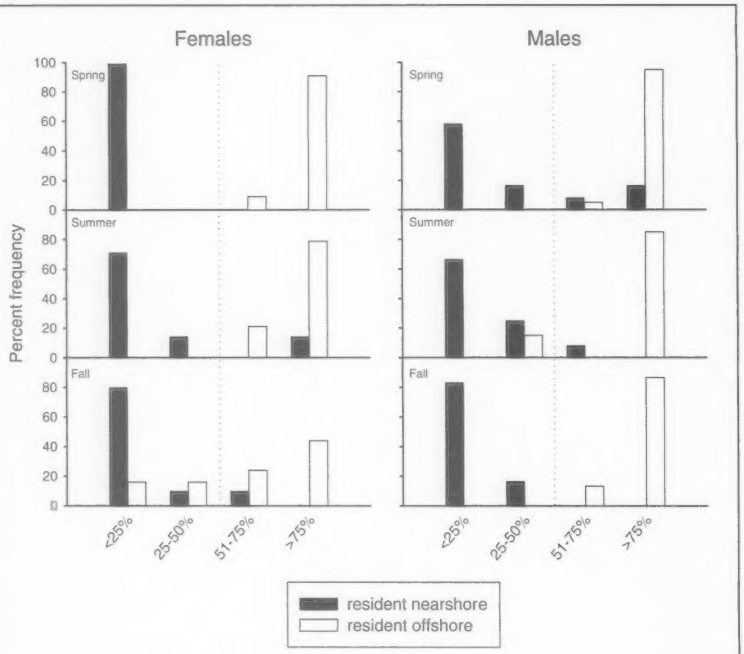

Figure 4

The percentage of gametogenic tissue of resident nearshore and resident offshore queen conch (*Strombus gigas*) by sex and season. The dotted line separates the categories that were combined for statistical analyses.

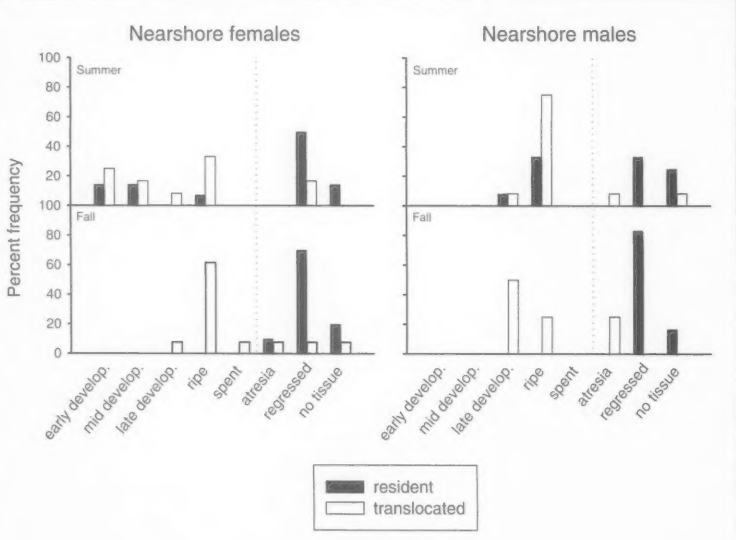

Figure 5

Gonadal maturity of resident nearshore and translocated nearshore queen conch (*Strombus gigas*) by sex and season. The dotted line separates the categories that were combined for statistical analyses.

a higher percentage of translocated nearshore females in some stage of gonadal development than resident nearshore females during the summer; in fact, about 30% of the translocated females were ripe (Fig. 5). By fall, the differences were even more extreme; over 60% of the translocated nearshore females were ripe, whereas all of the resident nearshore females were incapable of reproducing (Fig. 5). Although there was a significant difference in gonadal maturity between translocated nearshore and resident nearshore females during the summer, there was no significant difference in the percentage of gametogenic tissue (Table 5 and Fig. 6). However, by fall, there were significant differences in the percentage of gametogenic tissue between translocated nearshore and resident nearshore females (Table 5). Most translocated nearshore females had developed >75% of the gonad, whereas most resident nearshore females still had <25% gametogenic tissue (Fig. 6).

Histology: males

There were marked differences in gonadal condition of resident nearshore and resident offshore male conch (Fig. 2, D and E). There were significant differences in gonadal maturity between resident offshore and resident nearshore male conch during the spring, summer, and fall (Table 4). During the spring and summer, the gonads of most resident offshore males were categorized as ripe; by fall most were spent (Fig. 3). In contrast, at least half of the resident nearshore males were not capable of spawning during the spring and summer, although some were in the early stages of testicular development and some were even ripe (Fig. 3). However, all the sampled resident nearshore males were incapable of spawning by fall and none were identified as spent (Fig. 3). Histological examinations also revealed significant differences in the percentage of gametogenic tissue between resident offshore and resident nearshore males during the spring, summer,

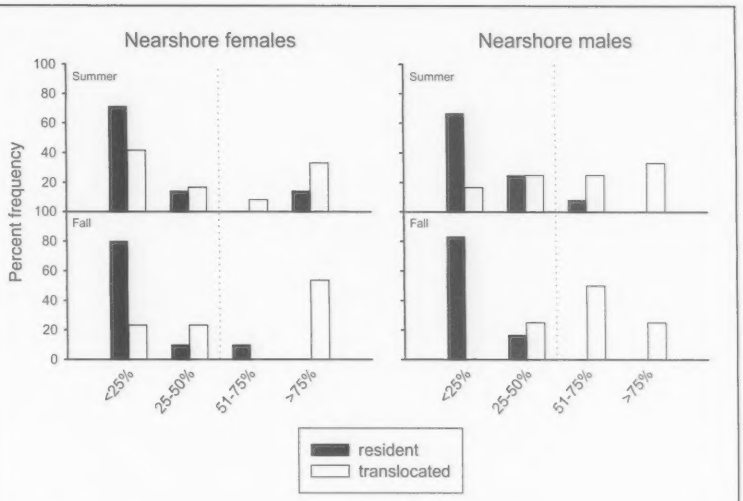

Figure 6

The percentage of gametogenic tissue of resident nearshore and translocated nearshore queen conch (*Strombus gigas*) by sex and season. The dotted line separates the categories that were combined for statistical analyses.

and fall (Table 4). Most resident offshore males had >75% gametogenic tissue throughout the study period, whereas most resident nearshore males had <25% (Fig. 4).

The gonadal condition of translocated nearshore males (Fig. 2F) improved in relation to the gonadal condition of resident nearshore males (Fig. 2D). There were significant differences in gonadal maturity between translocated nearshore and resident nearshore males during both the summer and fall (Table 5). Almost 80% of the translocated nearshore males were ripe during the summer, whereas about half of the resident nearshore males were incapable of reproducing (Fig. 5). By fall, most translocated nearshore males were still capable of reproduction, whereas none of the resident nearshore males were (Fig. 5). There were also significant differences in the percentage of gametogenic tissue between resident nearshore and translocated nearshore males during the summer and fall (Table 5). During the summer, the gonads of most of the resident nearshore males contained <25% gametogenic tissue, whereas translocated nearshore males were divided equally among the four gametogenic tissue categories (Fig. 6). During the fall, the gonads of most of the resident nearshore males still had <25% gametogenic tissue; however, most translocated nearshore males had developed >50% of the gonad (Fig. 6).

Table 5

Probabilities from Fisher's exact test of differences in gonadal maturity and the percentage of gametogenic tissue between resident nearshore and translocated nearshore conch by sex and season. *n* represents the total number of observations. Asterisks (*) indicate that the test was statistically significant.

	Females		Males	
	n	*P*	*n*	*P*
Gonadal maturity				
Summer	26	0.019*	24	0.045*
Fall	23	<0.001*	10	0.033*
% gametogenic tissue				
Summer	26	0.130	24	0.014*
Fall	23	0.038*	10	0.033*

Discussion

In the nearshore region of the Florida Keys, adult queen conch had severe deficiencies in reproductive behavior and gonadal development. Histological examinations of resident nearshore conch revealed that most were incapable of reproducing, whereas resident offshore conch exhibited a normal reproductive cycle (as described by Egan, 1985, and Stoner et al., 1992). Furthermore, our results suggest that female conch may be more sensitive to the negative effects of nearshore conditions than male conch. For example, during the spring and summer, some resident nearshore males were ripe (although their reproductive output would have been severely reduced because of a low percentage of gametogenic tissue), whereas the gonads of

most resident nearshore females contained no germ cells. The latter condition may have been due to the fact that egg production is more costly bioenergetically than sperm production (Ricklefs, 1990).

Mating and spawning do not occur among resident nearshore conch presumably because of their retarded gonadal development; however, the translocation of nearshore conch to the offshore region mitigated the deleterious effects that the nearshore environment had on their gonadal development. The reproductive tissues of translocated nearshore conch began to develop during the summer after the conch had spent about three months offshore. Most translocated female conch were in the early stages of gonadal development, whereas most translocated male conch were ripe. We believe this difference in gonadal development is due to the fact that the starting gonadal condition of nearshore females was worse than the starting condition of male conch. By fall, after six months offshore, most translocated females had become ripe. In addition, the percentage of gametogenic tissue in the gonads of both sexes increased through the summer and fall.

In conjunction with the improvement in gonadal condition, nearshore females translocated to the offshore region were observed spawning during the summer and fall; however, no mating was observed among nearshore conch translocated offshore. Resident offshore conch also had low mating frequencies (<6%). Similarly low mating frequencies have been reported in the Virgin Islands (Randall, 1964) and the Bahamas (Stoner et al., 1992). We suspect that the lack of observations of nearshore conch mating in the offshore region may have been an artifact of the low probability of encountering that activity due to the small number of nearshore conch translocated offshore. Nevertheless, we believe mating must have occurred because translocated nearshore conch were observed spawning. However, it is unknown if queen conch are capable of laying unfertilized egg masses.

The beginning of reproductive activity in queen conch is linked to the start of spring, when water temperatures begin rising (Randall, 1964; Stoner et al., 1992; Weil and Laughlin, 1984). This same seasonal pattern was observed in our study with resident offshore conch. They exhibited the highest mating and spawning frequencies during the spring and reproductive behavior decreased during the ensuing seasons. However, compared with the spawning pattern of resident offshore conch, peak spawning in translocated nearshore conch was delayed; peak spawning occurred during the fall. Nevertheless, there was evidence to suggest that the timing of reproductive behavior of both resident offshore and translocated nearshore conch might eventually become similar. Our results indicated that it takes at least three months after translocation for the negative effects of the nearshore environment to be mitigated and for gonadal maturation to occur. The out-of-phase spawning may have been prevented if the translocations had occurred earlier in the year (e.g., January, instead of March).

Identifying the causative factor or factors that inhibit the reproductive viability of nearshore queen conch requires further study. However, the juxtaposition of the nearshore conch aggregations with human population centers suggests that anthropogenic changes to the nearshore region may be partially responsible. Decreased reproductive output caused by anthropogenic contaminants has been observed in several marine invertebrates, including dogwinkles (*Nucella lapillus*) (Bryan et al., 1987; Gibbs and Bryan, 1986), scallops (Gould et al., 1988), sea urchins (Krause, 1994; Thompson et al., 1989), and shrimps and crabs (Wilson-Ormond et al., 1994). For example, chronic exposure to tributyltin has been shown to sterilize females of several species of mollusks (Matthiessen and Gibbs, 1998), and sublethal levels of copper greatly inhibited gamete production and maturation in scallops (Gould et al., 1988). There have also been numerous reports implicating eutrophication in nearshore habitat degradation in the Florida Keys (Lapointe et al., 1990; Lapointe and Clark, 1992; Szmant and Forrester, 1996); however, very little is known about the effects of increased nutrient levels at the organismal level.

The retarded gonadal condition in nearshore queen conch may also be due to environmental factors such as suboptimal habitat, poor food quality, or temperature extremes associated with shallow water. Research on bivalves has shown that habitat, diet, and food quality directly affect gamete production (Le Pennec et al., 1998; Madrones-Ladja et al., 2002). As they increase in age and size, queen conch undergo ontogenetic migrations from shallow, nearshore sites to deeper-water habitats (Randall, 1964; Sandt and Stoner, 1993; Stoner, 1989; Weil and Laughlin, 1984). It has been hypothesized that as conch grow larger and require more food, they migrate to take advantage of the augmented food supply in more productive offshore habitats (Sandt and Stoner, 1993; Stoner, 1989). However, nearshore queen conch in the Florida Keys are prevented from migrating offshore by Hawk Channel (Glazer and Berg, 1994). Therefore, translocating nearshore conch offshore would, in effect, link these isolated environments.

The implications of this study are of particular importance to the FWC-Florida Marine Research Institute's ongoing queen conch stock restoration program. Translocating naturally recruiting nearshore conch to offshore areas would be more cost effective than hatchery production of juvenile conch, especially because production costs are eliminated and survival of translocated conch is likely to be much greater than that of hatchery outplants (see Stoner, 1997, for a review of juvenile mortality in stock enhancement efforts). Translocations would also have a more immediate effect on reproductive output than would the release of hatchery-reared conch. A translocation program would focus on moving large juveniles and adults offshore, whereas a hatchery program must release small juveniles (to minimize production costs) that would then have to survive to maturity. Consequently, translocations would quickly alleviate the depensatory mechanisms described by Appeldoorn (1995) that can affect the recovery of queen conch stocks. Finally, translocations provide the added benefit of maintaining the genetic diversity of the population. Hatchery-reared conch are typically derived from a few egg masses and there is a concurrent loss in

rare alleles (Allendorf and Ryman, 1987). However, the use of wild conch to enhance the spawning aggregations eliminates this problem.

Queen conch appear to be a prime candidate for rehabilitation by translocation because they meet the criteria associated with successful translocations reported by Griffith et al. (1989). These factors include release within the historical range of the species or into areas of increased habitat quality (or both). Additionally, herbivorous animals stand a greater chance of translocation success than do carnivores or omnivores. Lastly, wild animals translocate more successfully than captive-bred animals. According to these parameters, queen conch are ideally suited for translocations.

However, before a full-scale translocation program can be implemented, there are some theoretical considerations that must be addressed. For example, Stoner and Ray-Culp (2000) reported that conch reproductive behavior reached an asymptotic level near 200 conch/ha.; therefore, it would seem advantageous to enhance reproductive aggregations to that density. However, without high habitat quality, translocations have low success rates regardless of how many animals are released (Griffith et al., 1989). First, we must ascertain if offshore habitats can support the added number of conch or if the translocated or native animals (or both) will simply disperse after release because of density-dependent factors (e.g., intraspecific competition for limited resources). Conch grazing has been shown to significantly reduce the biomass of seagrass macrodetritus and epiphytes (Stoner, 1989). In addition, the effects of removing nearshore conch from the nearshore environment need to be investigated.

Additionally, if increased recruitment is the ultimate goal of the translocation program, larvae must survive and be retained within the Florida Keys. At this point, it is unknown whether larvae produced from translocated nearshore conch are viable or as viable as the larvae produced by native offshore conch. Furthermore, the relative contribution of local and upstream sources to recruitment is unknown. Stoner et al. (1996, 1997) suggested that most of the queen conch larvae entering the Florida Keys come from upstream sources. If this is indeed the case, then local translocations will not be as effective as an international or regional management strategy. However, mechanisms for larval retention in the Florida Keys have been described by Lee and Williams (1999), who suggested that the periodic formation of gyres in the lower Keys may facilitate the retention and recruitment of locally produced larvae. If larvae are retained within the Florida Keys system, any increase in local larval production will increase larval supply and may increase recruitment. Therefore, translocation sites should be located in the lower Keys in order to ensure maximum larval retention and recruitment.

The present study has shown that translocation may be a viable method for rehabilitating queen conch populations in the Florida Keys. We have demonstrated that nearshore conch that were translocated offshore regained some of their reproductive capacity and abilities. Therefore, moving conch from nearshore larval sinks to offshore larval sources may be the key to expediting the recovery of queen conch stocks. Further research (e.g., larval retention studies, studies on the effect of water quality on larval survival, carrying capacity studies) and monitoring will determine the efficacy of this restoration strategy.

Acknowledgments

John Hunt, William Sharp, James Colvocoresses, Allan Stoner, and one anonymous reviewer provided insightful comments on the manuscript. Judy Leiby and Jim Quinn provided editorial comments. We thank Mary Enstrom and Sherry Dawson of The Nature Conservancy (TNC) as well as the numerous TNC volunteers who participated in the field surveys. Meaghan Darcy and other staff members at the Florida Marine Research Institute assisted in the field and in sample processing. This project was funded by Partnerships for Wildlife Grant no. P-3 from the U.S. Fish and Wildlife Service and by the Florida Fish and Wildlife Conservation Commission.

Literature cited

Allendorf, F. W., and N. Ryman.
1987. Genetic management of hatchery stocks. *In* Population genetics and fishery management (N. Ryman and F. Utter, eds.), p. 141–59. Washington Sea Grant, Washington D.C.

Appeldoorn, R. S.
1995. Potential depensatory mechanisms operating on reproductive output in gonochoristic molluscs, with particular reference to strombid gastropods. ICES Mar. Sci. Symp. 199:13–18.

Berg, Jr., C. J., and R. A. Glazer.
1995. Stock assessment of a large marine gastropod (*Strombus gigas*) using randomized and stratified towed-diver censusing. ICES Mar. Sci. Symp. 199:247–258.

Bryan, G. W., P. E. Gibbs, G. R. Burt, and L. G. Hummerstone.
1987. The effects of tributyltin (TBT) accumulation on adult dog-whelks, *Nucella lapillus*: Long-term field and laboratory experiments. J. Mar. Biol. Assoc. U.K. 67:525–544.

Edwards, A. J. and S. Clark.
1999. Coral transplantation: a useful management tool or misguided meddling? Mar. Pollut. Bull. 37:474–487.

Egan, B. D.
1985. Aspects of the reproductive biology of *Strombus gigas*. M.S. thesis, 147 p. Univ. British Colombia, Vancouver, Canada.

Garcia, A., R. Adaya, and G. Ceballos.
1996. Sea turtle conservation in Cuixmala, Jalisco: the role of nest translocation in small beaches. Bull. Ecol. Soc. Am. 77:155.

Gibbs, P. E., and G. W. Bryan.
1986. Reproductive failure in populations of the dog-whelk, *Nucella lapillus*, caused by imposex induced by tributyltin from antifouling paints. J. Mar. Biol. Assoc. U.K. 66:767–777.

Glazer, R. A., and C. J. Berg Jr.
1994. Queen conch research in Florida: an overview. *In* Queen conch biology, fisheries, and mariculture (R. S. Appeldoorn and B. Rodriguez, eds.), p. 79–95. Fundación Cientifica Los Roques, Caracas, Venezuela.

Glazer, R. A., and G. A. Delgado.
2003. Towards a holistic strategy to managing Florida's queen conch (*Strombus gigas*) population. *In* El Caracol *Strombus gigas*: conocimiento integral para su manejo sustentable en el Caribe (D. Aldana Aranda, ed.), p. 73–80. CYTED (Programa Iberoamericano de Ciencia y Technología para el Desarrollo), Yucatán, México.

Glazer, R. A., and I. Quintero.
1998. Observations on the sensitivity of queen conch to water quality: implications for coastal development. Proc. Gulf Carib. Fish. Inst. 50:78–93.

Gould, E., R. J. Thompson, L. J. Buckley, D. Rusanowsky, and G. R. Sennefelder.
1988. Uptake and effects of copper and cadmium in the gonad of the scallop *Placopecten magellanicus*: concurrent metal exposure. Mar. Biol. 97:217–223.

Griffith, B., J. M. Scott, J. W. Carpenter, and C. Reed.
1989. Translocation as a species conservation tool: status and strategy. Science 245:477–480.

Harig, A. L., K. D. Fausch, and M. K. Young.
2000. Factors influencing success of greenback cutthroat trout translocations. North Am. J. Fish. Manag. 20:994–1004.

Krause, P. R.
1994. Effects of an oil production effluent on gametogenesis and gamete performance in the purple sea urchin (*Strongylocentrotus purpuratus* Stimpson). Environ. Toxicol. Chem. 13:1153–1161.

Lapointe, B. E. and M. W. Clark.
1992. Nutrient inputs from the watershed and coastal eutrophication of the Florida Keys. Estuaries 15:465–476.

Lapointe, B. E., J. D. O'Connell, and G. Garrett.
1990. Nutrient couplings between on-site sewage disposal systems, groundwaters, and nearshore surface waters of the Florida Keys. Biogeochem. 10:289–307.

Le Pennec, M., R. Robert, and M. Avendano.
1998. The importance of gonadal development on larval production in pectinids. J. Shellfish Res. 17:97–101.

Lee, T. N., and E. Williams.
1999. Mean distribution and seasonal variability of coastal currents and temperature in the Florida Keys with implications for larval recruitment. Bull. Mar. Sci. 64:35–56.

Madrones-Ladja, J. A., M. R. dela Peña, and N. P. Parami.
2002. The effect of micro algal diet and rearing condition on gonad maturity, fecundity, and embryonic development of the window-pane shell, *Placuna placenta* Linnaeus. Aquaculture 206:313–321.

Matthiessen, P., and P. E. Gibbs.
1998. Critical appraisal of the evidence for tributyltin-mediated endocrine disruption in mollusks. Environ. Toxicol. Chem. 17:37–43.

McCarthy, K. J., C. T. Bartels, M. C. Darcy, G. A. Delgado, and R. A. Glazer.
2002. Preliminary observation of reproductive failure in nearshore queen conch (*Strombus gigas*) in the Florida Keys. Proc. Gulf Carib. Fish. Inst. 53:674–680.

Morgan, L. E. and L. W. Botsford.
2001. Managing with reserves: Modeling uncertainty in larval dispersal for a sea urchin fishery. *In* Spatial processes and management of marine populations (G. H. Kruse, N. Bez, A. Booth, M. W. Dorn, S. Hills, R. N. Lipcius, D. Pelletier, C. Roy, S. J. Smith, and D. Witherell, eds.), p. 667–684. Alaska Sea Grant, AK-SG-01-02. Univ. Alaska, Fairbanks, Alaska.

Randall, J. E.
1964. Contributions to the biology of the queen conch, *Strombus gigas*. Bull. Mar. Sci. 14:246–295.

Ricklefs, R. E.
1990. Ecology. 3rd ed., 896 p. W.H. Freeman and Co., New York, NY.

Rinkevich, B.
1995. Restoration strategies for coral reefs damaged by recreational activities: the use of sexual and asexual recruits. Restoration Ecology 3:241–251.

Sandt, V. J. and A. W. Stoner.
1993. Ontogenetic shift in habitat by early juvenile queen conch, *Strombus gigas*: patterns and potential mechanisms. Fish. Bull. 91:516–525.

Stoner, A. W.
1989. Winter mass migration of juvenile queen conch *Strombus gigas* and their influence on the benthic environment. Mar. Ecol. Prog. Ser. 56:99–104.
1997. The status of queen conch, *Strombus gigas*, research in the Caribbean. Mar. Fish. Rev. 59:14–22.

Stoner, A. W., R. A. Glazer, and P. J. Barile.
1996. Larval supply to queen conch nurseries: relationships with recruitment process and population size in Florida and the Bahamas. J. Shellfish Res. 15:407–420.

Stoner, A. W., N. Mehta, and T. N. Lee.
1997. Recruitment of *Strombus* veligers to the Florida Keys reef tract: relation to hydrographic events. J. Shellfish Res. 16:19–29.

Stoner, A. W. and M. Ray-Culp.
2000. Evidence for allee effects in an over-harvested marine gastropod: density-dependent mating and egg production. Mar. Ecol. Prog. Ser. 202:297–302.

Stoner, A. W., V. J. Sandt, and I. F. Boidron-Metairon.
1992. Seasonality in reproductive activity and larval abundance of queen conch, *Strombus gigas*. Fish. Bull. 90:161–170.

Szmant, A. M., and A. Forrester.
1996. Water column and sediment nitrogen and phosphorous distribution patterns in the Florida Keys, USA. Coral Reefs 15:21–41.

Thompson, B. E., S. M. Bay, J. W. Anderson, J. D. Laughlin, D. J. Greenstein, and D. T. Tsukada.
1989. Chronic effects of contaminated sediments on the urchin *Lytechinus pictus*. Environ. Toxicol. Chem. 8:629–637

van Treeck, P. and H. Schuhmacher.
1997. Initial survival of coral nubbins transplanted by a new coral transplantation technology-options for reef rehabilitation. Mar. Ecol. Prog. Ser. 150:287–292.

Weil, E., and R. Laughlin.
1984. Biology, population dynamics, and reproduction of the queen conch *Strombus gigas* Linne in the Archipielago de los Roques National Park. J. Shellfish Res. 4:45–62.

Wilson-Ormond, E. A., M. S. Ellis, and E. N. Powell.
1994. The effect of proximity to gas producing platforms on size, stage of reproductive development and health in shrimp and crabs. J. Shellfish Res. 13:306.

Zar, J. H.
1996. Biostatistical analysis, 3rd ed., 662 p. Prentice Hall, Upper Saddle River, NJ.

Genetic differentiation among Atlantic cod (*Gadus morhua*) from Browns Bank, Georges Bank, and Nantucket Shoals

Christopher Lage

Department of Biological Sciences
Murray Hall
University of Maine
Orono, Maine 04469

Kristen Kuhn

Irv Kornfield

School of Marine Sciences
Murray Hall
University of Maine
Orono, Maine 04469

E-mail address (for I. Kornfield, contact author): irvk@maine.edu

Abstract—This study examines genetic variation at five microsatellite loci and at the vesicle membrane protein locus, pantophysin, of Atlantic cod (*Gadus morhua*) from Browns Bank, Georges Bank, and Nantucket Shoals. The Nantucket Shoals sample represents the first time cod south of Georges Bank have been genetically evaluated. Heterogeneity of allelic distribution was not observed ($P>0.05$) between two temporally separated Georges Bank samples indicating potential genetic stability of Georges Bank cod. When Bonferroni corrections ($\alpha=0.05$, $P<0.017$) were applied to pairwise measures of population differentiation and estimates of F_{ST}, significance was observed between Nantucket Shoals and Georges Bank cod and also between Nantucket Shoals and Browns Bank cod. However, neither significant differentiation nor significant estimates of F_{ST} were observed between Georges Bank and the Browns Bank cod. Our research suggests that the cod spawning on Nantucket Shoals are genetically differentiated from cod spawning on Browns Bank and Georges Bank. Managers may wish to consider Nantucket Shoals cod a separate stock for assessment and management purposes in the future.

Manuscript approved for publication 5 November 2003 by Scientific Editor.

Manuscript received 20 January 2004 at NMFS Scientific Publications Office.

Fish. Bull. 102:289–297 (2004).

The Atlantic cod (*Gadus morhua*) is a migratory gadid found on both sides of the North Atlantic. In the Northwest Atlantic, cod are distributed nearly continuously along the continental shelf from Greenland to North Carolina, spawning in relatively discrete, temporally stable areas, and different regions are regarded as different management units defined primarily by latitude and bathymetry (Ruzzante et al., 1998). Atlantic cod historically supported economically important fisheries in the Northwest Atlantic (Halliday and Pinhorn, 1996). In U.S. waters, cod are assessed and managed as two stocks: 1) Gulf of Maine and 2) Georges Bank and southward (including Nantucket Shoals). Growth rates differ between the two stocks; growth is slower in the Gulf of Maine compared to growth in Georges Bank (Pentilla et al., 1989); each stock is exploited by the same gear type and may show similar biological responses towards such gear selection. Although both stocks support important commercial and recreational fisheries, each is overexploited and remains at a low biomass level (Mayo and O'Brien, 1998; O'Brien and Munroe, 2001; Mayo et al., 2002). Overexploitation may result in significant life-history changes such as a decline in time to reproductive maturity which has been observed in Georges Bank cod (O'Brien, 1998); such changes may be a compensatory response to overfishing but may also be influenced by shifts in underlying genetic control (Policansky, 1993).

Commercial fisheries are conducted year round, using primarily otter trawls and gill nets. The Canadian fishery on Georges Bank is managed under an individual quota system. United States cod fisheries are managed under the New England Fishery Management Council's Northeast Multispecies Fishery Management Plan (FMP)[1] as implemented by the U.S. Federal Register, 50 CFR Part 648 (U.S. Federal Register, 2003). Under this FMP, cod are included in a complex of 15 groundfish species managed by time and area closures, trip limits, gear restrictions, minimum size limits, days-at-sea restrictions, and a permit moratorium. The FMP's goal is to reduce fishing mortality to levels that will allow stocks within the complex to initially rebuild above minimum biomass thresholds, and, ultimately, to remain at or near target levels.

When ecological and evolutionary processes are responsible for stock structuring, it is necessary to incorpo-

[1] New England Fishery Management Council. 2003. Northeast Multispecies Fishery Management Plan. NEFMC, 50 Water St., Mill 2, Newburyport, MA, 01950

rate them into strategies designed to manage exploited species (Avise, 1998). High dispersive capabilities of many marine fish often correlate with low levels of population divergence over vast areas (Ward et al., 1994; Graves, 1998) and may be particularly true for species characterized by high fecundity, large population size, and potentially long-distance egg and larval dispersal. Although marine fish predominantly have high dispersal rates and low levels of population structuring, migratory species with continuous distributions may develop and maintain stock structure if they show fidelity to natal spawning sites or limited egg and larval dispersal. Fidelity to natal grounds has been shown in Greenland-Iceland cod (Frank, 1992) and Georges Bank haddock (Polacheck et al., 1992). Genetic divergence between areas originates when populations are formed or through the restriction of gene flow. Cod in some regions are known to migrate long distances, whereas in other regions they are nearly stationary (Lear and Green, 1984). Tagging studies in the Gulf of Maine show little exchange between the region east of Browns Bank and Georges Bank, and the inner Gulf of Maine (Hunt et al., 1999); however exchange has been reported among Bay of Fundy, southern Nova Scotia, Browns Bank, and Georges Bank populations (Klein-MacPhee, 2002). Such exchange among cod from different management areas may be important for stock assessments and management practices. Determining underlying genetic structure of spawning stocks is paramount to the conservation and management of overexploited species.

In the last 30 years the use of molecular-based studies in fisheries science has become common (Shaklee and Bentzen, 1998). In cod, a number of studies have used allozymes (Moller, 1968; Jamieson, 1975; Cross and Payne, 1978; Dahle and Jorstad, 1993), but their use and sensitivity are limited because of weak statistical power resulting from low levels of polymorphism and because of processes of balancing selection (Mork et al., 1985; Pogson et al., 1995). Mitochondrial DNA (mtDNA) characterization among Northwest Atlantic cod indicates that there is limited, albeit significant, population structuring throughout most the species' range (Smith et al., 1989; Carr and Marshall, 1991; Pepin and Carr, 1993; Carr et al., 1995; Arnason and Palsson, 1996). Genetic divergence at the vesicle membrane protein locus, pantophysin (*Pan*I), originally called *GM*798 and identified as synaptophysin (*Syp*I) (Fevolden and Pogson, 1997), has been reported among populations of cod from the Northwest Atlantic (Pogson, 2001; Pogson et al., 2001), Norway and the Arctic (Fevolden and Pogson, 1997), and Iceland (Jonsdottir et al., 1999, 2002). High levels of variation have been reported at nuclear RFLP loci (Pogson et al., 1995; Pogson et al., 2001), and especially at microsatellite loci (Bentzen et al., 1996; Ruzzante et al., 1996a, 1996b, 1997, 1998; Beacham et al., 1999; Miller et al., 2000; Ruzzante et al., 2000, 2001). By using microsatellites, significant genetic structuring has been detected among cod populations on major continental shelves and on neighboring banks that are separated by deep channels and have gyre-like circulation patterns hypothesized to act as retention mechanisms for eggs and larvae (Ruzzante et al., 1998). Although both Browns and Georges Bank maintain persistent gyre-like circulation patterns that may act to retain eggs and larvae, they are separated by the Fundian Channel (>260 m) which may pose a barrier to juvenile and adult migration (Klein-MacPhee, 2002). Evaluation of Northwest Atlantic haddock by using microsatellites showed similarly significant stock structuring from Newfoundland to Nantucket Shoals (Lage et al., 2001). Current assessment and management of cod in U.S. waters combine Georges Bank with the regions to its south including Nantucket Shoals. This study investigates genetic stock structure among cod from this region and provides additional insight for scientists and managers.

Materials and methods

Sampling

Samples of adult cod were collected through the U.S. National Marine Fisheries Service and the Canadian Department of Fisheries and Oceans groundfish surveys between 1994 and 2000. Adult cod were obtained from each of the following spawning grounds (Fig. 1): Browns Bank (July 1994, n=30), Georges Bank (March 1994, n=48; March 1999, n=96; Σn=144), and Nantucket Shoals (March 2000, n=97). Blood or tissue (or both) was obtained from individual fish and preserved in 95% ethanol for subsequent DNA extraction.

DNA extraction, amplification, and visualization

DNA was extracted by using either a Qiamp DNA Mini Kit (Qiagen Inc., Valencia, CA) or by following a published protocol designed for nucleated blood cells (Ruzzante et al., 1998). Five microsatellite loci—*Gmo*1, *Gmo*132 (Brooker et al., 1994), *Gmo*8, *Gmo*19, *Gmo*34 (Miller et al., 2000), and the pantophysin locus, *Pan*I (Fevolden and Pogson, 1997; Pogson, 2001)—were used to evaluate genetic diversity. Polymerase chain reactions (PCR) of all loci were performed in an Eppendorf Mastercycler Gradient thermal cycler. Final concentrations of reagents in a 25 μL PCR cocktail were as follows: ~10 ng of genomic DNA, 1×PCR buffer pH 9.5 [10 mM KCl, 20 mM Tris-HCl pH 8.3, 10 mM $(NH_4)_2SO_4$], 1.5 mM $MgCl_2$, 200 μM each dNTP, 0.15 μM forward primer, 0.15 μM reverse primer (unlabeled for the *Pan*I locus and 5'-labeled with a TET, FAM, or HEX ABI dye for all microsatellite loci), and 0.75 units of Taq DNA polymerase. PCR conditions were as follows: initial 5 min at 95°C, 30 cycles of denaturing at 95°C for 1 min, annealing at 50°C (*Gmo*8, *Gmo*19, and *Gmo*34), 55°C (*Pan*I), and 57°C (*Gmo*1 and *Gmo*132) for 1 min 30 s, and extending at 72°C for 1 min 30 s with a final extension of 72°C for 10 min. *Gmo*19 and *Gmo*34, as well as *Gmo*1 and *Gmo*132, were multiplexed in two 25 μL PCR reactions. Flourescent microsatellite PCR products were visualized on an ABI377 automated DNA sequencer (Perkin-Elmer Corporation, Foster City, CA) and were analyzed by using GeneScan (vers. 2.1) and Genotyper (vers. 2.1) software programs (Perkin-Elmer Corporation, Foster City, CA). *Pan*I PCR

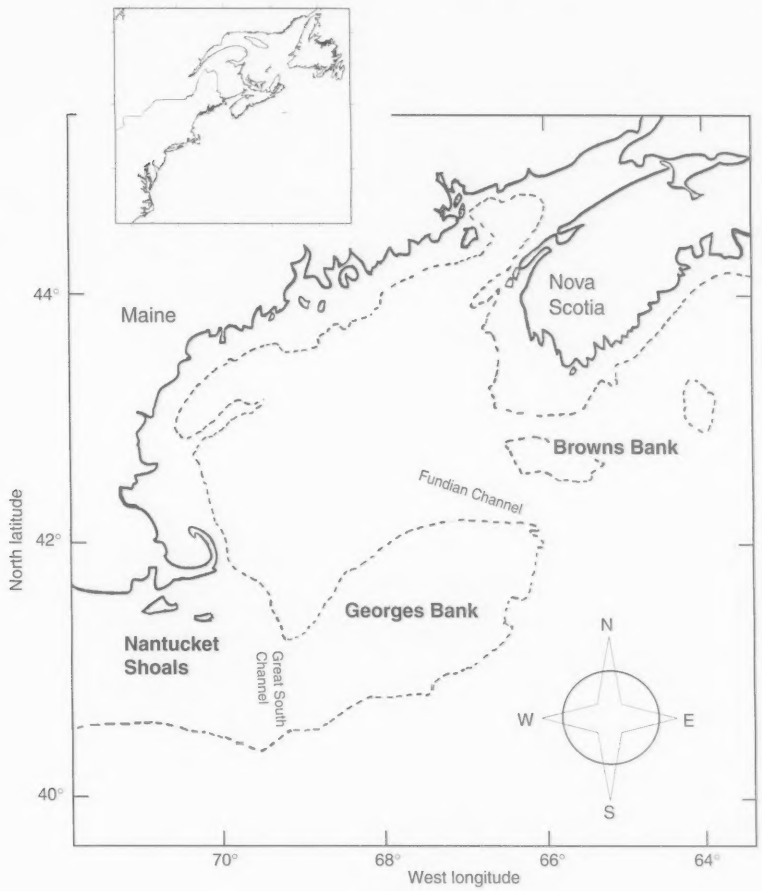

Figure 1

Map of Northwest Atlantic sampling regions for Atlantic cod (*Gadus morhua*). Dashed lines indicate the 100-m isobath.

products were digested with the restriction endonuclease *Dra*I for at least 2 hours at 37°C and visualized on 2% agarose gels to determine presence of *Pan*I^{A} or *Pan*I^{B} (or both) allelic variants.

Genetic analyses

Samples were tested for conformation to Hardy-Weinberg equilibrium (HWE) expectations by the Markov chain method (Guo and Thomson, 1992) by resampling 2000 iterations per batch for 200 batches with GENEPOP vers. 3.1d (CEFE/CNRS, Montpelier, France; available at http://www.cefe.cnrs-mop.fr/) (Raymond and Rousset, 1995); the null hypothesis tested was random union of gametes within a population. All loci were tested for genotypic disequilibrium across the entire data set, as well as for individual populations by using Markov chain resampling with 2000 iterations per batch for 200 batches in GENEPOP vers. 3.1d; the null hypothesis tested was that the genotypes at one locus are independent from genotypes at the other locus.

Tests of allelic and genotypic differentiation among and between population samples were conducted by using FSTAT 2.9.1 (UNIL, Lausanne, Switzerland; available at http://www.unil.ch/izea/softwares/fstat.html) (Goudet, 1995); the null hypothesis tested was homogeneous distributions across samples. Because alleles can be considered as independent when samples conform to HWE, it is valid to permute alleles among samples to test for population differentiation. On the other hand, when HWE is rejected within samples, alleles within an individual cannot be considered independent, and thus permuting genotypes among samples is the only valid permutation scheme. In both cases, contingency tables were generated and classified by using the log-likelihood statistic G (Goudet et al, 1996). Estimates of among- and between-sample F_{ST}'s were generated according to Weir and Cocherham (1984) with FSTAT vers. 2.9.1 and GENETIX vers. 4.04 (available

Table 1

Genetic variation in sampled populations of Atlantic cod (*Gadus morhua*) and *P*-value (in parentheses) for among sample population differentiation. n = observed number of alleles; H_0 = observed heterozygosity; F_{ST} = the among-sample *P*-value); bp = base pairs; * = significant deviation from HWE (α=0.05, P<0.0083); † = P <0.05; ‡ P= ≤0.001

			Browns Bank		Georges Bank		Nantucket Shoals			
Locus	Σn	Allelic range	H_0	n	H_0	n	H_0	n	F_{ST}	Differentiation
*Pan*I	2	*Pan*I^A/*Pan*I^B	0.0385	2	0.0397	2	0.0222	2	−0.0052 (0.767)	0.7820
*Gmo*1	5	96–110 bp	0.1000	4	0.1319	5	0.1505	5	0.0019 (0.307)	0.3210
*Gmo*8	23	118–201 bp	0.8929	17	0.8370	19	0.8444*	20	0.0001 (0.437)	0.5200
*Gmo*19	26	120–237 bp	0.8846	17	0.8148*	25	0.7975*	23	−0.0021 (0.857)	0.8320
*Gmo*34	11	82–120 bp	0.7778	5	0.5683	11	0.6630	7	−0.0033 (0.797)	0.8400
*Gmo*132	21	105–155 bp	0.8333	13	0.8214	17	0.7727	16	0.0255 (0.000)‡	0.0010‡
All loci	88	—	—	—	—	—	—	—	0.0047 (0.001)‡	0.0240†

at http://www.univ-montp2.fr/~genetix/genetix/genetix.htm) (Belkhir et al.[2]). Significance of F_{ST} estimates was determined with 2000 randomizations. Tests of population differentiation and estimations of F_{ST} were calculated at each locus individually and at all loci combined. To correct for simultaneous comparisons, standard Bonferroni corrections were applied by using a global significance level of 0.05 (Rice, 1989).

Results

Genetic variation

Observed numbers of alleles, allelic ranges, heterozygosities, and deviations from HWE are presented in Table 1. All tests of genotypic linkage disequilibrium were nonsignificant at the global and population levels. When Bonferroni corrections for multiple tests were applied to tests of HWE (α=0.05, P<0.0083), the pooled Georges Bank sample deviated significantly at *Gmo*19, and the Nantucket Shoals sample deviated at *Gmo*8 and at *Gmo*19. Interestingly, these two loci have the greatest variation based on number of alleles and heterozygosity. In each case, the cause of deviation was due to an excess of homozygotes. Population samples that generally conform to expectations of random mating but show a lack of concordance to HWE at one or more loci may be due to a number of processes including null alleles, genetic drift, admixture, selection, and insufficient sampling (e.g., Ruzzante, 1998). Possible explanations of homozygote excess include sample admixture (Wahlund effect) or drift; however these explanations are unlikely because one would expect to see similar results at all loci. More likely explanations are the presence of null alleles or selection. Deviations of HWE at *Gmo*8 and *Gmo*19 were not observed in all population samples, indicating that null alleles were not present at a global-level but may be present at the population-level for these two loci. Subsequently, any significant population structuring observed at these loci should be viewed with caution (see below).

Population structure

Tests of population structure are shown in Table 2. Although *Gmo*8 and *Gmo*19 showed significant deviations from HWE, they did not support any significant population structuring even when tests of population differentiation were performed without assuming conformation to HWE (i.e., permuting among genotypes rather than alleles). Heterogeneity of allelic distribution was not observed (P>0.05) between the 1994 and 1999 Georges Bank samples at each locus individually and at all loci combined, thus indicating potential genetic stability of Georges Bank cod. These samples were subsequently pooled to form a single Georges Bank population sample to facilitate statistical analyses by allowing for better estimations of allele frequencies and by reducing the number of pairwise tests. Tests of population differentiation among samples showed significant divergence at *Gmo*132 (P<0.01) and at all loci combined (P<0.05). When Bonferroni corrections were applied to pairwise measures of divergence (α=0.05, P<0.017), significance was observed between Nantucket Shoals and Georges Bank at *Gmo*132 and at all loci combined, and also between Nantucket Shoals and Browns Bank at *Gmo*132. No significant differentiation was observed between individual or pooled Georges Bank samples and the Browns Bank sample.

Significant among-population F_{ST} values were estimated at *Gmo*132 (0.0255, P<0.001) and at all loci combined (0.0047, P<0.01). When Bonferroni corrections were applied, significant pairwise-population F_{ST} values were estimated between Nantucket Shoals and Browns Bank at *Gmo*132 (0.0624, P<0.001) and at all loci combined

[2] Belkhir K., P. Borsa, L. Chikhi, N. Raufaste, and F. Bonhomme. 2002. GENETIX 4.04, logiciel sous Windows TM pour la génétique des populations. Laboratoire Génome, Populations, Interactions, CNRS UMR 5000, Université de Montpellier II, Montpellier (France).

Table 2

Genetic structuring in sampled populations of Atlantic cod (*Gadus morhua*): Above diagonal are *P*-values for pairwise differentiation. Below diagonal are pairwise F_{ST} values; upper values are for all loci combined; lower values are for *Gmo*132. * = $P < 0.0167$ ($\alpha = 0.05$ for three comparisons); ** = $P \leq 0.001$.

	Browns Bank	Georges Bank	Nantucket Shoals
Browns Bank	—	0.5440	0.2970
	—	0.1120	0.0020*
Georges Bank	0.0012	—	0.0030*
	0.0124	—	0.0010**
Nantucket Shoals	0.0114*	0.0045*	—
	0.0624**	0.0226**	—

(0.0114, $P<0.017$), and between Nantucket Shoals and Georges Bank at *Gmo*132 (0.0226, $P<0.001$) and at all loci combined (0.0045, $P<0.017$). Estimates of F_{ST} values between Browns Bank and Georges Bank samples were all nonsignificant. No significant genetic structuring was observed in any comparison when *Gmo*132 was excluded from the analysis.

Discussion

Georges Bank, a large, shallow offshore bank located along the southern edge of the Gulf of Maine off the U.S. and Canadian coasts (Fig. 1), supports a large fish biomass. High primary productivity and tightly bound system energetics on the bank result in relatively stable levels of overall biomass and total fish production, although major shifts in species composition routinely occur (Fogarty and Murawski, 1998). The largest spawning aggregation of cod on Georges Bank is found on the Northeast Peak, a gravel region that is an important habitat for the early demersal phase of cod, and may represent a limiting resource for this stock (Lough and Bolz 1989; Langton et al., 1996). The bank maintains its own circulation pattern in a slow clockwise gyre which may act as a transportation and retention mechanism for planktonic eggs and larvae (Smith and Morse, 1984; Lough and Bolz, 1989). There may be exchange of biota among regions by episodic fluxes of shelf water carrying eggs and larvae away from the Scotian Shelf and Browns Bank onto Georges Bank (Cohen et al., 1991; Townsend and Pettigrew, 1996; Bisagni and Smith, 1998). Once on Georges Bank, planktonic eggs and larvae may, depending on depth, be entrained and transported to gravel settlement sites along the western edge of Georges Bank (Smith and Morse 1984; Lough and Bolz, 1989; Werner et al., 1993). However, wind-driven advection may cause egg and larval loss from the Northeast Peak and southern flank of Georges Bank (Lough et al., 1989). Cod spawned in the Gulf of Maine usually drift southeasterly towards Georges Bank because of the counterclockwise Gulf of Maine gyre, but the extent of egg and larval exchange between these regions is unknown (Serchuk et al., 1994).

Cod have been found from the surface to depths greater than 450 meters; however few cod proximate to the Gulf of Maine occur deeper than 180 meters (Klein-MacPhee, 2002). Browns Bank and Georges Bank are bathymetrically separated by the relatively deep (>260 meters) Fundian Channel which may act as a barrier to adult migration, whereas Georges Bank and Nantucket Shoals are separated by the relatively shallow (<100 meters) Great South Channel. Although the latter channel is probably not a significant barrier to adult migration, it is an area of strong recirculation towards Georges Bank and could limit egg and larval dispersal. Tagging studies show little exchange of adults between the inner Gulf of Maine and the region east of Browns Bank and Georges Bank (Hunt et al., 1999), but limited exchange has been reported among the Bay of Fundy, southern Nova Scotia, Browns Bank, and Georges Bank (Klein-MacPhee, 2002).

The likelihood of determining correct population structure increases when population differentiation is stable over time (Waples, 1998). Results from this study are concordant with observations of temporal stability of microsatellite variation observed in Atlantic cod (Ruzzante et al., 1996a, 1997, 2001). Tests of population differentiation and subdivision cannot reject the maintenance of genetic homogeneity among Georges Bank cod from 1994 to 1999 and thus may indicate some degree of temporal genetic stability among adult Georges Bank cod.

Our results indicate that cod from Nantucket Shoals are genetically distinct from those from Browns Bank and Georges Bank, and cod from the two Banks are more genetically similar. The observed lack of heterogeneity between Browns Bank and Georges Bank is consistent with gene flow—perhaps due to episodic larval transport and some level of limited adult exchange. Nantucket Shoals cod may be genetically distinct because of egg and larval isolation by entrainment in the Georges Bank gyre or because of limited movement of adults between regions (or a combination of both). Eggs and larvae spawned on Nantucket Shoals most likely do not enter the Georges Bank gyre system; these early life history forms may be retained on the shoals or transported to the southwest by prevailing circulation (Fogarty and Murawski, 1998). Some North Atlantic cod stocks have shown substantial differences in

growth rate, reproductive capacity, and maturity schedules related to temperature (Brander, 1994). Cod within our study zone generally avoid water temperatures greater than 10°C, but Nantucket Shoals cod are abundant in temperatures as warm as 15°C (Klein-MacPhee, 2002). This differential thermal tolerance may support genetic structuring of Nantucket Shoals cod by selecting against individuals from other areas.

Closely related gadid species such as cod and haddock may exhibit similar patterns of population genetic structuring associated with similar life histories, selective pressures, and ecological constraints. Our results are concordant with a previous study suggesting that haddock from Browns Bank and Georges Bank are genetically similar and that haddock from Nantucket Shoals are distinct (Lage et al., 2001). However, Ruzzante et al. (1998) observed significant genetic differentiation between cod from Browns Bank and Georges Bank. Our results do not agree with this previously observed heterogeneity between Browns Bank and Georges Bank and may be due to the examination of different loci, different sampling comparisons, or small sample sizes used in both studies (or to a combination of these variables) (Ruzzante, 1998; Smouse and Chevillon, 1998).

Among loci, the greatest genetic differentiation was observed at locus *Gmo*132. Indeed, observed statistical significance of population differentiation and F_{ST} depends entirely on *Gmo*132. Length variation at *Gmo*132 is a function of mutations in the repetitive array and of an indel in a flanking region (Ruzzante et al., 1998) causing bimodal allele distributions in some populations. When compared to other microsatellite loci, *Gmo*132 has shown the greatest differentiation among other Northwest Atlantic cod populations (Bentzen et al., 1996; Ruzzante et al., 1998, 2001) and among Northwest Atlantic haddock populations (Lage et al., 2001) by an order of magnitude. Other loci examined have not shown similarly strong measures of population structuring. Observed genetic structuring may be due to forces currently determining regional larval and adult distributions, including bathymetry and oceanographic patterns. However, because similar genetic structuring is not observed at all loci, another potential explanation is that structuring at *Gmo*132 is due to forces that acted during the formation of populations rather than to forces presently maintaining strong reproductive isolation. Once genetic structure was generated during the formation of these populations subsequent to the last ice age, biological and oceanographic forces may have maintained such structure; other loci may show an absence of structure simply because it may not have been present when populations were formed. Pogson et al. (2001) reported that the recent age of populations, rather than extensive gene flow, may be responsible for weak population structure in Atlantic cod, and that interpreting limited genetic differences among populations as reflecting high levels of ongoing gene flow should be made with caution. This suggests that the observed lack of heterogeneity between Browns Bank and Georges Bank may not be due to high levels of ongoing gene flow, but to similarities between recently generated populations maintained by small but adequate levels of gene flow.

Alternatively, significant structuring associated with *Gmo*132 in both cod and haddock may suggest that selection is acting at this or at a linked locus. Although microsatellites themselves may be generally considered neutral, there is, in theory, potential for physical linkage or drift-generated linkage disequilibrium between microsatellite and functional loci. There is however, recent evidence of selection acting directly on microsatellite loci in tilapia in high-salinity environments. Streelman and Kocher (2002) found a strong functional genotype-environment interaction and suggested that microsatellite repeats of varying length might induce promoter conformations that differ in their capacity to bind transcriptional regulators. A potential selective mechanism to support the observed genetic structuring of Nantucket Shoals cod (and haddock) may be differential thermal tolerance, although this hypothesis remains untested.

There is strong evidence for an unusual mix of balancing and directional selection at the pantophysin (*Pan*I) locus in cod but no evidence of stable geographically varying selection among North Atlantic populations (Pogson, 2001; Pogson et al., 2001). In the present study, the *Pan*I locus showed little variation and no significant genetic structuring (Table 1). The observed lack of geographic structuring at *Pan*I provides no evidence for local adaptation. However, our observations may be due to strong balancing selection among the geographically proximate populations examined or, if *Pan*I is not under selection, insufficient variation to resolve genetic structure. Alternatively, this observed lack of genetic divergence at *Pan*I could be due to similarities among recently generated populations of North Atlantic cod.

Our research suggests that the cod spawning on Nantucket Shoals are genetically differentiated from cod spawning on Browns Bank and Georges Bank. Managers may wish to consider Nantucket Shoals cod as a separate stock for assessment and management purposes in light of current practices that combine Georges Bank with regions to the south as one management unit. Cod from within the Gulf of Maine can potentially migrate along the coast to Nantucket Shoals where there is little geographic barrier to adult movement. If this is true, the Nantucket Shoals sample that we analyzed may actually be representative of a mixed Gulf of Maine and Nantucket Shoals population. Additional analyses are needed to evaluate the hypothesis that Nantucket Shoals cod are genetically distinct from cod spawning within the Gulf of Maine. Further studies should address the issues of temporal stability and robust sampling and should incorporate cod samples from within the Gulf of Maine.

Acknowledgments

We thank three anonymous reviewers for their insightful comments. We thank the captains, crews, and scientists from the Canadian Department of Fisheries and Oceans and the United States. National Marine Fisheries Service. In particular, we would like to thank Chris Taggart, Nina Shepard, and Holly McBride for assistance in obtaining

samples. IK thanks Maryhaven for support. This work was funded by OCE9806712 from the U.S. National Science Foundation.

Literature cited

Arnason, E., and S. Palsson.
1996. Mitochondrial cytochrome b DNA sequence variation of Atlantic cod (*Gadus morhua*) from Norway. Mol. Ecol. 5:715–724.

Avise, J. C.
1998. Conservation genetics in the marine realm. J. Hered. 89:377–382.

Beacham, T. D., J. Brattey, K. M. Miller, L. D. Khai, and R. E. Withler.
1999. Population structure of Atlantic cod (*Gadus morhua*) in the Newfoundland and Labrador area based on microsatellite variation. DFO Canadian Stock Assessment Secretariat Research Document 99/35:1–32.

Bentzen, P., C. T. Taggart, D. E. Ruzzante, and D. Cook.
1996. Microsatellite polymorphism and the population structure of Atlantic cod (*Gadus morhua*) in the northwest Atlantic. Can. J. Fish. Aquat. Sci. 53:2706–2721.

Bisagni, J. J., and P. C. Smith.
1998. Eddy-induced flow of Scotian Shelf water across Northeast Channel, Gulf of Maine. Continental Shelf Res. 18:515–539.

Brander, K. M.
1994. Patterns of distribution, spawning, and growth in North Atlantic cod: the utility of inter-regional comparisons. International Council for the Exploration of the Seas (ICES) Marine Science Symposia 198:406–413.

Brooker, A. L., D. Cook, P. Bentzen, J. M. Wright, and R. W. Doyle.
1994. The organization of microsatellites differs between mammals and cold water fishes. Can. J. Fish. Aquat. Sci. 51:1959–1966.

Carr, S. M., and H. D. Marshall.
1991. Detection of intraspecific DNA sequence variation in the mitochondrial cytochrome b gene of Atlantic cod (*Gadus morhua*) by the polymerase chain reaction. Can. J. Fish. Aquat. Sci. 48:48–52.

Carr, S. M., A. J. Snellen, K. A. Howse, and J. S. Wroblewski.
1995. Mitochondrial DNA sequence variation and genetic stock structure of Atlantic cod (*Gadus morhua*) from bay and offshore locations on the Newfoundland continental shelf. Mol. Ecol. 4:79–88.

Cohen, E. B., D. G. Mountain, and R. O'Boyle.
1991. Local-scale versus large-scale factors affecting recruitment. Can. J. Fish. Aquat. Sci. 48:1003–1006.

Cross, T. F., and R. H. Payne.
1978. Geographic variation in Atlantic cod, *Gadus morhua*, off Eastern North America: a biochemical systematics approach. J. Fish. Res. Board Can. 35:117–123.

Dahle, G., and K. E. Jorstad.
1993. Haemoglobin variation in cod- a reliable marker for Arctic cod (*Gadus morhua* L.). Fish. Res. 16:301–311.

Fevolden, S. E., and G. H. Pogson.
1997. Genetic divergence at the synaptophysin (*Syp*I) locus among Norwegian coastal and north-east Arctic populations of Atlantic cod. J. Fish. Biol. 51:895–908.

Fogarty, M. J., and S. A. Murawski.
1998. Large-scale disturbance and the structure of marine systems: fishery impacts on Georges Bank. Ecol. Appl. 8:S6–S22.

Frank, K. T.
1992. Demographic consequences of age-specific dispersal in marine fish populations. Can. J. Fish. Aquat. Sci. 49:2222–2231.

Goudet, J.
1995. FSTAT (vers. 1.2): a computer program to calculate F-statistics. J. Hered. 86:485–486.

Goudet, J., M. Raymond, T. De Meeus, and F. Rousset.
1996. Testing divergence in diploid populations. Genetics 144:933–940.

Graves, J. E.
1998. Molecular insights into population structure of cosmopolitan marine fishes. J. Hered. 89:427–437.

Guo, S. W., and E. A. Thomson.
1992. Performing the exact test of Hardy-Weinberg proportions for multiple alleles. Biometrics 48:361–372.

Halliday, R. G., and A. T. Pinhorn.
1996. North Atlantic fishery management systems: a comparison of management methods and resource trends. J. Northw. Atl. Fish. Sci. 20:1–143.

Hunt, J. J., W. T. Stobo, and F. Almeida.
1999. Movement of Atlantic cod, *Gadus morhua*, tagged in the Gulf of Maine area. Fish. Bull. 97:842–860.

Jamieson, A.
1975. Enzyme type of Atlantic cod stocks on the North American banks. *In* Isozymes IV: Genetics and evolution (C. L. Markert (ed.), p. 491–515. Academic Press, New York, NY.

Jonsdottir, O. D. B., A. K. Imsland, A.K., Danielsdottir and G. Marteinsdottir.
2002. Genetic heterogeneity and growth properties of different genotypes of Atlantic cod (*Gadus morhua* L.) at two spawning sites off south Iceland. Fish. Res. 55:37–47.

Jonsdottir, O. D. B., A. K. Imsland, A.K., Danielsdottir, V. Thorsteinsson, and G. Naevdal.
1999. Genetic differentiation among Atlantic cod in south and south-east Icelandic waters: synaptophysin (*Syp*I) and haemoglobin (*Hbl*) variation. J. Fish. Biol. 54:1259–1274.

Klein-MacPhee, G.
2002. Cods. Family Gadidae. *In* Bigelow and Shroeder's fishes of the Gulf of Maine III (B. B. Collette and G. Klein-MacPhee, eds.), p. 223–260. Smithsonian Institution Press, Washington D.C.

Lage, C. R., M. Purcell, M. Fogarty, and I. Kornfield.
2001. Microsatellite evaluation of haddock (*Melanogrammus aeglefinus*) stocks in the northwest Atlantic ocean. Can. J. Fish. Aquat. Sci. 58:982–990.

Langton, R. W., R. S. Steneck, V. Gotceitas, F. Juanes, and P. Lawton.
1996. The interface between fisheries research and habitat management. N. Am. J. Fish. Manag. 16:1–7.

Lear, W. H., and J. M. Green.
1984. Migration of the "northern" Atlantic cod and the mechanisms involved. *In* Mechanisms of migration in fishes (J. D. McCleave, ed.), p. 309–315. Plenum, New York, NY.

Lough, R. G., and G. R. Bolz.
1989. The movements of cod and haddock larvae onto the shoals of Georges Bank. J. Fish. Biol. (suppl. A) 35:71–79

Lough, R. G., P. C. Valentine, D. C. Potter, P. J. Auditore, G. R. Bolz, J. D. Jielson, and R. I. Perry.
1989. Ecology and distribution of juvenile cod, and haddock in relation to sediment type and bottom currents on eastern Georges Bank. Mar. Ecol. Prog. Ser. 56:1–12.

Mayo, R. K., and L. O'Brien.
1998. Atlantic cod. *In* Status of fishery resources off the northeastern United States for 1998 (S. H. Clark, ed.), p. 49–52. NOAA Tech. Memo. NMFS-NE-115.

Mayo, R. K., E. M. Thunberg, S. E. Wigley, and S. X. Cadrin.
2002. The 2001 assessment of the Gulf of Maine Atlantic cod stock. Northeast Fish. Sci. Cent. Ref. Doc. 02-02, 154 p.

Miller, K. M., K. D. Le, and T. D. Beacham.
2000. Development of tri- and tetranucleotide repeat microsatellite loci in Atlantic cod (*Gadus morhua*). Mol. Ecol. 9:238–239.

Moller, D.
1968. Genetic diversity in spawning cod along the Norwegian coast. Hereditas 60:1–32.

Mork, J., Ryman, N., Stahl, G., Utter, F. and G. Sundness.
1985. Genetic variation in Atlantic cod (*Gadus morhua*) throughout its range. Can. J. Fish. Aquat. Sci. 42:1580–1587.

O'Brien, L.
1998. Factors influencing rates of maturation in the Georges Bank and the Gulf of Maine Atlantic cod stocks. NAFO Sci. Counc. Res. Doc. 98/104, 34 p.

O'Brien, L., and N. J. Munroe.
2001. Assessment of the Georges Bank Atlantic cod stock for 2001. Northeast Fish. Sci. Cent. Ref. Doc. 01-10, 126 p.

Pentilla, J. A., G. A. Nelson, and J. M. Burnett III.
1989. Guidelines for estimating lengths at age for 18 northwest Atlantic finfish and shellfish species. NOAA Tech. Memo. NMFS-F/NEC-66, 39 p.

Pepin, P., and S. M. Carr.
1993. Morphological, meristic, and genetic analysis of stock structure in juvenile Atlantic cod (*Gadus morhua*) from the Newfoundland shelf. Can. J. Fish. Aquat. Sci. 50:1924–1933.

Pogson, G. H.
2001. Nucleotide polymorphism and natural selection at the pantophysin (*Pan*I) locus in the Atlantic cod, *Gadus morhua* (L.). Genetics 157:317–330.

Pogson, G. H., K. A.Mesa, and R. G. Boutilier.
1995. Genetic population structure and gene flow in the Atlantic cod, *Gadus morhua*: a comparison of allozyme and nuclear RFLP loci. Genetics 139:375–385.

Pogson, G. H., C. T. Taggart, K. A. Mesa, and R. G. Boutilier.
2001. Isolation by distance in the Atlantic cod, *Gadus morhua*, at large and small geographic scales. Evolution 55:131–146.

Polacheck, T., D. Mountain, D. McMillan, W. Smith, and P. Berrien.
1992. Recruitment of the 1987 year class of Georges Bank haddock (*Melanogrammus aeglefinus*): the influence of unusual larval transport. Can. J. Fish. Aquat. Sci. 49: 484–496.

Policansky, D.
1993. Fishing as a cause of evolution in fishes. *In* The exploitation of evolving populations (T. K. Stokes, J. M. McGlade, and R. Law, eds.), p. 2–18. Springer-Verlag, Berlin.

Raymond, M., and F. Rousset.
1995. GENEPOP (vers. 1.2): population genetics software for exact tests and eumenism. J. Hered. 86:248–249.

Rice, W. R.
1989. Analyzing tables of statistical tests. Evolution 43: 223–225.

Ruzzante, D. E.
1998. A comparison of several measures of genetic distance and population structure with microsatellite data: bias and sampling variance. Can. J. Fish. Aquat. Sci. 55:1–14.

Ruzzante, D. E., C. T. Taggart, and D. Cook.
1996a. Spatial and temporal variation in the genetic composition of a larval cod (*Gadus morhua*) aggregation: cohort contribution and genetic stability. Can. J. Fish. Aquat. Sci. 53:2695–2705.

Ruzzante, D. E., C. T. Taggart, and D. Cook.
1998. A nuclear basis for shelf- and bank-scale population structure in northwest Atlantic cod (*Gadus morhua*): Labrador to Georges Bank. Mol. Ecol. 7:1663–1668.

Ruzzante, D. E., C. T. Taggart, D. Cook, and S. Goddard.
1996b. Genetic divergence between inshore and offshore Atlantic cod (*Gadus morhua*) off Newfoundland: microsatellite DNA variation and antifreeze level. Can. J. Fish. Aquat. Sci. 53:634–645.

Ruzzante, D. E., C. T. Taggart, D. Cook, and S. Goddard.
1997. Genetic differentiation between inshore and offshore Atlantic cod (*Gadus morhua*) off Newfoundland: a test and evidence of temporal stability. Can. J. Fish. Aquat. Sci. 54:2700–2708.

Ruzzante, D. E. C. T. Taggart, R. W. Doyle, and D. Cook.
2001. Stability in the historical pattern of genetic structure of Newfoundland cod (*Gadus morhua*) despite the catastrophic decline in population size from 1964 to 1994. Cons. Genetics 2:257–269.

Ruzzante, D. E., J. S. Wroblewski, C. T. Taggart, R. K. Smedbol, D. Cook, and S. V. Goddard.
2000. Bay-scale population structure in coastal Atlantic cod in Labrador and Newfoundland, Canada. J. Fish. Biol. 56:431–447.

Serchuk, F. M., M. D. Grosslein, R. G. Lough, D. G. Mountain, and L. O'Brien.
1994. Fishery and environmental factors affecting trends and fluctuations in the Georges Bank and Gulf of Maine Atlantic cod stocks: an overview. ICES Mar. Sci. Symp. 198:77–109.

Shaklee, J. B., and P. Bentzen.
1998. Genetic identification of stocks of marine fish and shellfish. Bull. Mar. Sci. 62:589–621.

Smith, P. J., A. J. Birley, A. Janieson, and C. A. Bishop.
1989. Mitochondrial DNA in the Atlantic cod, *Gadus morhua*: lack of genetic divergence between eastern and western populations. J. Fish. Biol. 34:369–373.

Smith, W., and W. W. Morse.
1984. Retention of larval haddock *Melanogrammus aeglefinus* in the Georges Bank region, a gyre-influenced spawning area. Mar. Ecol. Prog. Ser. 24:1–13.

Smouse, P. E., and C. Chevillon.
1998. Analytical aspects of population-specific DNA fingerprinting for individuals. J. Hered. 89:143–150.

Streelman, J. T, and T. D. Kocher.
2002. Microsatellite variation associated with prolactin expression and growth of salt-challenged tilapia. Physiol. Genomics 9:1–4.

Townsend, D. W., and N. R. Pettigrew.
1996. The role of frontal currents in larval fish transport on Georges Bank. Deep-Sea Res.II. 43:1773–1792.

United States Federal Register.
2003. 50 CFR Part 648. [Available at http://www.gpoaccess.gov; accessed 1 May 2003.]

Waples, R. S.
1998. Separating the wheat from the chaff: patterns of

genetic differentiation in high gene flow species. J. Hered. 89:438–450.

Ward, R. D., M. Woddwark, and D. O. F. Skibinski.
1994. A comparison of genetic diversity levels in marine, freshwater, and anadromous fishes. J. Fish. Biol. 44: 213–232.

Weir, B. S., and C. C. Cockerham.
1984. Estimating F-statistics for the analysis of population structure. Evolution 38:1358–1370.

Werner, F. E., F. H. Page, D. R. Lynch, J. W. Loder, R. G. Lough, R. I. Perry, D. A. Greenberg, and M. Sinclair.
1993. Influences of mean advection and simple life behavior on the distribution of cod and haddock early life stages on Georges Bank. Fish. Oceanogr. 2:43–64.

Conserving oyster reef habitat by switching from dredging and tonging to diver-harvesting

Hunter S. Lenihan
Bren School of Environmental Science and Management
University of California, Santa Barbara
Santa Barbara, California 93106-5131
E-mail address: Lenihan@bren.ucsb.edu

Charles H. Peterson
Institute of Marine Sciences
University of North Carolina at Chapel Hill
Morehead City, North Carolina 28557

Abstract—A major cause of the steep declines of American oyster (*Crassostrea virginica*) fisheries is the loss of oyster habitat through the use of dredges that have mined the reef substrata during a century of intense harvest. Experiments comparing the efficiency and habitat impacts of three alternative gears for harvesting oysters revealed differences among gear types that might be used to help improve the sustainability of commercial oyster fisheries. Hand harvesting by divers produced 25–32% more oysters per unit of time of fishing than traditional dredging and tonging, although the dive operation required two fishermen, rather than one. *Per capita* returns for dive operations may nonetheless be competitive with returns for other gears even in the short term if one person culling on deck can serve two or three divers. Dredging reduced the height of reef habitat by 34%, significantly more than the 23% reduction caused by tonging, both of which were greater than the 6% reduction induced by diver hand-harvesting. Thus, conservation of the essential habitat and sustainability of the subtidal oyster fishery can be enhanced by switching to diver hand-harvesting. Management schemes must intervene to drive the change in harvest methods because fishermen will face relatively high costs in making the switch and will not necessarily realize the long-term ecological benefits.

Manuscript approved for publication 25 November 2003 by Scientific Editor.
Manuscript received 20 January 2004 at NMFS Scientific Publications office.
Fish. Bull. 102:298–305 (2004).

Commercial fishing for demersal fishes and benthic invertebrates, such as mollusks and crabs, is commonly undertaken with bottom-disturbing gear that can inflict damage to seafloor habitats (Dayton et al., 1995; Engel and Kvitek, 1995; Jennings and Kaiser, 1998; Watling and Norse, 1998). Habitat damage from dredges and analogous gear, designed to excavate invertebrates that are partially or completely buried beneath the surface of the seafloor, is generally much more severe than the damage caused by bottom trawls (Collie et al., 2000). Furthermore, impacts on and recovery from bottom-disturbing fishing gear vary with habitat type; generally smaller effects and more rapid rates of recovery are found for infauna in sedimentary habitats and the most severe and long-lasting damage in biogenic habitats that emerge from the seafloor (Peterson et al., 1987; Collie et al., 2000). Such biogenic habitats include seagrass beds, fields of sponges and bryozoans, and invertebrate reefs. Biogenic reefs that provide important ecosystem services such as habitat for other organisms include not only tropical coral reefs but also temperate reefs constructed by oysters (Bahr and Lanier, 1981; Lenihan et al., 2001), polychaetes like *Petaloproctus* (Wilson, 1979; Reise, 1982), and vermetid gastropods (Safriel, 1975). The recovery of such emergent invertebrate reefs is a slow process because of the relative longevity of the organisms that provide structure for the reef after they die and because of the nature of reefs as accumulations of multiple generations of reef builders.

One widespread temperate reef builder, the American oyster (*Crassostrea virginica*, also known as the "eastern oyster," Am. Fish. Soc.), has been especially affected by bottom-disturbing fishing gear as the target of fisheries. More than one hundred years of dredging and tonging oysters in the Chesapeake Bay and Pamlico Sound have caused severe degradation of the oyster reef matrix (deAlteris, 1988; Hargis and Haven, 1988), such that reef area and elevation have been dramatically reduced (Rothschild et al., 1994; Lenihan and Peterson, 1998). Reduction in reef height has a serious consequence for the oyster population because one function of naturally tall subtidal oyster reefs is to elevate the oysters up into the mixed surface layer of the estuary; this layer of mixed surface water allows them to avoid mass mortality from persistent exposure to seasonally anoxic and hypoxic bottom water (Lenihan and Peterson, 1998). Reef height and structure also control reef hydrodynamics (e.g., flow speed, turbulent mixing, and particle delivery and deposition), which influence oyster population dynamics and production (Lenihan, 1999). Consequently, harvest-related reef destruction and degradation are considered major factors that have led to declines of American oys-

ters in many estuaries located along the coasts of the Atlantic Ocean and Gulf of Mexico (Lukenbach et al., 1999).

Loss of oysters and the biogenic habitat that they provide appears from archaeological and paleontological evidence to be a worldwide phenomenon in temperate estuaries (Jackson et al., 2001). Oyster loss hurts not only the oyster fishery but, more importantly, imperils the ecosystem services provided by the oysters. These include, especially, the provision of emergent habitat and reef-dependent prey resources for many fish and crustacean populations of commercial and recreational importance (Peterson et al., 2000; Lenihan et al., 2001; Peterson et al., 2003), the filtration of estuarine waters (Newell, 1988), and the promotion of estuarine biodiversity by provision of hard-bottom habitat in fields of mobile sediments (Wells, 1961).

Because of the importance of restoring and sustaining oysters and their reefs to serve both the oyster fishery and the ecosystem, we designed a field test of the habitat impacts of three oyster harvesting methods: dredging, tonging, and hand extraction by divers (diver-harvesting). Our study is a gear comparison, in which we assess not only the traditional response variable of quantitative harvest per unit of effort with each gear but also the degree of reef habitat damage induced by the extraction of the oysters (analogous to Peterson et al., 1983). We additionally examine the quality of the oysters harvested as a function of gear type. The results indicate that diver-harvesting is a more environmentally sound way of harvesting oysters than traditional methods with dredges and tongs and may be more compatible with conserving oyster reef habitat.

Methods

Study site

Gear comparisons were conducted on subtidal oyster reefs in the Neuse River estuary, North Carolina (35°00′20″N, 76°33′50″W). Environmental conditions of this estuary are well described elsewhere (Paerl et al., 1998; Lenihan, 1999). Briefly, the estuary is mesohaline, an optimal habitat for the American oyster, and was once an important oyster fishery ground (Lenihan and Peterson, 1998). The estuary contains remnants of many large, natural subtidal oyster reefs that have been intensely mined by oyster harvesting gear for over a century. Dredging is the most common fishing practice. Mining of the reef matrix has combined with sediment loading and eutrophication-associated hypoxia (Paerl et al., 1998) to degrade the oyster reef habitats and greatly reduce oyster populations (Lenihan and Peterson, 1998). In harvested areas, reefs that were 2–3 m tall in quantitative surveys in the late 1800s (n=8 reefs) were all <1 m tall in our survey conducted in 1994—a modification of habitat caused entirely by the removal of oysters and shells during harvesting with dredges and tongs (Lenihan and Peterson, 1998). To help maintain oyster harvests, the North Carolina Division of Marine Fisheries (NCDMF) restores oyster reefs throughout many locations in the estuary by creating piles of oyster shell, or marl, on the seafloor. These restored oyster reefs are also targeted by oyster fishermen using dredges and, less often, using manual oyster tongs (Marshall[1]).

Experimental oyster reefs

Gear comparisons were conducted in March 1996 on 16 subtidal oyster reefs that had previously been created in July 1993 as part of a reef restoration experiment (Lenihan and Peterson, 1998; Lenihan, 1999) in collaboration with NCDMF. The experimentally restored reefs (referred to as "experimental reefs" in this gear-comparison study) were piles of oyster shells 1 m tall, 6–7 m in diameter (28.3–38.5 m^2 in area), and generally hemispherical in shape. Natural subtidal reefs located elsewhere in the estuary are typically larger, rectangular biogenic structures, ranging from 8–13 m wide and 20–30 m long. Experimental reefs were constructed in 3–4 m of water on a firm and sandy bottom, and were separated by at least 50 m. From the time of their construction until use in our experiments, the restored oyster reefs remained research sanctuaries, protected from commercial and recreational shellfishing.

As oysters settle and undergo metamorphosis on the shells of other (live and dead) oysters, to which they are attracted by chemical cues (Tamburri et al., 1992), they help cement together and add to the shell matrix of the reef over years. Prior to our harvest treatments, the experimentally restored reefs were colonized by at least three generations of oysters, many of which grew to adult size (range of oyster sizes on experimental reefs at the start of our experiment: 2–11 cm in shell height). Consequently, the shell matrices of the reefs had become somewhat cohesive, although probably less so than natural oyster reefs. In February 1996, before initiation of experimental harvests, there was no significant difference in the mean density of adult (>1 cm in shell height) oysters (mean ±SD 179.1 ±18.4/m^2) among the four sets of four experimental reefs randomly selected to receive the four harvesting treatments (one-way ANOVA; $F_{3,12}$=0.29; mean square error=285.06; P=0.83). Experimental reefs in the Neuse River usually had slightly higher oyster densities nearer their base and larger oysters near the crest (see Lenihan, 1999).

Experimental harvests

We compared three types of oyster-harvesting techniques: dredging, hand-tonging, and diver-harvesting. In March 1996, each of 16 reefs was either dredged, tonged, diver-harvested, or left unharvested as a control (four replicates of each treatment). Experimental dredging and hand-tonging were conducted in the manner applied by commercial oyster fishermen. The dredge, 25 kg in weight and 1 m in width, was pulled behind a powerboat operated by NCDMF personnel with commercial oyster-dredging experience. Hand-tonging was also conducted by a professional oyster

[1] Marshall, M. 1999. Personal commun. North Carolina Division of Marine Fisheries, 3431 Arendell St., Morehead City, NC 28557.

fisherman, R. A. Cummings. Oysters and shell material collected by dredges and tongs were separated aboard the boat on a culling board, using the common culling techniques (i.e., breaking apart oysters and shell with hammers, mallets, and chisels). As mandated by law, oyster shell and undersized oysters (<7 cm in height) were thrown overboard above the reef from which they had been collected.

Hand collections of oysters were conducted by scuba divers (J. H. Grabowski and H. S. Lenihan). Unlike professional oyster divers in Chesapeake Bay and other areas, who rake large quantities of shell and attached oysters into baskets that are pulled aboard ship to be culled, the divers in this trial adopted a different method designed to preserve reef habitat. Instead of collecting shell and oysters indiscriminately, the divers chose only those oysters that appeared alive and of market-size. Selected oysters were hand picked from the reef and placed in heavy plastic mesh baskets that, when full, were subsequently pulled aboard the boat with haul lines.

To standardize fishing effort, each of the 12 harvested reefs was harvested for 2 hours, regardless of the number of oysters collected. A 2-h harvest period for each 28.3–38.5 m^2 reef was considered to be a thorough but not excessive level of harvesting by the professional fishermen. The numbers of oysters collected in the final three or four dredge hauls and oyster tongs were typically lower (by ~10–20%) than the preceding dredge hauls and tongs. This reduction in the catch per unit of effort was great enough that a fisherman foraging optimally would normally cease harvesting at that time and move on to another reef. Similarly, after 2 hours of diver-harvesting, most of the clearly visible market-size oysters had been harvested.

Quantifying reef structure

Measurements of oyster reef height and diameter were conducted on all 16 experimental reefs both before and after application of the three fishing methods. In February 1996, the preharvest height and radius of each oyster reef were measured by scuba divers using a custom-made "square angle," consisting of two pieces (2 m and 5 m long) of 3-cm wide steel angle-iron, each with an attached 1-m long carpenter's level. Both pieces of angle iron were marked at 1-cm intervals. The 5-m long (cross) piece was attached to the 2-m long (upright) piece by a roller-joint. The roller-joint allowed the cross piece to move up and down the upright piece, thus providing a measure of reef height, and to move horizontally in relation to the upright piece, thus providing a measurement of reef radius. The 2-m long piece also had a 0.75-m long piece of angle iron attached perpendicularly near its bottom so that it would not sink into the seafloor when placed upright.

One diver held the 2-m long angle iron perpendicular to the seafloor at the edge of a reef, while the other diver placed the 5-m long angle iron parallel to the seafloor, so that one end rested on the highest point of a reef and the other end met the upright angle iron at the reef's edge. The height and radius of the reef were then measured by recording the height at which the cross piece met the upright piece, and the distance at which the upright piece met the cross-piece. For each reef, a mean diameter was calculated by measuring three separate radii (oriented at three compass bearings, all 120° apart), multiplying the radii by two to estimate diameters, and then averaging the three diameters. This averaging procedure was undertaken because the reefs were not perfectly circular. Measurements of reef height and radius were repeated in March, two–five days after experimental harvests were completed.

Sampling oyster populations

We sampled live and dead oysters on each treatment and control reef before (late February 1996) and immediately after (late March) experimental harvests to estimate the proportion of oysters incidentally killed but not harvested by each harvesting treatment. Specifically, oyster data was collected within 30 hours of the application of the harvest treatment on each replicate reef. Densities of live and dead oysters were quantified by divers who haphazardly placed eight 0.5-m^2 weighted PVC quadrats on the reef surface at haphazard locations and recorded the number of live and dead oysters greater >1 cm in height. The density of dead oysters was measured by counting the number of oyster shells that were articulated and appeared relatively fresh (i.e., not black in color or decayed), or oysters with somatic tissue exposed because of cracked, broken, or punctured shells. Oysters with exposed somatic tissue almost certainly die because of predation by fishes and crabs in the Neuse River estuary (Lenihan, 1999; and see Lenihan and Micheli, 2000). Mean proportions of dead oysters were computed (dead oysters/dead+alive oysters), as well as mean densities of live and dead oysters on each reef.

Catch per unit of effort

The relative efficiency of each harvesting method was determined by comparing the numbers of bushels (1 bushel=36.4 L) of market-size oysters taken per hour of fishing. We quantified numbers of bushels for each harvesting method aboard the boat by placing oysters of legal size in premeasured mesh baskets. After being counted, and upon termination of the harvest trial, many of the oysters were returned to other nearby reefs not involved in the experiment.

Statistics

One-way analysis of variance (ANOVA) was used to compare the following across harvest treatments and controls: 1) changes in mean reef height and diameter; 2) catch per unit of effort; 3) the proportion of oysters found dead on reefs before harvest; 4) the proportion of oysters found dead on reefs after harvest; and 5) the absolute difference in the proportion of oysters found dead before versus after harvesting ([*after* minus *before*]). Data from all treatment (dredging, tonging, and diver-harvesting; n=4 for each treatment) and the control (n=4) reefs were used in

Table 1

Results of one-way ANOVAs comparing differences in reef height (cm), reef diameter (cm), and catch per unit of effort (number of oysters collected per hour) among experimental reefs harvested by different methods (dredging, tonging, diver-harvesting, and controls). df = degrees of freedom; ms = mean square; F = F-value; P = P-value; ss = sum of squares. Partial r^2= treatment ss/total ss.

	Reef height					Reef diameter				Catch per unit of effort			
Source	df	ms	F	P	partial r^2	ms	F	P	partial r^2	ms	F	P	partial r^2
Harvesting treatment	3	0.09	36.90	0.0001	0.90	0.07	15.79	0.0002	0.80	3.21	17.84	0.0001	0.11
Residual	12	0.003				0.005				0.08			
Total	15			Total ss: 0.31					0.27				9.64

the ANOVA. Before ANOVA, homogeneity of variances was tested by using Cochran's method (α=0.05). All data passed this test. After ANOVA, *post hoc* differences among means were compared by using Student-Newman-Keuls (SNK) tests (α=0.05).

Results

Reef height and diameter

Dredge harvesting on experimental reefs removed the largest amount of shell material from the reefs, based on the reduction of reef height (Fig. 1A) and on the qualitative assessment of increases in numbers of oyster shells found on the seafloor around the reefs. Hand-tonging removed an intermediate amount of reef materials, and diver-harvesting removed far less shell matrix than either dredging or tonging. All harvesting methods reduced the height of restored oyster reefs (Fig. 1A), but dredging (34% of reef height) and tonging (23%) had greater impacts than did diver-harvesting (6%). ANOVA demonstrated significant differences among harvest treatments in mean change in reef height (Table 1); all harvest treatments induced a loss in reef height as compared with unharvested control reefs (SNK; P<0.05). Dredging reduced reef height more than any other treatment (SNK, P<0.05), and tonging reduced reef height more than diver-harvesting (SNK, P<0.05). The reduction in reef height caused by diver-harvesting was small (mean ±SD: 6 ±3 cm). However, diver-harvesting nearly eliminated the veneer of live market-size oysters on reefs, which provides substantial structure on reef surfaces.

Oyster harvesting either slightly increased or slightly decreased reef diameter, depending upon method (Fig. 1B). Reef material was apparently removed from edges of reefs by tonging, thereby reducing reef diameter. Shell was spread around the reefs by dredging, thereby increasing reef diameter after application of that harvesting method. The effects of oyster harvesting on reef diameter proved significant (Table 1). Tonging significantly reduced reef size compared with controls and the other two harvesting treatments (SNK; P<0.05), whereas dredging

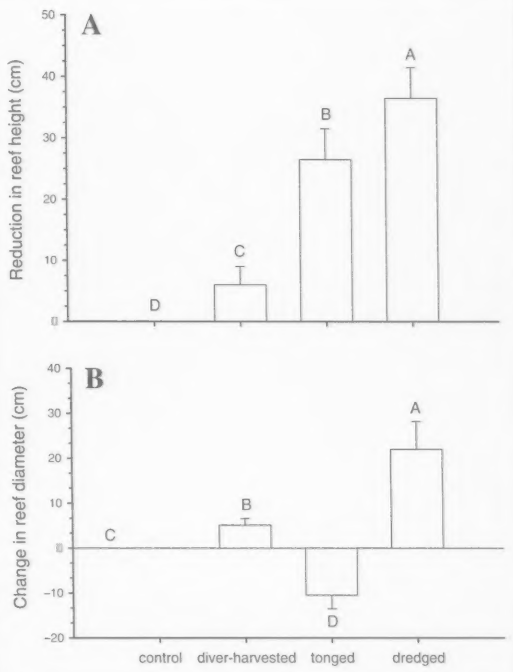

Figure 1

Modification of reef size and structure caused by various harvesting techniques. (**A**) Mean (+SE) reduction in the height of experimentally restored oyster reefs caused by three types of oyster harvesting: hand-harvesting by divers, hand tonging, and dredging. Dredges are pulled behind power boats. Reefs were located in the Neuse River estuary, North Carolina. Letters represent results of SNK *post hoc* tests: dredged>tonged>diver-harvested>control at P<0.05. (**B**) Mean (+SE) change in the diameter of experimental oyster reefs caused by different oyster-harvesting techniques. Letters represent results of SNK *post hoc* tests: dredged>diver-harvested>control>tonged at P<0.05.

Table 2

Results of one-way ANOVAs comparing differences in the proportion of oysters found dead ("mortality") on reefs before and after harvesting by different methods (dredging, tonging, diver-harvesting, and controls), and the absolute difference ([*after–before*]) in the proportion of dead oyster found before versus after harvesting. df = degrees of freedom; ms = mean square; F = F-value; P = P-value; ss = sum of squares. Partial r^2 = treatment ss/total ss.

	Before mortality					After mortality				Difference in mortality			
Source	df	ms	F	P	partial r^2	ms	F	P	partial r^2	ms	F	P	partial r^2
Harvesting treatment	3	0.001	0.49	0.69	0.11	0.02	7.90	0.004	0.58	0.01	7.56	0.004	0.57
Residual	12	0.001				0.002				0.08			
Total	15			Total ss: 0.01					0.08				0.04

increased reef diameter compared to the other treatments (SNK; $P<0.05$). The increase in diameter of diver-harvested reefs was also greater than that for controls (SNK; $P<0.05$). The substantial increase in shell material (with oysters of all sizes) spread out on the seafloor on dredged reefs indicates that the collection efficiency of dredges is less than 100%.

Catch per unit of effort

Catch per unit of effort of oysters included the time required to collect oysters from the reef and the time needed to separate (i.e., cull) them from undersized oysters and shell material. Two of the harvesting methods, hand-tonging and oyster dredging, are one-man operations in which one fisherman can operate the harvesting gear, cull oysters, and drive the boat. Therefore, measurements of catch per unit of effort for dredging and tonging represent the numbers of bushels of oysters one fisherman can collect per hour. In contrast, scuba diving is rarely attempted alone and it is usually necessary for someone else to tend the diver (e.g., helping him or her in and out of the water) and to haul oysters up to the boat when given a signal by the diver on the reef. Divers should preferably work as a team using the "buddy" system for safety reasons. Data for diver-collections are given in bushels per hour collected by one diver but hauled up to the boat and culled by a second person.

There was a significant difference in the numbers of bushels collected per hour by the different harvesting techniques (Table 1). Diver-harvesting had a higher catch efficiency than all other treatments (SNK; $P<0.05$; Fig. 2). Diver-harvesting was about 25% more time efficient than dredge harvesting and 32% more efficient than tonging. There was no statistically significant difference in efficiency between dredging and tonging (SNK; $P>0.05$).

Incidental oyster mortality

The proportion of oysters found dead on experimental reefs in February 1996 (~20%), prior to experimental harvesting, was similar to that found on other nearby experimental and natural reefs in the Neuse River estuary in preceding years (e.g., Lenihan and Peterson, 1998; Lenihan 1999). In February, the proportions of dead oysters did not differ among the four sets of reefs destined to be experimentally harvested (Table 2, Fig. 3A). In contrast, there was a large and statistically significant difference in the proportions of dead oysters on the reefs after harvesting (Table 2, Fig. 3A). The proportions of dead oysters on reefs that had been tonged and dredged were significantly greater than on diver-harvested and control reefs (SNK; $P<0.05$).

Before-after-control-impact (BACI) comparison of the change in proportions of dead oysters from before to after harvesting ([*after–before*]), a direct estimate of incidental mortality caused by harvesting gear, showed a similar pattern to mortality inferred from *in situ* proportions of dead oysters in March after harvesting (Table 2, Fig. 3B).

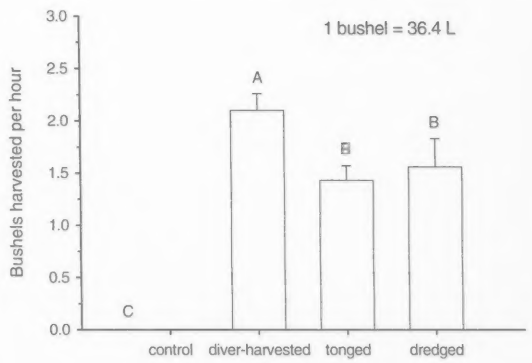

Figure 2

Mean (+SE) number of bushels collected per hour on experimental reefs by different oyster-harvesting techniques. Letters represent results of SNK *post hoc* tests: diver-harvested>dredged and tonged>control at $P<0.05$.

A significant treatment effect in the *after* period (Table 2) indicated that the change over time in proportion of dead oysters varied among harvest treatments. Tonging and dredging increased the fraction of dead among *in situ* oysters on reefs (SNK; $P<0.05$; Fig. 3B), but diver-harvesting did not. Immediately after harvesting, divers found that many oysters on tonged and dredged reefs had been broken open, severely cracked, or punctured.

Discussion

Our comparisons of gear revealed relatively unambiguous differences in their harvesting efficiency for oyster dredges, tongs, and hands of divers. Dredging and tonging had similar and statistically indistinguishable catch efficiencies, which seems reasonable given that both techniques are commonly employed in the same locations and times in the oyster fishery. Presumably, fishermen choose between these two gears on the basis of personal preference, history, and skill, as well as on the basis of water depth, bottom type, and other factors that did not vary in our study. Diver-harvesting of oysters resulted in higher rates of harvest per hour, but this enhancement in catch efficiency required the presence of two people, one diver beneath the surface and another person on deck involved in hauling baskets of oysters onto the deck and culling out marketable oysters. Because the increase in efficiency was only 25–32%, this enhancement falls short of the 100% required to compensate each fisherman to the same degree that dredging and tonging provide. Nevertheless, the immediate economics of diver-harvesting could prove competitive or even superior if the single deckhand could serve two or more divers, which seems likely from our experience with the workload on deck, and if the oysters taken are priced more favorably because of larger size or less damage, which seems possible. A complete short-term economic comparison would need to include higher costs for fuel in dredging and costs of filling air tanks for diving, as well as depreciation of gear.

This discussion of the basic efficiencies and economics of the methods of commercial oyster fishing is based upon short-term considerations only. That short-term time perspective is the cause of failures to achieve sustainability in fisheries quite generally (Ludwig et al., 1993; Botsford et al., 1997). We show that adoption of hand-harvesting by divers would result in substantially less fishery-induced reduction in reef height by a factor of four to six, implying greater preservation of the habitat and thus a more sustainable fishing practice. Our data on the changes in area covered by reefs as a function of harvest treatment revealed only small differences among treatments. The height of a reef is a critical variable in sustaining the reef as an engine of oyster production because short reefs can be easily covered by sediment (Lenihan, 1999), can be abraded by sediment transport (Lenihan, 1999), and can fail to extend above hypoxic bottom waters (Lenihan and Peterson, 1998). Tall reefs (i.e., reefs not degraded by harvesting) produce faster flow speeds and more turbulence for oyster populations, which in turn increase oyster growth rate, increase

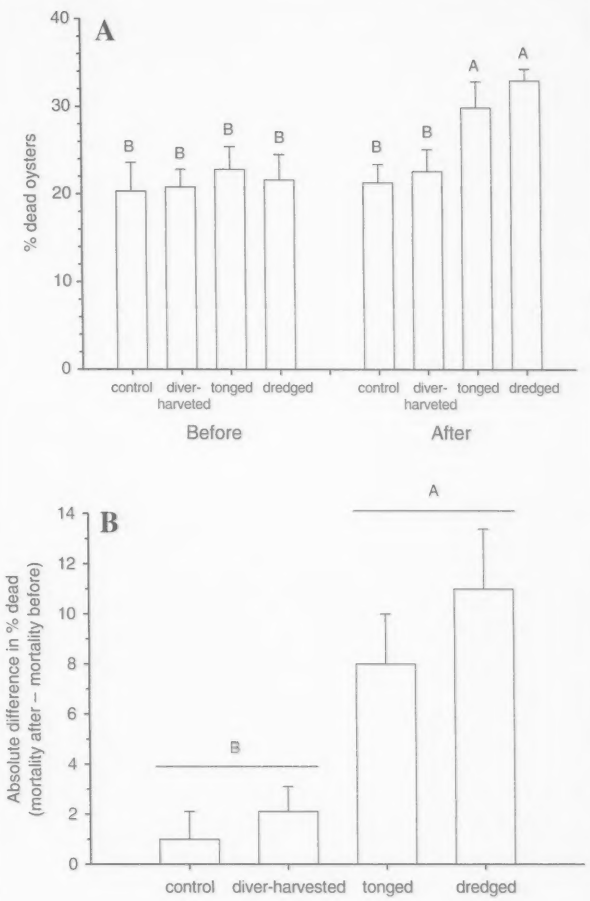

Figure 3

Mortality of oysters caused by various harvesting techniques. (**A**) Mean (+SE) % dead within oyster populations on experimental reefs before and after being harvested by three different harvesting techniques: dredging, tonging, and diver-harvesting. Control reefs were not harvested. Letters represent results of SNK *post hoc* tests: dredged, after>tonged, after>all other treatments at $P<0.05$. There was no difference among treatments before harvesting. (**B**) Mean (+SE) absolute difference in the % dead oysters on experimental reefs before and after harvesting. Difference calculated by: [% *after*–% *before*]. Letters represent results of SNK *post hoc* tests: dredged and tonged>diver-harvested and control at $P<0.05$.

physicalogical condition, reduce disease incidence and intensity, and decrease mortality (Lenihan, 1999). Consequently, assessment of economics of the oyster fishery over longer time frames would likely demonstrate higher returns from practicing diver-harvesting, assuming that this technique conserved reef structure. Diver-harvesting also killed fewer of the oysters that remained on the bottom, thereby sustaining future harvests better through reduced wastage and by retention of more live oysters that would produce more reef material.

Although the relative advantage of diver-harvesting for conserving reef structure is evident, the absolute conservation of reef habitat under the various oyster harvesting methods is not clear from our study. Our data on impacts of diver-harvesting revealed slight declines in reef height, but whether these same declines would apply to an older reef, as opposed to a recently restored reef, is open to question. The level of cementation that binds the shells of the reef is not as great on recently restored reefs, making them more susceptible to degradation with physical disturbance. Our study measured only the immediate drop in reef elevation after fishing at a level that removed a large fraction of legally marketable oysters. In a well-managed fishery, this drop in reef elevation would represent virtually an entire season's decline, after which substantial reef growth would occur through recruitment and growth of smaller oysters before a new harvesting season. Thus, a healthy oyster reef may well be able to compensate for the modest reduction in elevation caused by diver-harvesting. If so, oyster reef sanctuaries now being created throughout the Chesapeake Bay (Luckenbach et al., 1999) could conceivably be opened to diver-harvesting (without implements) and still preserve the reef services to the ecosystem. This possibility deserves to be evaluated in order to minimize conflicts between the goals of restoring oyster reef habitat for conservation purposes and restoring oyster reefs for the restoration of lost fisheries.

Application of the results of our gear comparisons to management of oyster fisheries will likely encounter some impediments. Although various artisanal fisheries worldwide have employed free diving as a fishing technique and some modern fisheries, including the American oyster fishery, involve the use of scuba, diving is not a skill possessed by most oyster fishermen and probably is not a method under consideration for oyster fishing in general. In addition, the peak of oyster harvesting season on the Atlantic and Gulf coasts is usually during winter months (e.g., November–March) when water temperatures in estuaries are quite low (0–10°C). Such conditions require cold-water diving equipment (e.g., dry-suits), which will further increase the cost of this new harvesting technique. Thus acceptance of diver-harvesting by the industry would require training in diving skills and safety, education and demonstration of the advantages of this gear, and perhaps even investment of public funds to defray costs of the transition from traditional dredges and tongs to scuba or hookah. Because the gains of switching to diver-harvesting accrue to the industry over the long term, while individual fishermen who switch may suffer economically in the short-term, gear choice represents a modified example of the tragedy of the commons (Ludwig et al., 1993). Only when armed with some form of ownership rights and an attendant long-term perspective would an individual oyster fisherman choose to switch to diver-harvesting. The precipitous declines of over 99% in oyster landings in mid-Atlantic estuaries (Rothschild et al., 1994; Lenihan and Peterson, 1998) mean that oyster fishermen can hardly be expected to bear the costs of switching fishing methods. Therefore, government intervention would be required to convert subtidal oyster dredge and tong fisheries into diver-harvesting operations for two reasons; the need for compensation of start-up costs and the need to overcome the tragedy of the commons. Given the dire state of oyster fisheries today (Rothschild et al., 1994), the habitat destruction in these declines (deAlteris, 1988; Hargis and Haven, 1998; Rothschild et al., 1994; Lenihan and Peterson, 1998), the broad ecosystem services provided by healthy oyster reefs (Jackson et al., 2001; Lenihan et al. 2001), and the very real potential for restoring oysters and their reefs (Luckenbach et al., 1999; Lenihan, 1999), a mandate to switch fishing methods for subtidal oyster fisheries could pay large dividends.

Acknowledgments

We thank Mike Marshall, Jeff French, and those many NCDMF people working on deck for initially creating experimental reefs to our specifications and for later applying the experimental dredge harvesting treatment. We thank Robert A. Cummings for applying the hand-tonging treatment, and Jonathan H. Grabowski for helping with diver-harvesting of reefs. This work was funded by the North Carolina General Assembly through the Cooperative Institute of Fisheries Oceanography (to C. H. Peterson), and NOAA-Chesapeake Bay Program Oyster Disease Program (to H. S. Lenihan, C. H. Peterson, and F. Micheli)

Literature cited

Bahr, L. M., and W. P. Lanier.
1981. The ecology of intertidal oyster reefs of the South Atlantic coast: a community profile. U.S. Fish Wildl. Serv. Office of Biological Services FWS/OBS-81/15.

Botsford, L. W., J. C. Castilla, and C. H. Peterson.
1997. The management of fisheries and marine ecosystems. Science 277:509–515.

Collie, J. S., S. J. Hall, M. J. Kaiser, and I. R. Poiner.
2000. A quantitative analysis of fishing impacts on shelf-sea benthos. J. Anim. Ecol. 69:785–798.

Dayton, P. K., S. F. Thrush, M. T. Agardy, and R. J. Hoffman.
1995. Environmental effects of marine fishing. Aquat. Conserv. Mar. Fresh. Ecosyst. 5:205–232.

deAlteris, J. T.
1988. The geomorphologic development of Wreck Shoal, a subtidal oyster reef of the James River, Virginia. Estuaries 11:240–249.

Engel, J., and R. G. Kvitek.
1995. Effects of otter trawling on a benthic community in

Monterey Bay National Marine Sanctuary. Conserv. Biol. 12:1204–1214.

Hargis, W. J., Jr., and D. S. Haven.
1988. The imperiled oyster industry of Virginia: a critical analysis with recommendations for restoration. Special report 290 in applied marine science and ocean engineering, 145 p. Virginia Sea Grant Marine Advisory Services, Virginia Institute of Marine Science, Gloucester Point, VA.

Jackson, J. B. C., M. X. Kirby, W. H. Berger, K. A. Bjorndal, L. W. Botsford, B. J. Bourque, R. H. Bradbury, R. Cooke, J. Erlandson, J. A. Estes, T. P. Hughes, S. Kidwell, C.B. Lange, H. S. Lenihan, J. M. Pandolphi, C. H. Peterson, R. S. Steneck, M. J. Tegner, and R. R. Warner.
2001. Historical overfishing and the recent collapse of coastal ecosystems. Science 293:629–638.

Jennings, S., and M. J. Kaiser.
1998. The effects of fishing on marine ecosystems. Adv. Mar. Biol. 34:201–352.

Lenihan, H. S.
1999. Physical-biological coupling on oyster reefs: how habitat structure influences individual performance. Ecol. Monogr. 69:251–276.

Lenihan, H. S., and F. Micheli.
2000. Biological effects of shellfish harvesting on oyster reefs: resolving a fishery conflict by ecological experimentation. Fish. Bull. 98:86–95.

Lenihan, H. S., and C. H. Peterson.
1998. How habitat degradation through fishery disturbance enhances impacts of hypoxia on oyster reefs. Ecol. Appl. 8:128–140.

Lenihan, H. S., C. H. Peterson, J. E. Byers, J. H. Grabowski, G. W. Thayer, and D. R. Colby.
2001. Cascading of habitat degradation: oyster reefs invaded by refugee fishes escaping stress. Ecol. Appl. 11:764–782.

Luckenbach, M. A., R. Mann, and J. A. Wesson (eds.).
1999. Oyster reef restoration: a synopsis and synthesis of approaches, 366 p. Virginia Institute of Marine Sciences Press, Gloucester Point, VA.

Ludwig, D., R. Hilborn, and C. Walters.
1993. Uncertainty, resource exploitation, and conservation: lessons from history. Science 260:17–18.

Newell, R. I. E.
1988. Ecological changes in the Chesapeake Bay: Are they the result of overharvesting the American oyster, *Crassostrea virginica*? *In* Understanding the estuary: advances in Chesapeake Bay research (M. P. Lynch, E. C. Krome, eds.), p. 536–546. Chesapeake Bay Research Consortium, Publ 129 CBP/TRS 24/88, Gloucester Point, VA.

Paerl, H. W., J. L. Pinckney, J. M. Fear, and B. L. Peierls.
1998. Ecosystem responses to internal and watershed organic matter loading: consequences for hypoxia in the eutrophying Neuse River Estuary, North Carolina, USA. Mar. Ecol. Prog. Ser. 166:17–25.

Peterson, C. H., H. C. Summerson, and S. R. Fegley.
1983. The relative efficiency of tow clam rakes and their contrasting impacts on seagrass biomass. Fish. Bull. 81:429–434.
1987. Ecological consequences of mechanical harvesting of clams. Fish. Bull. 85:281–298.

Peterson, C. H., H. C. Summerson, E. Thomson, H. S. Lenihan, J. H. Grabowski, L. Manning, F. Micheli, and G. Johnson.
2000. Synthesis of linkages between benthic and fish communities as a key to protecting essential fish habitat. Bull. Mar. Sci. 66:759–774.

Peterson, C. H., J. H. Grabowski, and S. P. Powers.
In press. Quantitative enhancement of fish production by oyster reef habitat: restoration valuation. Mar. Ecol. Prog. Ser.

Reise, K.
1982. Long-term changes in the macrobenthic invertebrate fauna of the Wadden Sea: are polychaetes about to take over? Neth. J. Sea Res. 16:29–36.

Rothschild, B. J., J. S. Ault, P. Goulletquer, and M. Héral.
1994. Decline of the Chesapeake Bay oyster population: a century of habitat destruction and overfishing. Mar. Ecol. Prog. Ser. 111:29–39.

Safriel, U. N.
1975. The role of vermetid gastropods in the formation of Mediterranean and Atlantic reefs. Oecologia 20:85–101.

Tamburri, M. N., R. K. Zimmer-Faust, and M. L. Tamplin.
1992. Natural sources and properties of chemical inducers mediating settlement of oyster larvae: a re-examination. Biol. Bull. 183:327–337.

Watling L., and E. A. Norse.
1998. Disturbance of the seabed by mobile fishing gear: a comparison to forest clearcutting. Cons. Biol. 12:1180–1197.

Wells, H. W.
1961. The fauna of oyster reefs with special reference to the salinity factor. Ecol. Monogr. 31:239–266.

Wilson, W. H., Jr.
1979. Community structure and species diversity of the sediment reefs constructed by *Petaloproctus socialis* (Polychaeta: Maldanidae). J. Mar. Res. 37:623–641.

Fecundity, egg deposition, and mortality of market squid (*Loligo opalescens*)

Beverly J. Macewicz
J. Roe Hunter
Nancy C. H. Lo
Erin L. LaCasella

Southwest Fisheries Science Center
National Marine Fisheries Service, NOAA
8604 La Jolla Shores Drive
La Jolla, California 92037-1508

E-mail address (for B. J. Macewicz): Bev.Macewicz@noaa.gov

Abstract—*Loligo opalescens* live less than a year and die after a short spawning period before all oocytes are expended. Potential fecundity (E_P), the standing stock of all oocytes just before the onset of spawning, increased with dorsal mantle length (L), where $E_P = 29.8L$. For the average female squid (L of 129 mm), E_P was 3844 oocytes. During the spawning period, no oogonia were produced; therefore the standing stock of oocytes declined as they were ovulated. This decline in oocytes was correlated with a decline in mantle condition and an increase in the size of the smallest oocyte in the ovary. Close agreement between the decline in estimated body weight and standing stock of oocytes during the spawning period indicated that maturation and spawning of eggs could largely, if not entirely, be supported by the conversion of energy reserves in tissue. *Loligo opalescens*, newly recruited to the spawning population, ovulated about 36% of their potential fecundity during their first spawning day and fewer ova were released in subsequent days. *Loligo opalescens* do not spawn all of their oocytes; a small percentage of the spawning population may live long enough to spawn 78% of their potential fecundity.

Loligo opalescens are taken in a spawning grounds fishery off California, where nearly all of the catch are mature spawning adults. Thirty-three percent of the potential fecundity of *L. opalescens* was deposited before they were taken by the fishery (December 1998–99). This observation led to the development of a management strategy based on monitoring the escapement of eggs from the fishery. The strategy requires estimation of the fecundity realized by the average squid in the population which is a function of egg deposition and mortality rates. A model indicated that the daily total mortality rate on the spawning ground may be about 0.45 and that the average adult may live only 1.67 days after spawning begins. The rate at which eggs escape the fishery was modeled and the sensitivity of changing daily rates of fishing mortality, natural mortality, and egg deposition was examined. A rapid method for monitoring the fecundity of the *L. opalescens* catch was developed.

Manuscript approved for publication 19 December 2003 by Scientific Editor.
Manuscript received 20 January 2004 at NMFS Scientific Publications Office.
Fish. Bull. 102:306–327 (2004).

Many loliginid squid populations depend entirely upon the reproductive output of the preceding generation because individuals live less than a year (Yang et al., 1986; Hatfield, 1991, 2000; Natsukari and Komine, 1992; Arkhipin, 1993; Arkhipin and Nekludova, 1993; Jackson, 1993, 1994; Jackson et al., 1993; Boyle et al., 1995; Jackson and Yeatman, 1996; Jackson et al., 1997; Moltschaniwskyj and Semmens, 2000; Semmens and Moltschaniwskyj, 2000). In California waters, *Loligo opalescens* (market squid, also known as the opalescent inshore squid [FAO]) live only 6–12 months (Butler et al., 1999) and die after spawning (McGowan, 1954; Fields, 1965). Thus, fecundity of *L. opalescens* is a critical life history trait and, in addition, must be known in order to estimate the biomass with either egg deposition or larval production methods (Hunter and Lo, 1997). *Loligo opalescens* is one of the most valuable fishery resources in California waters and is monitored under the Coastal Pelagics Species Fishery Management Plan of the Pacific Fishery Management Council as market squid.

Laptikhovsky (2000) pointed out that squid fecundity estimates would be biased if the females spawned ova prior to capture, if oocytes remained in the ovary after death, or if some of the standing stock of oocytes were lost because of atresia. Previous field work on squid fecundity has been limited to the traditional method of simply counting oocytes or ova (or both) of animals taken on the spawning grounds, and none of the biases identified by Laptikhovsky (2000) have been evaluated (Boyle and Ngoile, 1993; Coelho et al., 1994; Guerra and Rocha, 1994; Boyle et al., 1995; Collins et al., 1995; Moltschaniskyj, 1995; Lopes et al., 1997; Laptikhovsky, 2000). On the other hand, laboratory studies (Ikeda et al., 1993; Bower and Sakurai, 1996; Sauer et al., 1999; and Maxwell and Hanlon, 2000) have indicated that oocytes remain in the ovaries after spawning and death. Additionally, atresia was found to occur in all stages of oocytes of *Loligo vulgaris reynaudii* (Melo and Sauer, 1998). Modern approaches to estimating lifetime fecundity in fishes take the potential biases of past spawning history, residual fecundity, and atresia into account (Hay et al., 1987; Hunter et al., 1992; Macewicz and Hunter, 1994; Kjesbu et al., 1998). The initial objectives of the present study were to estimate the fecundity of *L. opalescens* by using a modern approach that considers such biases, and to provide a histological description of those aspects of ovarian structure upon which modern fecundity analyses are based. As our work progressed, we realized that it might be practical to manage the market squid fishery by monitoring egg escapement based on fecundity measurements. Thus, we added two new objectives: to conduct a preliminary evaluation of the use of egg escapement as a tool for management of the market squid fishery; and to develop a method

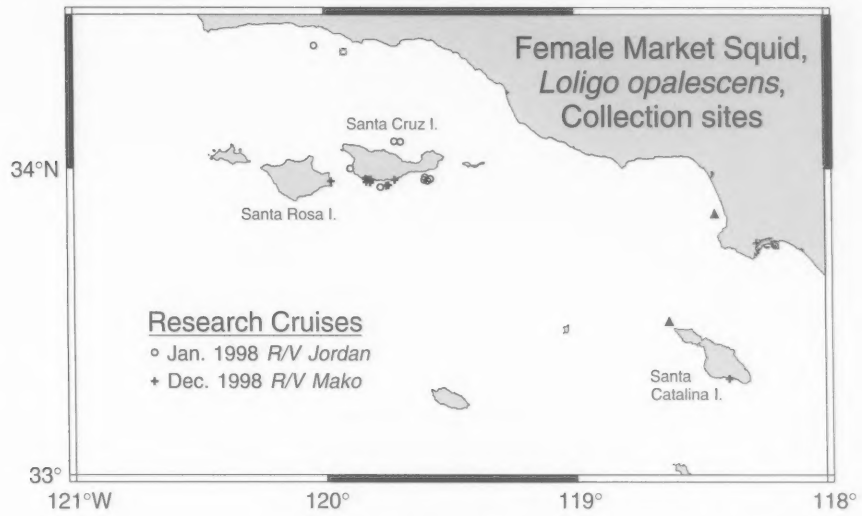

Figure 1

Collection locations for female *Loligo opalescens* during two joint research cruises during 1998 by California Department of Fish & Game (CDF&G) and National Marine Fisheries Service (NMFS) and for three immature females (triangles) collected during February 2000 (CDF&G).

to monitor the fecundity of the catch that avoids the costly process of counting all oocytes and ova.

In this study we consider four aspects of the fecundity of *L. opalescens*: potential fecundity, minimum residual fecundity, maximum fecundity, and the fecundity deposited by the average female in the population. *Potential fecundity,* or *potential lifetime fecundity,* is the standing stock of all oocytes in the ovary just before the onset of the first ovulation. Because *L. opalescens* are semelparous, the standing stock of all oocytes in the ovary just before first ovulation equals their potential lifetime fecundity. Clearly, once ovulation and spawning (deposition of ova in egg capsules on the sea floor) begin, the standing stock of oocytes can no longer be considered a measure of the potential fecundity of the female. *Minimum residual fecundity* is the minimum number of oocytes that might be expected to remain in the ovary at death. Because ovaries of dying *L. opalescens* contain oocytes (Knipe and Beeman, 1978), only a portion of the potential fecundity will be spawned in their lifetime. We use ancillary information on *L. opalescens* (an index of mantle condition and extent of ovarian development) to project what the minimum residual may be. *Maximum fecundity* (potential fecundity less the minimum residual fecundity) is the maximum number of eggs a female might be expected to deposit in a lifetime. We also estimate the fraction of the potential fecundity deposited by the average female, a key vital rate we approximate by modeling the daily rates of total mortality and egg deposition. Lastly, the term "standing stock of oocytes" is used throughout this article to indicate the total number of oocytes at all stages in an ovary. Whether the standing stock of a particular female is to be considered a potential fecundity, a residual fecundity, or something in between, depends upon ancillary information (i.e., presence of postovulatory follicles in the ovary, ova in the oviduct, mantle condition, or the level of ovarian maturity).

Materials and methods

We collected *Loligo opalescens* during two southern California research cruises in 1998 (7–15 January and 3–10 December) (Fig. 1). Most specimens were taken at night by using trawls, jigging, or by removing them from commercial purse-seine catches at sea; some specimens were collected during the day by using bottom trawls. We measured dorsal mantle length (mm), weighed the whole body (g), and classified the ovary and preserved it with viscera and oviduct attached in 10% neutral buffered formalin. To determine reproductive state we decided not to use the familiar ovary classification systems but rather tabulated gross anatomical characters and, later on, selected the most useful characteristics. See Table 1 for characters selected for scoring.

Preserved ovaries and oviducts were reclassified in the laboratory and weighed (to nearest 0.001 g). A piece of the preserved ovary from each of the 135 female *L. opalescens* from January and the 117 females from December was sectioned and stained (hematoxylin and eosin). Analyses of the histological sections included identification of the oocytes in the various development stages (I–VI) as described by Knipe and Beeman (1978), and identification of atresia and postovulatory follicles (Fig. 2). We use the term "ova" to indicate an ovulated mature oocyte (stage VI).

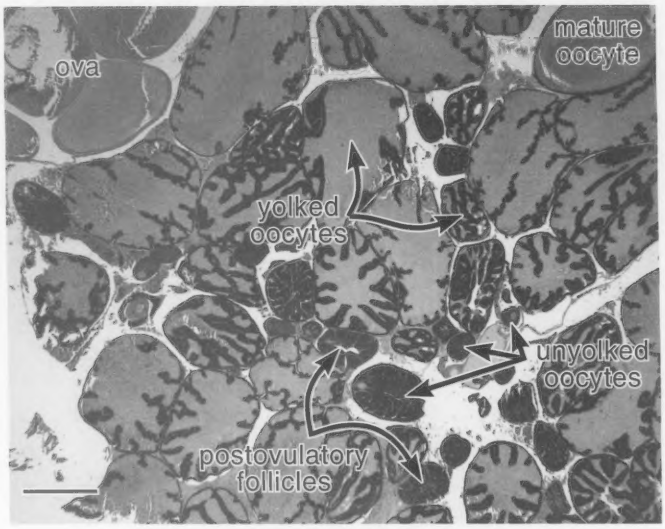

Figure 2

Slide of the ovary (stained with hematoxylin and eosin) of a mature spawning female *L. opalescens*. Bar = 1.0 mm.

Table 1

Classification system for the gross anatomical characteristics of the reproductive system of female market squid (*Loligo opalescens*).

Female organs	Character	Grade
Nidamental gland	length	millimeters
Accessory nidamental gland	color	0=clear, 1=whitish, 2= pink, 3=peach, 4=reddish-orange
Oviduct	number of large clear eggs	1=none, 2=1–20, 3=21–200, 4=>200
Ovary	number of large clear oocytes	1=none, 2=1–20, 3=21–200, 4=>200
Ovary	number of opaque or white oocytes	1=none, 2=1–20, 3=21–200, 4=>200

Postovulatory follicles were classified as either new, degenerating, or very degenerative. We assigned the females to one of the following reproductive categories on the basis of the histology of their ovaries (numerical stages in Knipe and Beeman, 1978):

Immature — Ovary contains only unyolked oocytes; oocyte development ranged from stages I (oogonia) to IV (follicular invagination oocyte) and requires microscopic examination.

Mature preovulatory — No postovulatory follicles are present. Ovaries contain oocytes with yolk (stage V, yolking begins about 1.1 mm in size); ovary usually contains unyolked oocytes.

Mature spawning — Ovary contains postovulatory follicles (POFs) of any degree of degeneration (none to extensive); more than one degenerative POF class may be present. Oocyte development stages III–VI are often present but stages Ic–II are rare. (2% of the ovaries have late stage Ic oocytes and none have any of the earliest stages, Ia or Ib.)

In some histological sections of ovaries we saw 1–10 yolking oocytes (development stage V) with a broken follicle layer, and the yolk seemed to be oozing out between the other oocytes. Because this may have been an artifact of handling, we did not use such females to estimate fecundity.

We used the gravimetric method (Hunter et al., 1985, 1992) to estimate the standing stock of oocytes in 98 *L. opalescens* ovaries. The gravimetric method overestimated the total number of oocytes of *Loligo pealeii*, but the difference between a count of all oocytes and a weight-based estimate was slight (Maxwell and Hanlon, 2000). We did not compare our estimates with a count of all oocytes in the ovary because we used a portion of the ovary for our histological examinations, and each value is the mean of the counts from two tissue samples (average coefficient of variation between samples was 0.12). All oocytes in each tissue sample were macroscopically classified (Fig. 3) as either unyolked, yolked, mature, or atretic; they were then counted by class and all stages were summed. "Atretic" was defined as oocytes in the alpha stage of atresia (Hunter and Macewicz, 1985b), recognizing, however, that poor preservation can create oocytes of similar macroscopic appearance. The number of ova in the oviduct was also counted directly (usually when n was less than 300) or the mean number was estimated from two tissue samples by using the gravimetric method. To illustrate the form of the oocyte-size distribution in the ovary, we measured (to 0.01 mm) the major axis of all the oocytes in one tissue sample from each ovary of six females by using a digitizer linked by a video camera to a dissection microscope. In all other ovaries used for fecundity estimation, we measured only the smallest and largest oocyte in the sample. The length of the major axis of the smallest oocyte (D) was used as an index of the extent of ovarian maturity. D is a crude index of time elapsed during the spawning period—as long as oocyte maturation continues throughout the spawning period and no new oocytes are produced—both of which appear to be true for *L. opalescens*.

To monitor body condition we cut a tissue sample disc from the mantle using a number 11 cork borer (area of 251.65 mm^2) and removed the outer dermis and the inner membrane. The mantle sample discs were frozen and subsequently dried at 56°C to a constant weight. An index of mantle condition (C) was calculated as the weight of the dry mantle in milligrams divided by disc surface area and is expressed as mg/mm^2.

We evaluated the extent that body reserves might be used to support egg production by comparing dry weight of the eggs and capsules to prespawning female body dry weight. For these calculations we made the following measurements: 1) the mean dry weight of one squid egg was 0.00177 g, including a fraction of the egg capsule because the value is based on the dry weight of 34 egg capsules (1–2 days old) containing 2 to 403 eggs each (total of 7341 eggs, capsules collected from La Jolla Canyon 6 July and 11 September 2000); 2) the relationship of dorsal mantle length (L) and whole-body wet weight (W_w) for immature and mature preovulatory females of $W_w = 0.000051L^{2.8086}$, where W_w is in grams and L is in mm (Fig. 4); and 3) the mean wet weight to dry weight conversion factor of 0.24 (2SE=0.001), based on the wet and dry weights of mantle tissue sampled from 214 mature females. The latter conversion factor was constant regardless of mantle condition index; apparently, in *L. opalescens*, starvation does not result in the replacement of muscle tissue with water as it does in fishes (Woodhead, 1960).

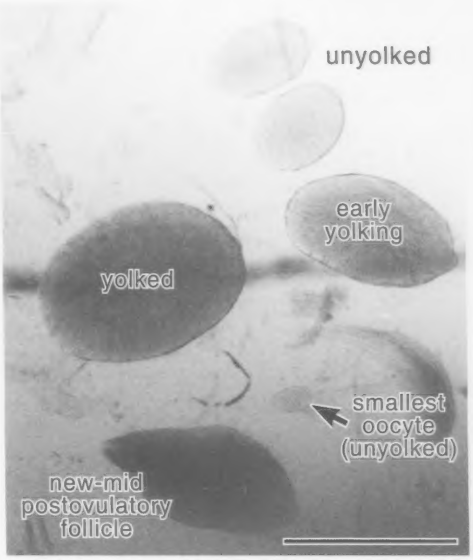

Figure 3

Whole *L. opalescens* oocytes as viewed under a dissection microscope used for counting and classifying oocytes. Bar = 1.0 mm.

In addition to the specimens taken during the research surveys, we also estimated the fecundity of 60 *L. opalescens* from the commercial catch sampled by California Department of Fish & Game (CDF&G) during 1998 and 1999. Landed specimens were not analyzed histologically because their ovarian tissues had begun to deteriorate before preservation. The 60 females were selected by dorsal mantle length and mantle condition index to provide a wide and uniform distribution of length and mantle condition. The number of oocytes in the ovaries was estimated (as described above) and the number of ova in the oviducts were predicted from oviduct weight (Fig. 5). CDF&G also provided data on the dry mantle disc weights of 1275 mature females taken from the catch from December 1998 through December 1999 as random samples taken during the Southern Californian Bight market squid fishery. About 100,000 tons of market squid were landed during this sampling period .

Modeling egg deposition

To identify egg deposition and mortality rates most consistent with our current understanding of spawning biology, we developed a model to estimate the proportion of the potential fecundity deposited by a cohort in its lifetime. The mean proportion of the potential fecundity deposited is the proportion of eggs deposited weighted by the propor-

Figure 2

Slide of the ovary (stained with hematoxylin and eosin) of a mature spawning female *L. opalescens*. Bar = 1.0 mm.

Table 1

Classification system for the gross anatomical characteristics of the reproductive system of female market squid (*Loligo opalescens*).

Female organs	Character	Grade
Nidamental gland	length	millimeters
Accessory nidamental gland	color	0=clear, 1=whitish, 2= pink, 3=peach, 4=reddish-orange
Oviduct	number of large clear eggs	1=none, 2=1–20, 3=21–200, 4=>200
Ovary	number of large clear oocytes	1=none, 2=1–20, 3=21–200, 4=>200
Ovary	number of opaque or white oocytes	1=none, 2=1–20, 3=21–200, 4=>200

Postovulatory follicles were classified as either new, degenerating, or very degenerative. We assigned the females to one of the following reproductive categories on the basis of the histology of their ovaries (numerical stages in Knipe and Beeman, 1978):

Immature — Ovary contains only unyolked oocytes; oocyte development ranged from stages I (oogonia) to IV (follicular invagination oocyte) and requires microscopic examination.

Mature preovulatory — No postovulatory follicles are present. Ovaries contain oocytes with yolk (stage V, yolking begins about 1.1 mm in size); ovary usually contains unyolked oocytes.

Mature spawning — Ovary contains postovulatory follicles (POFs) of any degree of degeneration (none to extensive); more than one degenerative POF class may be present. Oocyte development stages III–VI are often present but stages Ic–II are rare. (2% of the ovaries have late stage Ic oocytes and none have any of the earliest stages, Ia or Ib.)

In some histological sections of ovaries we saw 1–10 yolking oocytes (development stage V) with a broken follicle layer, and the yolk seemed to be oozing out between the other oocytes. Because this may have been an artifact of handling, we did not use such females to estimate fecundity.

We used the gravimetric method (Hunter et al., 1985, 1992) to estimate the standing stock of oocytes in 98 *L. opalescens* ovaries. The gravimetric method overestimated the total number of oocytes of *Loligo pealeii*, but the difference between a count of all oocytes and a weight-based estimate was slight (Maxwell and Hanlon, 2000). We did not compare our estimates with a count of all oocytes in the ovary because we used a portion of the ovary for our histological examinations, and each value is the mean of the counts from two tissue samples (average coefficient of variation between samples was 0.12). All oocytes in each tissue sample were macroscopically classified (Fig. 3) as either unyolked, yolked, mature, or atretic; they were then counted by class and all stages were summed. "Atretic" was defined as oocytes in the alpha stage of atresia (Hunter and Macewicz, 1985b), recognizing, however, that poor preservation can create oocytes of similar macroscopic appearance. The number of ova in the oviduct was also counted directly (usually when n was less than 300) or the mean number was estimated from two tissue samples by using the gravimetric method. To illustrate the form of the oocyte-size distribution in the ovary, we measured (to 0.01 mm) the major axis of all the oocytes in one tissue sample from each ovary of six females by using a digitizer linked by a video camera to a dissection microscope. In all other ovaries used for fecundity estimation, we measured only the smallest and largest oocyte in the sample. The length of the major axis of the smallest oocyte (D) was used as an index of the extent of ovarian maturity. D is a crude index of time elapsed during the spawning period—as long as oocyte maturation continues throughout the spawning period and no new oocytes are produced—both of which appear to be true for *L. opalescens*.

To monitor body condition we cut a tissue sample disc from the mantle using a number 11 cork borer (area of 251.65 mm^2) and removed the outer dermis and the inner membrane. The mantle sample discs were frozen and subsequently dried at 56°C to a constant weight. An index of mantle condition (C) was calculated as the weight of the dry mantle in milligrams divided by disc surface area and is expressed as mg/mm^2.

We evaluated the extent that body reserves might be used to support egg production by comparing dry weight of the eggs and capsules to prespawning female body dry weight. For these calculations we made the following measurements: 1) the mean dry weight of one squid egg was 0.00177 g, including a fraction of the egg capsule because the value is based on the dry weight of 34 egg capsules (1–2 days old) containing 2 to 403 eggs each (total of 7341 eggs, capsules collected from La Jolla Canyon 6 July and 11 September 2000); 2) the relationship of dorsal mantle length (L) and whole-body wet weight (W_w) for immature and mature preovulatory females of $W_w = 0.000051L^{2.8086}$, where W_w is in grams and L is in mm (Fig. 4); and 3) the mean wet weight to dry weight conversion factor of 0.24 (2SE=0.001), based on the wet and dry weights of mantle tissue sampled from 214 mature females. The latter conversion factor was constant regardless of mantle condition index; apparently, in *L. opalescens*, starvation does not result in the replacement of muscle tissue with water as it does in fishes (Woodhead, 1960).

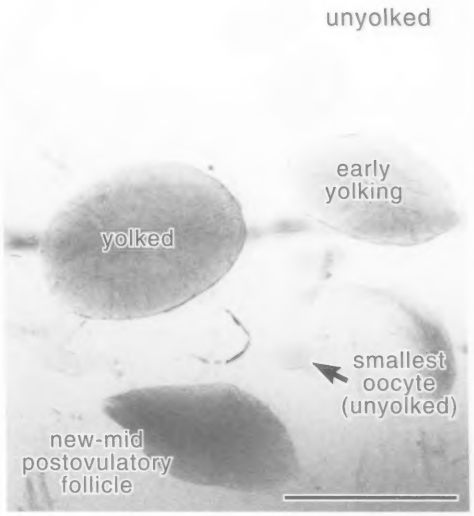

Figure 3

Whole *L. opalescens* oocytes as viewed under a dissection microscope used for counting and classifying oocytes. Bar = 1.0 mm.

In addition to the specimens taken during the research surveys, we also estimated the fecundity of 60 *L. opalescens* from the commercial catch sampled by California Department of Fish & Game (CDF&G) during 1998 and 1999. Landed specimens were not analyzed histologically because their ovarian tissues had begun to deteriorate before preservation. The 60 females were selected by dorsal mantle length and mantle condition index to provide a wide and uniform distribution of length and mantle condition. The number of oocytes in the ovaries was estimated (as described above) and the number of ova in the oviducts were predicted from oviduct weight (Fig. 5). CDF&G also provided data on the dry mantle disc weights of 1275 mature females taken from the catch from December 1998 through December 1999 as random samples taken during the Southern Californian Bight market squid fishery. About 100,000 tons of market squid were landed during this sampling period .

Modeling egg deposition

To identify egg deposition and mortality rates most consistent with our current understanding of spawning biology, we developed a model to estimate the proportion of the potential fecundity deposited by a cohort in its lifetime. The mean proportion of the potential fecundity deposited is the proportion of eggs deposited weighted by the propor-

tion of the cohort that died. Both the proportion of eggs deposited and squid that died were expressed as negative exponential functions. The cumulative eggs deposited up to elapsed time t (days) for a mature female *L. opalescens* is the difference of two terms: $E_{SP,t} = E_P - E_{YD,t}$ where $E_{SP,t}$ is the total eggs deposited by one female up to time t, E_P is the potential fecundity, and $E_{YD,t}$ is the standing stock of oocytes in the ovary plus the standing stock of ova in the oviduct remaining in the body at time t. If we assume that $E_{YD,t}$ declines at an exponential rate from E_P: $E_{YD,t} = E_P e^{-vt}$, where v is the daily rate of eggs deposited, then $E_{SP,t} = E_P(1-e^{-vt})$. We constructed the cumulative egg deposition curve as $Q_{SP,t} = E_{SP,t}/E_P = 1-e^{-vt}$. Assuming the mortality (survival) curve for the squid is e^{-zt}, where z is adult daily total mortality rate ($z=m+f$, where m is natural and f is fishing mortality), we computed the mean fraction of the potential fecundity deposited ($Q_{SP,t}$):

$$Q_{SP} = \frac{\int_0^{t_{\max}} ze^{-zt}(1-e^{-vt})dt}{\int_0^{t_{\max}} ze^{-zt}dt} \quad (1)$$

$$= 1 - \frac{z(1-e^{-(z+v)t_{\max}})}{(z+y)(1-e^{-zt_{\max}})} \cong \frac{v}{z+v} \text{ for large } t_{\max},$$

where $t_{\max}$ is the total elapsed time (days).

The mean fraction of the potential fecundity that remains in the average female (standing stock of oocytes and ova) over her lifetime is $1 - Q_{SP}$, and mean Q_{SP} is always less than one because of mortality. The mean duration of the spawning period in days is computed as the elapsed time corresponding to the mean fraction of eggs deposited (Q_{SP}: Eq. 1 and by setting $Q_{SP}=1-e^{-vt}$):

$$t_{Q_{SP}} = \ln(1 - Q_{SP})/(-u). \quad (2)$$

We evaluated various rates of adult daily total mortality (z) and egg deposition (v) using these models to determine the combination of rates that would provide estimates of fecundity nearest to our observed field data.

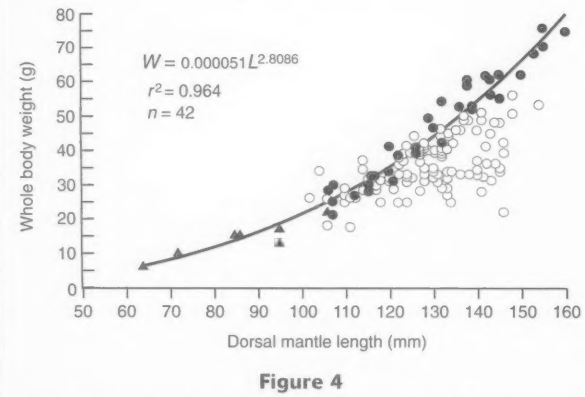

Figure 4

Female squid whole body weight (W) as a function of dorsal mantle length (L) for the 158 females with fecundity analyses. The line expresses the length-weight relation of females before weight losses associated with spawning and was fitted to the combined data for immature females (solid triangles), mature preovulatory females (solid circles), and mature females judged by their mantle condition to be new recruits to the spawning ground (solid circles). Open circles indicate females that have spawned.

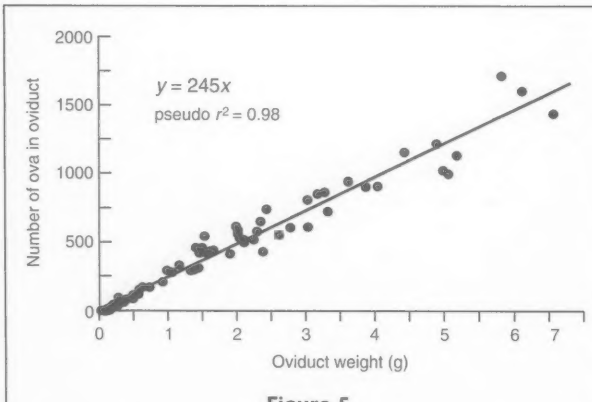

Figure 5

Number of ova in each oviduct shown as a function of the oviduct weight; n equals 91 mature females, pseudo r^2 = 1 – *residual ss/total ss*.

Modeling the effect of fishing effort on egg escapement

In theory we could manage the market squid fishery by monitoring egg escapement, that is, the fraction of the fecundity realized by the average female. Under such a management scheme, egg escapement would be maintained at a specified level by changing fishing effort whenever escapement of eggs fell below it. In this section we develop a model to explore the relative effects of fishing effort on egg escapement. We use this model to discuss some of the biological issues related to using egg escapement as a management tool.

In the modeling process, we follow one cohort of spawners. The elapsed time 0 is defined as the time when squid start spawning. The total escapement of eggs for a given elapsed time (t_k in days) is the sum of three sources of egg escapement: E_C, the total number of eggs deposited by mature females in the catch; E_M, the total number of eggs deposited by mature females dying of natural causes; and E_A, the total number of eggs deposited by females

alive and not taken by the fishery up to time t_k, and $t_k < t_{max}$. The egg escapement rate, R_{e,t_k}, up to time t_k is the sum of the three sources of egg escapement divided by the total number of eggs that would have been spawned if no fishery existed (E):

$$R_{e,t_k} = \frac{E_C + E_M + E_A}{E}. \quad (3)$$

Egg escapement rate at the maximum elapsed time (t_{max}) is

$$R_{e,t_{max}} = \frac{E_C + E_M}{E}, \quad (4)$$

where $t_k = t_{max}$.

Because there are no survivors at time t_{max}, no eggs can be deposited and E_A is zero.

Each term in Equation 3 can be expressed as functions of the mean cumulative number of eggs deposited up to time t_k, $\overline{E_{SP,t_k}} = \overline{E_P} - \overline{E_{YD,t_k}} = \overline{E_P}(1-e^{-vt_k})$, and total mortality ($z$) of the cohort; z includes both natural morality (m) and fishing mortality (f). For practicality, we considered cases when $t_k = t_{max}$, where E_A is zero. For formulas of any t_k, see appendix. The total number of eggs deposited by the females in the catch (E_C) is

$$E_C = \int_0^{t_{max}} \overline{E_{SP,t}} N_0 e^{-(m+f)t} f dt = \overline{E_P} N_0 \int_0^{t_{max}} (1-e^{-vt}) e^{-(m+f)t} f dt \quad (5)$$

$$= \overline{E_P} N_0 f \frac{v}{(m+f)(m+f+v)}, \quad (6)$$

where $\overline{E_P}$ = the mean number of oocytes in the ovary per mature female prior to spawning; and
N_0 = the number of mature females at time 0.

From the fishery data, we can estimate the total number of eggs deposited by the females in the catch (E_C) as

$$\hat{E}_C = N_C\left(\hat{\overline{E_P}} - \hat{\overline{E_{YD}}}\right), \quad (7)$$

where $\hat{\overline{E_P}}$ and $\hat{\overline{E_{YD}}}$ = sample estimates from the catch; and
N_C = the total number of spawners in the catch.

The total number of eggs deposited by *L. opalescens* prior to death due to natural mortality (E_M) is

$$E_M = \int_0^{t_{max}} \overline{E_{SP,t}} N_0 e^{-(m+f)t} m dt = \overline{E_P} N_0 \int_0^{t_{max}} (1-e^{-vt}) e^{-(m+f)t} m dt \quad (8)$$

$$= \overline{E_P} N_0 m \frac{v}{(m+f)(m+f+v)}. \quad (9)$$

The total eggs that would be deposited for the cohort without fishing mortality is

$$E = \int_0^{t_{max}} \overline{E_{SP,t}} N_0 m e^{-mt} dt = \overline{E_P} N_0 \int_0^{t_{max}} (1-e^{-vt}) m e^{-mt} dt \quad (10)$$

$$E = \overline{E_P} N_0 \frac{v}{m+v}, \quad (11)$$

where t_{max} (days) = the maximum elapsed time; and
time 0 = the time at the onset of egg deposition.

Egg escapement based on Equation 4 is

$$R_{e,t_{max}} = \frac{f\frac{v}{(m+f)(m+f+v)} + m\frac{v}{(m+f)(m+f+v)}}{\frac{v}{v+m}} = \frac{m+v}{m+f+v}. \quad (12)$$

Thus, egg escapement reduces down to a simple ratio, $\left(\frac{m+v}{m+f+v}\right)$ involving three daily instantaneous rates: natural mortality (m), egg deposition (v), and fishing mortality (f). $R_{e,t_{max}} = 1$ when there is no fishing and thus $R_{e,t_k} < 1$ with fishing mortality. The lower bound of the egg escapement rate for the cohort is equal to the ratio of the eggs escaping the fishery (E_C) to the total eggs deposited if no fishery existed (E):

$$R_e = E_C / E. \quad (13)$$

Results

Oocyte maturation and production

Immature ovaries contain many small unyolked oocytes with a pronounced peak at about 0.15 mm in size distribution (Fig. 6A). As development continues and vitellogenesis begins, the peak diminishes and shifts to a larger size class of unyolked oocytes (Fig. 6B). Just before the onset of spawning, the size distribution of oocytes becomes relatively flat without pronounced modes (Fig. 6C) and remains so through the rest of the spawning period (Fig. 6, D–F). The standing stock of oocytes declines throughout the spawning period. The minimum size of oocytes in the ovary gradually increases after the onset of yolking, indicating that new oocytes are not produced. We saw no primary oogonia in our histological sections of mature ovaries, another indication that new oocytes are not produced in mature ovaries. Knipe and Beeman (1978) reached the

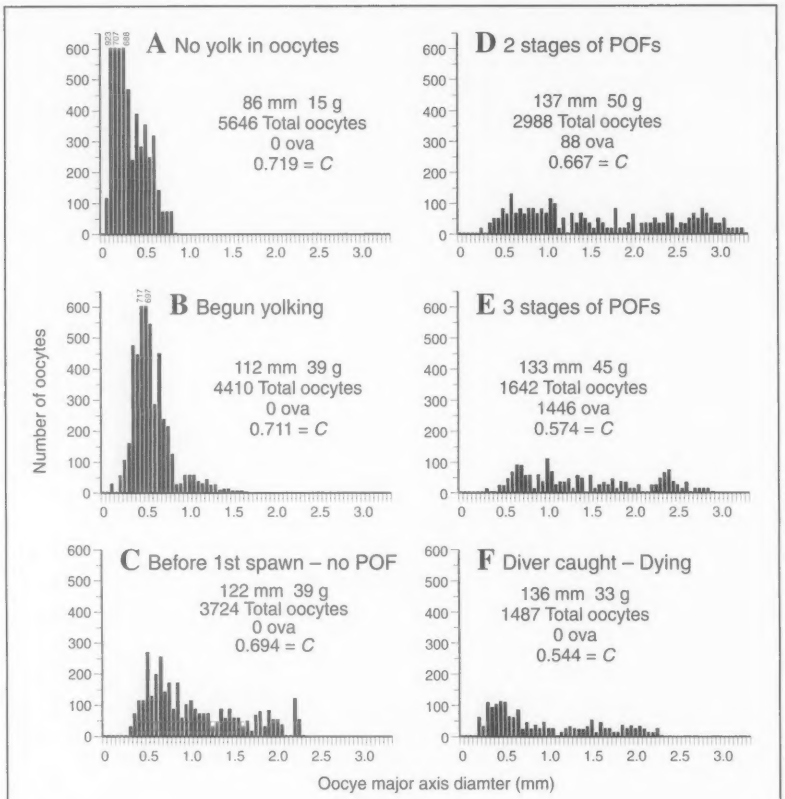

Figure 6

Oocyte-size distribution for six female *Loligo opalescens*. Dorsal mantle length (mm), body weight (g), the total number of oocytes in the ovary, and the number of ova are indicated for each specimen. (**A**) Female that is immature. (**B** and **C**) Females that are considered to be mature and preovulatory because neither has postovulatory follicles (POFs) in their ovaries nor ova in their oviducts. Although the oocytes have just begun yolking in the ovary of female B, female C has well-yolked oocytes and is close to its first ovulation. (**D–F**) Females are mature spawning females and their ovaries contained postovulatory follicles. Female F was caught by a scuba diver and appeared to be dying.

same conclusion from their histological analysis of *L. opalescens* ovaries. Thus, potential fecundity in *L. opalescens* probably becomes fixed near the onset of spawning. Not all oocytes are deposited, however, because all spawning females had some oocytes and many oocytes were counted in the ovary of a dying female (Fig. 6F).

In *L. opalescens* the migration of the oocyte nucleus begins early in the maturation process shortly before the onset of vitellogenesis, whereas in fishes, migration is near the end of vitellogenesis. The follicle of a migratory-nucleus-stage oocyte (late stage IV) of *L. opalescens* has a very large granulosa cell layer (in relation to the size of the oocyte) and is highly folded and perhaps fully developed. Subsequent maturation of the oocyte seems to consist primarily of the massive addition of yolk and fluid and the consequent stretching and unfolding of the follicle, ending with the formation of a chorion. Apparently, the formation of the chorion compacts the yolk because many mature oocytes (endpoint of stage V) have a smaller major axis than advanced yolked oocytes prior to chorion formation. Thus, maximum oocyte size is not a good proxy for oocyte maturation in *L. opalescens* and is not an indicator of the time remaining before spawning of the next batch. More importantly, the ovary of *L. opalescens* seems well adapted for rapid oocyte vitellogenesis, maturation, and spawning because nuclear migration and follicle cell proliferation is completed at an early stage.

Ovulation appears to occur in small batches. The distribution of oocyte sizes in spawning *L. opalescens* was flat (e.g., Fig. 6, D–F) and lacked the separate and distinct mode of hydrated oocytes that is typical in fishes. Batch sizes of mature oocytes ranged from 5 to 246 and averaged 50 (n=72

females). The maximum number of mature oocytes (246) was never close to the maximum number of ova (1726) in the oviduct. In addition, spawning females with 900 or more ova in their oviduct had in every case three or more distinctly different stages of postovulatory follicles in their ovaries (Table 2). Thus the oviduct is probably filled by a series of ovulation bouts separated by enough time to produce distinct age classes of degenerating follicles in the ovary.

Table 2

Percentage of spawning female market squid classed by the number of eggs in their oviducts and by the number of ages (stages of degeneration) of postovulatory follicles (POFs) in their ovaries.

Number of eggs in the oviduct	Number of females	Percentage of females	
		1 or 2 ages of POFs	≥3 ages of POFs
0	1	100	0
1–300	36	22	78
301–600	20	35	65
601–900	10	20	80
901–1200	7	0	100
1201–1500	2	0	100
1501–1800	2	0	100

Potential fecundity (E_P)

Potential fecundity (E_P) is the standing stock of oocytes of all stages in the ovary of a mature female just prior to the first ovulation. Finding females at this point in their reproductive cycle was difficult because nearly all specimens had already ovulated. The ovaries of 94% of the 247 mature females, from our research cruises, contained postovulatory follicles, indicating that they had recently ovulated and would not be suitable for estimating E_P. As can be seen in Figure 7A, spawning females had fewer oocytes in their ovaries than did mature preovulatory females. The relation between fecundity and squid size is best expressed in terms of dorsal mantle length (L) because *L. opalescens* lose weight during spawning (Figs. 4, 7C). The data from thirteen mature preovulatory females were used to establish the relationship between potential fecundity and L:

$$E_P = 85.62L - 6715, \qquad [r^2 = 34.3\%] \tag{14}$$

where L = dorsal mantle length in mm.

Because the constant was not significant (P=0.146) and the coefficient was (P=0.036), we forced the regression through zero which resulted in the equation

$$E_P = 29.8L. \tag{15}$$

Thus, the average female (129 mm) according to Equation 15 had a potential fecundity of 3844 oocytes (SE=317).

Clearly it would be preferable if the sample size for the estimate of potential fecundity were larger because thirteen females may not accurately represent the *L. opalescens* stock. Although the landed catch provides an unlimited supply of specimens, histological detection of postovulatory follicles is not possible because of deterioration of the ovaries. An alternative approach is to use mantle condition of mature females from the catch as a proxy for the preovulatory state. As can be seen in Figure 7C, the mantle condition index (C) of mature females declines as oocyte maturation continues and females deposit eggs. The mature preovulatory females (n=11, two discs were lost) had a mean C of 0.73 mg/mm^2 (SE=0.02). We believe that the twenty-two mature females from the landed catch with $C \geq 0.7$ mg/mm^2 had not begun to deposit eggs (Table 3). Because many of them had ovulated, we combined our estimates of the standing stock of oocytes (E_Y) with those of ova (E_D) to calculate total fecundity ($E_Y + E_D = E_{YD}$), and then regressed total fecundity on length. Although the regression was not significant, the average total fecundity of 3890 oocytes (Table 3) was within 5% of the potential fecundity of 4083 oocytes computed by substituting the mean length of the twenty-two females (137 mm) in Equation 15. The close agreement between these two values increases our confidence that the potential fecundity equation is accurate despite the low n. On the other hand, this rough comparison is not a substitute for increasing the sample size of specimens analyzed histologically, because females from the catch may have spawned some of their ova before they were captured.

Maximum fecundity ($E_P - E_R$)

Few if any *L. opalescens* live to realize their full potential fecundity (E_P). The literature on *L. opalescens* indicates that females that were described as "spawned out," dying, or dead had oocytes in all stages of development except the earliest previtellogenic stage (Knipe and Beeman 1978). In addition, all the spawning females that we collected had some oocytes in their ovaries. Thus, the maximum fecundity that *L. opalescens* might be expected to realize is the potential fecundity less an estimate of the number of oocytes that might be left in the ovary at death (residual fecundity [E_R]). To estimate residual fecundity we examined the relationship of the standing stock of oocytes in the spawning period with mantle condition index (C), size of the smallest oocyte (D), and dorsal mantle length (L).

The standing stock of oocytes in ovaries of mature females declines rapidly with decreasing mantle condition, between a C of 0.8 and 0.6 mg/mm^2, and more gradually over lower mantle conditions (Fig. 7C). A curvilinear relationship also exists between oocyte standing stock and the size of the smallest oocyte (Fig. 7B). Thus the number of past spawnings (decline in oocyte standing stock) appears to be inversely correlated with C and directly correlated with the extent of ovarian maturation as measured by D. To quantify how the standing stock of oocytes changes during the spawning period we fitted a nonlinear model to the fecundity data of 75 mature spawning females (Fig. 7) from our research cruises:

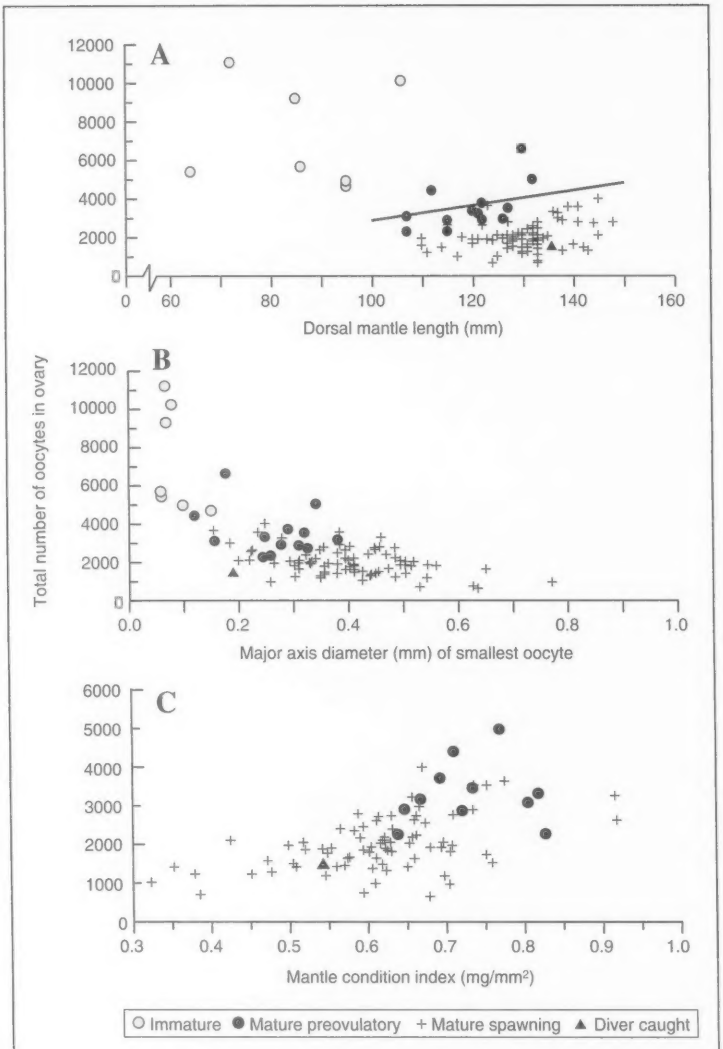

Figure 7

The number of oocytes in ovaries of 98 *Loligo opalescens* as a function of dorsal mantle length (**A**) and the diameter of the major axis of the smallest oocyte (**B**). In (**C**), the number of oocytes is plotted as a function of mantle condition index (the dry weight per surface area of a mantle tissue disc) for 87 mature females (4 discs were lost and the 7 immature were not included). Line in A expresses potential fecundity as a function of length (E_P=29.8L) for the 13 mature preovulatory females (solid circles); open circles represent immature females; plus signs represent spawning females; and the triangle represents a dying mature female.

$$E_R = 30283e^{(-1.24D - 6.19C - 0.024L + 0.059LC)}, \quad (16)$$

where C = mantle condition index;
D = size of the smallest oocyte; and
L = dorsal mantle length.

Substituting into the model (Fig. 8) the maximum observed D (0.771 mm) and the minimum observed C (0.323 mg/mm^2) from our research survey data set, we estimated that a female *L. opalescens* with L of 129 mm may have a minimum residual fecundity of 834 oocytes (CV=0.12).

Table 3

Mean fecundity, gonad weight, and dorsal mantle length for 60 mature female market squid (*Loligo opalescens*) sampled at the ports December 1998 to December 1999.

Mantle condition index (mg/mm^2)		Fecundity (mean number)			Mean gonad weight (g)	Dorsal mantle length (mm)		Number of females
Class	Mean	Oocytes in ovary (E_Y)	Ova in oviduct (E_D)	Total (E_{YD})		Mean	Range	
0.347–0.499	0.432	1134	231	1365	2.215	132	106–146	22
0.500–0.699	0.613	2072	522	2594	4.959	125	102–154	16
0.700–0.951	0.824	2589	1301	3890	8.988	137	106–160	22
0.347–0.951	0.624	1917	701	2618	5.397	132	102–160	60

A 129-mm *L. opalescens* with a potential fecundity of 3844 oocytes would have a maximum fecundity of 3010 eggs (3844–834 eggs) or about 78% of the potential fecundity. Very few females would be expected to deposit 78% of their potential because this maximum is based on extreme values for both mantle condition index and ovarian maturation. In a much larger set of mantle samples from the catch (Table 4), only 1.5% of the females had values of C less than 0.35 mg/mm^2. Clearly very few squid live to deposit 78% of their potential fecundity.

Another approach is to count the number of oocytes remaining in the ovaries of females presumed, from their behavior and appearance, to be dying. Although *L. opalescens* has been observed to be dying or dead on the bottom on video from a remotely operated vehicle (Cossio[1]), capturing such females was not attempted at the time. A female *L. opalescens* (136 mm) believed to be dying was opportunistically collected by a diver 6 July 2000 on the La Jolla Canyon spawning grounds (McGowan, 1954). There were no ova and the ovary contained 1487 oocytes—substantially more oocytes than our estimate of the minimum residual fecundity. In fact, the female had deposited only about 63% of her potential fecundity.

Table 4

Distribution of mantle condition index for 1275 mature female *L. opalescens* sampled from the landed catch from December 1998 to December 1999.

Mantle condition index (mg/mm^2)	Mature females	
	Number	Percentage
0.263–0.299	4	0.3
0.300–0.349	15	1.2
0.350–0.399	29	2.3
0.400–0.449	54	4.2
0.450–0.499	91	7.1
0.500–0.549	128	10.0
0.550–0.599	207	16.2
0.600–0.649	210	16.5
0.650–0.699	216	16.9
0.700–0.749	137	10.7
0.750–0.799	94	7.4
0.800–0.849	53	4.2
0.850–0.899	18	1.4
0.900–0.949	10	0.8
0.950–0.999	6	0.5
1.000–1.043	3	0.2

Role of body reserves

We used weight relationships to evaluate the extent to which body reserves might be used to support the reproduction of spawning female *L. opalescens*. In these crude energetic calculations we did not include metabolism, conversion efficiencies, or caloric values of tissues. We used the average dry weight of squid eggs, length to body weight conversion, potential fecundity equation, and the conversion factor from wet to dry mantle weight. We assumed preovulatory mantle condition index (C) for an average mature female of 130 mm was 0.798 mg/mm^2, the mean for values (n=41) of $C \geq 0.700$ mg/mm^2 in the our fecundity data set. We calculated that the potential fecundity of a 130-mm *L. opalescens* (i.e., 3874 encapsulated eggs) has a dry weight of 6.86 g which is equivalent to 64.8% of the whole-body dry weight (10.58 g) of that female just before spawning. If mantle condition is reduced in proportion to the dry weight of all the eggs, our hypothetical female would have a C of about 0.281mg/mm^2 (0.798 × [(10.58–6.86)/10.58]). This end point (C=0.281, egg=0) and the beginning point for the mature preovulatory female (C=0.798, eggs=3874) create a hypothetical

[1] Cossio, A. 2000. Personal commun. Southwest Fisheries Science Center, National Marine Fisheries Service, 8604 La Jolla Shores Dr., La Jolla, CA 92037

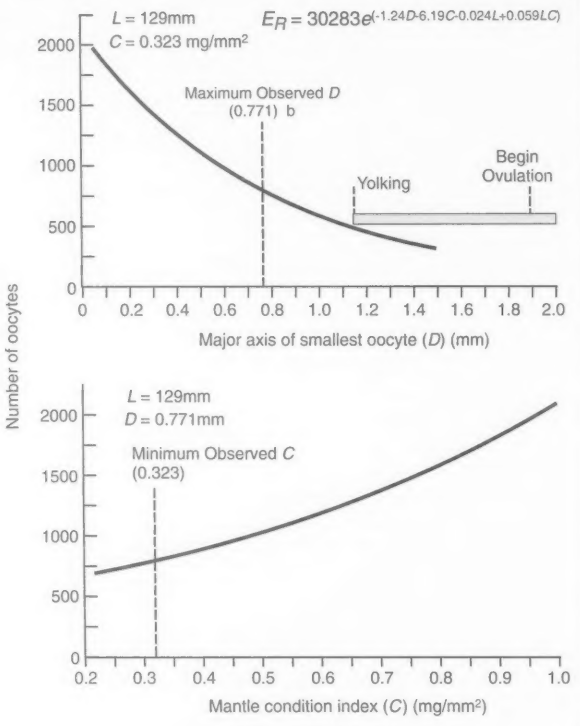

Figure 8

Changes in the standing stock of oocytes predicted by Equation 16 (equation also given at top of panel) when major axis of smallest oocyte (D) is varied and mantle condition index (C) held constant (upper panel), and when C is varied and D held constant (lower panel). The major axis size of oocyte when yoking begins and when ovulation begins is also indicated, as are the maximum observed D and minimum observed C. Substitution of the latter two values into the equation yields the standing stock of oocytes of females close to the end of their reproductive activity and is considered to be a minimum estimate of residual fecundity.

line that expresses oocyte standing stock for the average mature female of 130 mm as a function of mantle condition. In addition to the hypothetical line, we plotted the total standing stock of oocyte and ova (E_{YD}) and mantle condition index for all 147 mature females used for direct fecundity determinations (Fig. 9). Our hypothetical line, based on direct proportionality between egg dry weight and body dry weight, follows the general trend in the data, indicating that energy reserves in mantle tissue may largely support the production and spawning of eggs. Of course, actual energy costs would be higher because metabolism, other somatic tissue, and conversion efficiency of mantle tissue to eggs are not considered. The lowest observed C in the fecundity data set was 0.323 and the lowest C observed in the 1275 mature females from the landed catch was 0.263. Using the above preovulatory C (0.798 mg/mm^2), we determined that these values of C are equivalent to 60% and 67% losses in body dry weight for these individuals. Fields (1965) suggested body wet weight declined by as much as 50%, which is consistent with our results.

These rough calculations support the long held belief that oocyte maturation is supported primarily by body reserves. Some feeding occurs during spawning; *L. opalescens* has been observed feeding under lights at night on the spawning grounds (Butler[2]). Maxwell and Hanlon (2000) observed *L. pealeii* feeding between egg-laying bouts when they were held in the laboratory. Feeding between spawning bouts by the more robust spawners that may migrate on and off the grounds each day seems quite

[2] Butler, J. 2000. Personal commun. Southwest Fisheries Science Center, National Marine Fisheries Service, 8604 La Jolla Shores Dr., La Jolla, CA 92037.

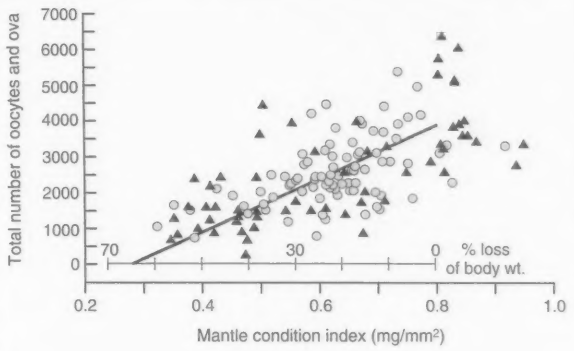

Figure 9

Standing stock of oocytes and ova as a function of mantle condition index for 60 mature females taken in the fishery (triangles) and 87 mature females taken in research surveys (circles). The line (not drawn to the data points plotted) represents a possible relation if losses in body weight were equivalent to the weight of the spawn released, computed for an average female (130 mm) where the starting point is her potential fecundity of 3874 oocytes and ends with 0 eggs and a mantle condition index of 0.281 mg/mm².

possible, but it seems unlikely for the nearly exhausted *L. opalescens* that are near the end of their life.

Longevity and egg deposition rates

Inferences regarding the longevity of adult spawning *L. opalescens* are the best proxy we have for the mortality rates of spawning adults. Previous observers (McGowen, 1954; Fields, 1965) suggested that females deposited all their eggs in one night and death soon followed. On the other hand, it is unreasonable to expect that a reduction of 60% in body weight and the maturation and deposition of up to 78% of the potential fecundity could take place in 24 hours. Our data on fecundity and mantle condition show an initial rapid decline in the number of oocytes followed by a more gradual decline (Fig. 7C), indicating an initial period of intense egg laying may be followed by a longer one where fewer eggs are deposited. It is also important to recognize that ovaries of spawning animals contain a wide range of oocyte sizes (Fig. 6), including many small unyolked oocytes (0.3–1 mm) that may mature and be deposited during the spawning period. It is unlikely that all these processes (body resorption, dynamic changes in rates of egg deposition, and maturation of small unyolked oocytes) could occur in one 24-hour period. Spawning periods longer than two weeks also seem unlikely because mature *L. opalescens* females may require extensive feeding periods and prolonged absences from the spawning grounds; these behaviors are inconsistent with our energetic analysis in the preceding section. Our analysis indicated that the observed reduction in eggs can be fairly well explained by the observed reduction in squid dry weight.

Egg deposition rates provide another way to infer the longevity of spawning squid. The best evidence for the rate of egg deposition is provided by females judged, on the basis of their high mantle condition ($C \geq 0.700$ mg/mm²), to be new recruits to the spawning grounds. Considering only those new recruits that have ovulated (postovulatory follicles present or ova in the oviduct), the difference between their average oocyte standing stock (E_Y=2571) and their average potential fecundity (E_P=4020) was equivalent to a reduction of 1449 oocytes or 36% of their potential fecundity (Table 5). If the difference is spawned in 24 hours or less, then 36% can be considered as an average for the first day of egg deposition. Instead of using the reduction of oocyte standing stock, one could consider the standing stock of ova (E_D) to be equivalent to the first day (24-hour period) of spawning in these new recruits. Their average E_D was 1073 or 27% of their potential fecundity. Thus depending on the criteria, the first day of spawning might be 27% to 36% of the potential fecundity. We prefer 36% because it is unaffected by any losses due to egg deposition.

The standing stock of ova (E_D) of spawning females with lower mantle condition (C<0.7 mg/mm²) averaged 9% of their potential fecundity. If the average E_D from these females is a crude measure of daily egg deposition rates after the first day, then we calculate it would take seven additional days [(100%–36%)/9%] to use up the remaining potential fecundity or a total spawning period of eight days. Eight days is an extreme value because an adult *L. opalescens* has never been taken with zero oocytes. The minimum residual fecundity was 22% of the potential which is roughly equivalent to about two days of egg deposition. Thus, six days may be a better guess of the maximum longevity of spawning *L. opalescens*.

Table 5

The mean fecundity for various classes of mantle condition for spawning *Loligo opalescens* and the grand mean weighted by the frequency of mantle condition classes in fishery samples 1998–99.

Class of mantle condition (mg/mm^2)	Number of spawning females	Mean fecundity (SE)			Dorsal mantle length in mm	Mean potential fecundity[1] (SE)	Number of eggs deposited $E_{SP} = E_P - E_{YD}$	Weighting factors (Table 4)
		Oocytes in ovary (E_Y)	Ova in oviduct (E_D)	Total (E_{YD})	Mean (SE)			
≤0.499	31	1212 (93)	207 (40)	1419 (100)	133 (2.08)	3954 (384)	2535	0.151
0.500–0.699	70	2008 (84)	437 (49)	2496 (100)	128 (1.20)	3813 (340)	1317	0.597
≤0.700	34	2571 (202)	1073 (109)	3657 (210)	135 (2.37)	4020 (385)	363	0.252
0.323–0.951	135	1967 (83)	544 (47)	2541 (102)	131 (1.01)	3897 (336)	1356	
				2599[2]	129.5	3859 (320)	1260[3]	

[1] Potential fecundity (E_P) estimated by $E_P = 29.8L$, where L = dorsal mantle length in millimeters.

[2] Product of population E_P and weighted average of the fraction of potential fecundity remaining in spawners):
$3859 \times [(1419/3954 \times 0.151) + (2496/3813 \times 0.597) + (3657/4020 \times 0.252)] = 2599$; or the population E_P less $E_{SP(weighted)}$ which is 3859–1260.

[3] Weighted average of the number of eggs deposited $[(2535 \times 0.151) + (1317 \times 0.597) + (363 \times 0.252)]$.

Probably very few females would be expected to survive six days because only a small percentage of the spawning population (Table 4) met the mantle criteria for minimum residual fecundity.

In summary, our best guess of the maximum longevity of squid on the spawning grounds is about six days. Our best description of daily egg deposition is a rate that ends the first day with 36% of the potential fecundity deposited and averages about 9% of the potential per day over the remaining five days and where only a small percentage of the females live to deposit 78% or more of their potential fecundity.

Egg escapement

We examine the spawning dynamics of *Loligo opalescens* from the standpoint of possibly using fecundity of the catch to monitor and ultimately regulate escapement of eggs from the fishery. The key variable in this approach is the fraction of the potential fecundity that is actually deposited as eggs on the bottom because this value can be directly estimated from the fecundity of the catch. Two other important parameters are the daily rate of total mortality (z) on the spawning grounds and the daily rate of egg deposition (v). Neither of these parameters can be directly estimated but they are approximated by values that are most consistent with our observations by using a model (Eq. 1). Our observations consist of the fecundity of the catch and the inferences regarding longevity and egg deposition, presented in the previous section. We use our approximations for egg deposition and total mortality in a second model (Eq. 12) to gain an idea of how natural mortality and fishing mortality may affect egg escapement. Lastly, we present a rapid method for monitoring the fecundity of the catch which does not require direct counting of oocytes or ova.

Fraction of the potential fecundity spawned (Q_{SP}) In a spawning population of *L. opalescens*, the mean standing stock of oocytes and ova ($\overline{E_{YD}}$), when expressed as a fraction of potential fecundity, is equivalent to the fraction of the potential fecundity of the population that remains in the spawners ($\overline{E_{YD}}/\overline{E_P}$). When subtracted from one ($1-[\overline{E_{YD}}/\overline{E_P}]$), the difference becomes the fraction of the potential fecundity of the population that is actually spawned (Q_{SP}). For this interpretation to be correct, samples must be randomly drawn from the population and represent all spawners according to their abundance on the spawning grounds—from the newly recruited to those that have been spawning for extended periods.

Neither the females taken from our research cruises nor those used to estimate fecundity from the landed catch were random samples of the spawning population. First, not all of the specimens taken during the two research cruises were from the spawning grounds. Second, the 60 females from the commercial catch were not randomly chosen but were selected to represent a full range of L and C. However, by weighting our fecundity estimates by a random sample of mantle condition from the fishery, it was possible to approximate a random fecundity sample of spawners. The population we used for weighting was based on the mantle condition index (C) of 1275 randomly taken specimens from the commercial catch sampled December 1998 through December 1999 (Table 4). The weighted and unweighted mean standing stocks of oocytes and ova ($\overline{E_{YD}}$) were similar (Table 5), indicating that our previous selection of specimens by C did not introduce a large bias. For the unweighted data, $\overline{E_{YD}}$ was 2541 and was 2599

Table 6

Estimates of number of days of egg deposition, the mean number of eggs deposited, mean standing stocks of oocytes and ova remaining in female *L. opalescens*, mean number of eggs deposited at the end of the first night (all means are expressed as a fraction of the potential fecundity), for various combinations of possible egg deposition (v) and total adult mortality (z) rates. Model provided estimate nearest observed data when $z = 0.45$, $v = 0.25$, and $t_{max} = 8$ days.

Daily total mortality (z)	Daily egg deposition rate (v)	Fraction of potential fecundity deposited Q_{SP} (Equation 1)	Fraction of potential fecundity remaining in females $(1 - Q_{SP})$	Mean number of nights of egg deposition $t_{Q_{SP}}$ (Equation 2)	Fraction of eggs deposited at the end of the first night $(1 - e^{-v})$	Days to reach 78% eggs deposited
0.2	0.25	0.458	0.542	2.45	0.221	6.057
0.2	0.45	0.617	0.383	2.13	0.362	3.365
0.2	0.65	0.706	0.294	1.88	0.478	2.329
0.45	0.25	0.341	0.659	1.67	0.221	6.057
0.45	0.45	0.486	0.514	1.48	0.362	3.365
0.45	0.65	0.580	0.420	1.33	0.478	2.329
0.8	0.25	0.237	0.763	1.08	0.221	6.057
0.8	0.45	0.359	0.641	0.99	0.362	3.365
0.8	0.65	0.447	0.553	0.91	0.478	2.329
Observed		0.326 (SE 0.075)	0.674		0.36	6.0

when the data were weighted by the distribution of mantle conditions in the catch. The mean fraction of the potential fecundity deposited (Q_{SP}) by *L. opalescens* was 0.326 (1–2599/3859). That much of the fecundity had escaped (eggs were deposited) before the market squid were taken by the fishery does not seem unreasonable because 22–36% of E_P may be deposited during the first day of spawning. The mean Q_{SP} is an important index because it measures egg escapement as a fraction of potential fecundity over its lifetime (Eq. 1). It is used in subsequent sections to identify a daily total mortality rate and egg escapement rate for the average female in the population that best characterizes the sampled *L. opalescens* population.

Preferred mortality and egg deposition rates We used Equation 1 to evaluate which combination of a range of plausible values for the rates of daily total mortality (z of 0.2, 0.45, and 0.8) and daily egg deposition (v of 0.25, 0.45, and 0.65) provides an estimate closest to observed Q_{SP} ($\overline{E_{SP}}/\overline{E_P}$) (Table 6). The combination of an adult daily total mortality (z) rate of 0.45, a daily egg deposition (v) rate of 0.25, and using a $t_{\max}$ of 8 days gave an estimate that was most consistent with the observed value for Q_{SP} of 0.326 (Table 6, Fig. 10). This combination of rates also gave an egg depletion of 78% of the potential fecundity in 6 days which was consistent with our best guess for maximum longevity and maximum fecundity. On the other hand, the model (using $1-e^{-vt}$ and t=1) predicts that about 22% of the potential is deposited by the end of the first 24 hours (day 1) which is less than our preferred estimate (36%) based on the reduction in standing stock of oocytes but is closer to the one based on the standing stock of ova (27%). A possible biological explanation for the difference might be that some of the ova produced during the first day of deposition might remain in the oviduct and then be deposited on the second day. Regardless of the uncertainties regarding the fit for the initial day of egg deposition, a daily total mortality rate of 0.45 and daily egg deposition rate of 0.25 are most consistent with the field data known at the present time. This means that the average spawning period is very short; the average female lives only 1.67 days after spawning begins (ln(0.659)/–0.25; Eq. 2). It is interesting that 1.67 days for the average animal is not a radical departure from Fields's (1965) original conclusion of a single night of spawning.

Egg escapement from the fishery In *L. opalescens*, where the fishery targets spawning adults that die after spawning, it is important to know the effect of fishing mortality on the egg escapement rate with respect to the lifetime fecundity deposited, $R_{e,t\max}$ (Eq. 12). However, not all terms in Equation 12 are observable and it may be practical to manage the fishery by monitoring the fraction of the potential fecundity that is deposited on the bottom (Q_{SP}= $1-[\overline{E_{YD}}/\overline{E_P}]$). Nevertheless, we examined the potential effects of fishing mortality (f) on the egg escapement rate, $R_{e,t\max}$, when natural mortality (m) is 0.1, 0.25, or 0.4, and egg deposition (v) is 0.25, 0.45, or 0.65 (Fig. 11). Because our preferred rates from the previous section are $v = 0.25$ and $z = 0.45$, then m is <0.45 with fishing because $z = m + f$. If we use $v = 0.25$ and set daily natural mortality rate high (m=0.4), then f is 0.05 and $R_{e,t\max}$ is 93%. Doubling the fishing mortality (to 0.1) produces an absolute difference of 6% in egg escapement (Fig. 11C). Thus at a high m of 0.4, escapement is relatively insensitive to changes in daily

fishing mortality. At lower natural mortalities, a change in fishing mortality has a greater effect on escapement. At $m = 0.1$ and $f = 0.35$ $R_{e,t_{max}}$ is 50%. Doubling the fishing morality to 0.7 $R_{e,t_{max}}$ would be 33%, producing a loss of 17% in escapement (Fig. 11A). Increasing the rate of daily egg deposition (v) from our preferred value of 0.25 to 0.65 also diminishes the effect of fishing mortality on escapement but the effect of fishing on egg escapement is most marked at the low natural mortality of m = 0.1 and is relatively minor when natural mortality reaches $m = 0.4$. Thus, uncertainties regarding the true initial values of egg deposition seem relatively unimportant at these high mortality rates. It is important to remember that in this discussion that we are discussing daily mortality rates that last only a few days or weeks of the life of a semelparous animal; hence the rates are very high and resemble the typical daily mortality rates of small pelagic fish eggs (Alheit, 1993) that also exist for short periods.

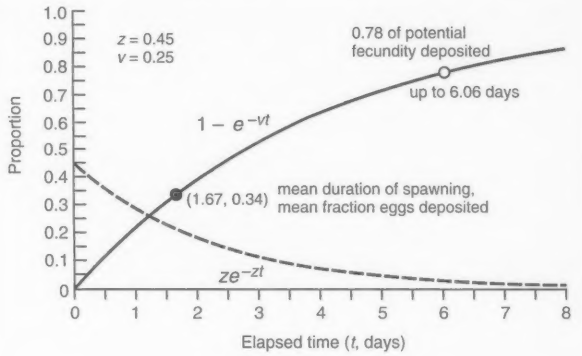

Figure 10

The cumulative egg release curve (solid line) and the density function of longevity on the spawning grounds of adult females (dashed line) of *Loligo opalescens* for a total mortality rate (z) of 0.45 and a egg release rate (v) of 0.25. The plotted solid circle represents mean egg deposition estimated by the model as a proportion of the potential fecundity and model estimate of the mean duration of the spawning period.

Cost effective methods for monitoring fecundity If egg escapement were adopted as a monitoring and management tool for the market squid fishery, a cost-effective method for monitoring fecundity of *L. opalescens* would be needed. A direct estimation of the standing stock of oocytes in an ovary by using a microscope and video system (as preformed in this study) is too time consuming for routine monitoring of the fishery because it takes about 4 hours per specimen.

Our first approach for an indirect estimator was to use the measurements routinely taken by CDF&G staff who sample the catch. These measurements were dorsal mantle length, mantle condition index, and an oviduct classification system for approximating the numbers of ova. To estimate the oocyte standing stock (E_Y) of the catch females, using only length and mantle condition, we fitted a nonlinear model to the data for all squid classed as mature (spawning individuals and pre-ovulatory) in our 1998 research survey data set. This yielded the equation

$$E_Y = 220.453e^{(1.99C + 0.0079L)}, \quad (17)$$

where L = dorsal mantle length; and
C = mantle condition index.

Equation 17 for E_Y explains only 33% of the variability within the survey data set (n=90) and therefore is rather imprecise. Using this model we estimated E_Y to average about 2221 oocytes in the ovaries of the mature females

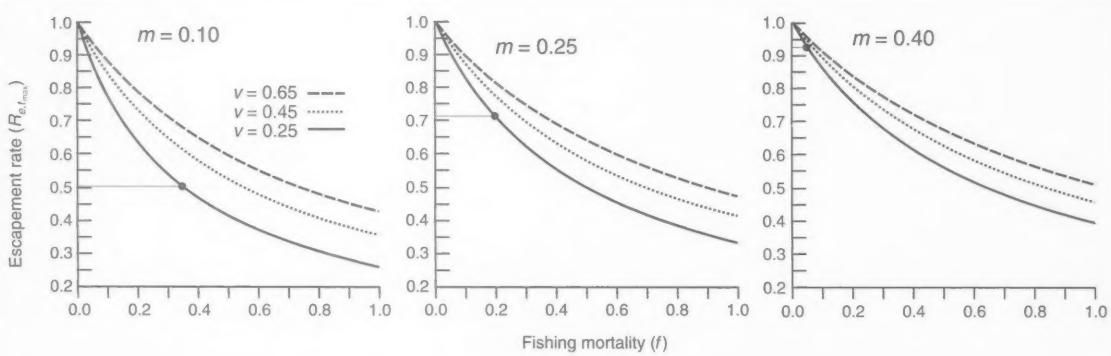

Figure 11

The egg escapement rate, $R_{e,t_{max}}$ (Eq. 12) of *L. opalescens* as a function of various daily natural adult mortality rates (m), daily egg deposition rates (v), and daily fishing mortality rates (f). In each panel, the solid circle indicates the f value for preferred values: $z = 0.45$ and $v = 0.25$.

(n=1275) sampled from catch during the period 1998–99 (Fig. 12); this estimate is equivalent to approximately 58% of the potential fecundity calculated from mean length (129 mm).

Our second approach was to estimate total fecundity (E_{YD}, standing stock of oocytes and ova) indirectly using the combined formalin wet weight of the ovary and the oviduct, in addition to mantle condition. Combining ovary and oviduct in one weight is more efficient than weighing them separately because much less time is required for dissection. Dorsal mantle length was also considered as a variable but it was not significant. The final equation for the total standing stock of oocytes and ova in a mature female squid is

$$E_{YD} = 378.28e^{(2.33C + 0.2447G - 0.24CG)}, \qquad (18)$$

where C = mantle condition index; and
G = gonad (ovary and oviduct) weight.

The predicted fecundity related well to the observed with a pseudo r^2 of 0.60 (df=143). We also used generalized additive models to estimate fecundity (GAM, pseudo r^2=0.64), as well as regression on the first principal component which explained 86% of the total variation (pseudo r^2=0.55). Although the GAM gave a slightly higher pseudo r^2 than the parametric nonlinear regression, we chose the later for easier interpretation and implementation. A pattern existed in the residuals from our model (Fig. 13); the model overestimated some fecundities at high mantle condition and underestimated fecundity at low mantle condition. This pattern in the residuals is probably related to the differences in density and size of oocytes in the ovary. Regardless of the minor problem with the residuals, this proxy (Eq. 18) for the standing stock of oocyte and ova is preferred because it gives a much more precise estimate at the minor additional cost of preserving and subsequently determining the combined weight of ovary and oviduct. Although formalin weight of ovary and oviduct are not presently monitored in the fishery, it is a variable that could be added to fishery protocols at a minor increase in cost. Another benefit of this more precise approach using E_{YD} is that oviduct is included in the estimate. If an estimate of the removal of fecundity by the fishery is needed, ova must be included. Because ova are not included in Equation 17, to add them requires using the oviduct classification system (Table 1) to estimate the average number of ova—a system that is imprecise but cheap. One could, of course, use Equation 17 for E_Y and either count the ova in the oviduct or weigh the oviduct, but that would take more work than applying Equation 18 for E_{YD}.

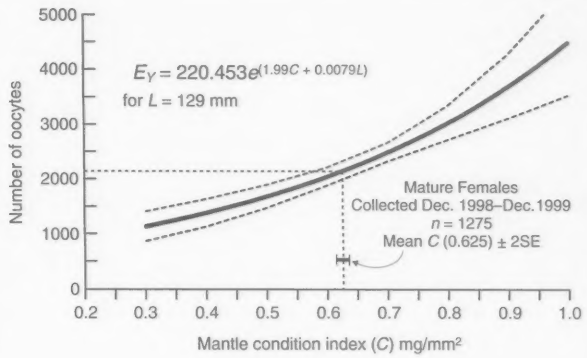

Figure 12

Standing stock of oocytes in the ovary (E_Y) as a function of mantle condition index (C) for a 129-mm mature female *L. opalescens* as predicted by Equation 17 (equation also given on top of panel; L is dorsal mantle length). Dashed lines are ±2SE. The mean E_Y for the females taken in the fishery was 2221 oocytes.

Discussion

Potential fecundity

Our estimate of *Loligo opalescens* potential fecundity is based on a regression of the standing stock of oocytes on dorsal mantle length for mature preovulatory females having yolked oocytes in their ovaries. The accuracy of this approach depends upon the assumption that these females are at the point in life when the standing stock of oocytes in their ovaries is equivalent to their potential lifetime fecundity. This key assumption would not hold if some of the mature squid classed histologically as preovulatory had in fact spawned. We do not know how long postovulatory follicles are distinguishable from atretic structures in the ovary of *L. opalescens* and, as far as we know, the rate of degeneration has not been determined for any loliginid. We know from our work on anchovy (Hunter and Goldberg, 1980; Hunter and Macewicz, 1985a), although it is not a cephalopod, that postovulatory follicles are distinguishable from atretic structures in the ovary of anchovy for about two to three days after spawning when the water temperature is about 16°C. This means that for undetected spawning to occur in *L. opalescens,* the interval between ovulation periods would likely need to exceed three days. This may be a minimum estimate because *L. opalescens* spawn at lower temperatures (9–13°C, Butler[2]) than do anchovy. Definitely a laboratory study on the rate of degeneration is necessary because postovulatory follicles in fish degenerate slower at lower temperatures (Fitzhugh and Hettler, 1995). In addition to the absence of postovulatory follicles, the oviduct must be empty for a spawning act to be undetected. Undetected ovulation and spawning seems unlikely because females with multiple stages of postovulatory follicles were common (87% of 247 mature females), females with only old postovulatory follicles were not detected, and the average life span on the spawning grounds may only be a few days.

Atretic losses of oocytes are another possible bias in estimating potential fecundity. Atresia (degeneration and resorption of an oocyte and its follicle) appears to be a

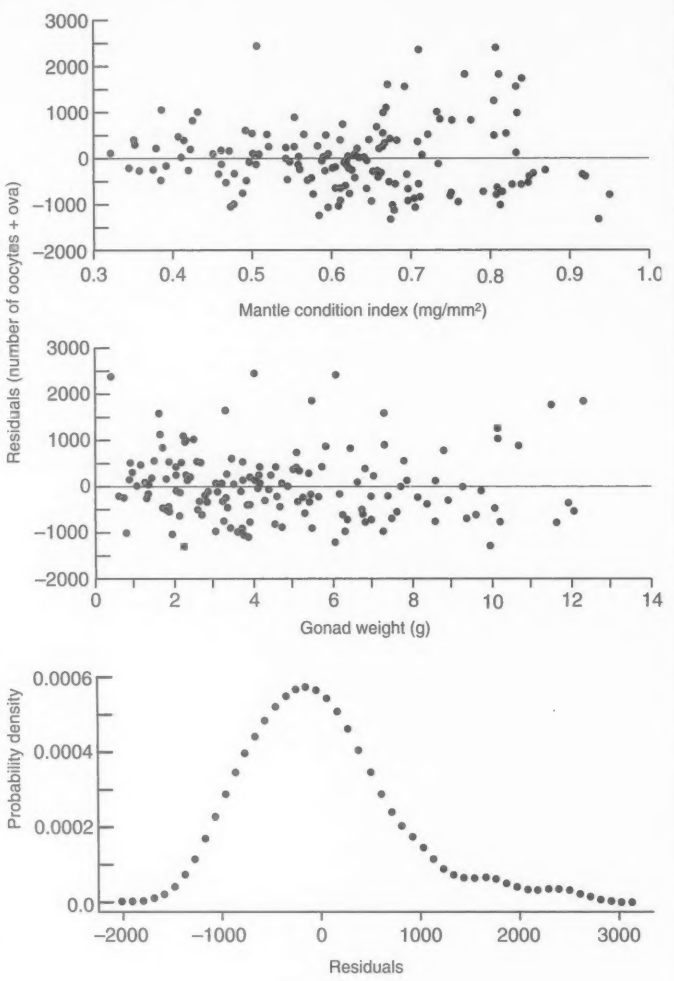

Figure 13

Residual plots of number of oocytes and ova from the equation $E_{YD} = 378.28e^{(2.33C+0.2447G-0.24CG)}$ (Eq. 18) where standing stock of oocytes and ova (E_{YD}) are predicted from mantle condition index (C) and gonad weight (G). Bottom panel shows probability density of residuals.

normal part of ovarian maturation in *L. oplaescens*, as it is the case for *L. v. reynaudii* (Melo and Sauer, 1998). Our evidence for this is that the standing stock of oocytes in immature female *L. opalescens* declines sharply as their ovaries mature (D increases, Fig. 7B). Clearly a narrow window of opportunity exists for an unbiased estimate of the potential fecundity of *L. oplaescens*. If the count is made too early in the ovarian maturation process, the count will either be low because extensive primary oogonia production may be still be occurring (64-mm female, Fig. 7A) or too high because additional oocytes will be absorbed before the female reaches maturity. If the count is made too late, it will be impossible to find a female that has not ovulated. Our selection criteria "presence of yolked oocytes" (which roughly begins at a oocyte size of about 1.1 mm) filtered out the very high counts of oocytes associated with immature ovaries.

From the practical standpoint, dealing with atretic losses that may continue into the spawning period is much less important for *L. opalescens* than for *L. v. reynaudii* (Melo and Sauer, 1998; Sauer et al., 1999) or *L. pealeii* (Maxwell and Hanlon, 2000). In these squid, where the spawning period may last weeks or months, atresia may seriously bias potential fecundity estimates. In the pres-

ent study all atretic losses would be attributed, of course, to ovulation and spawning but the chances of this being a major error seem low. Because we counted atretic as well as normal oocytes, atretic losses would be erroneously attributed to spawning only if atresia had proceeded to the point that the atretic structure could not be identified as that of an oocyte in whole-mount preparations under a light microscope (64× power). The time at stage for atretic oocytes in *L. opalescens* ovaries, as well as other squid, is unknown. The duration of alpha-stage atresia of yolked oocytes in anchovy is about a week at 16°C (Hunter and Macewicz, 1985b) and we suspect for the larger *L. opalescens* yolked oocyte that the alpha-stage duration may be even longer. The disappearance of unyolked atretic oocytes, as an oocyte-like structure that would be counted, is more difficult to dismiss because so little is known about this atretic stage and its duration. If our estimate of the average longevity of spawning female is only about 1.67 days, then atretic losses of even small unyolked oocytes is probably not an important bias. It would be useful if a way could be found to estimate oocyte resorption rates in squid although it may be very difficult. It seems more important to validate our preliminary estimate of the average longevity of spawning squid, because if true, any concerns regarding atresia could be dismissed.

Mature females without postovulatory follicles in their ovaries made up only 6% of the 247 females examined histologically. The rarity of these females in our collections reduced the precision of our potential fecundity estimate. Only thirteen of the fifteen females classed as a mature preovulatory female were usable for estimating potential fecundity, further reducing the sample size. Such a small sample size not only results in a low precision but raises the concern that the sample may not be representative of the stock as a whole. The fact that the average total fecundity of females with high mantle condition from the catch was close to the predicted value based on the thirteen females, indicates that the latter estimate may not be biased. Clearly a larger sample size is needed, particularly if egg escapement is used to monitor the fishery. It would be helpful, in obtaining more samples, if we knew the reason for the apparent rarity of mature preovulatory *L. opalescens* females. One possibility is that females might pass rapidly from the initial vitellogenesis to ovulation, perhaps in the course of a single day or some fraction of it, and ovulation might begin sometime in the evening when *L. opalescens* are the most vulnerable to fishing. Another possibility is that mature preovulatory females aggregate in regions not heavily fished by either our trawl or the fishery.

Egg escapement

A practical suggestion from this study is the idea of managing spawning-ground loliginid fisheries by monitoring the fecundity of the catch and computing the fraction of the potential fecundity spawned. Monitoring the escapement of eggs from the fishery is an attractive approach for *Loligo opalescens* because costs are moderate, unlike the high cost for monitoring egg beds that cover many locations offshore and occur at any time of the year, and because traditional fishery assessment models are difficult to apply or inappropriate at the present time (PFMC, 2002). To proceed with escapement fecundity as a management tool, it would be necessary to set a target level for egg escapement and to relate escapement to egg-per-recruit analysis so that fishing effort could be adjusted to alter egg escapement rates. Conceptual work along these lines has been completed (Maxwell[3]).

As mentioned earlier, as a practical matter in applying the egg escapement method, one would need to use Q_{SP}, the mean fraction of the potential fecundity escaping (Eq. 1), as a proxy for the more comprehensive and more useful measure of egg escapement $R_{e,t_{\max}}$, the fraction of the expected lifetime fecundity deposited (Eq. 12). Obviously, Q_{SP} will always be lower than $R_{e,t_{\max}}$ because the denominator of Q_{SP} (the fraction $\overline{E_{SP}/E_P}$) is potential fecundity which will always be larger than the denominator for $R_{e,t_{\max}}$, which is expected lifetime fecundity (E). Although quite a different value, Q_{SP} is a useful proxy for $R_{e,t_{\max}}$. If natural mortality (m) and egg deposition rates (v) are constant, changes in fishing mortality will result in changes in Q_{SP} that are proportional to the change in $R_{e,t_{\max}}$.

However, changes will not be proportional if either v or m varies. If there is reason to believe that m and v are varying significantly, the use of Q_{SP} as a proxy for $R_{e,t_{\max}}$ should be undertaken with caution.

A point of concern in applying this method is that it may be difficult to substantially change escapement of eggs by regulating fishing effort. Our model indicated that egg escapement may be relatively insensitive to changes in fishing mortality if natural mortality rates are as high as we believe them to be. Of equal importance to management is the need to protect egg beds from damage by nets and to monitor the catch to prevent any change that might result in the capture of significant numbers of female *L. opalescens* before they begin to deposit eggs. Thus the fraction of the catch that is immature females must be monitored if the stock is managed by using the egg escapement method. For simplicity, our calculations of escapement were based on only mature females because immature females were only 2.6% of the females in the catch (1998–99) and their inclusion had little effect on parameter estimates. Egg escapement would decrease with an increase in the fraction of immature in the catch. As none of the fecundity of a captured immature female escapes the fishery, a relatively small increase in the fraction of immature animals in the catch can have significant consequences.

From the standpoint of fishery management, the most important unanswered question regarding the reproductive biology of *L. opalescens* is "how long do they remain on the spawning grounds?" or the equivalent question "what

[3] Maxwell, M. R., L. D. Jacobson, and R. Conser. Unpubl. data. Managing squid stocks using catch fecundity in an eggs-per-recruit model. Southwest Fisheries Science Center, National Marine Fisheries Service, 8604 La Jolla Shores Dr., La Jolla, CA 92037.

is the daily natural mortality of the spawners?" *Loligo opalescens* have only one spawning period in their life time (McGowan, 1954; Fields, 1965; Butler et al., 1999) but how long that period lasts remains unknown. Melo and Sauer (1999) concluded that the spawning period of *L. v. reynaudii* consisted of more than one spawning bout but neither the number of bouts nor the duration of each spawning period is known. In a laboratory study of *L. pealeii* (Maxwell and Hanlon, 2000), the number of bouts varied from one to ten, the interval between bouts was highly variable, and the life span after the first spawning bout was from 3 to 50 days. Our best guess for *L. opalescens* under fishing conditions was an average life on the spawning grounds of only 1.67 days and a maximum longevity of about 6 days. These estimates were based on a simple exponential model, constrained by various proxies for egg deposition rate, longevity, and the fraction of the potential fecundity in the catch (the only directly measured value). We believe that two of our estimates, 36% of the potential fecundity is deposited in the first 24 hours of spawning and minimum residual fecundity is about 22% of the potential fecundity, are on relatively firm ground but our estimate of the maximum longevity on the spawning grounds as 6 days is speculative. New information on mortality is needed because, over a wide range of daily mortality rates, our model yields values that are consistent with observed average fraction of potential fecundity in the catch. Because direct measurement of mortality on the spawning grounds may be difficult, it may be useful to develop some indirect approaches. For example, a laboratory study could be designed to generate an energy-based model that converts squid mantle tissue loss to deposited eggs. This mantle-to-egg conversion rate could be used to assign an age (time elapsed after first egg deposition) to modes of mantle condition from fishery samples. Mortality could then be computed by following modes of mantle condition through time.

Acknowledgments

This study was a cooperative project between the California Department of Fish & Game (CDF&G) and the National Marine Fisheries Service (NMFS) from start to finish. We worked closely with CDF&G personnel throughout the study with port-sampling data, cruise time, and partial financial support was provided by CDF&G. We worked particularly closely with M. Yaremko, A. Henry, and D. Hanan of CDF&G. J. Welsh assisted in the fecundity work. Others that contributed include J. Butler, T. Kudroschoff, N. Smith, A. Preti, K. Lazar, A. Cossio, and at sea K. Barsky, T. Bishop, S Charter, R. Dotson, D. Fuller, C. Graff, D. Griffith, P. Hamdorf, A. Hays, B. Horandy, M. Levy, I. Taniguchi, J. Ugoretz, and L. Zeidberg. We wish to thank the crews of the research vessels *Jordan* and *Mako*. We especially wish to thank diver J. Hyde who observed, collected, and photographed squid in La Jolla Canyon. M. Maxwell and two anonymous reviewers read the manuscript and provided constructive comments. R. Allen and H. Orr improved our illustrations.

Literature cited

Alheit, J.
1993. Use of the daily egg production method for estimating biomass of clupeoid fishes: a review and evaluation. Bull. Mar. Sci. 53:750–767.

Arkhipkin, A.
1993. Statolith microstructure and maximum age of *Loligo gahi* (Myopsida: Loliginidae) on the Patagonian shelf. J. Mar. Biol. Assoc. U.K. 73:979–982.

Arkhipkin, A., and N. Nekludova.
1993. Age, growth and maturation of the loliginid squids *Alloteuthis africana* and *A. subulata* on the west African shelf. J. Mar. Biol. Ass. U.K. 73:949–961.

Bower, J. R., and Y. Sakurai.
1996. Laboratory observations on *Todarodes pacificus* (Cephalopoda: Ommastrephidae) egg masses. Am. Malacological Bull. 13(1/2):65–71.

Boyle, P. R., and M. A. K. Ngoile.
1993. Assessment of maturity state and seasonality of reproduction in *Loligo forbesi* (Cephalopoda: Loliginidae) from Scottish waters. *In* Recent advances in fisheries biology (T. Okutani, R. K. O'Dor, and T. Kubodera, eds.), p. 37–48. Tokai Univ. Press, Tokyo, Japan.

Boyle, P. R., G. J. Pierce, and L. C. Hastie.
1995. Flexible reproductive strategies in the squid *Loligo forbesi*. Mar. Biol. 121:501–508.

Butler, J., D. Fuller, and M. Yaremko.
1999. Age and growth of market squid (*Loligo opalescens*) off California during 1998. Calif. Coop. Oceanic Fish. Invest. Rep. 40:191–195.

Coelho, M. L., J. Quintela, V. Bettencourt, G. Olavo, and H. Villa.
1994. Population structure, maturation patterns and fecundity of the squid *Loligo vulgaris* from southern Portugal. Fish. Res. 21:87–102.

Collins, M. A., G. M. Burnell, and P. G. Rodhouse.
1995. Reproductive strategies of male and female *Loligo forbesi* (Cephalopoda: Loliginidae). J. Mar. Biol. Assoc. U.K. 75:621–634.

Fields, W. G.
1965. The structure, development, food relations, reproduction, and life history of the squid, *Loligo opalescens* Berry. Calif. Dep. Fish Game Fish Bull. 131, 108 p.

Fitzhugh, G. R., and W.F. Hettler
1995. Temperature influence on postovulatory follicle degeneration in Atlantic menhaden, *Brevoortia tyrannus*. Fish. Bull. 93:568–572.

Guerra, A., and F. Rocha.
1994. The life history of *Loligo vulgaris* and *Loligo forbesi* (Cephalopoda: Loliginidae) in Galician waters (NW Spain). Fish. Res. 21:43–69.

Hatfield, E. M. C.
1991. Post-recruit growth of the Patagonian squid *Loligo gahi* (D'Orbigny). Bull. Mar. Sci. 49(1–2)349–361.
2000. So some like it hot? Temperature as a possible determinant of variability in the growth of the Patagonian squid, *Loligo gahi* (Cephalopoda: Loliginidae). Fish. Res. 47:27–40.

Hay, D. E., D. N. Outram, B. A. McKeown, and M. Hurlburt.
1987. Ovarian development and occyte diameter as maturation criteria in Pacific herring (*Clupea harengus pallasi*). Can. J. Fish. Aquat. Sci. 44:1496–1502.

Hunter, J. R., and S. R. Goldberg.
1980. Spawning incidence and batch fecundity in northern anchovy, *Engraulis mordax*. Fish. Bull. 77:641–652.

Hunter, J. R., and N. C. H. Lo.
1997. The daily egg production method of biomass estimation: some problems and potential improvements. Ozeanografika 2:41–67.
Hunter, J. R., N. C. H. Lo, and R. J. H. Leong.
1985. Batch fecundity in multiple spawning fishes. *In* An egg production method for estimating spawning biomass of pelagic fish: application to the northern anchovy (*Engraulis mordax*) (R. Lasker, ed.), p. 67–77. NOAA Tech. Rep. NMFS 36.
Hunter, J. R., and B. J. Macewicz.
1985a. Measurement of spawning frequency in multiple spawning fishes. *In* An egg production method for estimating spawning biomass of pelagic fish: application to the northern anchovy (*Engraulis mordax*) (R. Lasker, ed.), p. 79–94. NOAA Tech. Rep. NMFS 36.
1985b. Rates of atresia in the ovary of captive and wild northern anchovy, *Engraulis mordax*. Fish. Bull. 83:119–136.
Hunter, J. R., B. J. Macewicz, N. C. H. Lo, and C. A. Kimbrell.
1992. Fecundity, spawning, and maturity of female Dover sole *Microstomus pacificus*, with an evaluation of assumptions and precision. Fish. Bull. 90:101–128.
Ikeda, Y., Y. Sakurai, and K. Shimazaki.
1993. Maturation process of the Japanese common squid *Todarodes pacificus* in captivity. *In* Recent advances in fisheries biology (T. Okutani, R. K. O'Dor, and T. Kubodera, eds.), p. 179–187. Tokai Univ. Press, Tokyo, Japan.
Jackson, G. D.
1993. Seasonal variation in reproductive investment in the tropical loliginid squid *Loligo chinensis* and the small tropical sepioid *Idiosepius pygmaeus*. Fish. Bull. 91:260–270.
1994. Statolith age estimates of the loliginid squid *Loligo opalescens* (Mollusca: Cephalopoda): corroboration with culture data. Bull. Mar. Sci. 54:554–557.
Jackson, G. D., A. I. Arkhipkin, V. A. Bizikov, and R. T. Hanlon.
1993. Laboratory and field corroboration of age and growth from statoliths and gladii of the loliginid squid *Sepioteuthis lessoniana* (Mollusca: Cephalopoda). *In* Recent advances in fisheries biology (T. Okutani, R. K. O'Dor, and T. Kubodera, eds.), p. 189–199. Tokai Univ. Press, Tokyo, Japan.
Jackson, G. D., J. W. Forsythe, R. F. Hixon, and R. T. Hanlon.
1997. Age, growth, and maturation of *Lolliguncula brevis* (Cephalopoda: Loliginidae) in the northwest Gulf of Mexico with a comparison of length-frequency versus statolith age analysis. Can. J. Fish. Aquat. Sci. 54:2907–2919.
Jackson, G. D., and J. Yeatman.
1996. Variation in size and age at maturity in *Photololigo* (*Mollusca: Cephalopoda*) from the northwest shelf of Australia. Fish. Bull. 94:59–65.
Kjesbu, O. S., P. R. Witthames, P. Solemdal, M. G. Walker.
1998. Temporal variations in the fecundity of Arcto-Norwegian cod (*Gadus morhua*) in response to natural changes in food and temperature. J. Sea Res. 40: 303–321.
Knipe, J. H., and R. D. Beeman.
1978. Histological observations on oogenesis in *Loligo opalescens*. *In* Biological, oceanographic, and acoustic aspects of the market squid, *Lolgio opalescens* Berry (C. W. Recksiek and H. W. Frey, eds.), p. 23–33. Calif. Dep. Fish Game Fish Bull. 169.
Laptikhovsky, V.
2000. Fecundity of the squid *Loligo vulgaris* Lamarck, 1798 (Myopsida, Loliginidae) off northwest Africa. Scientia Marina 64(3):275–278.
Lopes, S. S., M. L. Coelho, and J. P. Andrade.
1997. Analysis of oocyte development and potential fecundity of the squid *Loligo vulgaris* from the waters of southern Portugal. J. Mar. Biol. Assoc. U.K. 77:903–906.
Macewicz, B. J., and J. R. Hunter.
1994. Fecundity of sablefish, *Anoplopoma fimbria*, from Oregon coastal waters. Calif. Coop. Oceanic Fish. Invest. Rep. 35:160–174.
Maxwell, M. R., and R. T. Hanlon.
2000. Female reproductive output in the squid *Loligo pealeii*: multiple egg clutches and implications for a spawning strategy. Mar. Ecol. Prog. Ser. 199:159–170.
McGowan, J. A.
1954. Observations on the sexual behavior and spawning of the squid, *Loligo opalescens*, at La Jolla, California. Calif. Fish Game Fish Bull. 40(1):47–55.
Melo, Y. C., and W. H. H. Sauer.
1998. Ovarian atresia in cephalopods. S. Afr. J. Mar. Sci. 20:143–151.
1999. Confirmation of serial spawning in the chokka squid *Loligo vulgaris reynaudii* off the coast of South Africa. Mar. Biol. 135:307–313.
Moltschaniwskyj, N. A..
1995. Multiple spawning in the tropical squid *Photololigo* sp.: what is the cost in somatic growth? Mar. Biol. 125:127–135.
Moltschaniwskyj, N. A., and J. M. Semmens.
2000. Limited use of stored energy reserves for reproduction by the tropical loliginid squid *Photololigo* sp. J. Zool. Lond. 251:307–313.
Natsukari, Y., and N. Komine.
1992. Age and growth estimation of the European squid, *Loligo vulgaris*, based on statolith microstructure. J. Mar. Biol. Assoc. U.K. 72:271–280.
PFMC
2002. Report of the Stock Assessment Review (STAR) panel for market squid, Appendix 3. *In*, Status of the Pacific Coast coastal pelagic species fishery and recommended acceptable biological catches: stock assessment and fishery evaluation—2002, 17 p. Pacific Fishery Management Council. Portland, OR
Quinn, T. J., and R. B. Deriso.
1999. Quantitative fish dynamics. Biological resource Mmanagement series, 542 p. Oxford Univ. Press, New York, NY.
Sauer, W. H. H., Y. C. Melo, and W. de Wet.
1999. Fecundity of the chokka squid *Loligo vulgaris reynaudii* on the southeastern coast of South Africa. Mar. Biol. 135:315–319.
Semmens, J. M., and N. A. Moltschaniwskyj.
2000. An examination of variable growth in the loliginid squid *Sepioteuthis lessoniana*: a whole animal and reductionist approach. Mar. Ecol. Prog. Ser. 193:135–141.
Woodhead, A. D.
1960. Nutrition and reproductive capacity in fish. Nutrition Society Proceedings 19:23–28.
Yang, W. T., R. F. Hixon, P. E. Turk, M. E. Krejci, W. H. Hulet, and R. T. Hanlon.
1986. Growth, behavior, and sexual maturation of the market squid, *Loligo opalescens*, cultured through the life cycle. Fish. Bull. 84:771–798.

Appendix I

Terms

E_P potential fecundity (standing stock of oocytes in the ovary of mature females prior to spawning)

$E_{SP,t}$ the total eggs deposited on the bottom up to time t (t in days)

E_C total number of eggs deposited by mature females in the catch or total number of eggs escaped

E_M total number of eggs deposited by mature females prior to death due to natural mortality

E_A total number of eggs deposited by females alive and not caught by fishery

E total number of eggs that would have been spawned during a squid's lifetime if no fishery existed

E_Y standing stock of oocytes in the ovary

E_D standing stock of ova in the oviduct

E_{YD} total fecundity, the sum of both the number of oocytes in the ovary and ova in the oviduct

E_{YD,t_k} stocking stock of oocytes in the ovary plus those ova in the oviduct after spawning has begun and up to the elapsed time t_k, where t_k is $\le t_{\max}$

$t_{\max}$ maximum elapsed time with the time 0 being the time when mature females are about to ovulate or total elapsed time (in days) of spawners on the spawning ground

E_R standing stock of oocytes remaining in ovary at death

m daily adult natural mortality rate

f daily fishing mortality rate for adults

v daily egg deposition rate

$Q_{SP,t} = E_{SP,t} / E_P = 1 - e^{-vt}$ fraction of potential fecundity deposited up to time t

e^{-zt} mortality (survival) curve

N_0 number of mature females at time 0

N_C total number of spawners in the catch

R_{e,t_k} egg escapement rate = ratio of eggs deposited to total number of egg which would be spawned if there was no fishery, at a given elapsed time (t_k)

$R_{e,t_{\max}}$ egg escapement rate up to the maximum elapsed time ($t_{\max}$)

Appendix II

For any elapsed time t_k, formulas for E_C, E_M, E_A and E:

$$E_C = \overline{E_P} N_0 f \left[\frac{1-e^{-(m+f)t_k}}{m+f} - \frac{1-e^{-(m+f+v)t_k}}{m+f+v} \right]$$

$$E_M = \overline{E_P} N_0 m \left[\frac{1-e^{-(m+f)t_k}}{m+f} - \frac{1-e^{-(m+f+v)t_k}}{m+f+v} \right]$$

$$E_A = (\overline{E_P} - \overline{E_{YD,t_k}}) N_k = N_0 e^{-(m+f)t_k} \overline{E_P} (1-e^{-vt_k})$$

$$E = \overline{E_P} N_0 \left[\frac{v}{v+m} - e^{-mt_k} \left(1 - \frac{m}{v+m} e^{-vt_k} \right) \right].$$

The derivation for E_A is straight forward and the derivations for E_C, E_M, and E, similar among one another, are as follows:

$$E_C = \int_0^{t_k} \overline{E_{SP,t}} dC_t = \int_0^{t_k} \overline{E_P} (1-e^{-vt}) dC_t$$

$$= \overline{E_P} N_0 \int_0^{t_k} (1-e^{-vt}) e^{-(m+f)t} f dt,$$

where

$$C_t = N_0 \frac{f}{m+f} (1-e^{-(m+f)t})$$

is the number of removals of the cohort due to fishing up to time t (Quinn and Deriso, 1999).

$$E_M = \int_0^{t_k} \overline{E_{SP,t}} dD_{m,t} = \int_0^{t_k} \overline{E_P} (1-e^{-vt}) dD_{m,t}$$

$$= \overline{E_P} N_0 f \frac{v}{(m+f)(m+f+v)},$$

where

$$D_{m,t} = N_0 \frac{m}{m+f} \left(1-e^{-(m+f)t} \right)$$

is the number of removals of the cohort due to natural mortality up to time t (Quinn and Deriso, 1999) and E (when no fishing takes place):

$$E = \int_0^{t_k} \overline{E_{SP,t}} dD_t = \int_0^{t_k} \overline{E_P}(1-e^{-vt}) dD_t$$

$$= \overline{E_P} N_0 \int_0^{t_k} (1-e^{-vt}) e^{-mt} m dt,$$

where $D_t = N_0(1-e^{-mt})$ is the number of removals of the cohort due to natural mortality when no fishing takes place.

The dusky rockfishes (Teleostei: Scorpaeniformes) of the North Pacific Ocean: resurrection of *Sebastes variabilis* (Pallas, 1814) and a redescription of *Sebastes ciliatus* (Tilesius, 1813)

James W. Orr

Resource Assessment and Conservation Engineering Division
Alaska Fisheries Science Center
National Marine Fisheries Service, NOAA
7600 Sand Point Way NE
Seattle, Washington 98115
E-mail address: James.Orr@noaa.gov

James E. Blackburn

Alaska Department of Fish and Game
211 Mission Road
Kodiak, Alaska 99615-9988

Abstract—The dusky rockfish (*Sebastes ciliatus*) of the North Pacific Ocean has been considered a single variable species with light and dark forms distributed in deep and shallow water, respectively. These forms have been subjected to two distinct fisheries separately managed by federal and state agencies: the light deep form is captured in the offshore trawl fishery; the dark shallow form, in the nearshore jig fishery. The forms have been commonly recognized as the light dusky and dark dusky rockfishes. From morphological evidence correlated with color differences in some 400 specimens, we recognize two species corresponding with these color forms. *Sebastes ciliatus* (Tilesius) is the dark shallow-water species found in depths of 5–160 m in the western Aleutian Islands and eastern Bering Sea to British Columbia. The name *Sebastes variabilis* (Pallas) is resurrected from the synonymy of *S. ciliatus* to apply to the deeper water species known from depths of 12–675 m and ranging from Hokkaido, Japan, through the Aleutian Islands and eastern Bering Sea, to Oregon. *Sebastes ciliatus* is uniformly dark blue to black, gradually lightening on the ventrum, with a jet black peritoneum, a smaller symphyseal knob, and fewer lateral-line pores compared to *S. variabilis*. *Sebastes variabilis* is more variable in body color, ranging from light yellow to a more usual tan or greenish brown to a nearly uniform dark dorsum, but it invariably has a distinct red to white ventrum. Synonymies, diagnoses, descriptions, and geographic distributions are provided for each species.

Manuscript approved for publication 22 December 2003 by Scientific Editor.

Manuscript received 20 January 2004 at NMFS Scientific Publications Office.

Fish. Bull. 102:328–348 (2004).

Among the approximately 92 species of *Sebastes* found in the North Pacific, two commercially important species long identified under the name *Sebastes ciliatus* have been taxonomically problematic. The name *S. ciliatus* (Tilesius, 1813) has been commonly applied to specimens considered to represent a single variable species ranging from northern Japan to British Columbia (Barsukov, 1964; Westrheim, 1973; Shinohara et al., 1994; Mecklenburg et al., 2002), and the name *S. variabilis* (Pallas, 1814) has been treated as a junior synonym (Jordan and Gilbert, 1881; Eigenmann and Beeson, 1894; Jordan and Evermann, 1898; Blanc and Hureau, 1968). Two color forms within *S. ciliatus* have been reported and hypothesized to be distinct species (Quast and Hall, 1972; Eschmeyer et al., 1983; Kessler, 1985; Fig. 1). The typically light-colored form, commonly known as the light dusky rockfish, is often found in large aggregations over the outer continental shelf and upper slope at depths down to 675 m, and less frequently in nearshore habitats. The dark-blue to black form, commonly known as the dark dusky rockfish, is found in more shallow habitats from nearshore rocky reefs to depths no greater than 160 m.

These forms have been subjected to two distinct fisheries separately managed by U.S. federal and Alaska state agencies since 1998. The light-colored deep form is captured in the offshore trawl fishery and is the dominant species of the pelagic shelf rockfish fisheries complex regulated by the National Marine Fisheries Service (NMFS). Specific catch limits are set under the designation "dusky rockfish." The occasional catch of the dark form in these offshore waters has also been considered "dusky rockfish." The dark-colored shallow form is found commonly in the nearshore jig fishery regulated by the Alaska Department of Fish and Game. The dark form, routinely misidentified as *S. melanops*, may comprise up to 25% of the catch in the "black rockfish" jig fishery off Kenai Peninsula (Clausen et al.[1]) and is managed only as "other rockfish" bycatch within the fishery.

Early allozyme analyses (Tsuyuki et al., 1965, 1968) indicated significant genetic differences among samples identified as *S. ciliatus*. A more detailed analysis of several *Sebastes* species (Seeb, 1986) and a later study focused

[1] Clausen, D. M., C. R. Lunsford, and J. T. Fujioka. 2002. Pelagic shelf rockfish. *In* Stock assessment and fishery evaluation report for the groundfish resources of the Gulf of Alaska for 2002, p. 383–417. North Pacific Fishery Management Council, 605 W 4th Ave, Suite 306, Anchorage, AK 99501.

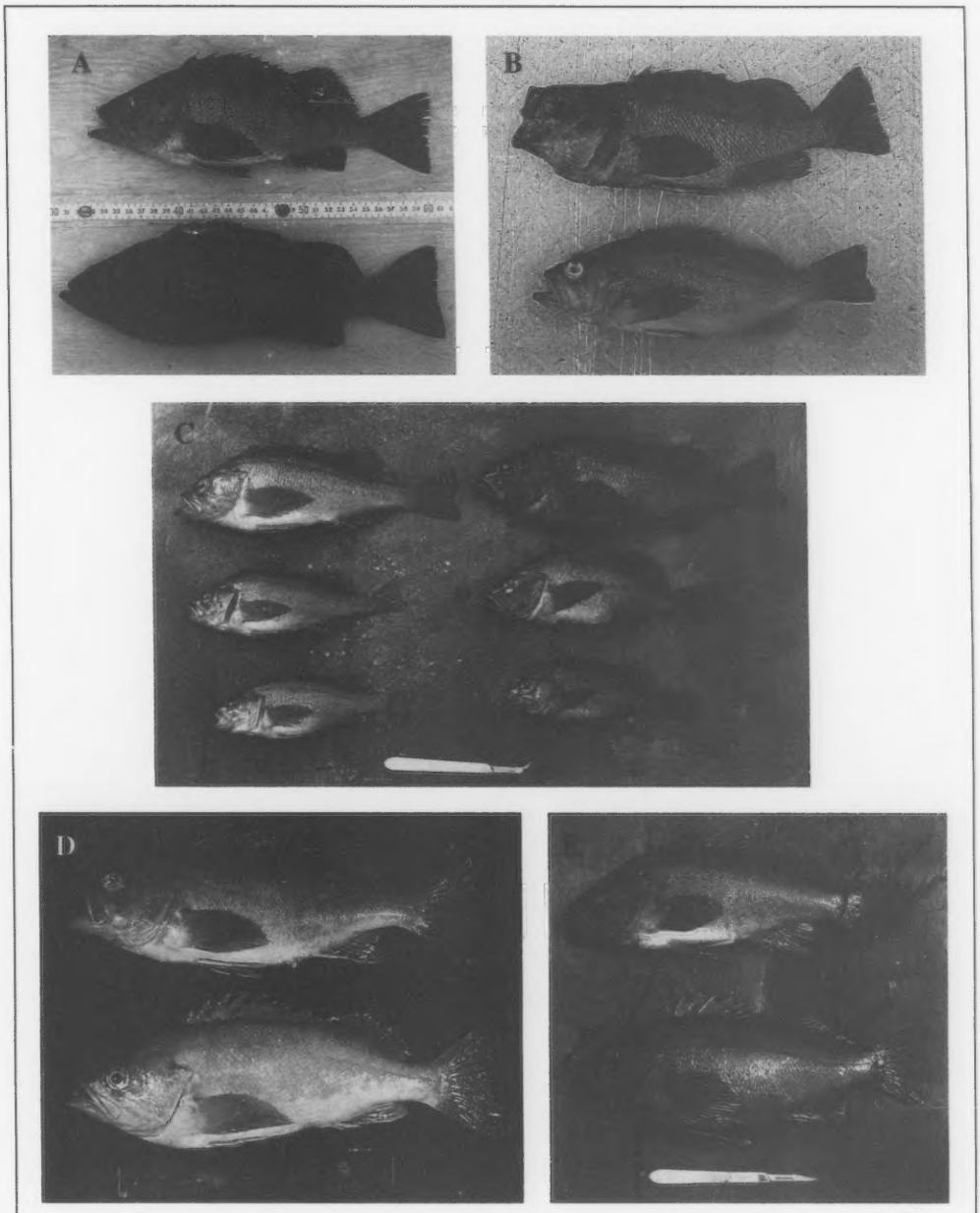

Figure 1

(**A**) *Sebastes variabilis* (top), UW 43494, 225.2 mm, and *S. ciliatus* (bottom), UW 43493, neotype, 266.4 mm, collected at 37 and 25 m depth, respectively, in Lynn Canal near Funter Bay, southeast Alaska. (**B**) *Sebastes ciliatus* (top), UW 45512, 235.2 mm, and *S. variabilis* (bottom), UW 45511, 206.2 mm, collected syntopically at 67 m depth in the northern Gulf of Alaska, 57.38061°N, 154.8009°W. (**C**) *Sebastes variabilis* (left), UW 43494, 150.6–225.2 mm, and *S. ciliatus* (right), UW 43492, 153.7–241.1 mm, collected at 37 and 25 m depth, respectively, in Lynn Canal near Funter Bay, southeast Alaska. (**D**) *Sebastes variabilis*, UW 43251, 390 mm (top) and 410 mm (bottom), northern Gulf of Alaska, 59.50446°N, 145.2262°W, 135 m depth. (**E**) *Sebastes melanops* (top), UW 43490, and *S. ciliatus* (bottom), UW 43484, 313 mm, collected at 25 m depth in Soapstone Cove, southeast Alaska.

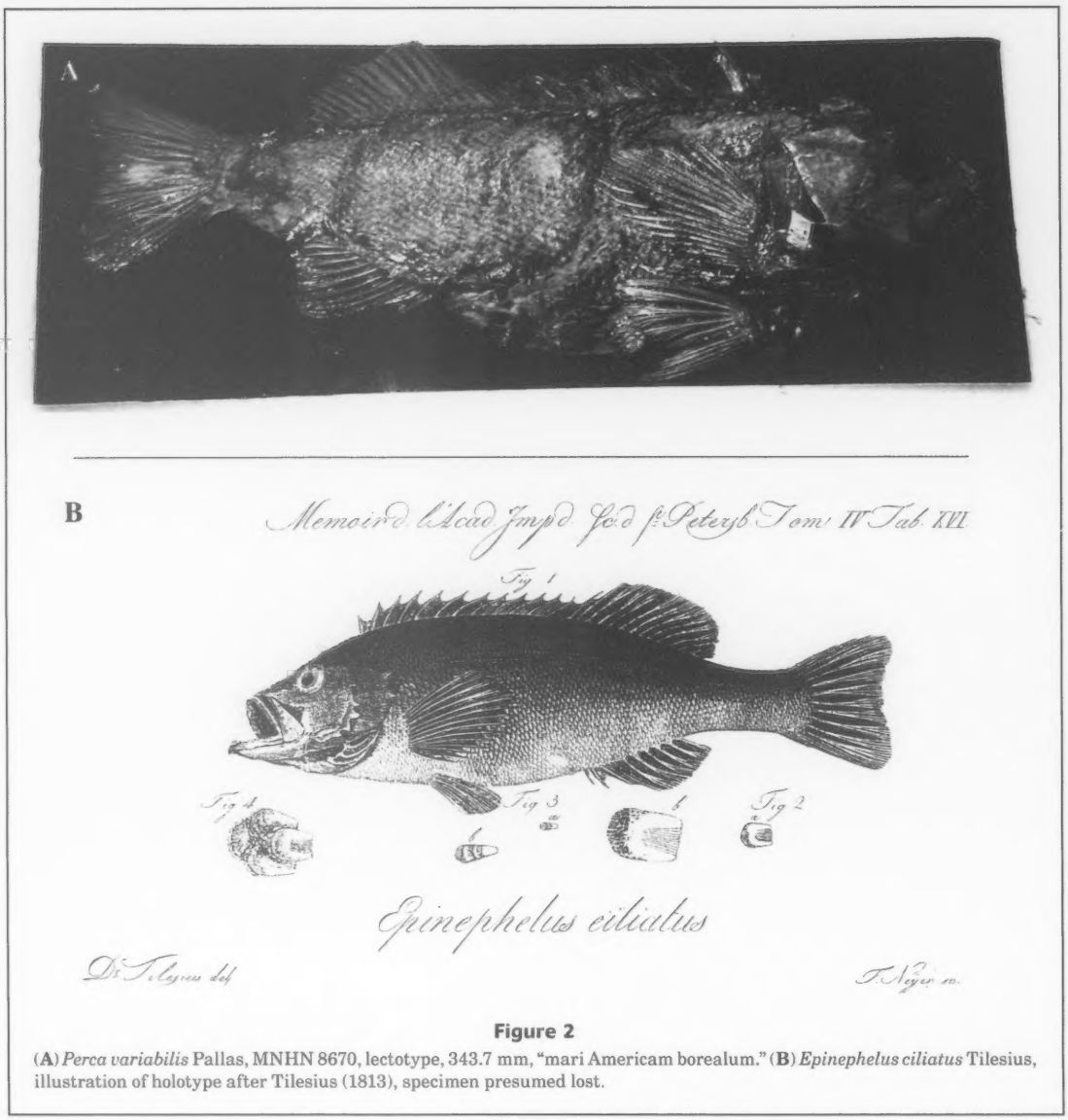

Figure 2

(**A**) *Perca variabilis* Pallas, MNHN 8670, lectotype, 343.7 mm, "mari Americam borealum." (**B**) *Epinephelus ciliatus* Tilesius, illustration of holotype after Tilesius (1813), specimen presumed lost.

on *S. ciliatus* (Westrheim and Seeb[2]) concluded that the two color forms were distinct sister species. Seeb's recent work with microsatellite DNA data has revealed discrete genetic differences between the two, as well as some evidence for infrequent hybridization (Seeb[3]). Sequence data from NADH dehydrogenase subunit regions of the mitochondrial genome, however, have not revealed differences between the two forms (López[4], Gray[5]), nor have sequence data from other work on closely related species of *Sebastes* (Bentzen et al., 1998; Sundt and Johansen, 1998; Roques et al., 2001).

[2] Westrheim, S. J., and L. W. Seeb. 1997. Unpubl. manuscript. Investigation of the *Sebastes ciliatus* species group, 36 p. Fisheries and Oceans Canada, Pacific Biological Station, Nanaimo, BC, Canada V9R 5K6.

[3] Seeb, L. W. 2002. Personal commun. Alaska Department of Fish and Game, 333 Raspberry Road, Anchorage, AK 99518-1599.

[4] López, J. A. 2000. Personal commun. Iowa State Univ., Ames, IA 50014.

[5] Gray, A. 2000. Personal commun. Fisheries Division, School of Fisheries and Ocean Sciences, Univ. Alaska Fairbanks, 11120 Glacier Highway, Juneau, AK 99801.

In this study, we provide morphological evidence from examination of about 400 specimens collected throughout the geographic and bathymetric range of the species to correlate color differences with meristic and shape differences. In thus recognizing two species, *S. ciliatus* and *S. variabilis*, previously referred to the name *S. ciliatus* (Tilesius, 1813), we discuss the nomenclatural consequences of this decision. Both species were originally described (as *Epinephelus ciliatus* Tilesius and *Perca variabilis* Pallas) on the basis of early Russian collections from along the Aleutian Islands (Svetovidov, 1978, 1981). The type series of one species is now represented by a single extant specimen (Fig. 2A) and the other by the illustration of a single, now lost, specimen (Svetovidov, 1978, 1981; Fig. 2B). Although workers since the turn of the century have associated the name *S. ciliatus* with the variably light-colored species (Jordan, 1896; Jordan and Evermann, 1898; Barsukov, 1964; Orr et al., 1998, 2000; Mecklenburg et al., 2002), the original description and accompanying illustration (Fig. 2B) appear to describe the uniformly dark species. We have also identified the remaining syntype (Fig. 2A) of *Perca variabilis* as the light species. Therefore, we refer the dark, shallow-water species (the dark rockfish) to *Sebastes ciliatus* (Tilesius, 1813) and resurrect the name *Sebastes variabilis* (Pallas, 1814) for the typically light, deeper-water species (the dusky rockfish).

Methods and materials

Counts and measurements follow Hubbs and Lagler (1958), except as noted below. Unless indicated otherwise, standard length (SL) is used throughout and was always measured from the tip of the snout. Depth at pelvic-fin base was measured from the origin of the dorsal fin to the base of the pelvic fins (at the articulation of the pelvic-fin spine); depth at anal-fin origin, from the base of the last dorsal-fin spine to the anal-fin origin; depth at anal-fin insertion, from dorsal-fin insertion to anal-fin insertion; body thickness, at pectoral-fin base; head thickness, at the posterior orbital rim; prepelvic- and preanal-fin length, from pelvic-fin base or anal-fin origin to the tip of the snout; pelvic-fin to anal-fin length from pelvic-fin base to anal-fin origin; caudal peduncle dorsal length from dorsal-fin insertion to caudal-fin base; caudal peduncle ventral length from anal-fin insertion to caudal-fin base. The small anterior notch in the orbit between the frontal bone and lateral ethmoid was excluded from orbit length and snout length measurements. Accessory scales are small scales located beyond the posterior field of major scales. The swimbladder musculature was examined after dissection according to the methods of Hallacher (1974). Institutional abbreviations follow Leviton et al. (1985) and Leviton and Gibbs (1988), as modified by Poss and Collette (1995).

Individuals were identified by body and peritoneum color (see species descriptions below) for grouping in ANOVA and ANCOVA, as well as for labeling individuals in graphs of principal components analysis scores. Univariate and multivariate analyses were conducted by using Statgraphics Plus 4.1 (Manugistics, Rockville, MD) and Splus 2000 (Mathsoft, Inc., Seattle, WA). Differences were considered significant at $P < 0.05$.

Arcsine-transformed morphometric ratios (with SL or head length as denominator) and meristic characters were tested to meet the assumptions of normality required for ANOVA. The following characters exhibited normal distributions and did not differ significantly in variance between species and were subjected to ANOVA: head length, orbit length, snout length, interorbital width, suborbital depth, gill-raker length, body thickness, pectoral-fin base width, pectoral-fin ray length, caudal peduncle ventral length, predorsal length, spinous dorsal-fin base, soft dorsal-fin base, and counts of lateral-line pores and gill rakers.

For morphometric characters, significant differences were also identified by using an analysis of covariance (ANCOVA) of log-10-transformed measurements with SL or head length (HL) as covariates when assumptions of normality and the homogeneity of slopes were satisfied. The ANCOVA model included species as a factor, SL or HL as a covariate, and a species/(SL or HL) interaction (e.g., $HL=C+Species+SL+(Species\times SL)$). A residual analysis was done for each model to determine the appropriateness of the model. Whenever the interaction was not significant (at the 5% level), a reduced model was used by dropping the interaction and forcing the slopes to be the same ($BD=C+Species+SL$). This removed the effect of SL and HL and allowed testing for significant differences between species. The following morphometric characters met the assumptions required for ANCOVA: head length, snout length, interorbital width, gill-raker length, pectoral-fin base width, pectoral-fin ray length, caudal peduncle ventral length, predorsal length, spinous dorsal-fin-base length, and soft dorsal-fin-base length.

On a dataset of specimens with all characters, sheared principal components analysis (SPCA) for a size-free analysis (Bookstein et al., 1985) was conducted by using morphometric characters, and a standard principal components analysis (PCA) was conducted by using all meristic characters. Raw morphometric data were log-transformed and the covariance matrix was subjected to SPCA, as was the correlation matrix of raw meristics. Differences between species were illustrated by plotting scores of sheared PC2 against sheared PC3 and sheared morphometric PC2 against the standard meristic PC1. Separate analyses were also conducted on three groupings: 1) each species by depth, 2) each species by sex, and 3) shallow-water populations of *S. ciliatus* and *S. variabilis* primarily collected in the vicinity of the Triplet Islands and Monashka Bay, on the northeast side of the Kodiak Island Archipelago, and the vicinity of Lynn Canal, Alaska. Shallow collections were defined as those made at less than 50 m depth, and deep collections were taken at depths greater than 50 m.

These plots were also examined for groupings indicative of geographic differences in body shape and meristics. Geographic areas were defined as follows: British Columbia, from the Straits of Juan de Fuca to Dixon Entrance; southeast Alaska, from Dixon Entrance to Chatham Strait; Gulf of Alaska, from Chatham Strait to the tip of the Alaska Pennisula; Aleutian Islands and Bering Sea,

Table 1

Proportional morphometrics and meristics of *Sebastes ciliatus* and *S. variabilis* from all depths and regions. Morphometric data are in %SL or %HL. X = statistically significant difference at 0.05 level, as evaluated by ANOVA and ANCOVA, when appropriate; ns = not statistically significant at 0.05 level. *n* = number of fish in sample.

	S. ciliatus			*S. variabilis*				
	n	Range	Mean ±SD	*n*	Range	Mean ±SD	ANOVA	ANCOVA
Meristics								
Dorsal-fin spines	138	12–14	13.0 ±0.2	194	13–14	13.0 ±0.1		
Dorsal-fin rays	138	13–17	15.0 ±0.5	194	13–16	15.0 ±0.4		
Anal-fin rays	139	7–9	7.9 ±0.4	195	7–9	7.9 ±0.4		
Pectoral-fin rays (left)	138	17–19	18.2 ±0.5	194	17–19	18.0 ±0.3		
Pectoral-fin rays (right)	137	16–19	18.2 ±0.4	195	16–19	18.0 ±0.4		
Unbranched pectoral-fin rays (left)	136	8–10	9.2 ±0.5	195	7–11	9.1 ±0.4		
Unbranched pectoral-fin rays (right)	108	8–11	9.2 ±0.5	188	7–11	9.1 ±0.5		
Lateral-line pores (left)	138	39–50	45.4 ±2.3	188	43–54	48.5 ±1.9	X	
Lateral-line pores (right)	125	40–54	45.3 ±2.4	172	42–54	48.5 ±1.9	X	
Lateral-line scales	132	44–60	50.6 ±2.7	177	47–63	52.8 ±2.7		
Gill rakers	137	32–37	34.8 ±1.1	184	32–37	34.7 ±0.9	X	

continued

from the tip of the Alaska Peninsula west and north into the Bering Sea.

Results

Color

Body color in life and in preservation differs consistently between *S. ciliatus* and *S. variabilis* (Fig. 1; see detailed description below). In life, *S. ciliatus* is uniformly bluish-black to gray, with slight gradual lightening on the belly; the peritoneum is invariably jet black. In contrast, *S. variabilis* varies in background color from golden yellow to greenish brown to dark gray, with a distinct break between the darker dorsum and the invariably white to pink ventrum, particularly at the base of the anal fin; the peritoneum is gray to black. In *S. variabilis* preserved for up to 30 years, the distinct break along the ventrum is retained and differs from the uniformly dark preserved color of *S. ciliatus*. This combination of characteristic body and peritoneum color was used initially to identify individuals as either *S. ciliatus* or *S. variabilis* as the basis for univariate statistical analyses.

Meristic characters

Lateral-line pore and gill-raker counts differed significantly between *S. ciliatus* and *S. variabilis* from all depths and regions, *S. ciliatus* having a lower range and mode of counts (Tables 1–3). In shallow water, only lateral-line pore counts showed significant differences (Table 4). Slight clinal variation was evident for lateral-line pores in *S. ciliatus* between southeast Alaska collections and northern Gulf of Alaska material (Table 2). In the PCA, counts of lateral-line pores, gill rakers, and pectoral-fin rays were most heavily loaded along the first PC axis, confirming that *S. ciliatus* has typically lower lateral-line pore and gill-raker counts and tends to have a higher pectoral-fin ray count (Tables 1–3, 5; Fig. 3B).

Morphometric characters

Among morphometric characters meeting statistical assumptions for ANOVA or ANCOVA, head length, interorbital width, suborbital depth, lower-jaw length, gill-raker length, body thickness, pectoral-fin base width, predorsal length, and soft-dorsal-fin-base length differed significantly between *S. ciliatus* and *S. variabilis* across all depths and regions (Table 1). Between shallow-water *S. ciliatus* and *S. variabilis*, all the above characters, except head length, interorbital width, and predorsal length, differed significantly (Table 4). No significant differences were found in analyses within species by depth or sex.

In the PCA for specimens collected across all regions and depths, clusters of *S. ciliatus* and *S. variabilis* showed broad overlap and only slight discrimination among individuals along the PC2 axis (Fig. 3A). Principal component 2, the primary shape component, described 1.8% of the total variation, and PC1, the size component having all loadings positive, described 96.4% of the variation. Characters loading most heavily along the PC2 axis included suborbital depth, gill-raker length, orbit length, body

Table 1 (continued)

	S. ciliatus			*S. variabilis*				
	n	Range	Mean ±SD	*n*	Range	Mean ±SD	ANOVA	ANCOVA
Morphometrics								
Standard length	132	83.8–340.0		192	77.7–430.8			
Head length/SL	113	28.7–35.5	32.9 ±1.2	129	28.1–36.2	32.5 ±1.2	X	ns
Orbit length/HL	111	21.5–30.6	25.6 ±2.0	121	20.6–33.5	25.6 ±2.1	ns	
Snout length/HL	111	18.2–26.0	21.4 ±1.6	121	17.1–27.1	21.4 ±1.8	ns	ns
Interorbital width/HL	111	22.9–29.3	25.9 ±1.3	121	22.5–30.4	26.4 ±1.4	X	X
Suborbital depth/HL	111	4.1–7.8	6.0 ±0.8	121	4.3–8.1	6.2 ±0.7	X	
Upper jaw length/HL	111	43.6–51.1	47.4 ±1.5	121	42.7–54.0	47.8 ±2.0		
Lower jaw length/HL	105	53.4–60.5	56.5 ±1.7	108	52.8–62.7	58.3 ±2.2	X	
Gill raker length/HL	98	11.3–20.7	15.0 ±1.6	110	11.6–19.9	15.5 ±1.7	ns	X
Depth at pelvic-fin base/SL	111	32.5–42.7	37.0 ±1.9	121	29.2–40.9	36.2 ±1.7		
Depth at anal-fin origin/SL	111	27.4–35.8	31.2 ±1.7	121	26.7–35.4	30.5 ±1.6		
Depth at anal-fin insertion/SL	109	13.8–18.5	15.9 ±1.0	116	13.1–18.0	15.4 ±0.9		
Body thickness/SL	111	14.9–22.3	18.0 ±1.2	120	12.9–20.9	17.3 ±1.5	X	
Pectoral-fin base width/SL	111	9.5–11.9	10.7 ±0.5	121	9.4–11.2	10.2 ±0.4	X	X
Pectoral-fin ray length/SL	111	24.6–31.8	28.5 ±1.3	121	23.5–31.0	28.2 ±1.4	ns	ns
Pectoral-fin length/SL	111	25.5–33.6	29.8 ±1.5	117	24.2–35.1	29.2 ±1.7		
Pelvic-fin ray length/SL	111	20.5–26.0	22.7 ±1.1	119	19.2–29.2	22.0 ±1.5		
Pelvic-fin ray/Pelvic-fin spine length	111	52.4–67.4	59.9 ±4.3	121	44.9–70.7	59.9 ±5.5		
Anal-fin spine I length/SL	83	3.6–9.1	5.2 ±0.9	107	3.3–8.8	5.3 ±1.0		
Anal-fin spine II length/SL	84	7.5–14.2	10.6 ±1.2	106	5.8–13.6	10.5 ±1.5		
Anal-fin spine III length/SL	84	10.0–14.6	12.4 ±1.1	107	9.5–15.6	12.2 ±1.3		
Anal-fin ray 1 length/SL	83	15.6–22.5	19.0 ±1.2	97	15.1–21.0	18.2 ±1.3		
Anal-fin ray 2 length/SL	84	14.5–23.4	20.2 ±1.2	97	15.3–23.1	19.5 ±1.3		
Caudal-fin length/SL	60	10.2–29.4	21.7 ±2.7	74	15.4–26.9	21.2 ±2.3		
Caudal peduncle depth/SL	111	9.3–13.7	11.4 ±0.7	121	9.5–12.2	10.9 ±0.5		
Caudal peduncle dorsal length/SL	111	11.9–16.2	13.8 ±0.8	121	12.6–16.4	14.1 ±0.8		
Caudal peduncle ventral length/SL	111	17.6–22.9	20.5 ±1.0	121	17.1–24.3	21.1 ±1.3	ns	ns
Preanal length/SL	111	60.0–77.4	68.7 ±2.5	121	59.4–77.9	68.1 ±2.6		
Pelvic- to anal-fin length/SL	105	26.1–43.2	32.5 ±3.1	111	25.9–41.7	31.6 ±2.9		
Predorsal length/SL	111	28.5–35.4	32.1 ±1.3	121	28.1–35.2	31.8 ±1.3	X	ns
Spinous dorsal-fin-base length/SL	111	32.1–43.6	37.2 ±2.1	121	31.6–41.9	37.0 ±2.1	ns	ns
Soft dorsal-fin-base length/SL	111	21.9–30.8	26.0 ±1.6	121	21.4–28.7	24.8 ±1.6	X	X
Anal-fin-base length/SL	111	13.9–18.9	16.5 ±1.0	121	13.1–18.4	16.3 ±1.0		
Prepelvic-fin length/SL	111	33.5–49.5	39.7 ±2.6	121	34.0–46.5	39.7 ±2.4		

thickness, caudal-peduncle dorsal length, and upper-jaw length (Table 6). No significant regional variation was observed within the overall PCA.

In the sheared PCA of differences in shape by depth, both species showed negligible differences within broadly overlapping clusters of individuals. In the depth analysis, loadings along the PC2 axis were strongest for suborbital depth, gill-raker length, and orbit length, and shallower individuals tended to have a greater suborbital depth, longer gill rakers, and longer orbit. In the combined morphometric and meristic shallow-water analysis, slight differences along the morphometric PC2 axis and the meristic PC1 axis reflected longer gill rakers and higher lateral-line pore counts in *S. variabilis*. No differences were found in the PCA comparing sex within species (Tables 7–8).

Table 2

Counts of lateral-line pores and gill rakers for *Sebastes ciliatus* and *S. variabilis* by region. AI or BS = Aleutian Islands or Bering Sea; GOA = Gulf of Alaska; SEAK = Southeast Alaska; BC = British Columbia.

		Lateral-line pores																		
Species	Region	39	40	41	42	43	44	45	46	47	48	49	50	51	52	53	54	*n*	Mean	SD
Sebastes ciliatus	AI or BS				2	3	8	4	8				1					26	44.73	1.66
	GOA	1		1	6	7	4	11	8	5	5	3	1					52	45.20	2.22
	SEAK					3	3	2	2	4	2	5	3					24	46.75	2.40
Sebastes variabilis	AI or BS							3	4	5	1	7	4	3				27	48.04	1.87
	GOA							5	4	14	11	15	13	8	3		1	74	48.68	1.95
	SEAK					1	1		3	5	9	5	14	4	2			44	48.75	1.94
	BC							1	3	1	2	3	4		1	1		16	48.63	2.25

		Gill rakers																		
Region		32	33	34	35	36	37											*n*	Mean	SD
Sebastes ciliatus	AI or BS	1	9	5	10	1												26	34.04	1.04
	GOA	2	17	23	7	2												51	33.80	0.87
	SEAK	1	1	6	13	3	1											25	34.77	0.92
Sebastes variabilis	AI or BS	3	1	10	8	2	1											25	34.22	1.13
	GOA	1	5	24	35	5												70	34.52	0.80
	SEAK		4	18	15	8	1											46	34.61	0.89
	BC		1	2	8	6												17	35.12	0.86

Systematics

Sebastes ciliatus (Tilesius, 1813)

Dark rockfish

Figs. 1–4; Tables 1–8

Epinephelus ciliatus Tilesius, 1813:406, pl. 16, figs. 1–4 (original description, one specimen: holotype apparently lost, sex unknown, approximately 413 mm TL, "Oceano orientali Camtschatcam et Americam alluenti").

Sebastichthys ciliatus: Jordan and Jouy, 1881:8 (in part, new combination).

Sebastodes ciliatus: Jordan and Gilbert, 1883:658 (in part, new combination).

Sebastostomus ciliatus: Eigenmann and Beeson, 1894:388 (in part, new combination).

Sebastes ciliatus: Westrheim, 1973:1230 (in part, new combination).

Sebastes sp. cf. *ciliatus*: Orr et al., 1998:26, 2000:26.

Neotype

UW 43493, 1(266.4 mm), Lynn Canal, north of Funter Bay, 58.2467°N, 134.899°W, 25 m depth, 13 July 1998.

Material examined

A total of 140 specimens, 83.8–340.0 mm, were examined, including the neotype above. See Appendix for catalog numbers and locality data.

Diagnosis

A species of *Sebastes* with the following combination of character states: body uniformly black to dark blue or gray, particularly at anal-fin base and ventral pectoral-fin rays; peritoneum jet black; symphyseal knob moderate to strong; extrinsic swimbladder muscle with anterior fascia separating sections of striated muscles, otherwise of type I (a–z) of Hallacher (1974); lateral-line pores 39–50, lateral-line scales 44–60; pectoral-fin (P1) rays 16–19; anal-fin (A) rays 7–9; dorsal-fin (D) rays 13–17; vertebrae 28 (11–12 + 16–17).

Description

D XII–XIV, 13–17; A III, 7–9; P1 16–19, 8–11 simple; lateral-line pores 39–50(54), scales 44–60; gill rakers 32–37 (10–11 + 22–27); vertebrae 28 (11–12 + 16–17). Meristic frequency and statistical data are presented in Tables 2–4.

Morphometric data and statistics are presented in Tables 1 and 4. Body relatively deep, especially at nape, depth at pelvic-fin base 32.5–42.7% SL; profile of dorsal margin of head steep from snout to nape above anterodorsal margin of gill slit, flattening to dorsal-fin origin; mouth large, with posterior end of maxilla extending between pupil and posterior rim of orbit, maxilla length 43.6–51.1% HL; symphyseal knob moderate to strong and having blunt tip, lower jaw length 53.4–60.5% HL; mandibular pores of moderate size. Cranial spines weak, in large adults covered by flesh, head smooth. Nasal spine invariably present; parietal ridge invariably present and small spine typically

Table 3

Counts of soft-dorsal-, anal-, and pectoral-fin rays for *Sebastes ciliatus* and *S. variabilis* by region. AI or BS = Aleutian Islands or Bering Sea; GOA = Gulf of Alaska; SEAK = Southeast Alaska; BC = British Columbia. *n* = number of fish in sample.

		Dorsal-fin rays							
Species	Region	13	14	15	16	17	*n*	Mean	SD
Sebastes ciliatus	AI or BS		2	21	3		26	15.04	0.45
	GOA	1	4	45	2		52	14.94	0.42
	SEAK		5	14	4	1	24	15.04	0.75
Sebastes variabilis	AI or BS			25	3		28	15.12	0.33
	GOA		7	54	9		70	15.03	0.49
	SEAK		4	40	3		47	14.98	0.39
	BC		1	16			17	14.94	0.24
		Pectoral-fin rays							
	Region	17	18	19			*n*	Mean	SD
Sebastes ciliatus	AI or BS	1	19	6			26	18.19	0.49
	GOA		44	8			52	18.16	0.37
	SEAK	2	16	6			24	18.17	0.56
Sebastes variabilis	AI or BS		23	4			27	18.17	0.38
	GOA	6	65				71	17.93	0.26
	SEAK	1	44	2			47	18.02	0.25
	BC		15	2			17	18.12	0.33
		Anal-fin rays							
	Region	7	8	9			*n*	Mean	SD
Sebastes ciliatus	AI or BS	4	21	1			26	7.88	0.43
	GOA	4	47				51	7.92	0.27
	SEAK	1	20	3			24	8.08	0.41
Sebastes variabilis	AI or BS	4	19	3			27	8.00	0.50
	GOA	8	63				71	7.88	0.32
	SEAK	5	41				46	7.89	0.31
	BC	1	15	1			17	8.00	0.35

present; postocular and tympanic spines absent or obsolete in adults (postocular present on at least one side in 23.2% and tympanic present on at least one side of 37.7% of specimens examined), most often present in juveniles. Interorbital region wide, 22.9–29.3% HL, strongly convex; parietal ridges weak, and area between ridges slightly convex; preopercular spines 5, directed posteroventrally; two opercular spines, upper spine directed posteriorly, lower spine directed posteroventrally; posttemporal and supracleithral spines present; lachrymal spines rounded, small; dorsal margin of opercle nearly horizontal; lower margin of gill cover with small spines: posteroventral tip of subopercle and anteroventral tip of interopercle rugose or with 1–2 small spines.

Dorsal-fin origin above anterodorsal portion of gill slit; dorsal fin continuous, gradually increasing in height to spine IV and decreasing in height to spine XII; spine XIII much larger, forming anterior support of soft dorsal fin; membranes of spinous dorsal fin moderately incised, less so posteriorly; soft dorsal fin with anterior rays longest, posterior rays gradually shortening. Anal-fin spine II shorter than III (7.5–14.2 vs. 10.0–14.6% SL), anterior rays longest on soft rayed portion of anal fin, posterior rays gradually shortening, posterior margin perpendicular to body axis or with slight posterior slant, anterior ray tips directly ventral to or forward of posterior tips, anterior tip of anal fin typically rounded. Pectoral fins with ray 10 longest, extending to or slightly anterior to vent, fin-ray length 24.6–31.8% SL, fin-base to ray-tip length 24.6–31.8% SL; fin-base width 9.5–11.9% SL. Pelvic fins extend about 60% of distance from pelvic-fin base to anal-fin origin, falling well short of vent, ray length 20.5–26.0% SL, spine length 52.4–67.4% ray length. Caudal fin shallowly emarginate, length 10.2–29.4% SL. Vent positioned below dorsal-fin spine 10, 1.6–5.8% SL from anal-fin origin.

Table 4

Selected proportional morphometrics and meristics of *Sebastes ciliatus* and *S. variabilis* from shallow-water collections. Morphometric data are in percent standard length (SL) or head length (HL). X = statistically significant difference at 0.05 level, as evaluated by ANOVA and ANCOVA, when appropriate; ns = not statistically significant at 0.05 level.

	S. ciliatus			*S. variabilis*				
	n	Range	Mean ±SD	*n*	Range	Mean ±SD	ANOVA	ANCOVA
Meristics	68			49				
Dorsal-fin rays		13–16	15.0 ±0.5		14–16	15.0 ±0.4	ns	
Anal-fin rays		7–9	7.9 ±0.4		7–9	8.0 ±0.3	ns	
Pectoral-fin rays (left)		17–19	18.1 ±0.5		17–19	18.0 ±0.2	ns	
Lateral-line pores (left)		40–50	45.2 ±2.1		42–51	47.9 ±2.0	X	
Gill rakers		32–37	34.3 ±1.1		32–36	34.6 ±1.0	ns	
Morphometrics								
Standard length		83.8–331.0			83.3–363.0			
Head length/SL		30.5–35.5	32.9 ±1.1		30.2–35.4	32.7 ±1.0	ns	ns
Orbit length/HL		21.5–30.6	25.6 ±2.1		23.6–30.0	26.4 ±1.6	ns	ns
Snout length/HL		18.2–26.0	21.3 ±1.6		18.2–24.0	20.9 ±1.4	ns	ns
Interorbital width/HL		22.9–28.2	25.6 ±1.2		23.0–28.8	25.8 ±1.1	ns	ns
Suborbital depth/HL		4.1–7.6	5.9 ±0.7		4.5–7.4	6.0 ±0.6	ns	ns
Upper jaw length/HL		43.6–50.4	47.3 ±1.5		43.9–54.0	47.3 ±2.0	ns	ns
Lower jaw length/HL		53.4–60.5	56.4 ±1.6		52.8–60.4	56.6 ±1.8	ns	X
Gill raker length/HL		11.8–20.7	15.2 ±1.5		13.3–19.9	16.1 ±1.6	X	X
Depth at pelvic–fin base/SL		34.0–40.8	36.7 ±1.5		33.7–38.6	36.2 ±1.2	ns	ns
Depth at anal–fin origin/SL		27.4–35.8	31.2 ±1.7		27.0–31.7	30.0 ±1.1	ns	ns
Body thickness/SL		14.9–21.3	17.9 ±1.2		12.9–20.9	17.1 ±1.8	X	ns
Pectoral-fin base width/SL		9.7–11.8	10.6 ±0.5		9.4–11.1	10.2 ±0.4	X	ns
Pectoral-fin ray length/SL		25.1–31.3	28.6 ±1.2		24.8–31.0	28.4 ±1.2	ns	ns
Caudal peduncle depth/SL		9.8–13.7	11.5 ±0.7		9.7–11.8	10.8 ±0.5	ns	ns
Caudal peduncle dorsal length/SL		11.9–16.2	14.0 ±0.8		12.6–15.3	13.9 ±0.7	ns	ns
Caudal peduncle ventral length/SL		18.2–22.5	20.6 ±1.0		17.1–24.3	21.3 ±1.5	X	X
Preanal length/SL		62.5–77.4	68.3 ±2.3		64.6–73.5	68.2 ±2.1	ns	ns
Predorsal length/SL		29.3–35.4	32.2 ±1.2		28.6–35.2	31.8 ±1.4	ns	ns
Spinous dorsal-fin-base length/SL		32.5–41.8	37.0 ±2.0		33.2–41.6	36.6 ±1.8	ns	ns
Soft dorsal-fin-base length/SL		22.1–29.6	26.2 ±1.4		21.4–28.7	25.0 ±1.6	X	X
Anal-fin-base length/SL		14.5–18.9	16.5 ±0.9		13.6–18.4	16.4 ±1.0	ns	ns
Prepelvic-fin length/SL		36.4–49.5	39.4 ±2.3		36.3–46.5	40.3 ±2.6	ns	ns

Table 5

Factor loadings for principal component (PC) analysis of meristic characters for *Sebastes ciliatus* and *S. variabilis* collected in all depths and regions.

	PC1	PC2	PC3
Lateral-line pores	−0.6139	−0.1000	−0.4151
Gill raker	−0.5993	0.1360	0.5217
Dorsal-fin rays	−0.2731	−0.5625	0.4739
Anal-fin rays	−0.0138	−0.7389	−0.3954
Pectoral-fin rays	0.4349	−0.3304	0.4180

Lateral body scales with many (ca. 5–7) accessory scales in posterior field. Maxilla and underside of mandible completely scaled; suborbital region scaled; branchiostegal rays scaled.

Gill rakers long, 11.3–20.7% HL, and slender on first arch, longest raker in joint between cerato- and hypobranchials, length of preceding and succeeding rakers progressively shorter; rudiments absent. Pseudobranchs 37–38.

Body color in life and after preservation dark, black to gray, lighter in deeper water, lightening ventrally on belly and occasional reddening from base of pectoral fin to base of anal fin, uniformly dark from soft dorsal fin to anal-fin base; vague darker mottling tapering from origin of soft

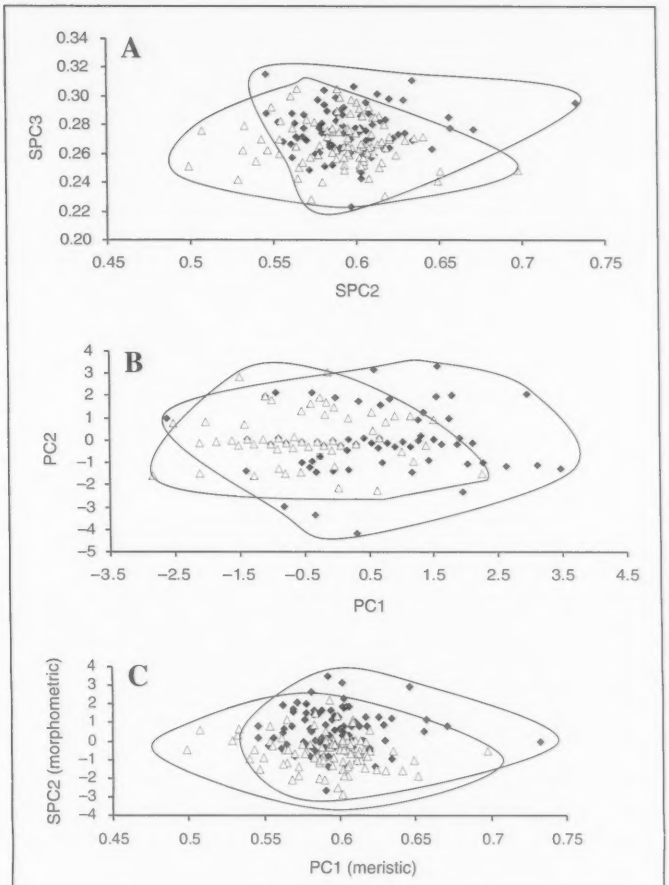

Figure 3

Plots of sheared (SPC) and standard principal component (PC) scores for morphometric and meristic characters for *Sebastes ciliatus* (diamonds) and *S. variabilis* (triangles). (**A**) Morphometric characters only, (**B**) meristic characters only, and (**C**) morphometric (SPC2) versus meristic characters (PC1).

dorsal fin ventrally and forward narrowing across lateral line, faint darker mottling also present farther posterior at soft dorsal-fin base. Head nearly uniformly dark, two faint bars extending from orbit to preopercle, a faint bar along anterior margin of maxilla. Median fins uniformly dark gray to black. Pectoral fins, including lower rays, gray to black. Pelvic fins dark. Peritoneum jet black; stomach, pyloric caeca, and intestines pale. See Figure 1 (A–C, E), and previously published color figures of Kessler (1985, "*S. ciliatus*, dark dusky rockfish"), Kramer and O'Connell (1986; "*S. ciliatus*, dark"), Kramer and O'Connell (1988, 1995; "*S. ciliatus*, Kodiak specimen," and "shallow water specimen"), Orr et al. (1998, 2000; "*S.* sp. cf. *ciliatus*, dark dusky rockfish"), Orr and Reuter (2002; "*S. ciliatus*, dark dusky"), and Mecklenburg et al. (2002; "*S. ciliatus*, dark phase"). Juveniles in life (Fig. 1C) similar to adults in general body color, often brassy on breast and head.

Largest specimen examined 340.0 mm (425 mm TL, 412 mm fork length; UW 46068). Maximum size confirmed 470 mm fork length (RACE Division[6]; Orr, personal observ.).

Distribution and natural history

The range of *Sebastes ciliatus* based on material examined extends from the western Aleutian Islands and east-

[6] RACE (Resource Assessment and Conservation Engineering) Division. 2002. Unpubl. data from RACE database. Alaska Fisheries Science Center, Natl. Mar. Fish. Serv., NOAA, 7600 Sand Point Way NE, Seattle, WA 98115.

Table 6

Factor loadings for sheared principal component (SPC) analysis of morphometric characters for specimens examined across all depths and regions for *Sebastes ciliatus* and *S. variabilis*.

	PC1	SPC2	SPC3
Head length	0.1526	0.1131	0.0416
Orbit length	0.1853	0.2090	0.0988
Depth at anal-fin origin	0.2564	0.1335	−0.0136
Snout length	0.2452	0.1109	0.0240
Interorbital width	0.5753	−0.8081	−0.0485
Suborbital depth	0.1905	0.1481	0.0675
Upper jaw length	0.1837	0.1394	0.0713
Lower jaw length	0.2332	0.2321	−0.9231
Gill raker length	0.1635	0.0768	0.0840
Body thickness	0.2045	0.1692	0.1404
Pectoral-fin base	0.2119	0.1146	0.1139
Pectoral-fin ray length	0.1551	0.0848	0.0105
Caudal peduncle depth	0.2113	0.1436	0.1757
Caudal peduncle dorsal length	0.1885	0.1561	0.0262
Caudal peduncle ventral length	0.1601	0.0829	0.0773
Pre-anal-fin length	0.1313	0.0732	0.0800
Predorsal-fin length	0.1516	0.1063	0.0456
Spinous dorsal-fin base length	0.1549	0.0976	0.0504
Soft dorsal-fin base length	0.1602	0.1271	0.1493
Anal-fin base length	0.1671	0.1266	0.1140

Table 7

Factor loadings for sheared principal component (SPC) analysis of morphometric characters for shallow water *Sebastes ciliatus* and *S. variabilis*.

	PC1	SPC2	SPC3
Head length	0.1149	0.0855	0.0497
Orbit length	0.1504	0.1223	0.0408
Depth at anal-fin origin	0.1876	0.1908	0.1111
Snout length	0.1586	0.0886	0.0687
Interorbital width	0.2465	0.1636	−0.0394
Suborbital depth	0.2428	0.1156	0.0024
Upper jaw length	0.5843	−0.8015	0.0042
Lower jaw length	0.1876	0.1565	0.0745
Gill raker length	0.2431	0.1866	−0.9189
Body thickness	0.1782	0.1386	0.0734
Pectoral-fin base	0.2103	0.1889	0.1819
Pectoral-fin ray length	0.2108	0.1308	0.1165
Caudal peduncle depth	0.1550	0.1033	0.0162
Caudal peduncle dorsal length	0.2126	0.1552	0.1930
Caudal peduncle ventral length	0.1854	0.1426	−0.0224
Pre-anal-fin length	0.1520	0.1098	0.0381
Predorsal-fin length	0.1499	0.1124	0.0603
Spinous dorsal-fin base length	0.1516	0.0953	0.0358
Soft dorsal-fin base length	0.1642	0.1395	0.1171
Anal-fin base length	0.1697	0.1061	0.1310

ern Bering Sea, through the Gulf of Alaska, to southeast Alaska. Other documented records extend its range south to Johnstone Strait, British Columbia (Peden and Wilson, 1976; Fig. 4). It is common throughout its range in shallow rocky habitats, and our material was collected at depths from 5 to 160 m, its total recorded depth range.

Sebastes ciliatus is commonly collected with *S. melanops* by trawl and hook-and-line gear in shallow waters, where *S. ciliatus* is commercially fished as part of the "black rockfish" fishery and has been often misidentified as *S. melanops*. In deeper (>100 m) trawls in Aleutian and Gulf of Alaska waters, *S. ciliatus* is commonly found in association with *S. alutus* (Pacific ocean perch), *S. polyspinis* (northern rockfish), and *S. variabilis* (dusky rockfish). Less frequently, *S. variegatus* (harlequin rockfish), *S. zacentrus* (sharpchin rockfish), and *S. proriger* (redstripe rockfish) are also captured with *S. ciliatus*. A large (320 mm; UW 47417) *S. ciliatus* was found in the stomach of a Pacific cod (*Gadus macrocephalus*) collected in the Aleutian Islands.

Females captured in summer (May–July) trawl surveys are most often ripe with eyed larvae. Near-term females and males were observed in July in shallow waters off southeast Alaska in contrast to individuals of *S. variabilis*, which were all immature at this time (Orr, personal observ.).

Table 8

Factor loadings for principal component (PC) analysis of meristic characters for shallow water *Sebastes ciliatus* and *S. variabilis*.

	PC1	PC2
Lateral-line pores	−0.5933	0.1677
Gill rakers	−0.4274	−0.6851
Dorsal-fin rays	−0.5742	−0.0777
Anal-fin rays	−0.3667	0.6191
Pectoral-fin rays	0.0325	−0.3364

Etymology

The specific name *ciliatus* is derived from the Latin word "cilium" for "eyelid" or "eyelash" and alludes to the numer-

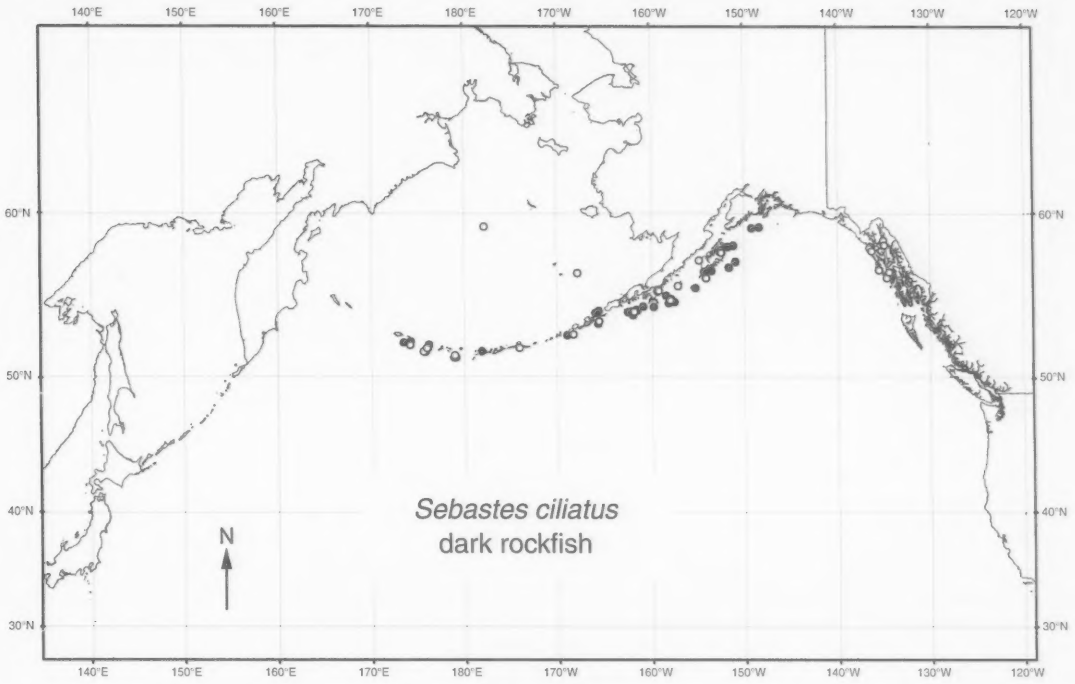

Figure 4

Distribution of *Sebastes ciliatus* based on material examined (open circles) and recent National Marine Fisheries Service survey data (closed circles) for the years 1999 to 2002. Each symbol may represent more than one capture.

ous accessory scales (similar to fringing eyelashes) that are found on the posterior field of the larger scales in most species of *Sebastes* (Tilesius, 1813).

Remarks

Tilesius (1813) based his description of *Epinephelus ciliatus* on a single specimen collected in the North Pacific "bordering Kamchatka and America," probably during the Krusenstern expedition of 1803–06 (Bauchot et al., 1997; Svetovidov, 1978, 1981; Pietsch, 1995). Although the illustration of the specimen was published (Tilesius, 1813; Fig. 2B), the specimen itself has since been lost, probably before the transfer of the Kunstkammer collection to the Zoological Museum of the Academy of Sciences, St. Petersburg (Svetovidov, 1978, 1981). Because *S. ciliatus* may easily be confused with other dark-colored *Sebastes* and *S. variabilis*, we have herein designated UW 43493, collected in Lynn Canal of southeast Alaska, as the neotype of *S. ciliatus*.

The illustration of the holotype of *E. ciliatus* Tilesius (1813) depicts a uniformly dark individual of *Sebastes*, and most of its reported meristics and other characters are consistent with both *S. ciliatus* and *S. variabilis*. However, its lateral-line pore count is low at 43, and although falling well within the range found in the material examined of *S. ciliatus*, the count is represented in only one individual of *S. variabilis* examined. Along with its low lateral-line pore count, a moderate symphyseal knob is illustrated, similar to that of *S. ciliatus*, excluding its identification as *S. melanops*, a common and similarly colored *Sebastes* found within the geographic range of *S. ciliatus*.

The anal-fin posterior margin of the specimen illustrated shows a moderate posterior slant, and tips of the posteriormost rays extend well past those of the anterior rays. *Sebastes ciliatus* may have an anal fin with a slight posterior slant, unlike *S. variabilis*, but it is never as pronounced as the illustration indicates. However, this character is not found in any other dark-colored species of *Sebastes* presently known from the Aleutian Islands and northern Gulf of Alaska west of Kodiak Island. *Sebastes entomelas* has an anal fin with a strong posterior slant to its posterior margin, but the northernmost record of this species is Kodiak Island (Allen and Smith, 1988; Love, 2002; Mecklenburg et al., 2002) where it is rare (RACE Division[6]). *Sebastes entomelas* also has a much higher count of lateral-line pores (50–60; Love et al., 2002).

One syntype of *Perca variabilis* was sent by Martin H. K. Lichtenstein (1780–1857), the director of the Berlin Zoological Museum in 1813, to Georges Cuvier at the Muséum National d'Histoire Naturelle in Paris, and has been preserved as MNHN 8670 (Svetovidov, 1981; Fig. 2A). Although originally from the collections of Carl Heinrich Merck (1761–1799; Svetovidov, 1981; Blanc and Hureau, 1968; Bauchot and Desoutter, 1986) and thus contempora-

neous with Tilesius's material, this specimen probably did not serve as the example for Tilesius's (1813) illustration. The illustration is of the left side of a whole fish, whereas MNHN 8670 is the dried skin and head of the right side. Counts and measurements taken from the original description and compared with the specimen indicate that it is improbable that the left side of this individual was the subject of the illustration. The counts provided by Tilesius (1813) include D XIII, (soft rays not given); A III, 8; P1 18; lateral-line pores 43. MNHN 8670 differs in counts of anal-fin rays (9) and in lateral-line pores (49). Although the symphyseal knob is reduced and the anal-fin margin is strongly slanted posteriorly in the Tilesius illustration, MNHN 8670 has a strong symphyseal knob and a perpendicular anal-fin margin with a distinctly pointed tip (Fig. 2, A and B).

Sebastes variabilis (Pallas, 1814)

Dusky rockfish

Figs. 1–3, 5; Tables 1–8

Perca variabilis Pallas, 1814:241 (original description, three? specimens; lectotype hereby designated, MNHN 8670, dried skin, sex unknown, 343.7 mm, "mari Americam borealum"; other syntypes apparently lost).

Sebastes variabilis: Cuvier, in Cuvier and Valenciennes, 1829:547 (new combination).

Sebastichthys ciliatus: Jordan and Jouy, 1881:8 (in part, new combination).

Sebastodes ciliatus: Jordan and Gilbert, 1883:658 (in part, new combination).

Sebastostomus ciliatus: Eigenmann and Beeson, 1894:388 (in part, new combination).

Sebastes ciliatus: Westrheim, 1973:1230 (in part, new combination).

Material examined

A total of 253 specimens, 48.0–430.8 mm, including the lectotype listed above, were examined. See Appendix for additional catalog numbers and locality data.

Diagnosis

A species of *Sebastes* with the following combination of character states: body light yellow to greenish brown to gray, typically greenish brown, with orange flecks variously present on sides, particularly light ventrally above anal-fin base and on ventral pectoral-fin rays; peritoneum light gray to jet black; symphyseal knob strong; extrinsic swimbladder muscle with a single section of striated muscle, lacking anterior fascia, otherwise of type I (a–z) of Hallacher (1974); lateral-line pores 43–54, lateral-line scales 47–63; pectoral-fin rays 16–19; anal-fin rays 7–9; dorsal-fin rays 13–16; vertebrae 28–29 (11–12 + 16–18).

Description

D XIII–XIV, 13–16; A III, 7–9; P1 16–19, 7–11 simple; lateral-line pores 43–54, scales 47–63; gill rakers 32–37 (10–11 + 22–26); vertebrae 28–29 (11–12 + 16–18) (one of ten specimens with 27 vertebrae, with one caudal vertebra bearing two neural and two haemal spines). Meristic frequency and statistical data are presented in Tables 2–4.

Morphometric data and statistics are presented in Tables 1 and 4. Body relatively deep, especially at nape, depth at pelvic-fin base 29.2–40.9% SL; profile of dorsal margin of head steep to nape above anterodorsal margin of gill slit, flattening to dorsal-fin origin. Mouth large, with posterior end of maxilla extending beyond pupil to or beyond posterior rim of orbit, maxilla length 42.7–54.0% HL; symphyseal knob strong with blunt tip, lower-jaw length 52.8–62.7% HL; mandibular pores of moderate size. Cranial spines weak, in large adults covered by flesh, head smooth. Nasal spines invariably present; parietal ridge invariably present and small spine typically present; postocular and tympanic spines typically absent or obsolete in adults (weak postocular spines present on at least one side in 29.7% and weak tympanic spines present on at least one side in 50.6% of specimens examined) are typically present in juveniles. Interorbital region wide, 22.5–30.4% HL, strongly convex; parietal ridges weak, and area between ridges slightly convex; preopercular spines 5, directed posteroventrally; two opercular spines, upper spine directed posteriorly, lower spine directed posteroventrally; posttemporal and supracleithral spines present; lachrymal spines rounded, small; dorsal margin of opercle nearly horizontal; lower margin of gill cover with small spines: posteroventral tip of subopercle and anteroventral tip of interopercle rugose or with 1 or 2 small spines.

Dorsal-fin origin above anterodorsal portion of gill slit; dorsal fin continuous, gradually increasing in height to spine IV or V and decreasing in height to spine XII; spine XIII much larger, forming anterior support of soft dorsal fin; membranes of spinous dorsal fin moderately incised, less so posteriorly; soft dorsal fin with anterior rays longest, posterior rays gradually shortening. Anal-fin spine II shorter than III (5.8–13.6 vs. 9.5–15.6% SL), anterior rays longest on soft rayed portion of anal fin, posterior rays gradually shortening, posterior margin perpendicular to body axis or with slight posterior slant, anterior ray tips directly ventral to posterior tips, anterior tip of anal fin typically pointed. Pectoral fins with ray 10 longest, extending to or slightly anterior to vent, fin-ray length 23.5–31.0% SL, fin base to ray tip length 24.2–35.1% SL; fin-base width 9.4–11.2% SL. Pelvic fins extend about 60% of distance from pelvic-fin base to anal-fin origin, falling well short of vent, ray length 19.2–29.2% SL, spine length 44.9–70.7% ray length. Caudal fin slightly emarginate, length 15.4–26.9% SL. Vent positioned below dorsal-fin spine 10, 2.2–7.0% SL from anal-fin origin.

Lateral body scales with many (ca. 5–7) accessory scales in posterior field. Maxilla and underside of mandible completely scaled; suborbital region scaled; branchiostegal rays scaled.

Gill rakers long, 11.6–19.9% HL, and slender on first arch, longest raker in joint between cerato- and hypobranchials, length of preceding and succeeding rakers progressively shorter; rudiments absent. Pseudobranchs 36–38.

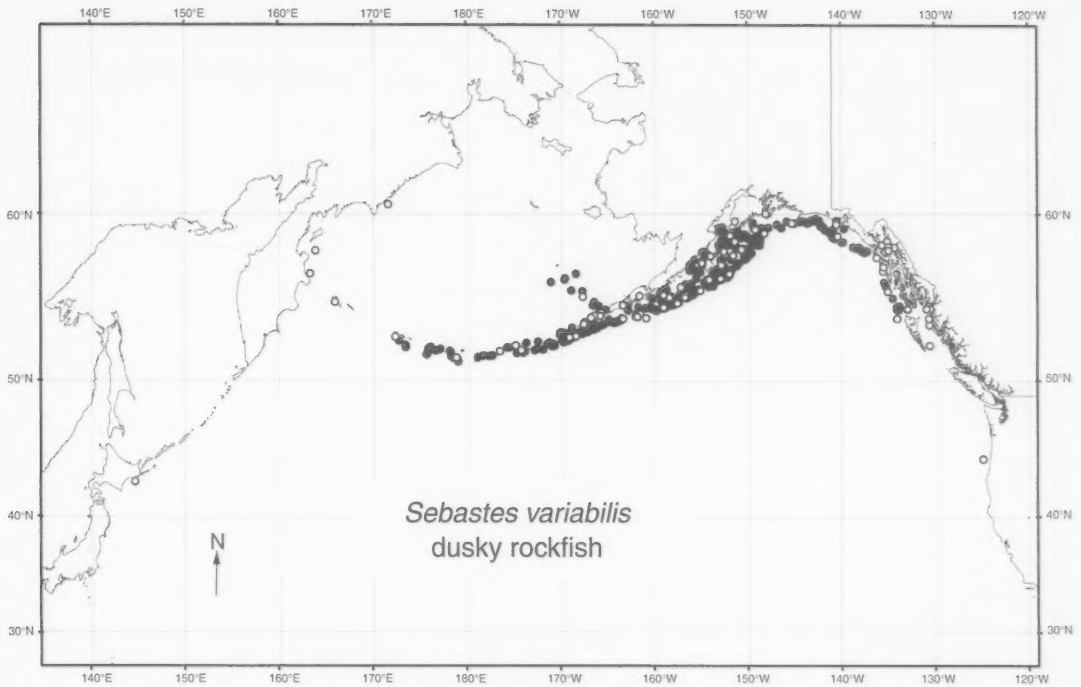

Figure 5

Distribution of *Sebastes variabilis* based on material examined (open circles) and recent National Marine Fisheries Service survey data (closed circles) for the years 1999 to 2002. Each symbol may represent more than one capture.

Body color in life variable (Fig. 1D); adults typically light, greenish-tan (Fig. 1B), often darker gray dorsally (Fig. 1D), rarely lighter yellow overall (Fig. 1D); invariably lightening ventrally to pinkish-white on head, belly, anal-fin base, and caudal peduncle; a clear demarcation between darker dorsum and light ventrum above anal-fin base; vague darker mottling tapering from origin of soft dorsal-fin ventrally and forward narrowing across lateral line, faint darker mottling also present farther posterior at soft dorsal-fin base, mottling most evident in tan individuals; brown to orange "flecks" present on sides of body on posterior fields of scales, appearing as darker speckling in juveniles. Head similar in background color to body, two prominent bars extending from orbit to preopercle, a prominent bar along anterior margin of maxilla in darker individuals (these bars obsolete in light individuals). Median fins and pelvic fins uniformly gray, lighter in light-bodied individuals. Pectoral fins brown to grayish pink; lower rays pink. Peritoneum light gray to jet black, typically dark gray; stomach, pyloric caeca, and intestines pale. See Figure 1 (A–D) and previously published color figures of Kessler (1985; "*Sebastes* sp., light dusky rockfish"), Kramer and O'Connell (1986; "*S. ciliatus,* light"), Kramer and O'Connell (1988, 1995; "*S. ciliatus,* light specimen"), Orr et al. (1998, 2000; "*S. ciliatus*, light dusky rockfish"), Orr and Reuter (2002; "light dusky"), Mecklenburg et al. (2002; "light phase").

Juveniles in life (Fig. 1C) lighter than adults, with dorsum light-brown to tan, background covered with orange-brown speckles, often with distinct dark band at base of soft dorsal fin; head brassy; ventrum pink on lower jaw, breast, and base of anal fin, lightening to white on belly.

Largest specimen examined 430.8 mm (527.7 mm fork length [FL], 541.3 mm TL; UW 44253). Maximum size reported 590 mm FL (RACE Division[6]).

Distribution and natural history

Sebastes variabilis is recorded from a single specimen off Hokkaido, Japan (Shinohara et al., 1994), and from other specimens collected from the east coast of Kamchatka to Cape Ol'utorskii (at 60°N) in the western Bering Sea, along the Aleutian Islands to 60°N in the eastern Bering Sea, through the Gulf of Alaska south to Johnstone Strait, British Columbia (Peden and Wilson, 1976; Richards and Westrheim, 1988; Fig. 5), and to central Oregon (based on a recently collected single specimen [UW 46575]). The earlier record of Schultz (1936) and Alverson and Welander (1952) from Washington at Neah Bay was reidentified by Westrheim (1968) as *S. entomelas.*

Although the depth of collection for material examined ranges from 6 to 370 m, and the species is recorded at depths to 675 m, large adults are commonly found along the edge of the continental shelf at depths of 100–300 m,

where the species is the target of commercial fisheries in the Gulf of Alaska. During trawl surveys, it is most commonly associated with *S. alutus* and *S. polyspinis*, and at greater depths with *S. aleutianus* (rougheye rockfish) throughout its range in Alaskan waters (Reuter, 1999; Ackley and Heifetz, 2001).

Females and males captured during summer (May–July) trawl surveys ranged widely in maturity state. Occasional ripe females were observed, although most females were maturing (Orr, personal observ.). A high percentage of females caught in trawl surveys during early April off southeast Alaska were releasing larvae, indicating that parturition occurs in the spring (Lunsford[7]). During July in shallower waters (ca. 40 m) of southeast Alaska, all *S. variabilis* collected were immature.

Etymology

The specific name *variabilis* is presumed to be a reference by Pallas (1814) to the wide range of body color in the species.

Remarks

Pallas (1814) described *Perca variabilis* from at least three specimens probably collected by Merck during the 1786–94 Billings expedition to the Russian Far East, including the Aleutian Islands, eastern Bering Sea, and northern Gulf of Alaska (Schmidt, 1950; Svetovidov, 1978, 1981; Pierce, 1990). One specimen was more completely described and used by him to obtain a set of counts and measurements. The other specimens were used to describe variation in the species, as in the following excerpt translated by the authors from the Latin text of Pallas (1814): "Body colored according to life and sex, varied, sometimes dark blue, belly white, fins blackish; female red below; those older wholly red or even purplish...." Pallas (1814) ultimately based the name *P. variabilis* on the supposed variability in color in this species.

Jordan and Evermann (1898) examined an individual from the Pallas collection, recognized by him as the "summer variety" of *P. variabilis* (ZMB 8145). They identified this "summer variety" as *Sebastes aleutianus* Jordan and Evermann (Jordan, 1884, 1885; Jordan and Evermann, 1898), a species easily distinguished from both *S. variabilis* and *S. ciliatus* by its full complement of eight pairs of strong cranial spines. These specimens have since been lost, probably during the destruction of the Berlin Zoological Museum during World War II (Paepke and Fricke, 1992). Although Jordan and Gilbert (1883) wrote that *S. proriger* was also confounded with *S. ciliatus*, Jordan (1885) and Jordan and Evermann (1898) corrected this statement, noting that only *S. ciliatus* and *S. aleutianus* were included within the material described as *E. ciliatus* and *P. variabilis* by Tilesius and Pallas.

[7] Lunsford, C. 2002. Personal commun. National Marine Fisheries Service, Auke Bay Laboratory, Alaska Fisheries Science Center, 11305 Glacier Highway, Juneau, AK 99801-8626.

Although MNHN 8670 (Fig. 2A) is from the Pallas collection (Svetovidov, 1978, 1981), it is apparently not the specimen used for the complete description. In his original account, Pallas (1814) listed the following meristic data (modified to standard notation): D XIII, 15; A III, 7; P1 17 (8 simple). Although the dorsal-fin ray count is identical with that of the MNHN 8670 specimen, both anal- and pectoral-fin ray counts differ. All elements are well preserved and easily counted.

Comparisons of proportions are more difficult to interpret because measurements had not been standardized at the time of the original description. However, of those measurements that can be readily compared, the following significant differences were found, providing additional evidence that this individual was not the specimen used for the primary description: total length (391.6 mm in Pallas [1814; "longitudo majoris speciminis"] vs. 414.0 mm taken from MNHN 8670), head length (101.6 mm ["capitis a summa maxilla ad operculum angulum"] vs. either 96.6 mm [standard head length] or 110.2 mm [head length to tip of lower jaw]). The specimen used by Pallas for the detailed meristics and morphometrics is presumed lost (Svetovidov, 1978).

Ayres (1854) misidentified *S. melanops* from the vicinity of San Francisco Bay as *S. variabilis*. Günther (1860) and Ayres (1862, 1863) placed *S. variabilis* of Ayres into the synonymy of *S. melanops*.

Comparisons

Sebastes variabilis is most similar to *S. ciliatus*; the latter is distinguished by its uniformly dark-blue to black color. *Sebastes ciliatus* is invariably dark at the base of the anal fin and on the lower pectoral rays, areas of lighter color in *S. variabilis* even in those individuals that have an overall dark body. The peritoneum of *S. ciliatus* is always jet black, unlike the usual gray peritoneum of *S. variabilis*, which however may often be dark or occasionally jet black. In combination with these color differences, a low count of 39–42 lateral-line pores will distinguish *S. ciliatus* from *S. variabilis*, although the total range of counts overlaps considerably.

The extrinsic morphological features of the swimbladder of both *S. ciliatus* and *S. variabilis* are of type I (a–z) of Hallacher (1974) in which the anterior muscle mass originates from the occipital region of the neurocranium, attaches to the pectoral girdle near the insertion of Baudelot's ligament, passes between the epineural and pleural ribs of vertebrae 3 and 4, passes ventral to the pleural rib of vertebrae 5, and continues posteriorly as three tendons that insert on the pleural ribs of vertebrae 8, 9, and 10. In *S. ciliatus* and not *S. variabilis*, the anterior striated muscle mass is separated into two sections by a thin fascia, similar to the condition reported in *S. paucispinis* alone among species of *Sebastes* (Hallacher, 1974). The morphological features of the complex differ significantly in *S. paucispinis*, however, in that the striated muscle does not attach to the pectoral girdle but bypasses it to insert by a single tendon into the posterior portion of the swimbladder. Only five specimens each of *S. ciliatus* and *S. varia-*

bilis were dissected in the present study to examine these muscles. Additional material should be examined to assess the intraspecific variability and systematic significance of this character complex.

Typical habitats of these two species also differ. Adult *S. ciliatus* are found in nearshore shallow habitats at maximum depths of 160 m and are abundant in protected coves on the outer coast of Alaska. *Sebastes variabilis*, in contrast, is found along the continental shelf margin at depths to 675 m. However, adult *S. variabilis* have also been collected in nearshore waters as shallow as 40 m (UW 43494). In areas of sympatry, such as the inside waters in Lynn Canal of southeast Alaska and Monashka Bay of Kodiak Island, *S. variabilis* is found at greater depths in stronger current, whereas *S. ciliatus* is found, often with *S. melanops*, among kelp (*Macrocystis*) on rocky ledges (Blackburn and Orr, personal observ.).

Other uniformly dark colored species of *Sebastes*, such as *S. melanops* and *S. mystinus*, may also be confused with *S. ciliatus* and darker individuals of *S. variabilis*, although both may be distinguished on the basis of color and morphological features. The body of *S. melanops* is dark bluish-black, has black speckling on the dorsum and lateral surfaces, and a distinctly white ventrum (in contrast with the slightly lighter ventrum of *S. ciliatus* [Fig. 1E]). Unlike *S. ciliatus*, in which the peritoneum is jet black, *S. melanops* has a white peritoneum. In *S. melanops*, five or six faint light blotches slightly larger than the orbit are present on the dorsum about midway between the lateral line and the dorsal-fin base. These blotches are especially prominent underwater, and in Alaska easily distinguish *S. melanops* from both *S. variabilis* and *S. ciliatus*, which lack blotches (Lauth[8]; see color figures of Love, 2002, and Stewart and Love, 2002). The symphyseal knob in *S. melanops* is obsolete, consisting only of a fleshy pad at the tip of the mandible, unlike the distinct bony knob of *S. ciliatus* and *S. variabilis*. Mandibular pores of *S. melanops* are obsolete, as compared with the larger, readily apparent pores of *S. ciliatus* and *S. variabilis*. Vertebral counts also differ, from 28–29 in *S. ciliatus* and *S. variabilis* to 26 in *S. melanops*. *Sebastes melanops* ranges from southern California to Atka Island in the Aleutian Islands (Mecklenburg et al., 2002) and the southern Bering Sea, where its presence is documented by a single recent collection (UW 47037). Most previous reports from the Bering Sea may be of *S. ciliatus*.

Sebastes mystinus is also similar to *S. ciliatus* but may be distinguished by the four distinct dark bars across its head and nape contrasting with its general body color of light mottled bluish-gray. The mouth of *S. mystinus* is smaller than that of *S. ciliatus*, and the maxilla extends only to the middle of the pupil rather than to the posterior portion of the orbit as in *S. ciliatus*. Like *S. melanops* and most Pacific *Sebastes*, *S. mystinus* has 26–27 vertebrae, compared to the 28–29 vertebrae of *S. ciliatus* and *S. variabilis*. *Sebastes mystinus* has been recorded from Sitka Harbor, Alaska (Kramer and O'Connell, 1995), to Punta Santo Tomas, northern Baja California (Hobson, 2002). Earlier reports from Kodiak Island, the Aleutian Islands, and Bering Sea are undocumented (Quast and Hall, 1972; Kramer and O'Connell, 1995; Mecklenburg et al., 2002) and probably refer to *S. ciliatus*.

Sebastes polyspinis is commonly caught in trawls and may be confused with *S. variabilis*, especially when preserved. It can be distinguished from *S. variabilis* by its modal count of 14 dorsal-fin spines and light (pink or white when live) oblique band across the lower rays of the pectoral fin, which remains prominent when recently preserved. In life, the overall color of *S. polyspinis* is reddish-orange to pink, overlaid with gray-green mottling and fine green spots. Evermann and Goldsborough (1907) considered the then undescribed *S. polyspinis* within the range of variation of "*S. ciliatus*," because at least one lot (USNM 6243) was misidentified by them as "*S. ciliatus*." They probably also confused *S. melanops* with *S. variabilis*, or possibly *S. polyspinis*, describing the color in life of *S. melanops* from Alaska as "olive-brown, blotched with dirty red." *Sebastes melanops* never has a trace of red, whereas the most common color pattern of *S. variabilis* could be adequately described by this phrase.

In the western Pacific, two species, the dark-colored *S. taczanowskii* and the light-colored *S. schlegelii*, may be confused with *S. ciliatus* and *S. variabilis*, respectively. Both may be distinguished from *S. ciliatus* and *S. variabilis* by modal counts of pectoral-fin rays (15 in *S. taczanowskii* and 17 in *S. schlegelii* vs. 18 in both *S. ciliatus* and *S. variabilis*) and vertebrae (26 in both *S. taczanowskii* and *S. schlegelii* vs. 28–29 in *S. ciliatus* and *S. variabilis*). *Sebastes schlegelii* may also be distinguished by its typical dorsal-fin spine count of 12 (vs. 13 in *S. ciliatus* and *S. variabilis*).

Implications for fisheries management

The dusky rockfish (*S. variabilis*) and the dark rockfish (*S. ciliatus*) have been subjected to two distinct fisheries separately managed by U.S. federal and Alaska state agencies: *S. variabilis* is captured in the offshore trawl fishery; *S. ciliatus*, in the nearshore jig fishery. Although the offshore fisheries for dusky rockfish only incidentally catch the dark rockfish and are managed for dusky rockfish, the nearshore fishery is not managed for dark rockfish, and instead the species has been routinely misidentified as black rockfish (*S. melanops*). *Sebastes ciliatus* has been found to comprise up to 25% of the catch in the "black rockfish" jig fishery of the northern Gulf of Alaska (Clausen et al.[1]).

Several differences in biologically significant parameters were evident from specimens examined in our study and from observations in survey data. The two species are typically found in different habitats, attain different maximum sizes, and show differences in reproductive seasonality. Recognizing the two as distinct species is the first step towards establishing a biologically based, species-specific management scheme.

[8] Lauth, R. R. 1998. Personal commun. Resource Assessment and Conservation Engineering Division, Alaska Fisheries Science Center, Natl. Mar. Fish. Serv., NOAA, 7600 Sand Point Way NE, Seattle, WA 98115.

Acknowledgments

We appreciate the early efforts of J. Geil and J. Westrheim to encourage this research through spirited discussion and by providing unpublished data, courtesy of Fisheries and Oceans Canada, Pacific Biological Station. We thank D. Clausen, C. Lunsford, T. W. Pietsch, D. E. Stevenson, and M. E. Wilkins for overall reviews and K. Mier for a statistical review. The care and transportation of specimens from Alaska is not a small task and we thank the many collectors who made this project possible: fisheries observers W. Benecki, M. Brown, K. Barber, T. Droz, J. Peeples, and J. Wiersema; personnel of the AFSC's RACE Division W. C. Flerx, R. Harrison, R. R. Lauth, G. R. Hoff, M. Martin, N. W. Raring, J. S. Stark, H. Zenger, and M. Zimmermann. For support of nearshore field work in southeast Alaska, we thank J. Fujioka, D. Clausen, and B. Wing. The University of Washington Fish Collection archived most of the fresh material examined for this study and we appreciate the support of the curator (T. W. Pietsch) and collections managers (K. E. Pearson and B. W. Urbain). We also thank the following curators and collections managers and their institutions for hosting visits for examination of material or for the loan of specimens: B. Wing (ABL), K. Sendall (BCPM), W. Eschmeyer, D. Catania (CAS), B. Sheiko (KIE), J.-C. Hureau, G. Duhamel, P. Pruvost (MNHN), D. F. Markle (OSU), and G. D. Johnson, S. Jewett, and S. J. Raredon (USNM).

Literature cited

Ackley, D. R., and J. Heifetz.
2001. Fishing practices under maximum retainable bycatch rates in Alaska's groundfish fisheries. Alaska Fish. Res. Bull. 8(1):22–44.

Allen, M. J., and G. B. Smith.
1988. Atlas and zoogeography of common fishes in the Bering Sea and northeastern Pacific. NOAA Tech. Rep. NMFS 66, 151 p.

Alverson, D. L., and A. D. Welander.
1952. Notes on the scorpaenid fishes of Washington and adjacent areas, with a key for their identification. Copeia 1952:138–143.

Ayres, W. O.
1854. [Descriptions of new species of California fishes.] Proc. Calif. Acad. Sci. 1:1–22.
1862. [Descriptions of fishes believed to be new.] Proc. Calif. Acad. Sci. 2:209–218.
1863. Notes on the sebastoid fishes occurring on the coast of California, U.S.A. Proc. Zool. Soc. London 26:390–402.

Barsukov, V. V.
1964. Key to the fishes of the family Scorpaenidae. Soviet Fisheries Investigations in the northeast Pacific. Soviet Fisheries Investigations in the northeast Pacific 53:226–262.

Bauchot, M.-L., J. Daget, and R. Bauchot.
1997. Ichthyology in France at the beginning of the 19th century: the histoire naturelle des poissons of Cuvier (1769–1832) and Valenciennes (1794–1865), p. 27–80. *In* Collection building in ichthyology and herpetology (T. W. Pietsch and W. D. Anderson Jr., eds.), 593 p. Am. Soc. Ichthyol. Herpetol. Spec. Publ. 3.

Bauchot, M.-L., and M. Desoutter.
1986. Catalogue critique des types de poissons du Muséum national d'Histoire naturelle. Sous-ordre des Percoidei (familles des Apogonidae, Centrachidae, Centropomidae, Dinolestidae, Glaucosomatidae, Grammatidae, Kuhliidae, Percidae, Percichthyidae, Plesiopidae, Priacanthidae, Pseudochromidae, Teraponidae). Bull. Mus. natl. Hist. nat., Paris, 4e sér., 8, sect. A, 4 suppl.: 51–130.

Bentzen, P., J. M. Wright, L. T. Bryden, M. Sargent, and K. C. T. Zwanenburg.
1998. Tandem repeat polymorphism and heteroplasmy in the mitochondrial control region of redfishes (*Sebastes*: Scorpaenidae). J. Hered. 89:1–7.

Blanc, M., and J. C. Hureau.
1968. Catalogue critique des types de poissons du Muséum national d'Histoire naturelle (poissons à joues cuirassées), 70 p. Publ. Diverces Mus. Natl. Hist. Nat. 23.

Bookstein, F. L., B. Chernoff, R. L. Elder, J. M. Humphries Jr., G. R. Smith, and R. E. Strauss.
1985. Morphometrics in evolutionary biology, 177 p. Acad. Nat. Sci. Spec. Publ. 15, Philadelphia, PA.

Cuvier, G., and A. Valenciennes.
1829. Histoire naturelle des poissons. Vol. 4, 518 p. Strasbourg.

Eigenmann, C. H., and C. H. Beeson.
1894. A revision of the fishes of the subfamily Sebastinae of the Pacific coast of America. Proc. U.S. Nat. Mus. 17:375–407.

Eschmeyer, W. N., E. S. Herald, and H. Hammann
1983. A field guide to Pacific coast fishes of North America. Houghton Mifflin Company, Boston, MA, 336 p.

Evermann, B. W., and E. L. Goldsborough.
1907. The fishes of Alaska. Bull. Bur. Fish. 26:219–360.

Günther, A. C. G.
1860. Catalogue of the fishes in the British Museum. Catalogue of the acanthopterygian fishes in the collection of the British Museum. Gobiidae to Notacanthi. Cat. Fishes 3:1–586.

Hallacher, L. E.
1974. The comparative morphology of extrinsic swimbladder musculature in the scorpionfish genus *Sebastes* (Pisces: Scorpaenidae). Proc. Cal. Acad. Sci. 40:59–86.

Hobson, T.
2002. *Sebastes mystinus*. *In* Rockfishes of the northeast Pacific (M. Love, M. Yoklavich, and L. Thorsteinson, eds.), p. 215–218. Univ. California Press, Los Angeles, CA.

Hubbs, C. L., and K. F. Lagler.
1958. Fishes of the Great Lakes region, revised ed. Cranbrook Inst. Sci. Bull. 26, 213 p.

Jordan, D. S.
1883. Notes on American fishes preserved in the museums at Berlin, London, Paris, and Copenhagen. Proc. Acad. Nat. Sci. Phila. 1884:281–293.
1885. A catalogue of fishes known to inhabit the waters of North America, north of the Tropic of Cancer, with notes on the species discovered in 1883 and 1884. Rep. U.S. Fish Comm. 13:789–973.
1896. Notes on fishes, little known or new to science. Proc. Calif. Acad. Sci. 6:201–244.

Jordan, D. S., and B. W. Evermann.
1898. The fishes of North and Middle America: a descriptive catalogue of the species of fish-like vertebrates found in the waters of North America, north of the Isthmus of Panama. Part II. Bull. U.S. Natl. Mus. 47:i–xxx, 1241–2183.

Jordan, D. S., and C. H. Gilbert.
1881. Description of *Sebastichthys mystinus*. Proc. U.S. Natl. Mus. 4:70–72.
1883. Synopsis of the fishes of North America. Bull. U.S. Natl. Mus. 16:i-liv + 1–1018.

Jordan, D. S., and P. L. Jouy.
1881. Checklist of duplicates of fishes from the Pacific coast of North America, distributed by the Smithsonian Institution in behalf of the U.S. National Museum. Proc. U.S. Natl. Mus. 4:8.

Kessler, D. W.
1985. Alaska's saltwater fishes and other sea life, 358 p. Alaska Northwest Publishing Co., Anchorage, AK.

Kramer, D. E., and V. O'Connell.
1986. Guide to northeast Pacific rockfishes genera *Sebastes* and *Sebastolobus*. Alaska Sea Grant, Mar. Adv. Bull. 25, 78 p.
1988. Guide to northeast Pacific rockfishes genera *Sebastes* and *Sebastolobus*. [1st revision.] Alaska Sea Grant, Mar. Adv. Bull. 25, 78 p.
1995. Guide to northeast Pacific rockfishes genera *Sebastes* and *Sebastolobus*. [2nd revision.] Alaska Sea Grant, Mar. Adv. Bull. 25, 78 p.

Leviton, A. E., and R. H. Gibbs Jr.
1988. Standards in herpetology and ichthyology. Standard symbolic codes for institutional resource collections in herpetology and ichthyology. Suppl. no. 1: additions and corrections. Copeia 1988:280–282.

Leviton, A. E., R. H. Gibbs Jr., E. Heal, and C. E. Dawson.
1985. Standards in herpetology and ichthyology: part I. Standard symbolic codes for institutional resource collections in herpetology and ichthyology. Copeia 1985:802–832.

Love, M. S.
2002. *Sebastes entomelas*. *In* Rockfishes of the northeast Pacific (M. Love, M. Yoklavich, and L. Thorsteinson, eds.), p. 172–174. Univ. California Press, Los Angeles, CA.

Love, M. S., M. Yoklavich, and L. Thorsteinson (eds.).
2002. The rockfishes of the northeast Pacific, 405 p. Univ. California Press, Los Angeles, CA.

Mecklenburg, C. W., T. A. Mecklenburg, and L. K. Thorsteinson.
2002. Fishes of Alaska, 1037 p. Am. Fish. Soc., Bethesda, MD.

Orr, J. W., M. A. Brown, and D. C. Baker.
1998. Guide to rockfishes (Scorpaenidae) of the genera *Sebastes*, *Sebastolobus*, and *Adelosebastes* of the northeast Pacific Ocean. NOAA Tech. Memo. NMFS-AFSC-95, 46 p.
2000. Guide to rockfishes (Scorpaenidae) of the genera *Sebastes*, *Sebastolobus*, and *Adelosebastes* of the northeast Pacific Ocean, 2nd ed. NOAA Tech. Memo. NMFS-AFSC-117, 48 p.

Orr, J. W., and R. Reuter.
2002. *Sebastes ciliatus*. *In* Rockfishes of the northeast Pacific (M. Love, M. Yoklavich, and L. Thorsteinson, eds.), p. 151–153. Univ. California Press, Los Angeles, CA.

Paepke, H.-J., and R. Fricke.
1992. Critical catalog of the types of the fish collection of the Zoological Museum Berlin. Part 4: Scorpaeniformes. Mitt. Zool. Mus. Berl. 68:267–293.

Pallas, P. S.
1814. Zoographia Rosso-Asiatica, sistens omnium animalium in extenso Imperio Rossico et adjacentibus maribus observatorum recensionem, domocilia, mores et descriptiones, anatomen atque iconem plurimorum. Petrop., Acad. Sci., vol. 3, 428 p.

Peden, A. E., and D. E. Wilson.
1976. Distribution of intertidal and subtidal fishes of northern British Columbia and southeastern Alaska. Syesis 9:221–248.

Pierce, R. A.
1990. Russian America: a biographical dictionary. Alaska Historical Commission Studies in History, No. 132, 555 p. Limestone Press, Fairbanks, AK.

Pietsch, T. W. (ed.)
1995. Historical portrait of the progress of ichthyology, from its origins to our own time, by Georges Cuvier, 366 p. Edited and annotated by T. W. Pietsch, translated from the French by A. J. Simpson. Johns Hopkins Univ. Press, Baltimore, MD.

Poss, S., and B. B. Collette.
1995. Second survey of fish collections in the United States and Canada. Copeia 1995:48–70.

Quast, J. C., and E. L. Hall.
1972. List of fishes of Alaska and adjacent waters with a guide to some of their literature. NOAA Tech. Rep. NMFS SSRF-658, 47 p.

Reuter, R. F.
1999. Describing dusky rockfish (*Sebastes ciliatus*) habitat in the Gulf of Alaska using historical data. Unpubl. MS thesis, 83 p. California State Univ., Hayward, CA.

Richards, L. J., and S. J. Westrheim.
1988. Southern range extension of the dusky rockfish, *Sebastes ciliatus*, in British Columbia. Can. Field-Nat. 102:251–253.

Roques, S., J.-M. Sévigny, and L. Bernatchez.
2001. Evidence for broadscale introgressive hybridization between two redfish (genus *Sebastes*) in the North-west Atlantic: a rare marine example. Mol. Ecol. 10:149–165.

Schmidt, P. Y.
1950. Fishes of the Sea of Okhotsk. Academy of Sciences of the USSR, Transactions of the Pacific Committee, vol. 6, Moscow-Leningrad, 392 p. [In Russian, 1965 transl. by the Israel Prog. Sci. Trans. Available from the National Technical Information Service, Springfield, VA.]

Schultz, L. P.
1936. Keys to the fishes of Washington, Oregon and closely adjoining regions. Univ. Washington Publ. Biol. 2:103–228.

Seeb, L.
1986. Biochemical systematics and evolution of the scorpaenid genus *Sebastes*. Ph.D. diss., 176 p. Univ. Washington, Seattle, WA.

Shinohara, G., M. Yabe, and T. Honma.
1994. Occurrence of the scorpaenid fish, *Sebastes ciliatus*, from the Pacific coast of Hokkaido, Japan. Bull. Biogeogr. Soc. Japan 49:61–64.

Stewart, E., and M. Love.
2002. *Sebastes melanops*. *In* Rockfishes of the northeast Pacific (M. Love, M. Yoklavich, and L. Thorsteinson, eds.), p. 204–207. Univ. California Press, Los Angeles, CA.

Sundt R. C., and T. Johansen.
1998. Low level of interspecific DNA sequence variation of the mitochondrial 16S rDNA in north Atlantic redfish *Sebastes* (Pisces, Scorpaenidae). Sarsia 83:449–452.

Svetovidov, A. N.
1978. The types of the fish species described by P. S. Pallas in "Zoographi Rosso-Asiatica" (with a historical account of publication of this book). Nauka, Leningrad, 35 p. [In Russian.]
1981. The Pallas fish collection and the Zoographia Rosso-Asiatica: an historical account. Arch. Nat. Hist. 10:45–64.

Tilesius, W. G. von.
1813. Iconum et descriptionum piscium Camtschaticorum continuatio tertia tentamen monographiae generis Agoni Blochiani sistens. Mem. Acad. Imp. Sci. St. Petersb. 4:406–478.

Tsuyuki, H., E. Roberts, and W. E. Vanstone.
1965. Comparative zone electropherograms of muscle myogens and blood hemoglobins of marine and freshwater vertebrates and their application to biochemical systematics. J. Fish. Res. Board Canada 22:203–213.

Tsuyuki, H., E. Roberts, R. H. Lowes, W. Hadaway, and S. J. Westrheim.
1968. Contribution of protein electrophoresis to rockfish (Scorpaenidae) systematics. J. Fish. Res. Board Canada 25:2477–2501.

Westrheim, S. J.
1968. First records of three rockfish species (*Sebastodes aurora*, *S. ciliatus*, and *Sebastolobus altivelis*) from waters off British Columbia. J. Fish. Res. Board Canada 25: 2509–2513.
1973. Preliminary information on the systematics, distribution, and abundance of the dusky rockfish, *Sebastes ciliatus*. J. Fish. Res. Board Can. 30:1230–1234.

Appendix

Material examined

Sebastes ciliatus Bering Sea: UW 45488, 1(329.7 mm), 56.65°N, 167.8167°W, 100 m depth, 5 February 2001; UW 22474, 1(221.7 mm), 59.25°N, 177.8167°W, 160 m depth, 1987. Aleutian Islands: UW 43447, 1(290 mm), 51.2534°N, 179.2689°E, 165 m depth, 26 July 1997; UW 45588, 2(240–380 mm), Aleutian Is., FV *Vesteraalen*, 1997; ABL 69-13, 2(228.8–250.9 mm), Amchitka I., Constantine Harbor, 51.4°N, 179.3667°E, 6 September 1968; UW 46489 (UK T002383), 1(279.7 mm), 51.2707°N, 179.2118°E, 98 m depth, 26 July 1997; UW 45498, 1(318.5 mm), 51.9921°N, 174.1031°W, 93 m depth, 6 July 1997; UW 43039, 4(83.8–206.5 mm), Amchitka I., Constantine Harbor, off Kirilof, 7 December 1961; UW 43423, 2(295.1–315.9 mm), Amchitka I., 51.3833°N, 178.9°E, 88 m depth, 20 April 1993; UW 43436, 12(272–315 mm), 51.7552°N, 175.6726°E, 94 m depth, 1 August 1997; UW 14416, 1(183 mm), Amchitka I., Constantine Harbor, 5 September 1955; UW 43458, 5(263.9–288.6 mm), 51.2707°N, 179.2118°E, 98 m depth, 26 July 1997; UW 4766, 1(189 mm), Atka I., Atka village, 18 August 1938; UW 46483, 2(230–253 mm), 51.9730°N, 176.0841°E, 78 m depth, 20 July 2000; UW 46484, 2(275–293 mm), 51.9638°N, 176.0288°E, 64 m depth, 20 July 2000; UW 47417, 1(320 mm), Aleutian Is., recovered from stomach of *Gadus macrocephalus*. Gulf of Alaska: UW 43242, 6(320–390 mm), 53.7345°N, 165.5425°W, 89 m depth, 25 June 1996; UW 43272, 5(274–325.5 mm), 55.093°N, 157.8048°W, 76 m depth, 10 June 1996; UW 43420, 1(334.7 mm), 55.9042°N, 157.0751°W, 101 m depth, 18 June 1996; UW 45508, 2(242.4–292.6 mm), 55.1056°N, 157.9594°W, 78 m depth, 2 June 1999; UW 45512, 1(235.2 mm), 57.3806°N, 154.8009°W, 67 m depth, 7 June 1999; UW 45509, 1(298 mm), 54.3215°N, 161.8107°W, 72 m depth, 23 May 1999; UW 47412, 1(323.7 mm), 52.8953°N, 168.297°W, 99 m depth, 21 May 2001; UW 46488, 1(270 mm), 56.3686°N, 154.0495°W, 69 m depth, 24 June 2001; UW 46584, 1(295 mm), 55.1056°N, 157.9594°W, 78 m depth, 2 June 1999; UW 46485, 1(320.1 mm), 55.01862°N, 157.882°W, 76 m depth, 8 June 2001. Kodiak Island area: UW 43059, 1(200.7 mm), Kodiak I., Monashka Bay, SW of Trenton Pt., 57.8367°N, 152.4°W, 28 July 1977; UW 47289, 2(169–203.7 mm), Kodiak I., Monashka Bay, 5 m depth, 57.8383°N, 152.4283°W, 5 m depth, 31 July 1982; UW 44035, 2(216.7–274.5 mm), Kodiak I., Monashka Bay, 57.8367°N, 152.4°W, 18 m depth, 2 August 1982; UW 44036, 11(178.2–263.7 mm), Kodiak I., Monashka Bay, 57.8383°N, 152.4283°W, 12 m depth, 3 August 1982; UW 44045, 19(140.6–307.8 mm), Kodiak I., Monashka Bay, 57.8383°N, 152.4283°W, 15 m depth, 12 August 1982; UW 44049, 1(291.6 mm), Kodiak I., Monashka Bay, 57.8383°N, 152.4283°W, 12 m depth, 11 September 1982; UW 44050, 1(331 mm), NE of Kodiak I., Triplets Is., 57.98°N, 152.48°W, 18 m depth, 1 July 1983; UW 44051, 1(319.7 mm), Kodiak I., Monashka Bay, 57.8367°N, 152.4°W, 6 m depth, 14 October 1982. Southeast Alaska: ABL 60-7, 1(164 mm), Kuiu I., Washington Bay, ca. 5 mi W of Petersburg, 2 June 1960; ABL 62-105, 1(224.5 mm), Little Port Walter, SE tip of Baranoff I.; ABL 68-295, 1(214.1 mm), NW tip of Lincoln I., ca. 5 mi N of Pt. Retreat, Lynn Canal, 7.5 m depth, 4 July 1968; ABL 87-15, 1(111.8 mm), Port Althorp, 58.1317°N, 136.3333°W, 126–146 m depth, 18 July 1982; UW 43484, 17(202.8–315 mm), Cross Sound, Chichagof I., Soapstone Cove, 58.1°N, 136.5°W, 25 m depth, 11 July 1998; UW 43485, 19(124.4–264.7 mm), Lisianski Strait, 57.925°N, 136.288°W, 10 m depth, 12 July 1998; UW 43492, 3(153.7–241.1 mm), Lynn Canal, Funter Bay, 58.2467°N, 134.8983°W, 25 m depth, 13 July 1998; UW 22426, 2(134.8–169.4 mm), Alexander Archipelago, Biorka Channel, S. of Sitka, 33 m depth, 21 February 1982.

Sebastes variabilis Japan: HUMZ 125816, 1(334.0 mm), Pacific coast off Kushiro, Hokkaido, 42.6833°N, 144.7667°E, 200 m depth, 2 March 1993. Bering Sea: KIE 1277, 1(320.3 mm), east coast of Kamchatka off Cape Ol'utorskii, 60.4667°N, 171.75°E, 370 m depth, 18 August 1994; KIE 1409, 2(334.5–344.7 mm), Commander Is., Bering I., 55°N, 166.05°E, 90–120 m depth, 30 April 1996; KIE uncat, 1(324.5 mm), Karaginskiy Bay, 1 August 1998; UW 43500, 1(314.5 mm), 55.3179°N, 167.5503°W, 147 m depth, 3 July 1998; UW 43499, 1(370 mm), 56.7°N, 163.4°W, 77 m depth, 18 June 1998; UW 43498, 3(330–340 mm), 54.4763°N, 159.6925°W, 4 June 1996; UW 40308, 1(180 mm), 55.36°N, 163.44°W, 84 m depth, 7 May 1990; UW 40311, 1(187 mm), 55.55°N, 163.75°W, 84 m depth, 3 May 1990; UW 44166, 1(339.3 mm), Alaska, "2-1-92" at 1800 hours; UW 44182, 2(258.2–266 mm), FV *Yukon Challenger*, haul 105, 8 March 1993; UW 44253, 1(430.8 mm), Aleutian Is., 52.3°N, 173.8–174.7°W, 106–113 m depth, 10 April 1991; UW 44255, 1(375.7 mm), 56.4192°N, 152.853°W, 182 m depth, 24 March 1990; UW 44261, 1(331.1 mm), 57.3333°N, 151.4167°W, 128 m depth; UW

47411, 1(360 mm), Bering Sea, winter 2001, P. J. Sullivan. Aleutian Islands: UW 43480, 1(370 mm), 51.2522°N, 179.199°E, 173 m depth, 20 July 1997; UW 43460, 1(340 mm), Aleutian Is., FV *Dominator*, summer 1997; UW 43438, 5(330–370 mm), 51.9252°N, 176.3817°W, 122 m depth, 23 July 1997; UW 43455 (KU T002038), 1(275 mm), 51.2707°N, 179.2118°E, 98 m depth, 26 July 1997; UW 45499, 2(327–330 mm), 51.9921°N, 174.1031°W, 93 m depth; UW 45632, 3(83.3–126.1 mm), Amchitka I., NE of Sand Beach Cove, 51.5°N, 179°E, 36 m depth, 20 August 1971; UW 45460, 1(98.7 mm), 54.0386°N, 166.6406°W, 85 m depth, 22 May 2000; UW 43441, 2(380–381 mm), 54.17902°N, 166.3255°W, 240 m depth, 12 June 1997; UW 43442, 1(355 mm), 54.0386°N, 166.6572°W, 90 m depth, 13 June 1997; UW 43445, 2(315–340 mm), 54.3773°N, 165.608°W, 90 m depth, 11 June 1997; UW 43459 (KU T002038), 1(264.2 mm), 51.2707°N, 179.2118°E, 98 m depth, 26 July 1997; UW 43461, 1(330 mm), 53.6905°N, 167.2648°W, 112 m depth, 13 June 1997; UW 43416, 1(290 mm), 54.796°N, 163.2772°W, 89 m depth, 1 June 1996; UW 43443, 1(230 mm), 52.8589°N, 172.4586°E, 146 m depth, 5 August 1997; UW 43444, 1(220 mm), 52.8589°N, 172.4586°E, 146 m depth, 5 August 1997; UW 45588, 2(350–350 mm), Aleutian Is., FV *Vesteraalen*, summer 1997; UW 46482, 4(175–225 mm), 52.8280°N, 168.9904°W, 44 m depth, 20 May 2001. Gulf of Alaska: UW 43204, 7(350–420 mm), 55.4327°N, 158.9439°W, 155 m depth, 8 June 1996; UW 43200, 6(320–390 mm), 55.2924°N, 156.6652°W, 114 m depth, 12 June 1996; UW 43214, 1(190 mm), 57.3175°N, 154.8356°W, 82 m depth, 21 June 1996; UW 43212, 1(300 mm), 54.9351°N, 157.4668°W, 153 m depth, 12 June 1996; UW 43201, 8(290–380 mm), 54.1125°N, 161.7306°W, 111 m depth, 1 June 1996; UW 43203, 8(305–405 mm), 54.1125°N, 161.7306°W, 111 m depth, 1 June 1996; UW 43211, 2(380–410 mm), 54.6806°N, 158.9407°W, 95 m depth, 8 June 1996; UW 43213, 1(345 mm), 53.9849°N, 163.2663°W, 108 m depth, 30 May 1996; UW 43416, 1(290 mm), 54.7960°N, 163.2772°W, 89 m depth, 1 June 1996; UW 43417, 1(241.4 mm), 55.2898°N, 158.3123°W, 130 m depth, 10 June 1996; UW 43377, 1(356.4 mm), 55.6441°N, 134.9706°W, 202 m depth, 26 July 1996; UW 45587, 4(325.3–376.2 mm), 55.4351°N, 156.5458°W, 167 m depth, 15 June 1996; UW 44123, 1(85.3 mm), 57.2128°N, 152.7898°W, 135 m depth, 24 October 1997; KU T3178, 1(348.7 mm), 58.8191°N, 140.3303°W, 185 m depth, 14 July 1999; KU T003215, 1(324.3 mm), 58.8191°N, 140.3303°W, 185 m depth, 14 July 1999; KU T003216, 1(373.9 mm), 58.8191°N, 140.3303°W, 185 m depth, 14 July 1999; USNM 32014, 1(240.1 mm), Tolstoi Bay, October 1882; UW 45477, 2(351.5–352.8 mm), 59.1787°N, 149.1194°W, 157 m depth, 29 June 1999; UW 45510, 4(335–370 mm), 58.9658°N, 148.1749°W, 251 m depth, 14 July 1996; UW 45511, 3(206.2–213.4 mm), 57.3806°N, 154.8009°W, 67 m depth, 7 June 1999; UW 46487, 1(333.1 mm), 52.8953°N, 168.297°W, 99 m depth, 21 May 2001; UW 43427, 1(350 mm), 54.2758°N, 161.4326°W, 122 m depth, 3 June 1996; UW 43428, 1(315 mm), 55.9042°N, 157.0751°W, 101 m depth, 18 June 1996; UW 43466, 1(380 mm), 59.4469°N, 140.4849°W, 226 m depth, 30 July 1993; UW 43471, 1(371.7 mm), 58.0895°N, 150.5977°W, 141 m depth, 5 August 1993; UW 43473, 1(342 mm), 59.4469°N, 140.4849°W, 226 m depth, 18 July 1996; UW 22475, 2(240–270 mm), 54.0167°N, 160.8°W, 170 m depth, 4 November 1981; UW 40912, 1(213.6 mm), Prince William Sound, 60.5658°N, 147.5866°W, 70 m depth, 2 October 1989; UW 43214, 1(187.9 mm), 57.3175°N, 154.8356°W, 82 m depth, 21 June 1996; UW 43251, 8(320–420 mm), 59.5045°N, 145.2262°W, 135 m depth, 17 July 1996. Kodiak Island area: ABL 66-890, 1(103 mm), Marmot Bay, Kodiak I., 57.9333°N, 152.1167°W, 1964; UW 44052, 1(215.5 mm), Kodiak; UW 44032, 1(93.4 mm), Cook Inlet, Kachemak Bay, 59.6°N, 151.3°W, "<50 m" depth, 8 September 1981; UW 44033, 2(95.7–112 mm), Cook Inlet, Kachemak Bay, 59.6°N, 151.3°W, "<50 m" depth, 10 October 1981; UW 47148, 5(95.5–112 mm), Cook Inlet, Kachemak Bay, 59.6°N, 151.3°W, 10 October 1981; UW 44034, 1(363 mm), NE of Kodiak I., Triplets Is., 57.98°N, 152.48°W, 20–24 m depth, 1 July 1982; UW 44037, 1(335 mm), E of Kodiak I., 57.72–57.87°N, 151.8–152.2°W, crab pot, 18 August 1982; UW 44038, 2(275.3–310 mm), 57.975°N, 151.8433°W, 144 m depth, 19 August 1982; UW 44039, 3(266.7–300.4 mm), Kodiak I., Monashka Bay, 57.8367°N, 152.4°W, 15 m depth, 31 August 1982; UW 44040, 5(269.7–303.7 mm), Kodiak I., Monashka Bay, 57.8367°N, 152.4°W, 20 m depth, 14 October 1982; UW 44041, 1(281.1 mm), NE of Kodiak I., Triplets Is., 57.98°N, 152.48°W, 20 m depth, 2 July 1983; UW 43381, 1(340 mm), Triplets Is., hook and line, 57.98°N, 152.48°W, 34 m depth, 15 July 1993; UW 44042, 2(199.5–215.8 mm), Shelikof Strait off mouth of Uyak Bay, 57.7°N, 153.92°W, 100 m depth, 2 April 1984; UW 44043, 12(231.3–271.3 mm), Shelikof Strait; UW 44044, 2(229.6–257.8 mm), Kodiak I., Monashka Bay, jig, 57.8367°N, 152.4°W, 15 m depth, 12 August 1982; UW 44046, 1(302 mm), E of Kodiak I., 58.5217°N, 151.3333°W, 154 m depth, 21 August 1982; UW 44047, 1(321.7 mm), E of Kodiak I., 58.85°N, 151.8167°W, 113 m depth, 21 August 1982; UW 44048, 1(318.3 mm), Kodiak I., Monashka Bay, 57.8367°N, 152.4°W, 18 m depth, 11 September 1982; UW 46486, 1(278.5 mm), 56.6941°N, 151.9115°W, 59 m depth, 27 June 2001; UW 47362, 3(122–219 mm), 56.3686°N, 154.0495°W, 69 m depth, 24 June 2001. Southeast Alaska: UW 43495, 1(262 mm), Lynn Canal, N of Funter Bay, 58.03°N, 134.8967°W, 40 m depth, 13 July 1998; ABL 66-156, 1(269.4 mm), Barlow Cove, 19 mi NW of Juneau, 58.3197°N, 134.8967°W, 12 February 1967; ABL 68-301, 1(249.8 mm), Lynn Canal, off reef at N end of Little I., ca. 9 mi N of Pt. Retreat, 58.5417°N, 135.0433°W, 3 August 1968; ABL 69-116, 2(77.7–136.3 mm), Chichagof I., Ogden Passage between Khaz Bay and Portlock Harbor, 57.6333°N, 136.1617°W, 10 September 1969; ABL 69-122, 2(82–82.1 mm), Chichagof I., Icy Strait off SE end of Pleasant I., 58.3333°N, 135.6333°W; ABL 70-103, 1(173.2 mm), Gastineau Channel, Marmion I., ca. 9 mi. S of Juneau, 58.2°N, 134.2533°W, 10 July 1970; UW 43494, 11(150.7–225.2 mm), Lynn Canal, Funter Bay, 58.2467°N, 134.8988°W, 37 m depth, 13 July 1998; UW 44117, 26(153.8–272.7 mm), Funter Bay, 58.2467°N, 134.8983°N, 40 m depth, 13 July 1998; UW 44118, 5(151.9–190.0 mm),

Funter Bay, 58.2467°N, 134.8983°W, 40 m in depth, 13 July 1998; UW 46526, 12(48.0–93.5 mm), Sitka Sound, Middle I., 57.1°N, 135.45°W, 4 June 2001; UW 48866, 3(78.1–156.7 mm), Alexander Archipelago, Biorka Channel, S of Sitka, 33 m depth, 21 February 1982. British Columbia: BCPM 974-0623-001, 5(342–367 mm), Hecate Strait, Moresby Gully, RV *G. B. Reed*, 52.31°N, 130.4867°W, 185–199 m depth, 14 September 1974; BCPM 974-416, 1(154.7 mm), Dundas I., Brundige Inlet, reef at entrance to E arm, 1–5 m depth; BCPM 974-419, 1(124.8 mm), Dundas Is., Brundige Inlet, just N of island at entrance to E arm, 54.6043°N, 130.8612°W, 6–15 m depth, 19 June 1974; BCPM 974-434, 2(108.3–113.8 mm), mouth of Brundige Inlet E shore, 8–12 m depth; BCPM 974-447, 2(168.9–175.6 mm), Welcome Harbour channel, 54.0225°N, 130.6133°W, 6–12 m depth, 2 July 1974; BCPM 974-467, 2(127.9–162.1 mm), off Parkin Islets (E side), 54.6261°N, 130.4639°W, 6–8 m depth, 12 July 1974; BCPM 974-468, 1(120 mm), off N tip of Birnie Is., 54.6045°N, 130.4508°W, 6–12 m depth, 13 July 1974; BCPM 974-485, 1(129.9 mm), off island in Griffith Harbor, 53.6011°N, 130.5486°W, 5–8 m depth, 20 July 1974; BCPM 974-489, 2(145.8–151.5 mm), Safa Islets, 54.7733°N, 130.6067°W, 6–18 m depth, 28 July 1974. Oregon: UW 46575, 1(355 mm), 44.4°N, 124.783°W, 265 m depth, 17 May 2002.

Significant comparative material examined

Sebastes melanops USNM 342, syntypes, Cape Flattery, Washington, and Astoria, Oregon; UW 47037, 1(350 mm), Bering Sea, 55.2333°N, 164.65°W, 2 February 2002; UW 43490, 3(195–230 mm), Cross Sound, Chichagof I., Soapstone Cove, 58.1°N, 136.5°W, 25 m depth, 11 July 1998; UW 47288, 2(163–182 mm), Kodiak I., Monashka Bay, 5 m depth, 57.8383°N, 152.4283°W, 5 m depth, 2 August 1982.

Sebastes mystinus USNM 27031, syntype, 1(346 mm), Monterey, California; USNM 27085, syntype, 1(269 mm), Monterey, California; USNM 26971, syntype, 1(212 mm), Monterey, California.

Sebastes polyspinis USNM 60243, 2(75.3–141.3 mm), Alaska, Chignik Bay, 13.6 km S of Tuliumnit Point, 56°N, RV *Alabatross*, Sta. 4285, 57–108 m depth, 10 August 1903.

Recruitment as an evolving random process of aggregation and mortality

Joseph E. Powers

Southeast Fisheries Science Center
National Marine Fisheries Service, NOAA
75 Virginia Beach Drive
Miami, FL 33149

E-mail address: joseph.powers@noaa.gov

Abstract—The dynamics of the survival of recruiting fish are analyzed as evolving random processes of aggregation and mortality. The analyses draw on recent advances in the physics of complex networks and, in particular, the scale-free degree distribution arising from growing random networks with preferential attachment of links to nodes. In this study simulations were conducted in which recruiting fish 1) were subjected to mortality by using alternative mortality encounter models and 2) aggregated according to random encounters (two schools randomly encountering one another join into a single school) or preferential attachment (the probability of a successful aggregation of two schools is proportional to the school sizes). The simulations started from either a "disaggregated" (all schools comprised a single fish) or an aggregated initial condition. Results showed the transition of the school-size distribution with preferential attachment evolving toward a scale-free school size distribution, whereas random attachment evolved toward an exponential distribution. Preferential attachment strategies performed better than random attachment strategies in terms of recruitment survival at time when mortality encounters were weighted toward schools rather than to individual fish. Mathematical models were developed whose solutions (either analytic or numerical) mimicked the simulation results. The resulting models included both Beverton-Holt and Ricker-like recruitment, which predict recruitment as a function of initial mean school size as well as initial stock size. Results suggest that school-size distributions during recruitment may provide information on recruitment processes. The models also provide a template for expanding both theoretical and empirical recruitment research.

Manuscript approved for publication
10 December 2003 by Scientific Editor.

Manuscript received 20 January 2004
at NMFS Scientific Publications Office.

Fish. Bull. 102:349–365 (2004).

The study of recruitment processes has traditionally addressed mortality (predation and starvation) and the effects of patchiness on mortality (Vlymen, 1977; Beyer and Laurence, 1980; Hunter, 1984; Rothschild, 1986); hence the importance of aggregation and mortality in recruitment processes of marine fish populations has long been noted. Ecological processes of starvation, growth, and predation of larval fish, coupled with oceanographic factors show the inherent variability in these processes (Koslow, 1992; Mertz and Myers, 1994, 1995; Pepin, 1991; Rickman et al., 2000; Comyns et al., 2003). In particular Rickman et al. (2000) have indicated the importance of the magnitude of fecundity in the variability of egg and larval mortality. Indeed, Koslow (1992) argued that fecundity and the associated variability in egg and larval mortality will limit our ability to determine stock-recruitment relationships.

Stock-recruitment models have generally emphasized the static results of recruitment processes rather than the dynamics themselves. Indeed, although the classic stock-recruitment models such as the Beverton-Holt and Ricker have been related to microscale processes (Beverton and Holt, 1957; Ricker, 1958; Paulik, 1973; Harris, 1975), the dynamics at those scales were not explored, primarily because there was not a theoretical basis for doing so (Rothschild, 1986). Nevertheless, there is a need to develop a theoretical understanding of small-scale interaction processes during recruitment, particularly as they relate to group formation.

Group-formation (aggregation of fish into schools), schooling (shoaling) behavior, and the evolutionary motivations for formation of schools continue to be important research topics (Pitcher and Parrish, 1993; Landa, 1998). Schooling behavior has variously been attributed to predator-avoidance, predator-attack dilution, and hydrodynamic and foraging advantages (see Pitcher and Parrish, 1993, for a review). One of the first models for school formation was that of Anderson (1981) in which he empirically observed skewed distributions in which small schools were more prevalent than larger ones. Subsequently, Bonabeau and Dagorn (1995), Gueron and Levin (1995), Niwa (1998), and Bonabeau et al. (1999), developed group-size distribution models. In particular, Bonabeau et al. (1999) in comparing group-size distributions of tunas, sardinella, and buffalo suggested that power-law distributions may be quite generic. Niwa (1998) noted that Anderson's original model allowed for power-law distributions. Power-laws are termed scale-free because they exhibit no intrinsic scale. Similarly, existence of a power-law is often referred to as "scaling."

Recently, power-law distributions have arisen in studies of the physics of small-world and evolving networks (for example the world wide web, actor collaborations, scientific citations [Barabási and Albert,1999], biological cellular networks [Fell and Wagner, 2000], and ecosystem structure [Solé and Montoya, 2001]). In particular, Barabási and Albert (1999) demonstrated that a randomly evolving network would result in a scale-free degree distribution if the network is growing

(the number of nodes is increasing) and if the new nodes were linked to existing nodes by preferential attachment. Preferential attachment (or the "rich-get-richer" phenomenon) occurs when a new node is linked to an existing node with a probability proportional to the number of links already attached to that node. More formally, the Barabasi and Albert model is created by adding a new node at each time step and by randomly linking it to m existing nodes proportional to the number of links at the existing nodes. After a large number of time steps, the probability of a node having k links (the degree distribution) scales as a power-law $P(k) \sim k^{-\gamma}$, where $\gamma = 3$, independent of m. The Barabási and Albert result differs from the classic random network model of Erdös and Rényi (1960) in which nodes are linked randomly to existing nodes, leading to $P(k) \sim exp(-\lambda k)$. Subsequent research has expanded on the Barabási and Albert model to examine aging, removal and rewiring of nodes, removal of links, fitness and attractiveness of nodes, and local modifications to preferential attachment (see Albert and Barabási, 2002, for a review of these developments)

The generic occurrence of scale-free school-size distributions suggest that modeling of aggregation and mortality processes using the analogy of random networks may be fruitful. The approach may provide insight into recruitment dynamics and a theoretical basis for further investigation. This study attempts to do that and is organized in the following manner. First, a simulation model of the recruitment process is developed in which aggregation and mortality occur based upon some simple rules of preferential attachment and random attachment. Attachment rules are presented as metaphors for more complex behaviors. Next, analytical models are created that mimic the simulations, and results of the simulations and analytical models are compared. Finally, the implications for existing stock-recruitment models and investigation of recruitment processes are discussed.

Methods

Simulation of individuals in ecology and population dynamics (individual-based models) have become increasingly popular (McCauley et al., 1993). However, it is often difficult to understand the dynamics of large individually based models (Pascual and Levin, 1999). Thus, it is important to obtain models that describe dynamics of groups that incorporate individual behavior (Flierl et al., 1999). The models that are developed here include an individually based model (simulation model) and an analytical model that describes "mean-field" dynamics of the individuals behavior.

Simulation model

The recruiting fish of a year class may be modeled as a network of fish in which a fish "links" to other fish to form schools. (Note that in this context it is assumed that a "school" includes aggregations consisting of a single fish). Thus, the process of aggregation is a process of adding links to nodes (aggregation of schools). Similarly, mortality is the removal of nodes (fish) and, if there are no more fish in the school, then the removal of schools. A simulation model with simple rules of mortality and aggregation was created to examine the dynamics of these processes.

The simulation model followed individual fish and schools through a recruitment period, i.e., the passage of time until an arbitrary time of recruitment. During a recruitment period fish and schools undergo encounters of mortality and aggregation. Starting at time $t=0$ with S fish, $N_{t=0}$ schools and $k_{i,t=0}$ fish in school i (i=1,2, … , N_0), simulations were conducted by randomly generating an encounter event (mortality or aggregation). If the event was a mortality, then a school was randomly selected by using the appropriate mortality rate model (m, discussed below). If the size of that school was greater than one, then that size was reduced by one. If the school size was equal to one, then the number of schools was reduced by one and this school was eliminated from the list.

If the event was an aggregation, then two distinct schools were randomly selected by using the appropriate aggregation rate model (w, also discussed below). The two schools were combined, leaving one school whose size was the sum of the two original ones and one fewer total number of schools. The probability of an event being a mortality was $m/(m+w)$ and the converse probability of an aggregation was $1-m/(m+w)$. Time increments of each event were computed using $\Delta t = m^{-1}$ for mortality events and $(mw)^{-1}$ for aggregation events. Results at time t were collated into the number of fish surviving to time t (denoted by R_t), the number of schools, N_t, the school size distribution, $P_t(k)$, and the average school size, $\bar{k}_t$. Note that $R_t = N_t \bar{k}_t$. Simulations were run until there were no fish left.

Encounter rates The encounter rates, m and w, were based upon random movements in statistical mechanics (Tolman, 1979) in which the encounter rate (U) of objects of type i with objects of type j is described by

$$U = (G_i + G_j)\, D_i D_j\, (v_i^3 + v_j^3)^{1/3}, \quad (1)$$

where G_i = the size of the detection space at which object detects object type j;
D_i = the density of objects of type i; and
v_i = the velocity (in three-dimensional space) at which object i moves in the environment.

For these simulations the G parameters were scaled to one and the velocity parameters (v's) were collapsed into two encounter rates: μ for mortality encounters (scaled to unity) and α for aggregation encounters.

Mortality rate In the simulations, mortality of fish is perpetrated by mortality agents. If the mortality agents randomly encounter schools of fish, then the probability of a successful mortality (the removal of a fish from the system) is proportional to the school size k. Under these conditions Equation 1 reduces to Equation 2 with

$$\begin{aligned} G_i = G_j = 1, & (v_i^3 + v_j^3)^{\frac{1}{3}} = \mu: \\ m = 2\mu E N k, & \end{aligned} \quad (2)$$

where E = the density of mortality agents; and
μ = the encounter rate of fish with mortality agents.

Note that on average Equation 2 reduces to $m = 2\mu E_t N_t \bar{k}_t = 2\mu E_t R_t = -dR/dt$. Hence, if the density of mortality agents is constant throughout the recruitment period, then mortality is density independent and mortality is proportional to abundance. An alternative interpretation of Equation 2 is that the mortality agents randomly encounter fish and that all encounters result in a successful mortality. The mortality model (Eq. 2) will be referred to as m_{di} (for density-independent). It is not expected that m_{di} is the most realistic, but rather it provides a basis for comparison.

A second mortality alternative is where mortality agents randomly encounter schools, whereupon they always perpetrate a successful mortality: $m_N = 2\mu E_t N_t$. This model, like m_{di}, assumes that the density of mortality agents are constant throughout the recruitment period.

For purposes of simulation, the density of mortality agents at the onset of the recruitment process was specified to be unity (E_0=1). For the two mortality models, m_{di} and m_N, this meant that E=1 throughout a simulation.

More realistic density-dependent mortality models are immediately suggested. The first is a density-dependent model in which the ratio of mortality-agent density to the number of schools remains constant throughout the recruitment period, i.e., E_t/N_t remains constant throughout the recruitment period. This leads to $m_{dN} = 2\mu N^2 k$, where E_t/N_t was set equal to one. In this model the ratio of mortality agents to schools is constant, agents and schools randomly encounter one another, and the probability of a successful mortality (given there is an encounter) is proportional to the number of fish that are in the school that is encountered (mortality success is related *preferentially* toward larger schools).

A second density-dependent model is where the mortality agent density is proportional to the number of fish (E_t/R_t is a constant set equal to one, $m_{dR}=2\mu R^2=2\mu N^2 k^2$). In this model the ratio of mortality agents to the number of fish in the population is constant; agents and schools randomly encounter one another; and the probability of a successful mortality (given there is an encounter) is proportional to the number of fish that are in the school that is encountered (mortality success related preferentially toward larger schools). Another interpretation of this model is that agents randomly encounter fish, at which time the fish suffers mortality at a probability independent of school-size characteristics.

A third density-dependent model depicts mortality-agent density proportional to school size (E_t/k_t is a constant set equal to one, $m_{dk}=2\mu Nk^2$). In this model the ratio of mortality agents to mean school size is constant, agents and schools randomly encounter one another, and the probability of a successful mortality (given that there is an encounter) is proportional to the number of fish that are in the school that is encountered. Another interpretation of this model is that agent density is proportional to the number of schools, agents encounter schools preferentially according to school size, and the probability of a successful mortality (given that there is an encounter) is proportional to the number of fish that are in the school that is encountered.

Subsequently it will be shown that the first density-dependent model is related to a Ricker-like stock-recruitment model and the second model is exactly equivalent to a Beverton-Holt model. Definitions of the mortality models are summarized in Table 1. Note that in the initial applications of these mortality models, it is assumed that a mortality encounter results in mortality of one fish. More detailed mortality models in which a number of fish greater than one are removed by mortality may be implemented in the future. Clearly, these would be more biologically realistic in many instances. However, the emphasis of this study is on the possible scaling behavior of school-size distributions. Barabasi and Albert (1999) showed that the scaling behavior of a growing random network is independent of the number of randomly selected links at each time step. With this analogy, simple increases in mortality per encounter are not expected to alter the scaling behavior of the school-size distributions. Therefore, the one-fish-per-mortality-encounter approach was used in these initial simulations.

Aggregation rate

Similar to mortality-rate encounters, aggregations were investigated as 1) random attachment of two unique schools ($w_N=2\alpha N(N-1)$) and 2) preferential attachment of two unique schools i and j ($w_{pa}=2\alpha N(N-1)k_i k_j$; [Table 1]). Note, the trivial alternative where there was no attachment, (α=0), results in equivalence between the mortality models m_{dN}, *and* m_{dR}; whereas m_{di} becomes a simple proportional mortality rate. Thus, results of models with α=0 are uninteresting in the context of this study and are not presented.

Initial conditions Each simulation was conducted with one of two alternative initial conditions. The first alternative was one of complete disaggregation in which simulations were initiated with S fish, S schools, and one fish in each school ($N_0=S$, $\bar{k}_0=1$). The second alternative initial condition was constructed from the population dynamics of a typical fish population. The main assertion of this alternative is that the eggs or larval fish produced by one female during spawning constitutes one school at the onset of the recruitment process. Thus, the fecundity per female at age is a measure of initial school size and the abundance of females at age is a measure of the frequency of schools of that size. More precisely, the initial condition was constructed for a population of females greater than five years of age (age of maturity), where their fecundity at age, F_{age}, is proportional to weight at age determined from a von Bertalanffy growth equation with parameters K=0.2 and L_∞=10, and an allometric parameter of 3: ($F_{age}=1000[(1-\exp(-\text{age}(0.2)))]^3$). Abundance at age, A_{age}, was computed with an instantaneous mortality rate of 0.2: [$A_{age}=X\exp(-0.2(\text{age}-5))$]. The scalar X was obtained from the approximate solution to $S=\Sigma F_{age} A_{age}$, where F and A were integer values and S was the initial number of fish

Table 1

Summary of definitons of the mortality models used in this study.

	Model	Definition
Mortality rates[1]:	$m_{di} = 2\mu Nk$	density-independent
	$m_{dN} = 2\mu N^2 k$	density-dependent, mortality agents proportional to N
	$m_{dR} = 2\mu N^2 k\bar{k}$	density-dependent, mortality agents proportional to R
	$m_{dk} = 2\mu Nk\bar{k}$	density-dependent, mortality agents proportional to k
	$m_N = 2\mu N$	random encounters with schools
Aggregation rates:	$w_N = 2\alpha N(N-1)$	random encounters with schools
	$w_{pa} = 2\alpha N(N-1)k_i k_j$	preferential attachment of schools i and j
Initial conditions:	Disaggregated	$N_0 = S, \bar{k}_0 = 1$
	Aggregated	(see text and Table 2)

Mean field equivalents used in analytical model (see text):

$m_{di} = 2\mu N\bar{k}$ $m_{dN} = 2\mu N\bar{k}^2$ $m_{dR} = 2\mu N^2\bar{k}^2$

$m_{dk} = 2\mu N\bar{k}^2$ $w_{pa} = 2N(N-1)\bar{k}^2$

Key to figures of simulation results:

Figure 1: *disaggregated*	m_{di}	w_{pa}	$\alpha = 10^{-6}$	$S = 10^6$
Figure 2: *disaggregated*	m_{di}	w_N	$\alpha = 10^{-6}$	$S = 10^6$
Figure 3: *aggregated*	m_{di}	w_{pa}	$\alpha = 10^{-6}$	$S = 10^6$
Figure 4: *aggregated*	m_{dN}	w_{pa}	$\alpha = 1.5\times10^{-6}$	$S = 2\times10^6$
Figure 5: *aggregated*	m_{dN}	w_N	$\alpha = 1.5\times10^{-6}$	$S = 2\times10^6$

[1] In all simulations, μ was set equal to 1.

Table 2

The aggregated initial school-size distribution, when S = 1,000,000. Per capita female fecundity at age is a measure of school size, number of females at age is a measure of frequency of schools. See text for details of computation.

School size	Freq. of schools	Freq. × size	School size	Freq. of schools	Freq. × size
252	348	87,696	857	47	40,279
341	284	96,844	882	38	33,516
427	233	99,491	903	31	27,993
508	190	96,520	920	25	23,000
581	156	90,636	934	21	19,614
596	1	596	946	17	16,082
646	128	82,688	955	14	13,370
703	104	73,112	963	11	10,593
751	85	63,835	970	9	8730
793	70	55,510	975	7	6825
828	57	47,196	979	6	5874

Sum of freq. × size = S = 1,000,000.

of a simulation. Then one school of an appropriate magnitude, M, was added such that the $M + \Sigma F_{age} A_{age}$ was exactly equal to S. Note that under this construction the school sizes in the distribution do not vary with S (except for the one school of size M), whereas the frequency of schools by size do. An example of the initial distribution with the use of this construction is given in Table 2.

Analytical models

Analytical models of aggregation and recruitment are presented, where the models are developed from first principles and the parameters have an interpretation in the physics and biology of the recruitment process. Hopefully, the nature of the parameters can guide model selection,

and the estimates may provide a theoretical framework for empirical research on recruitment processes.

Noting that $R_t=N_t\bar{k}_t$, the recruitment dynamics depicted in the simulations may be modeled by using Equations 3–6 in which recruitment is dependent on the particular mortality and aggregation models that are chosen (m and w; Table 1):

$$dR_t/ = -m = d(N_t\bar{k}_t"/dt = (d\bar{k}_t/dt"N_t + (dN_t/dt"\bar{k}_t \quad (3)$$

$$dN_t/dt = -w - m_1P_{1,t} \quad (4)$$

$$\begin{aligned} d\bar{k}_t/dt &= m_1P_{1,t}\left[(\bar{k}_t-1)/(N_t-1)\right] \\ &-(m-m_1P_{1,t})/N_t + w\bar{k}_t/(N_{t-1}) \end{aligned} \quad (5)$$

$$\begin{aligned} dP_{k,t}/dt &= (m_{k+1}P_{k+1,t} - m_kP_{k,t})/N_t - w_kP_{k,t}/N_t \qquad k>1 \\ &+w\sum_{i=1}^{k-1}P_iP_{k-i}/N_t \\ &= m_2P_{2,t}/N_t - m_1P_{1,t}(1-P_{1,t})/(N_t-1) \qquad k=1 \\ &-w_1P_{1,t}/N_t\ , \end{aligned} \quad (6)$$

where $P_{k,t}$ = the proportion of schools with k fish in them at time t.

Also, m_k and w_k denote encounter rates appropriate to schools of size k, whereas unsubscripted m and w denote mean field dynamics and, thus, the $k_{i,t}$'s are replaced by $\bar{k}_t$'s (see Table 1).

The first term in Equation 4 denotes the reduction in number of schools due to aggregation events; the second term denotes a reduction due to mortality events on schools with one fish in them. Similarly, the first term in the mean school-size equation (Eq. 5) describes the change in mean school size due to mortality events on schools of size equal to one; the second term is due to mortality events on schools of size greater than one; and the third term is due to aggregation events. Finally, the first term in Equation 6 describes the change in probability of school size k due to mortality; the second term describes loss due to aggregation; and the third describes gain due to aggregation. Of particular importance is $P_{1,t}$: when $P_{1,t}$ is zero, the loss of schools occurs only due to aggregation. When $P_{1,t}$ is positive, then loss of schools is accelerated due to mortality (Eq. 4).

The goal is to obtain solutions to Equations 3–6 as functions of α, μ, and the initial conditions. If one can be assured that there will not be a school composed of one fish during a particular recruitment period ($P_{1,t}=0$), then Equation 6 is eliminated, the $P_{1,t}$ terms drop out of Equations 4 and 5, and a numerical or analytical solution to the differential equations can be obtained, which is computationally feasible for use in fitting to stock-recruitment data. For example, when there is preferential aggregation (w_{pa}) and mortality agents are proportional to schools (m_{dN}), the equations reduce to

$$dN_t/dt = -w_{pa} = -2\alpha N_t(N_t-1)\bar{k}_t^2$$

$$d\bar{k}_t/dt = -m_{dN}/N_t + w_{pa}\bar{k}_t(N_1-1) = -2\mu N_t\bar{k}_t + 2\alpha N_t\bar{k}_t^3.$$

Analytical solutions were obtained for some of the mortality and aggregation models when $P_{1,t}=0$ throughout the recruitment process (Appendix 1). In particular for m_{dR} and w_{pa}:

$$R_t = S/(1+2\mu tS) \quad (7)$$

$$N_t = N_0 + (\alpha/\mu"\left[S - S/(\%+ 2\mu tS"\right] \quad (8)$$

$$\bar{k}_t = \bar{k}_0/[1+2\mu tS+2\alpha tS\bar{k}_0], \quad (9)$$

which is the Beverton-Holt stock-recruitment model expanded to include equations for the number of schools and the mean school size. Interestingly, Equation 9 indicates that monitoring the school-size distribution two or more times during a recruitment procession would yield estimates of the stock-recruitment parameters without having direct measures of the number of surviving fish. Equation 7 predicts recruitment by using one parameter, μ_t, the rate of mortality encounters during the recruitment period. However, spawning stock biomass is often used as a surrogate for the number of initial stock, S. Thus, another parameter is needed to convert spawning stock biomass to S in Equation 7. In that case the recruitment model becomes $R_t = aS/(1+2\mu taS)$, where a is another parameter related to fecundity. The additional parameter will be needed for all the models discussed here, if spawning stock biomass is the measure of initial stock.

The assumption that $P_{1,t}=0$ for all t of a recruitment period may not be justified in all situations. An approximation was developed (Appendix 2) to be applied when the initial conditions are disaggregated and when there is preferential attachment. In this circumstance, the differential equation (Eq. 6) when k=1 is replaced by

$$dP_{1,t}/dt = -wP_{1,t}/N_t + m(1-P_{1,t})/N_t. \quad (10)$$

Results

Simulations

Several hundred simulations were conducted under various initial stock sizes (S), aggregation parameters (α), initial aggregation conditions, and mortality and aggregation models (m and w). An example set of results are presented in Figures 1–5 (a key to figures is in Table 1).

A typical example of the evolution of the school-size distribution is given in Figure 1 for the disaggregated initial condition, $\alpha=10^{-6}$, $S=10^6$, mortality model m_{di} and aggregation model w_{pa}. In this example both the mortality and aggregation models exhibit preferential attachment, and the school-size distribution approaches scale-free behavior $P(k)\sim k^{-\gamma}$, although γ evolves over time. Eventually, a so-called "giant cluster" is formed by the aggregation process, in which all the fish attach to one school. This has

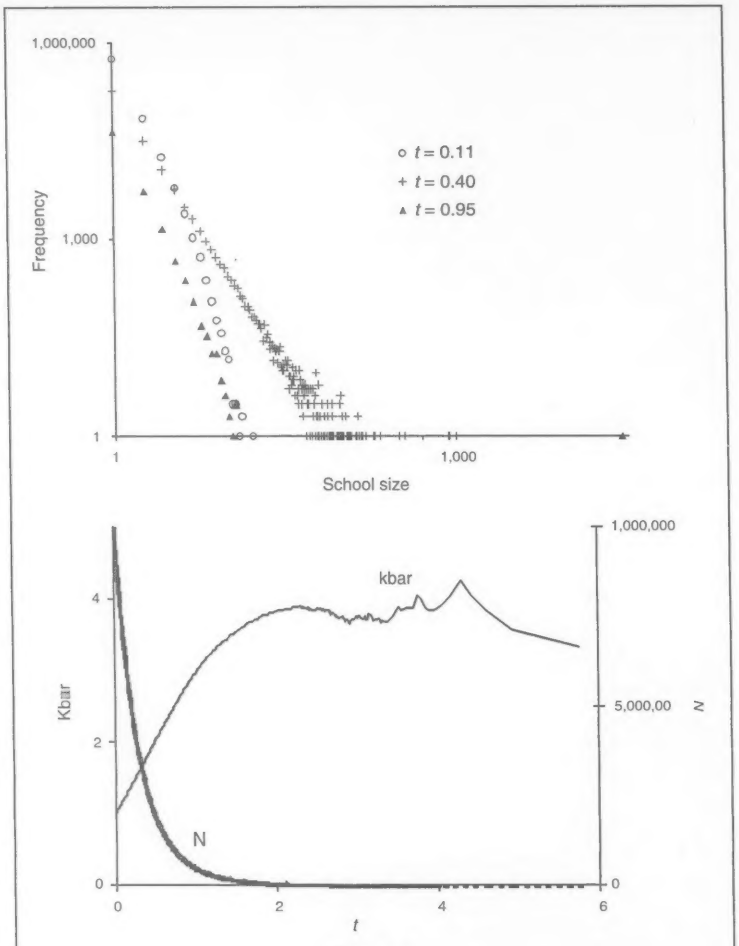

Figure 1

Simulated dynamics of school-size distributions with m_{di} as the mortality model and w_{po} as the aggregation model. This simulation started with disaggregated initial conditions (N_0=S), where S=10^6. The aggregation parameter was α=10^{-6}. The top panel shows school-size distributions (in log-log scale) at selected times (t). The lower panel gives the mean school size (*kbar*) and school abundance (N) versus time.

been shown to be an analog of Bose-Einstein condensation (Bianconi and Barabási, 2001; Dorogovtsev and Mendes, 2002) and gelation (Krapivsky et al., 2000). Greater mixing rates (α's) and larger densities (N's) accelerate the aggregation process and the formation of the giant cluster. The average size, $\bar{k}$, increases over time from the disaggregated initial condition until a giant cluster is formed. The number of schools declines over time because of both aggregation and the mortality of fish in schools that only have one fish in them.

When there is random aggregation beginning from a disaggregated initial condition (α=10^{-6}, S=10^6, m_{di}, w_N; Fig. 2), the school-size distribution exhibits exponential behavior $P(k)$~exp($-\lambda k$), with λ evolving over time. This is equivalent to the Erdös and Rényi (1960) results for random graphs. A comparison of Figure 2 with Figure 1 shows the difference between preferential attachment and random attachment, i.e., the difference between scale-free and exponential models.

Aggregated initial conditions (Figs. 3–5) result in a transition from the initial distribution to either scale-free or exponential distribution. During the transition, the size of the smallest school gradually becomes smaller until there is a finite probability of schools with one fish in

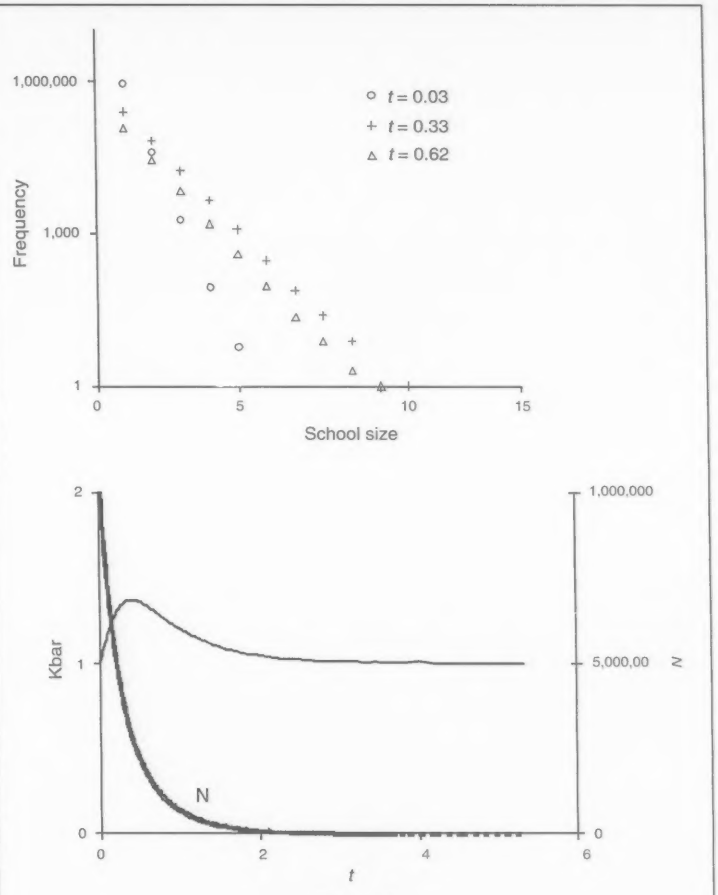

Figure 2

Simulated dynamics of school-size distributions with m_{di} as the mortality model and w_N as the aggregation model. This simulation started with disaggregated initial conditions (N_0=S), where S=10^6. The aggregation parameter was α=10^{-6}. The top panel shows school-size distributions (frequency in log) at selected times (t). The lower panel gives the mean school size ($kbar$) and school abundance (N) versus time.

them. At this point the reduction in the number of schools is accelerated because of the mortality of fish that are in "schools" in which they are the only member, and because of the loss of schools attributed to aggregation.

Model comparisons

Numerical integration of Equations 3–5 matched the simulation results (Fig. 6, when $P_{1,t}$=0), indicating that the mathematical model describes the simulation dynamics. The numerical techniques are sufficiently efficient to be used in a curve-fitting context. Evaluations of the approximation (Appendix 2) indicate that the approximation may be useful for predictions of recruitment, when compared with the simulations. However, the components of recruitment, $\overline{k}_t$ and N_t, were biased (Fig. 7). Further research is needed to develop estimates of $P_{1,t}$ and, more generally, $P(k)$ under other models and initial conditions.

Recruitment was compared between mortality models and aggregation models (Fig. 8). If the mortality model was either m_{di} or m_{dR}, then the mortality rate was not affected by the school-size distribution: random attachment and preferential attachment perform equally as well in terms of survival at a given time. But if mortality encounters proportional to school density (m_{dN}) were imposed, then there were better survival rates with preferential attachment than with random attachment (Fig. 8, A and B). Conversely, mortality encounters proportional to school

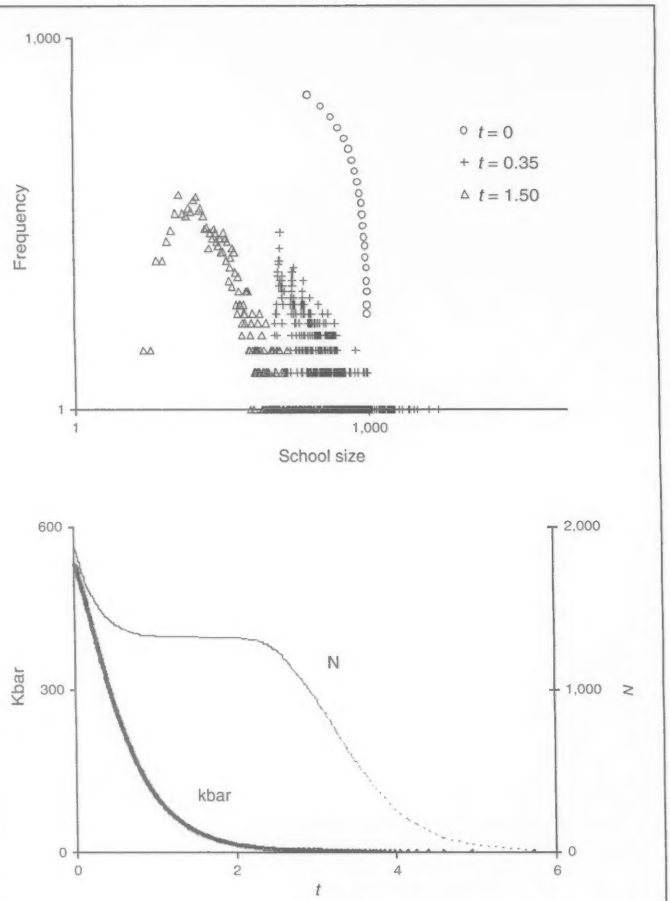

Figure 3

Simulated dynamics of school-size distributions using m_{di} as the mortality model and w_{pa} as the aggregation model. This simulation started with aggregated initial conditions (S=10^6). The aggregation parameter was α=10^{-6}. The top panel shows school-size distributions (in log-log scale) at selected times (t). The lower panel gives the mean school size (*kbar*) and school abundance (N) versus time.

size (m_{dk}) led to poorer survival with preferential attachment (Fig. 8, C and D).

Discussion

Koslow (1992), Rickman et al. (2000), and others have commented on the inherent variability in stock-recruitment data and the limited predictive power of deterministic stock-recruitment models. Therefore, there is no expectation that one could select the models described here over other stock-recruitment models on the basis of fits to data. Although the aggregation-mortality models may be fitted to stock-recruitment data, the real usefulness is as a guide to selection of stock-recruitment models used in management, as a mechanism for integrating research on recruitment processes, and as a tool for exploring the structure of recruitment variability.

The aggregation-mortality models were introduced by using an analogy with evolving random networks (Barabási and Albert, 1999) and were shown to be analytically equivalent (Appendix 2). Modeled fish are subjected to competing forces of organization (aggregation) and decay (mortality), as in a network in which links to nodes in the network are created, destroyed, and rewired (Albert and Barabási, 2002). An important finding of Barabási and

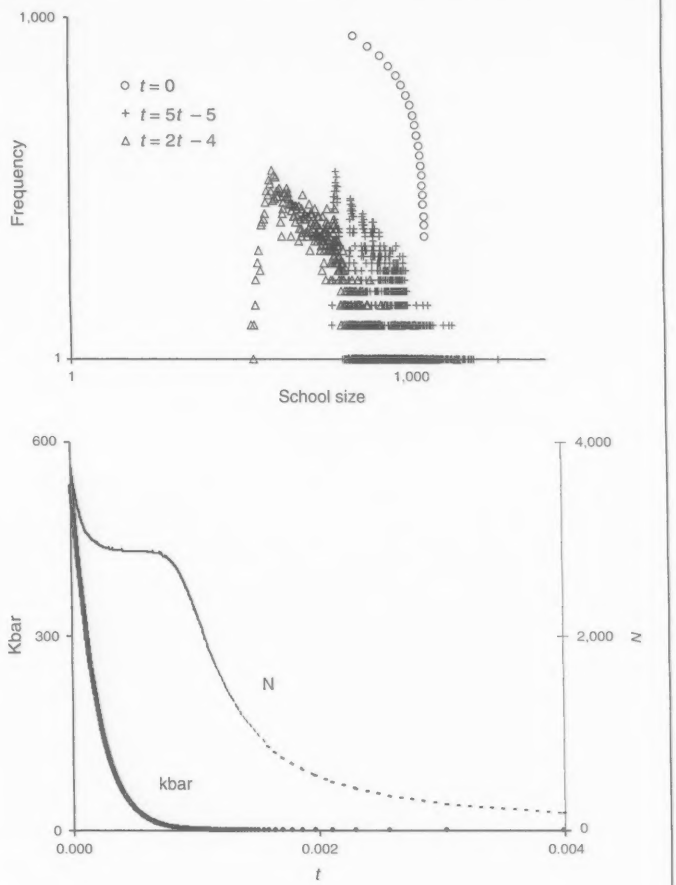

Figure 4

Simulated dynamics of school-size distributions using m_{dN} as the mortality model and w_{pa} as the aggregation model. This simulation started with aggregated initial conditions (S=2×10^6). The aggregation parameter was α=1.5×10^{-6}. The top panel shows school-size distributions (in log-log scale) at selected times (t). The lower panel gives the mean school size (*kbar*) and school abundance (N) versus time.

Albert (1999) was that scaling of the aggregate-size distribution was dependent on the type of aggregation, specifically preferential attachment. Bonabeau and Dagorn noted the generic occurrence of scaling of aggregation distributions in nature (Bonabeau and Dagorn, 1995) and this scaling of aggregation distributions motivated the development of the models presented here.

The emphasis of the aggregation models was on preferential attachment and on comparison of model results with results for models with random attachment strategies. The preferential attachment rule used in the simulations was that aggregation rates were proportional to the size of the school encountered. But, what is meant by preferential attachment and does preferential attachment occur in nature? Clearly, a fish, school or mortality agent has no global knowledge of the proportional size of a school that is encountered. However, preferential attachment in these models is a metaphor for aggregation strategies that are weighted toward larger school sizes. Indeed, studies of networks have shown that attachment may be proportional to a power of school size and still produce scale-free properties (Albert and Barabási, 2002). Also, network studies have shown that scale-free distributions occur when a wide number of attachment criteria are included, such as the "fitness" of the object being encountered and the attractiveness of local conditions (Bianconi and Barabási,

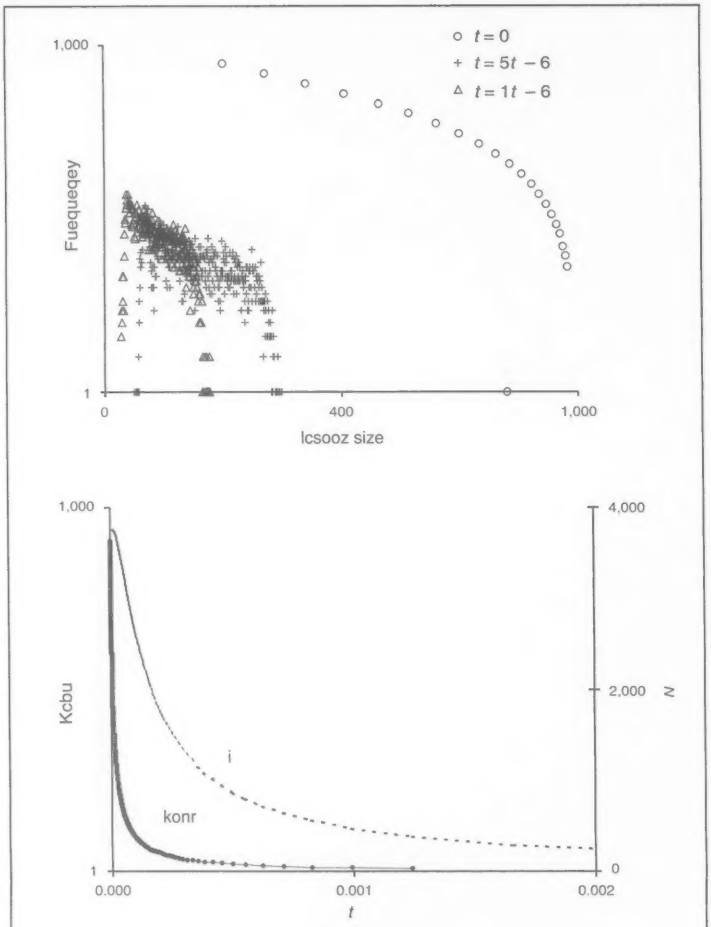

Figure 5

Simulated dynamics of school-size distributions using m_{dN} as the mortality model and w_N as the aggregation model. This simulation started with aggregated initial conditions (S=2×10^6). The aggregation parameter was α=1.5×10^{-6}. The top panel shows school-size distributions (in log-log scale) at selected times (t). The lower panel gives the mean school size (*kbar*) and school abundance (N) versus time.

2001; Calderelli et al., 2002; Vazquez, 2003). Biological concepts of fitness, feeding behavior, predator-avoidance behavior, and habitat suitability appear to fall within the attachment criteria examined in physics literature. Oceanographic stability (Myers and Pepin, 1994), assortative schooling by color patterns (Crook, 1999), chemosensory stimuli (Quinn and Busack, 1985), and larval fitness indices from RNA/DNA ratios (Pepin, 1991; Suneetha et al., 1999) may be mechanisms that directly or indirectly influence aggregation size and, thus, distribution.

The geometry of the school size itself may be sufficient to produce preferential attachment behavior, as well. In the models of this study, the detection spaces (G_i +G_j in Equation 1) were set to unity and assumed to be independent of school size. However, the detection space may be related to school size. For example, if a school of one fish has a spheroid detection space around itself with radius equal to 1, then using the geometry of an aggregation of k fish, the detection space of the aggregate would be proportional to $k^{1/3}$. Alternatively, if the detection space were a two-dimensional circle with a radius of 1, then the aggregate's detection space would be proportional to $k^{1/2}$. Substituting size-dependent detection spaces into the random mortality and aggregation models would be sufficient to induce pref-

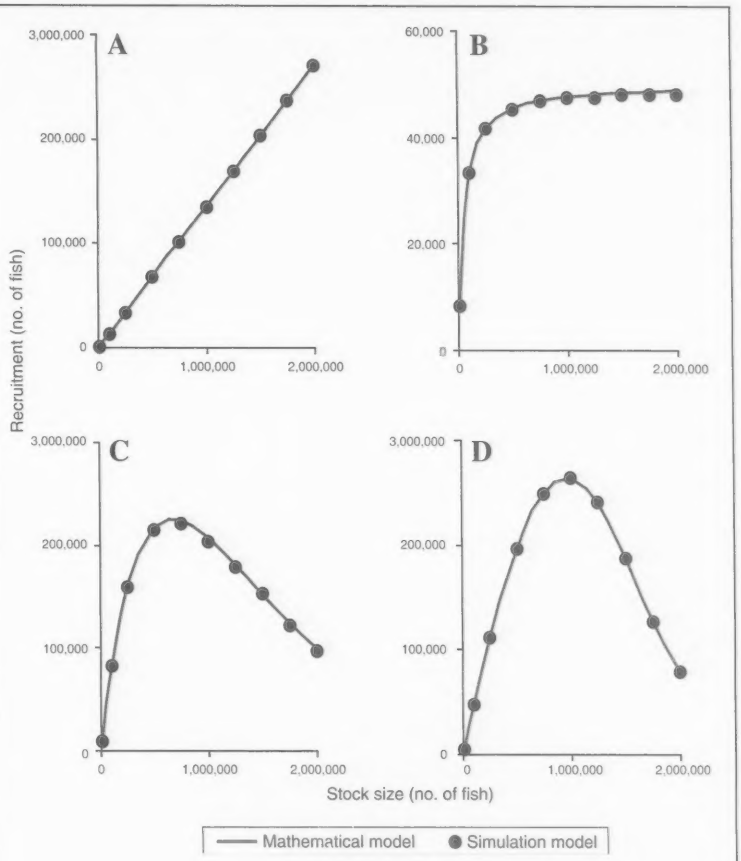

Figure 6

Stock-recruitment relationships from the mathematical models (Eqs. 3–5, aggregated initial conditions) compared with simulation results: (**A**) density-independent mortality (m_{di}) and preferential attachment (w_{pa}) evaluated at t=1, α=10^{-9}, μ=1; (**B**) density-dependent mortality proportional to fish (m_{dR}) and preferential attachment (w_{pa}) evaluated at t=10^{-5}, α=3×10^{-5}, μ=1; (**C**) density-dependent mortality proportional to schools (m_{dN}) and preferential attachment (w_{pa}) evaluated at t=5×10^{-4}, α=1.5×10^{-6}, μ=1; and (**D**) density-dependent mortality proportional to school size (m_{dk}) and preferential attachment (w_{pa}) evaluated at t=10^{-3}, α=2×10^{-6}, μ=1.

erential interaction even when encounters are random: schools are randomly encountered, but the encounter event itself is weighted toward larger schools. Thus, the shape of the detection space may be another mechanism by which preferential attachment may be exhibited.

In the models presented, it is blithely assumed that mortality is caused by undefined mortality agents. However, most larval recruitment research has been directed at starvation and predation as determinants of recruitment variability (Lasker, 1975; Hunter, 1984; Bailey and Houde, 1989; Chambers and Trippel, 1997, for example). The mortality models used here clearly fit within the predation paradigm: mortality from predation results from encounters with mortality agents of specific density and size. Whereas, mortality from starvation ensues from a lack of encounters with prey agents of sufficient density and size. In certain situations starvation processes might be aptly described by the predation-encounter approach used in this study. However, further research is needed to evaluate their appropriateness and to develop alternative modifications to Equations 3–6. A mechanism to do this may be the inclusion of fragmentation of schools into the models. In the models as they are now characterized, new schools are not created, the number of schools only becomes smaller through either aggregation or through mortality on schools of a single fish. Fragmentation might

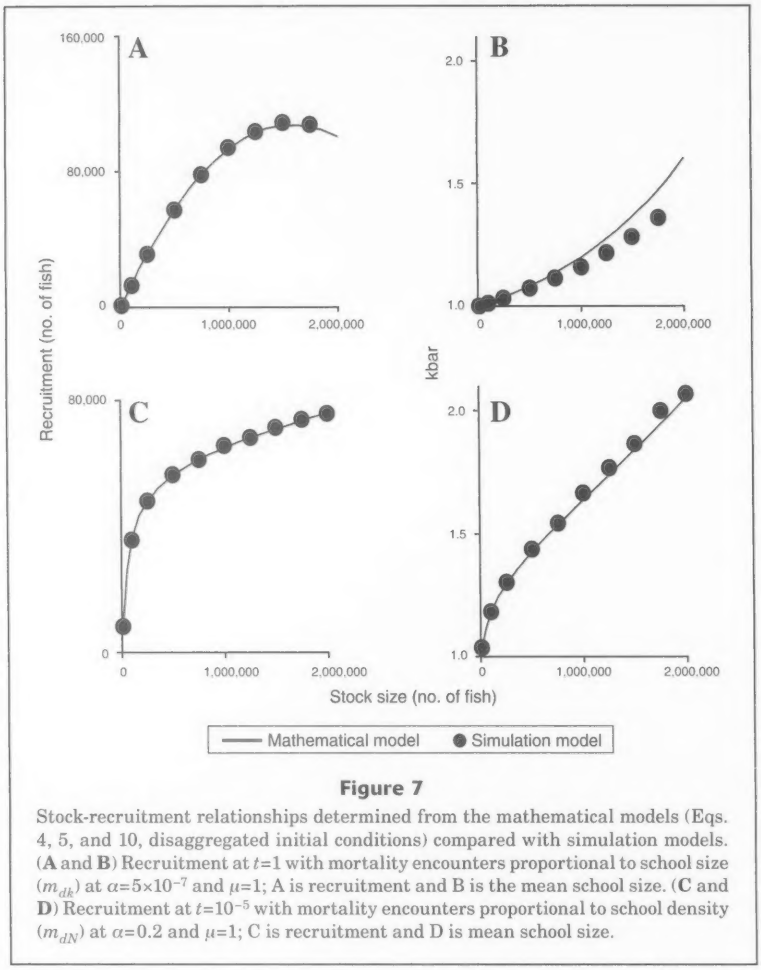

Figure 7

Stock-recruitment relationships determined from the mathematical models (Eqs. 4, 5, and 10, disaggregated initial conditions) compared with simulation models. (**A** and **B**) Recruitment at t=1 with mortality encounters proportional to school size (m_{dk}) at $\alpha=5\times10^{-7}$ and μ=1; A is recruitment and B is the mean school size. (**C** and **D**) Recruitment at $t=10^{-5}$ with mortality encounters proportional to school density (m_{dN}) at α=0.2 and μ=1; C is recruitment and D is mean school size.

occur due to secondary effects of mortality encounters, as well as other factors such as starvation. For example, Sogard and Olla (1997) have shown predation-risk and hunger to be related to group cohesion.

The formation of a giant cluster (a single school encompassing all the fish) is an important feature of the attachment process. The simulations showed that with preferential attachment the recruitment process passes through a phase where the size distribution is scale free, then a critical point is reached where a giant cluster is being formed, i.e. a single school begins to attract all the fish. Research on complex networks has shown the conditions for formation of the giant cluster (Aiello et al., 2000; Albert and Barabasi, 2002). This should be investigated for the school aggregation models because it is likely that the mortality models used in the present study would no longer be appropriate once the giant cluster is formed. Indeed in some fish stocks, schools may aggregate into giant clusters on a local scale and then aggregation may stop for reasons such as juveniles entering a benthic phase. The resulting distribution of school sizes may be the cluster distribution across benthic habitats. Spatial limitations of aggregation are an important feature of individually based models (Pascual and Levin, 1999). Again, this may be an important area for research.

What is the benefit of preferential attachment? If mortality encounters are proportional to school density, then recruitment survival rates are improved when there are fewer schools for a given number of fish, i.e. when preferential attachment is employed rather than random attachment (Fig. 8). Perhaps, preferential attachment strategies are a useful evolutionary hedge against uncertainty in the nature of the mortality dynamics. Conversely, when mortality encounters are proportional to school size, then better survival is achieved when schools are smaller, i.e. with random attachment (Fig. 8). If mortality by predators is related to larger schools, or if attainment of prey is inversely related to larger schools, then more solitary life

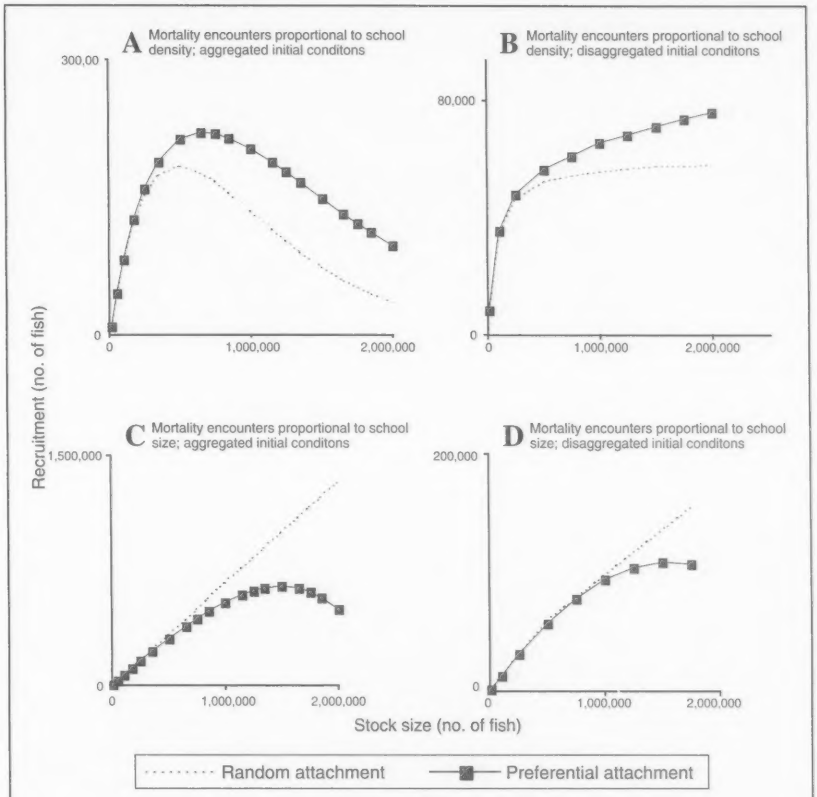
A Mortality encounters proportional to school density; aggregated initial conditons
B Mortality encounters proportional to school density; disaggregated initial conditons
C Mortality encounters proportional to school size; aggregated initial conditons
D Mortality encounters proportional to school size; disaggregated initial conditons
Recruitment (no. of fish)
Stock size (no. of fish)
300,00
80,000
1,500,000
200,000
0
1,000,000
2,000,000
Random attachment
Preferential attachment

Figure 8

Stock-recruitment results with preferential attachment compared with random attachment (w_{pa} versus w_N). (**A**) Recruitment at t=1 with mortality encounters proportional to school density (m_{dN}) at $\alpha=10^{-9}$ and $\mu=5\times10^{-4}$ with an aggregated initial condition; (**B**) recruitment at $t=10^{-5}$ with mortality encounters proportional to school density (m_{dN}) at α=0.2 and μ=1 with a disaggregated initial condition; (**C**) recruitment at t=1 with mortality encounters proportional to school size (m_{dk}) at $\alpha=10^{-9}$ and $\mu=5\times10^{-4)}$ with an aggregated initial condition; (**D**) recruitment at t=1 with mortality encounters proportional to school size (m_{dk}) at $\alpha=5\times10^{-7}$ and μ=1 with a disaggregated initial condition.

history strategies may evolve. Perhaps, the random aggregation model would be most effective for solitary predatory fish when their mortality is imposed by a m_{dk}-type model. For fish, this may be more likely to occur at later life stages than at recruitment. If mortality encounters are proportional to fish (m_{dR}), then results are intermediate and preferential attachment and random attachment perform equally as well.

The density-dependent mortality models implicitly incorporate a predator-prey interaction. Alternative predator-prey interactions examined were those in which predator density was proportional to fish, to schools, or to the number of fish within a school (school size) throughout a recruitment period. In reality mortality is perpetrated by a variety of agents at many different scales. Some agents act at the scale of the population ($N\bar{k}$), some at the scale of schools (N), some at the scale of mean school size ($\bar{k}$), and some at the scale of a local school (k_i). The mixture of predatory agents and their densities can cause various kinds of dynamics including oscillatory, chaotic, and stable behavior (Wilson 1996, Pascual and Levin 1999). Therefore, it is unlikely that the models in this study, in which predator-prey ratios are constant, would be predictive of anything other than average behavior during recruitment. However, the analytical approach allows changes in the scale of predator-prey interaction over time. We can model this as $m_t=2\mu N_t^a \bar{k}_t^b$, where a and b are dynamic (time-dependent) and, perhaps, correlated. Although we may wish to use the Beverton-Holt model ($a=b=2$) or the Ricker-like model ($a=2$, $b=1$) as a representation of average dynamics, it remains that recruitment variability will be influenced by the dynamics of the exponents, a and b. Numerical evalua-

tion of the differential equations by using random variates at each time step may be a mechanism to evaluate how the variability of a and b within a recruitment period are translated into the variability structure around a stock-recruitment relationship.

The model formulations used in the present study have been characterized from the underlying physical processes. By doing so, research may be directed at empirical and experimental measurement of specific stock-recruitment parameters, which opens the models to testing and verification. Additionally, results indicate that the school-size distribution contains a rich source of information on the mortality and aggregation processes and that monitoring of the distribution during recruitment could be useful for understanding recruitment variability and model structure.

Acknowledgments

I would like to thank the reviewers for their constructive comments and the National Marine Fisheries Service for allowing me the opportunity to conduct this research.

Literature cited

Aiello, W. F., F. Chung, and L. Lu.
2000. A random graph model for massive graphs. Proc 32nd ACM Symp. Theor. Comp., p. 171–180.

Albert, R., and A. Barabási.
2002. Statistical mechanics of complex networks. Rev. Mod. Phys. 74(1):47–98.

Anderson, J. J.
1981. A stochastic model for the size of fish schools. Fish. Bull. 79:315–323.

Bailey, K. M., and E. D. Houde.
1989. Predation on eggs and larvae of marine fishes and the recruitment problem. Adv. Mar. Biol. 25:1–83.

Barabási, A., and R. Albert.
1999. Emergence of scaling in random networks. Science 286:5098–512.

Bianconi, G., and A. Barabási.
2001. Bose-Einstein condensation in complex networks. Phys. Rev. Lett. 86:5632–5635.

Beverton, R. J. H., and S. J. Holt.
1957. On the dynamics of exploited fish populations. Fish. Invest. Lond. Ser. 2, 19 p.

Beyer, J. E., and G. C. Laurence.
1980. A stochastic model of larval fish growth. Ecol. Model. 8:109–132.

Bonabeau, E., and L. Dagorn.
1995. Possible universality in the size distribution of fish schools. Phys. Rev. E 51:R52220–R52223.

Bonabeau, E., L. Dagorn, and P. Freon.
1999. Scaling in animal group-size distributions. Proc. Natl. Acad. Sci. 96:4472–4477.

Caldarelli, G., A. Capocci, P. De Los Rios, and M.A. Munoz.
2002. Scale-free networks from varying vertex intrinsic fitness. Phys. Rev. Lett. 89, 258702.

Chambers, C., and E. A. Trippel.
1997. Early life history and recruitment in fish populations, 632 p. Chapman and Hall, London.

Comyns, B. H., R. F. Shaw, and J. Lyczkowski-Shultz.
2003. Small-scale spatial and temporal variability in growth and mortality of fish larvae in the subtropical northcentral Gulf of Mexico: implications for assessing recruitment success. Fish. Bull. 101:10–21.

Crook, A. C.
1999. Quantitative evidence for assortative schooling in a coral reef fish. Mar. Ecol. Prog. Ser. 176:17–23.

Dorogovtsev, S. N., and J. F. F. Mendes.
2000. Scaling behaviour of developing and decaying networks. Europhys. Lett. 52:33–39
2002. Evolution of networks. Adv. Phys. 51:1079–1187.

Erdös, P., and A. Rényi.
1960. On evolution of random graphs. Publ. Math. Inst. Hung. Acad. Sci. 5:17–61.

Fell, D. A., and A. Wagner.
2000. The small world of metabolism. Nat. Biotech. 18:1121–1122.

Flierl, G., D. Grunbaum, S.A. Levin, and D. Olson.
1999. From individuals to aggregations: the interplay between behavior and physics. J. Theor. Biol. 196:397–454.

Gueron, S., and S. A. Levin.
1995. The dynamics of group formation. Math. Biosci. 128:243–264.

Harris, J. G. K.
1975. The effect of density-dependent mortality on the shape of the stock and recruitment curve. J. Cons. Int. Explor. Mer 36:144–149.

Hunter, J. R.
1984. Inferences regarding predation on the early life stages of cod and other fishes. *In* The propagation of cod, *Gadus morhua* L. (E. Dahl, D. S. Danielssen, E. Moksness, and P. Solemdan, eds.), p. 533–562. Flodevigen Rapportser 1984.

Koslow, J. A.
1992. Fecundity and the stock-recruitment relationship. Can. J. Fish. Aquat. Sci. 49:210–217.

Krapivsky, P. L., S. Redner, and F. Leyvraz.
2000. Connectivity of growing random networks. Phys. Rev. Lett. 85:4629–4632.

Landa, J. T.
1998. Bioeconomics of schooling fishes: selfish fish, quasi-free riders, and other fishy tales. Environ. Biol. Fish. 53:353–364.

Lasker, R.
1975. Field criteria for survival of anchovy larvae: the relation between inshore chlorophyll maximum layers and successful first feeding. Fish. Bull. 73:453–462.

McCauley, E., W. G. Wilson, and A.M. de Roos.
1993. Dynamics of age-structured and spatially structured predator-prey interactions: individual-based models and population-level formulations. Am. Naturalist 142:412–442.

Mertz, G., and R. A. Myers.
1994. Match/mismatch predictions of spawning duration versus recruitment variability. Fish. Oceanogr. 3(4):236–245.
1995. Estimating the predictability of recruitment. Fish. Bull. 93:657–665.

Myers, R. A., and P. Pepin.
1994. Recruitment variability and oceanographic stability. Fish. Oceanogr. 3(4):246–255.

Niwa, H.-S.
1998. School size statistics of fish. J. Theor. Biol. 195:351–361.

Pascual, M., and S. A. Levin.
1999. From individuals to population densities: searching for the intermediate scale of nontrivial determinism. Ecology 80(7):2225–2236.
Paulik, G. J.
1973. Studies of the possible form of the stock-recruitment curve. Rapp. P.-v. Réun. Cons. Int. Explor. Mer 164: 303–315.
Pepin, P.
1991. Effect of temperature and size on development, mortality, and survival rates of early life history stages of marine fish. Can. J. Fish. Aquat. Sci. 48:503–518.
Pitcher, T. J., and J. K. Parrish.
1993. Functions of shoaling behaviour in teleosts. *In* Behaviour of teleost fishes (T. J. Pitcher, ed.), p. 363–439. Chapman and Hall, London.
Quinn, T. P., and C. A. Busack.
1985. Chemosensory recognotion of siblings in juvenile coho salmon *Oncorhynchus kisutch*. Anim. Behav. 33:51–56.
Ricker, W. E.
1958. Handbook of computations for biological statistics of fish populations, 119 p. Fish. Res. Board Can. Bull.
Rickman, S. J., N. K. Dulvy, S. Jennings, and J. D. Reynolds.
2000. Recruitment variation related to fecundity in marine fishes. Can. J. Fish. Aquat. Sci. 57:116–124.
Rothschild, B. J.
1986. Dynamics of marine fish populations, 269 p. Harvard Univ. Press, Cambridge, MA.
Sogard, S. M., and B. L. Olla.
1997. The influence of hunger and predation risk on group cohesion in a pelagic fish, walleye pollock *Theragra chalcogramma*. Environ. Biol. Fish. 50:405–413.
Solé, R. V., and J. M. Montoya.
2001. Complexity and fragility in ecological networks. Proc. R. Soc. London B. 268:2039–2045.
Suneetha, K.-B., A. Folkvord, and A. Johannessen.
1999. Responsiveness of selected condition measures of herring, *Clupea harengus*, larvae to starvation in relation to ontogeny and temperature. Environ. Biol. Fish. 54:191–204.
Tolman, R. C.
1979. The principles of statistical mechanics, 661 p. Dover Publs., New York, NY.
Vazquez, A.
2003. Growing networks with local rules: preferential attachment, clustering hierarchy and degree correlations. Phys. Rev. E 67:056104.
Vlymen, W. J.
1977. A mathematical model of the relationship between larval anchovy (*Engraulis mordax*) growth, prey microdistribution, and larval behavior. Environ. Biol. Fish. 2: 211–233.
Wilson, W. G.
1996. Lotka's game in predator-prey theory: linking populations to individuals. Theor. Pop. Biol. 50:368–393.

Appendix 1

Analytical solutions to Equations 3–5 for selected mortality and aggregation models. Solutions assume that $P_{1,t} = 0$ for all t evaluated and that the number of schools is large. No analytical solutions were found for (m_{dN},w_{pa}), (m_{dN}, w_{pa}), or (m_{dk},w_{pa}).

Mortality proportional to fish: m_{dR}
Preferential aggregation: w_{pa}

$$R_t = \frac{S}{1+2\mu St}$$

$$N_t = \frac{S}{\bar{k}_0} + \frac{\alpha}{\mu}\left(S - \frac{S}{1+2\mu St}\right)$$

$$\bar{k}_t = R_t / N_t = \frac{\bar{k}_0}{1+2\mu St + 2\alpha S\bar{k}_0 t}$$

Mortality proportional to fish: m_{dR}
Random aggregation: w_N

$$R_t = \frac{S}{1+2\mu St}$$

$$N_t = \frac{S}{S-(S-\bar{k}_0)e^{-2\alpha t}}$$

$$\bar{k}_t = R_t / N_t = \frac{S-(S-\bar{k}_0 e^{-2\alpha t}}{\%+\ 2\mu St}$$

Density-independent: m_{di}
Preferential aggregation: w_{pa}

$$R_t = Se^{-2\mu t}$$

$$N_t = \frac{S}{\bar{k}_0} - \frac{S^2}{2}\frac{\alpha}{\mu}(1-e^{-4\mu t})$$

$$\bar{k}_t = R_t / N_t = \frac{\bar{k}_0 e^{-2\mu t}}{1-\frac{S\bar{k}_0}{2}\frac{\alpha}{\mu}(1-e^{-4\mu t})}$$

Density-independent: m_{di}
Random aggregation: w_N

$$R_t = Se^{-2\mu t}$$

$$N_t = \frac{S}{S-(S-\bar{k}_0)e^{-2\alpha t}}$$

$$\bar{k}_t = R_t / N_t = e^{-2\mu t}\left(S-(S-\bar{k}_0)e^{-2\alpha}\right)$$

Mortality proportional to schools: m_{dN}
Random aggregation: w_N

$$R_t = Se^{-2\mu t}\left\{\frac{\bar{k}_0}{S-(S-\bar{k}_0)e^{-2\alpha t}}\right\}^{\frac{\mu}{\alpha}}$$

$$N_t = \frac{S}{S-(S-\bar{k}_0)e^{-2\alpha t}}$$

$$\bar{k}_t = R_t / N_t = \frac{\bar{k}_0^{\mu/\alpha} e^{-2\mu t}}{\left[S-(S-\bar{k}_0)e^{-2\alpha t}\right]^{\frac{\mu}{\alpha}-1}}$$

Mortality proportional to school size: m_{dk}
Random aggregation: w_N

$$R_t = \frac{S}{1+2\mu St - \frac{\mu}{\alpha}(S-\bar{k}_0)[1-e^{-2\alpha t}]}$$

$$N_t = \frac{S}{S-(S-\bar{k}_0)e^{-2\alpha t}}$$

$$\bar{k}_t = R_t / N_t = \frac{S-(S-\bar{k}_0)e^{-2\alpha t}}{1+2\mu St - \frac{\mu}{\alpha}(S-\bar{k}_0)[1-e^{-2\alpha t}]}$$

Random mortality encounters: m_N
Random aggregation: w_N

$$R_t = S - \frac{\mu}{\alpha}\ln\left\{\frac{S}{\bar{k}_0}(e^{2\alpha t}-1)+1\right\}$$

$$N_t = \frac{S}{S-(S-\bar{k}_0)e^{-2\alpha t}}$$

$$\bar{k}_t = R_t / N_t$$

Appendix 2

Characteristics of school-size distribution under preferential attachment

Much of the recent literature on evolving complex networks has been directed at determining the degree distribution, i.e., the probability $P(k)$ of a node having k links (Albert and Barabási, 2002). When the network grows or declines proportional to k or when links are rewired to be proportional to k, then $P(k)$ can be determined by using continuum theory (Dorogovtsev and Mendes, 2000; Albert and Barabási, 2002) leading to scale-free degree distributions. Therefore, when preferential attachment and nonrandom mortality are used, then the model may be couched as a scale-free network in the manner of Barabási and Albert (1999), Dorogovtsev and Mendes (2000) and Albert and Barabási (2002).

When the aggregation model is *preferential attachment* (w_{pa}) (ignoring for the moment the nonstationarity of N and R), then the partial differential of a school of size k_{it} with respect to R_t has been shown by Dorogovtsev and Mendes (2000) to asymptotically be

$$\partial k_{it} / \partial R_t = \beta_t (k_{it} / R_t), \tag{A1}$$

where β_t is the net rate of decay per each mortality event, i.e.,

$$\beta_t = 1 - w_{pa} / m. \tag{A2}$$

With specific-mortality models, β_t is

$$\begin{aligned}
m_{di}&: \ \beta_t = 1-(\alpha/\mu)(N_t-1)\bar{k}_t \approx 1-(\alpha/\mu)R_t \\
m_{dN}&: \ \beta_t = 1-(\alpha/\mu)(N_t-1)\bar{k}_t / N_t \approx 1-(\alpha/\mu)\bar{k}_t \\
m_{dR}&: \ \beta_t = 1-(\alpha/\mu)(N_t-1)/N_t \approx 1-(\alpha/\mu) \\
m_{dk}&: \ \beta_t = 1-(\alpha/\mu)(N_t-1) \approx 1-(\alpha/\mu)R_t/\bar{k}_t,
\end{aligned}$$

where the approximations on the right assume that the number of schools is large. The first term of (A2) denotes the removal of a fish proportional to school size for a mortality event; the second term denotes aggregation events proportional to school size. If β_t is independent of time ($\beta_t=\beta$), then Dorogovtsev and Mendes (2000) showed that under continuum conditions

$$P(k) \propto k^{-\gamma} \qquad \gamma = 1+1/\beta. \tag{A3}$$

Equation A3 is equivalent to the results of Dorogovtsev and Mendes (2000), Krapivsky et al. (2000), and Albert and Barabási (2002) and suggest that β_t may be a useful approximation for determining the power-law tail of the school-size distribution (Appendix Fig. 1).

The simulation results showed the dynamics of P_{kt}. When the aggregated initial condition was imposed, at the start of the simulations there were no schools with only one fish in them ($P_{1t}=0$). Eventually, as the number of schools and fish declined, P_{1t} became positive. Finally, as the distribution became scale-free, $-\partial P_{1t}/\partial k$ became negative and remained so throughout the remainder of the simulation or until a single giant cluster was formed (Appendix Fig. 1). Conversely, if the initial conditions began with schools being disaggregated, then $\partial P_{1t}/\partial k$ began as a negative number and remained so until either a giant cluster formed or there were no more fish remaining.

An approximation is suggested by the above results for circumstances when the initial conditions are disaggregated and when there is preferential attachment: the differential equation $dP_{k,t}/dt$ when $k=1$ (Eq. 6) is replaced by

$$dP_{1,t}/dt = -wP_{1,t}/N_t + m(1-P_{1,t})/N_t. \tag{A4}$$

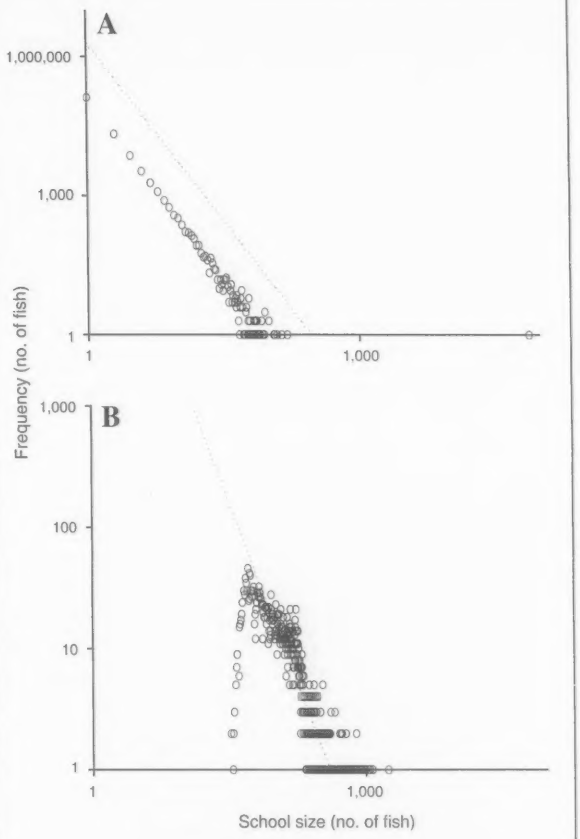

Appendix Figure 1

School-size distribution at selected times. (**A**) School-size distribution of a simulation starting with a disaggregated initial condition, $S=10^6$, $\alpha=10^{-6}$, where mortality is density-independent (m_{di}) and there is preferential attachment (w_{pa}). (**B**) Distribution starting with an aggregated initial condition, $S=2\times10^6$, $\alpha=1.5\times10^{-6}$, where mortality is density-dependent proportional to schools (m_{dN}) and with preferential attachment (w_{pa}). The dotted lines are the predictions of $\gamma=1+1/\beta$ from Equation A2, horizontally offset for viewing.

Diet shifts of juvenile red snapper (*Lutjanus campechanus*) with changes in habitat and fish size

Stephen T. Szedlmayer

Marine Fish Laboratory
Department of Fisheries
Auburn University
8300 State Highway 104
Fairhope, Alabama 36532
E-mail address: sszedlma@acesag.auburn.edu

Jason D. Lee

Barry Vittor & Associates
8060 Cottage Hill Rd.
Mobile, Alabama 36695

Abstract—We examined the diets and habitat shift of juvenile red snapper (*Lutjanus campechanus*) in the northeast Gulf of Mexico. Fish were collected from open sand-mud habitat (little to no relief), and artificial reef habitat (1-m^3 concrete or PVC blocks), from June 1993 through December 1994. In 1994, fish settled over open habitat from June to September, as shown by trawl collections, then began shifting to reef habitat—a shift that was almost completed by December as observed by SCUBA visual surveys. Stomachs were examined from 1639 red snapper that ranged in size from 18.0 to 280.0 mm SL. Of these, 850 fish had empty stomachs, and 346 fish from open habitat and 443 fish from reef habitat contained prey. Prey were identified to the lowest possible taxon and quantified by volumetric measurement. Specific volume of particular prey taxa were calculated by dividing prey volume by individual fish weight. Red snapper shifted diets with increasing size. Small red snapper (<60 mm SL) fed mostly on chaetognaths, copepods, shrimp, and squid. Large red snapper (60–280 mm SL) shifted feeding to fish prey, greater amounts of squid and crabs, and continued feeding on shrimp. We compared red snapper diets for overlapping size classes (70–160 mm SL) of fish that were collected from both habitats (Bray-Curtis dissimilarity index and multidimensional scaling analysis). Red snapper diets separated by habitat type rather than fish size for the size ranges that overlapped habitats. These diet shifts were attributed to feeding more on reef prey than on open-water prey. Thus, the shift in habitat shown by juvenile red snapper was reflected in their diet and suggested differential habitat values based not just on predation refuge but food resources as well.

Manuscript approved for publication 4 November 2003 by Scientific Editor.
Manuscript received 20 January 2004 at NMFS Scientific Publications Office.
Fish. Bull. 102:366–375 (2004).

Larval red snapper (*Lutjanus campechanus*) spend approximately 26 days in the plankton, prior to metamorphosis and first appearance on benthic substrate. For the most part the fish settle on open substrate, where peaks in recruitment are observed in August and September, after which they may move to more structured habitat sometime within the first year (Szedlmayer and Conti, 1999). The apparent advantage of this habitat shift would be increased food resources and protection from predators. To help clarify the value of increased food resources on reef habitats, comparisons of diets from the two habitats are necessary. Also, because many fish species shift diets with increasing size (Sedberry and Cuellar, 1993; Burke, 1995; Rooker, 1995; Lowe et al., 1996), we need to distinguish possible ontogenetic diet differences from shifts that are due to habitat.

Previous red snapper diet studies have focused on larger individuals and on small sample sizes for fish <250 mm SL (Camber, 1955; Moseley, 1966; Bradley and Bryan, 1975). Camber (1955) described the diets of 15 "small red snapper" from Campeche Banks, and reported that 14 of the 15 stomachs contained small penaeid shrimps. Moseley (1966) described the diets of 45 "juvenile red snapper" collected off the coasts of Texas, and 28 off Louisiana. Louisiana fish fed on fishes, shrimps, detritus, and stomatopods, and Texas fish fed on shrimps, crabs, and mysid shrimps.

Perhaps the most comprehensive red snapper diet study to date has been that of Bradley and Bryan (1975) which described the diets, by season, of trawl-collected (open sand-mud habitat) and hook-and-line reef "rough bottom areas" fish off the Texas coast. They described the diets of 258 open-habitat and 190 reef red snapper and found that juvenile red snapper (25–325 mm FL) were dependent on shrimp, crabs, and other crustaceans and that adults (325–845 mm FL) were dependent on fish, crabs, and other crustaceans. They described a change in juvenile red snapper diet as fish size increased, "young red snapper depend almost exclusively upon invertebrates," and showed a gradual increase in vertebrate prey with growth. However, they did not separate out the proportions of their "juvenile" red snapper that were collected from reef versus open habitat. Thus, the shift from open to reef habitat is still poorly understood. If and when this shift occurs and whether this shift is accompanied with a diet shift that is independent of fish-size effects needs to be defined.

The purpose of the present study is to describe the diet of red snapper off the coast of Alabama—from the juvenile stage (just after settlement) to one-year old fish. We examined overall

ontogenetic shifts in red snapper diet with increasing size and possible changes in diet with habitat shifts from open substrate to structured habitat (artificial reefs).

Materials and methods

Red snapper were collected from open-flat substrate (sand and mud) and reef habitats (artificial reefs; Fig. 1). The open habitat was located approximately 6 km south of Mobile Bay, Alabama (30°06′N, 88°03′W), and ranged in depth from 12 to 20 m. Previous studies showed very high concentrations of age-0 red snapper from these areas (Szedlmayer and Shipp, 1994; Szedlmayer and Conti, 1999). The artificial reef habitats were located in the Hugh Swingle artificial reef area, approximately 20 km south of Mobile Bay, AL, and ranged in depth from 18 to 23 m (Szedlmayer and Shipp, 1994; Szedlmayer, 1997).

We collected fish from open substrate by trawl (7.62-m head rope, 2.54-cm mesh, 2-mm codend mesh). Samples were taken every two weeks from June to December 1994; however. time between samples was longer in the winter because of poor weather. Each trawl was fished for 10 min, and all age-0 and age-1 red snapper collected were placed on ice, returned to the laboratory, and frozen for later analysis. Bottom dissolved oxygen, salinity, and temperature were sampled with a Hydrolab Surveyor II at each location (Szedlmayer and Conti, 1999).

Prior to diet analysis, red snapper were thawed, weighed to the nearest 0.1 g, and measured to the nearest 0.1 mm SL. The whole fish was preserved in 10% formalin if SL was <50 mm, whereas for larger fish, stomachs were removed and preserved. After 48 hours in formalin, stomach samples were transferred to 75% isopropyl alcohol.

Concrete block and PVC artificial reefs (1 m^3) were placed in the Hugh Swingle reef area in August 1992 and July 1993 (Szedlmayer, 1997). "Reef" is used here for defining these artificial habitats. Reefs were not sampled for a minimum of 3 months after placement. Red snapper were collected from June 1993 through December 1994. Fish were collected from these reefs by SCUBA divers first placing a drop net (3.0 m radius, 1.3 cm square mesh) over the reef and then releasing rotenone into the enclosed area. Reef fish were placed on ice in the field and transported back to the laboratory. Approximately 12–18 h after collection all reef fish were weighed to the nearest 0.1 g and measured to the nearest 1.0 mm. Stomachs were fixed in 10% formalin, and after 24 h transferred to 75% isopropyl alcohol. Red snapper size classes were also estimated by SCUBA visual surveys in July and August 1994. On each visual survey, divers counted red snapper by 50-mm size intervals. Bottom dissolved oxygen, salinity, and temperature were sampled with a Hydrolab Surveyor II during each survey.

All stomachs were dissected and contents placed in petri dishes. All prey were counted and identified to the lowest possible taxon. Volume was calculated by using an adaptation of the method described by Hellawell and Able (1971). Each prey taxon from each stomach was placed into a glass well of a known depth. A cover slide was placed on the well,

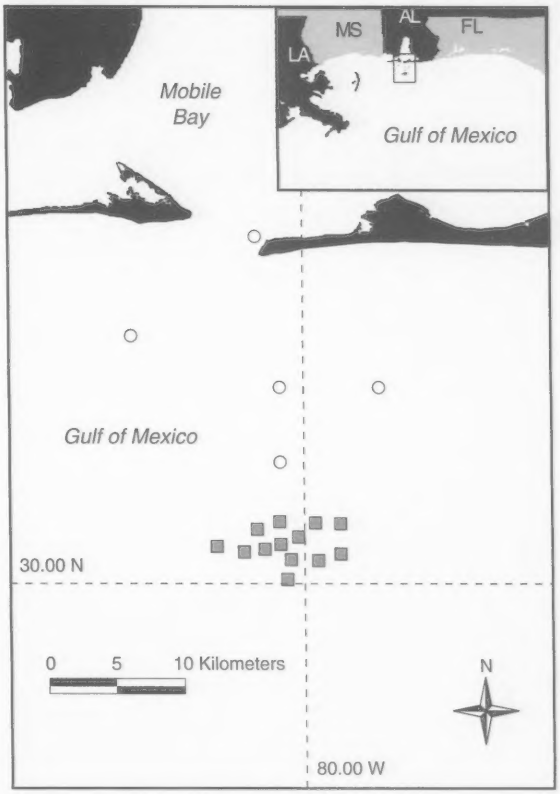

Figure 1

Collection sites for red snapper (*Lutjanus campechanus*) in the northern Gulf of Mexico. Open circles are open habitat trawl sites, and gray squares are 1-m^3 concrete or PVC artificial reefs.

depressing the prey taxon to a known depth (e.g., 1 mm). The prey were video taped with a high-8 Sony camera and images were digitized with Image Pro 2.0 software (Media Cybernetics, Silver Spring, MD). Image size was calibrated to 0.01 mm by a stage micrometer. The surface area of each preparation was measured by using Image Pro software. Volume was calculated by multiplying the surface area by the known depth. Specific volumes for particular prey taxa were calculated by dividing prey volume by individual fish weight (mm^3/fish wt g). Comparisons of diet shift by increasing fish size were made by grouping prey taxa into ten prey groups and by calculating specific volume for 10-mm-size intervals of red snapper.

A dissimilarity index (Bray-Curtis) was calculated from specific volumes of individual prey taxa, for overlapping size classes of red snapper both within and between habitats: Bray-Curtis = $\Sigma|Y_{ij}-Y_{ik}|/\Sigma(Y_{ij}+Y_{ik})$, where Y = specific volume of i^{th} species, and j and k are the samples being compared (Field et al., 1982). The dissimilarities were then used in a multidimensional scaling analysis (MDS; Schiffman et al., 1981). The MDS provided a two-dimensional "map" of the distances between samples (fish

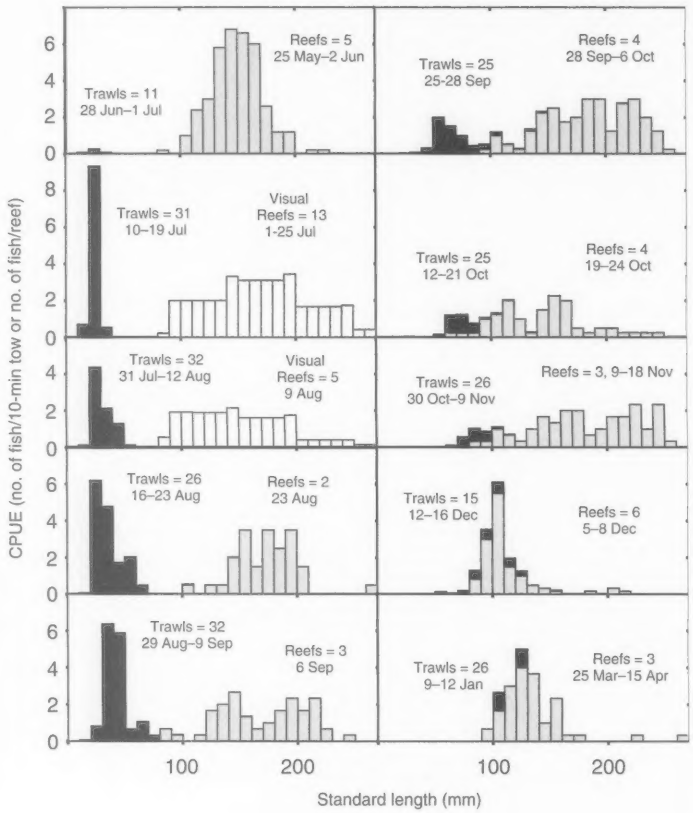

Figure 2

Movement patterns for age-0 red snapper (*Lutjanus campechanus*) from the northern Gulf of Mexico in 1994. Black bars represent trawl samples, grey bars represent reef drop-net samples, and white bars represent SCUBA visual surveys of concrete reefs.

size and habitat type) in Euclidian space based on the Bray-Curtis index. Thus, comparisons of red snapper diets were based on all prey taxa, yet independent of capture habitat and fish size.

Results

In the sampling areas during the summer and fall of 1994, salinity ranged from 30 to 35 ppt. Dissolved oxygen was 7 ppm in the early summer, decreased to 3 ppm in July and August, and increased to 7 ppm in the fall. Temperature was 22°C in June, increased to 28°C in late August, then dropped to just below 20°C by December. No significant differences were detected between trawl and reef sites for these environmental measures (*t*-test, $P \leq 0.05$).

Red snapper showed a clear shift in habitat during their first few months of life (Fig. 2). Fish first recruited to open habitat at the end of June, at sizes <40 mm SL. Fish continued to recruit to open habitat until early September, at which time they were larger (30 to 100 mm SL) and began shifting to more structured habitat. By mid-October most age-0 fish had moved to reef habitat. During the initial settlement no new recruits were collected or visually observed on the artificial habitats (Fig. 2). Overall, only red snapper <160 mm SL were collected from open habitat, whereas only red snapper >70 mm SL were collected from reef habitat. Size overlapped from 70.0 to 160 mm SL between habitats (Fig. 3).

A total of 1639 red snapper stomachs were analyzed: 570 from open substrate and 1069 from reef habitat. Prey were found in 789 (48%) of the total stomachs examined, 346 (61%) from the open habitat and 443 (41%) from the reef habitat (Fig. 3). Trawl-collected red snapper were mostly collected from site one, but sample sizes were also large (>30 with prey) at two other sites (Table 1). Total red

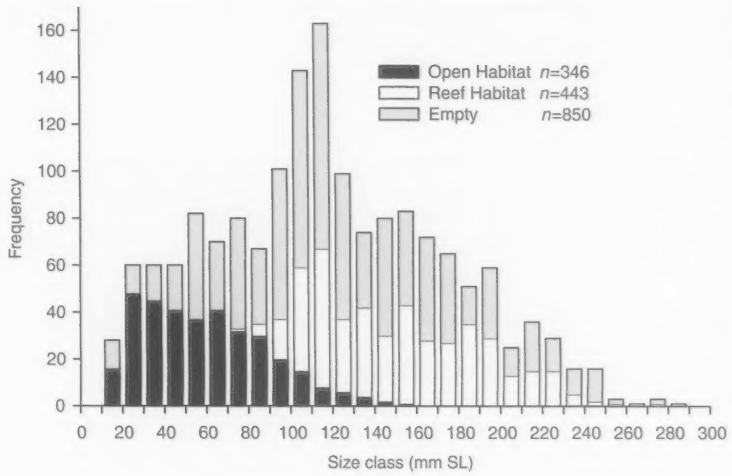

Figure 3

A comparison of red snapper (*Lutjanus campechanus*) length frequencies between open and reef habitats in the northern Gulf of Mexico. Gray bars = empty stomachs from both habitats.

Table 1

Number of red snapper (*Lutjanus campechanus*) stomachs sampled (*n*), and number of stomachs containing prey from open and reef habitat in the northeast Gulf of Mexico.

Open trawl sites		Reef habitats	
n	*n* with prey	*n*	*n* with prey
356	223	108	53
45	21	17	5
75	58	198	115
57	33	55	31
37	11	249	71
		50	23
		14	1
		89	45
		11	5
		209	74
		35	10
		22	4
		12	6

Table 2

Number of red snapper (*Lutjanus campechanus*) stomachs sampled (*n*), and number containing prey, by month and year, from open and reef habitat in the northeast Gulf of Mexico.

Open habitat			Reef habitat		
Month and year	*n*	*n* with prey	Month and year	*n*	*n* with prey
Jul 1994	56	43	Jun 1993	94	50
Aug 1994	169	109	Oct 1993	370	169
Sep 1994	187	98	May 1994	141	37
Oct 1994	97	52	Jun 1994	46	37
Nov 1994	16	12	Aug 1994	41	8
Dec 1994	45	32	Sep 1994	155	86
			Oct 1994	76	28
			Nov 1994	65	12
			Dec 1994	81	16

snapper collected from the reefs varied by site (from 11 to 249 fish), but large samples were collected from at least 6 different reefs (Table 1). Large sample sizes were collected during most months over open habitat, with the exception of November 1994 (n=12), and for most months (6 out of 9) from reef sites (Table 2). Only red snapper stomachs containing prey were used in our analyses.

Red snapper diets showed 55 different prey identified to the lowest possible taxon. In general, red snapper diets were dominated by fish (43%), squid (29.5%), shrimp (16.4%), and crabs (4.4%; Table 3). Specifically, the "shrimp" group included Mysidacea (mysid shrimps), Stomatopoda (mantis shrimps), Penaeidea (penaeid

Table 3

Specific volume (mm^3/fish weight g) for prey taxa from red snapper (*Lutjanus campechanus*). % = percent specific-volume of total volume, Habitat = prey habitat. General prey groups are noted in quotation marks. unid. = unidentified.

Prey taxa	Total volume	Percent	Lowest taxon	Specific volume	Percent	Habitat
Osteichthyes "fish"	5408.2	43.5	unid. fish	3465.9	27.9	
			Halichoeres spp.	650.4	5.2	reef
			Blenniidae	279.2	2.2	reef
			Serranidae	278.1	2.2	reef
			Serranus subligarius	240.8	1.9	reef
			Centropristis ocyurus	207.3	1.7	reef
			Engraulidae	117.9	0.9	open
			Ophichthidae	100.6	0.8	open
			Cynoglossidae	35.2	0.3	open
			Triglidae	20.8	0.2	open
			Ophichthus sp.	10.8	0.1	open
Cephalopoda "squid"	3665.6	29.5	Loliginidae	3665.6	29.5	open
Natantia "shrimp"	2033.7	16.4	unid. shrimp	544.6	4.4	
			Sicyoninae	359.6	2.9	reef
			Hippolytidae	345.7	2.8	reef
			Penaeidae	264.5	2.1	open
			Alpheidae	131.1	1.1	reef
			Sergestidae	24.2	0.2	open
			Luciferinae	22.6	0.2	open
			Ogyrididae	8.8	0.1	open
Stomatopoda "shrimp"			Squillidae	221.8	1.8	open
Mysidacea "shrimp"			Mysidacea	109.8	0.9	open
Reptantia "crabs"	550.8	4.4	Portunidae	302.0	2.4	mixed
			unid. crab	143.0	1.2	
			Diogeninae	51.6	0.4	open
			Leucosiidae	20.7	0.2	reef
			Xanthidae	16.7	0.1	reef
			Porcellanidae	7.3	0.1	reef
Chaetognatha	199.6	1.6	*Sagitta* spp.	199.6	1.6	open
Polychaeta	130.1	1.0	Polycheata	75.4	0.6	mixed
Polychaeta			Onuphidae	34.0	0.3	open
			Maldanidae	19.9	0.2	open
Ascidiacea "tunicate"	121.0	1.0	Ascidiacea	121.0	1.0	reef
Calanoida "copepod"	118.2	1.0	Calanoida	113.3	0.9	open
Octopodidae	93.6	0.8	*Octopus* sp.	93.6	0.8	reef
unid.	79.5	0.6	unid.	79.5	0.6	
Amphipoda	13.8	0.1	Amphipoda	9.4	0.1	mixed
Ostracoda	6.1	0.0	Ostracoda	6.1	0.0	open

shrimps), and Caridea (caridean shrimps). In addition, all Squillidae were probably *Squilla empusa*, according to Hopkins et al., (1987). Among fish, many were unidentified due to digestion, but if proportions of unidentified fish are similar to identified fish, then dominant fish prey included *Halichoeres* spp., (5.2%), Blenniidae (2.2%), and Serranidae (2.2%). Two prey fish were identified to species: *Serranus subligarius* (1.9%), and *Centropristis ocyurus* (1.7%).

Among the squid taxon, one genus dominated: *Lolliguncula* spp., (29.5%), but all squid were either *L. brevis* or *Loligo pealeii* (Hopkins et al., 1987). Among shrimp, dominant taxa included Sicyoninae (2.9%), Hippolytidae (2.8%), Penaeidae (2.1%), Squillidae (1.8%), and Alpheidae (1.1%). Among crabs, dominant taxa were mostly Portunidae (2.4%). Other groups showing greater than 1.0% included Chaetognatha (*Sagitta* sp. 1.6%), and Ascidiacea or tunicates (1.0%; Table 3).

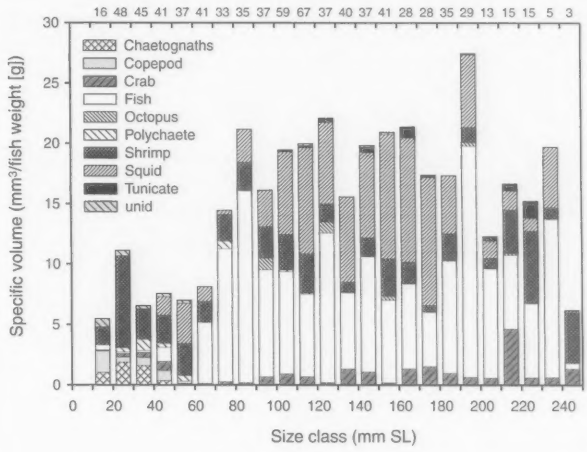

Figure 4

Stomach contents by specific-volume for ten higher taxonomic groups over 10-mm size classes of red snapper (*Lutjanus campechanus*) from both open and reef habitats in the northern Gulf of Mexico. Numbers on the upper axis are the number of red snapper that contained prey for each respective size class.

Red snapper shifted diets with increasing size. For red snapper <60.0 mm SL, diets were dominated by shrimp, chaetognaths, squid, and copepods. Large red snapper (60–280 mm SL) shifted to feeding on fish prey, greater amounts of squid and crabs, and continued feeding on shrimp (Fig. 4).

The diets of juvenile red snapper changed as they moved from open to reef habitats. Fish collected had overlapping sizes of 70.0 to 160.0 mm SL from both open and reef habitats, and the MDS analysis for this size range showed a clear separation of diets between the two habitats (Fig. 5). Two points that were outliers (R75, T155) were biased because they represented only one fish each, and the third outlier (R85) was difficult to explain.

The clear separation of red snapper diets shown by the MDS analysis can be attributed to several prey shifts that accompanied habitat shifts. For prey crabs, open-habitat red snapper diets were dominated by Xanthidae, and smaller amounts of Paguridae, Portunidae, Diogeninae, and Pinnotheridae (Fig. 6), whereas diets of red snapper from reef habitats shifted to a dominance by Portunidae and Diogeninae (Fig. 7). For prey shrimp, open habitat red snapper diets were dominated by Penaeidae and Mysidacea (Fig. 8), whereas diets from reef habitats shifted to a dominance of Sicyoninae, Hippolytidae, Alpheidae, and Squillidae (Fig. 9). For prey fish, open-habitat red snapper diets were dominated by Engraulidae (although most were unidentified; Fig. 10), whereas diets from reef habitat clearly reflected prey fish from reef habitats and included Blenniidae, Serranidae, and three prey fish identified to genera, *Centropristis* spp, *Halichoeres* spp., and *Serranus* spp. (Fig. 11).

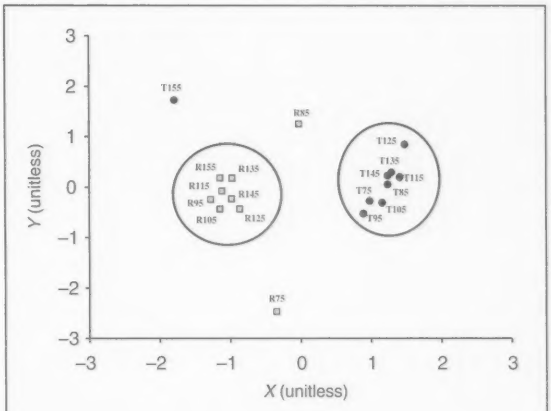

Figure 5

Multidimensional scaling of diets for red snapper (*Lutjanus campechanus*) based on the Bray-Curtis dissimilarity index computed for specific volume of prey taxa both within and between habitats for overlapping size classes (70.0 to 159.9 mm SL). The letter and number accompanying each point indicates the habitat and size class that each point represents (e.g., T = trawl, R = reef, 75 = 75 mm SL size class). Circles were drawn by hand. Axes are unitless.

Discussion

The present study provides a substantial sample size (n=1639) for red snapper diet analysis and a relatively

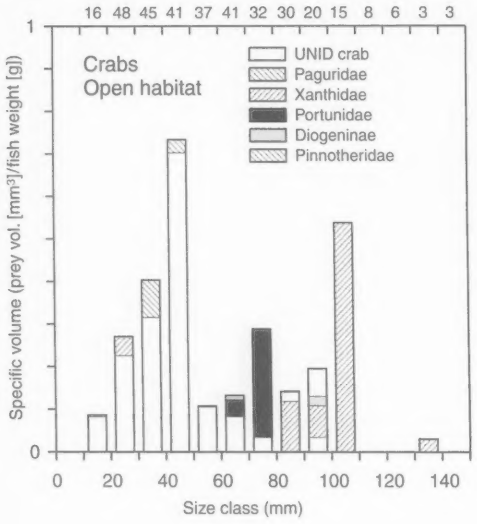

Figure 6

Crab prey from open habitat. Stomach contents by specific volume over 10-mm size classes of red snapper (*Lutjanus campechanus*) from the northern Gulf of Mexico. Numbers on the upper axis are the number of red snapper that contained prey for each respective size class.

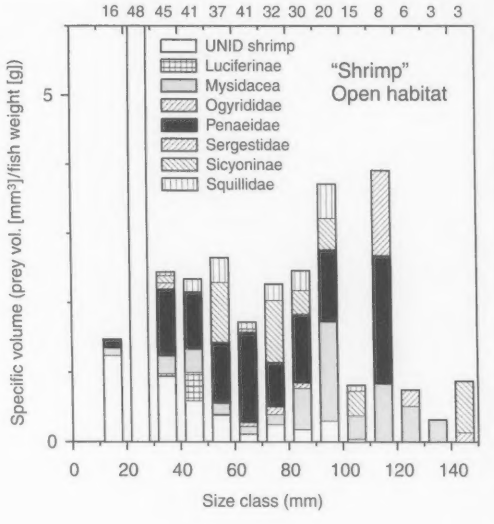

Figure 8

"Shrimp" prey from open habitat. Stomach contents by specific volume over 10-mm size classes of red snapper (*Lutjanus campechanus*) from the northern Gulf of Mexico. Numbers on the upper axis are the number of red snapper that contained prey for each respective size class.

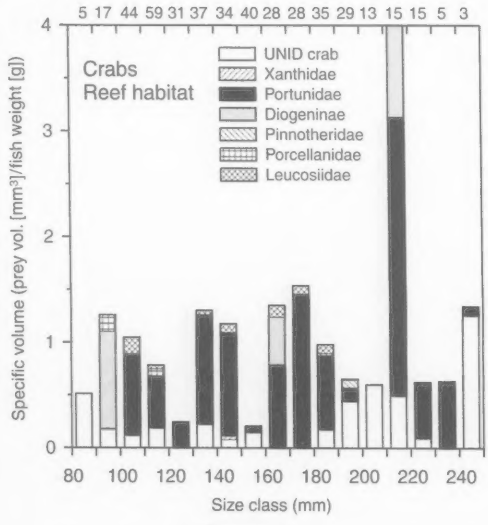

Figure 7

Crab prey from reef habitat. Stomach contents by specific volume over 10-mm size classes of red snapper (*Lutjanus campechanus*) from the northern Gulf of Mexico. Numbers on the upper axis are the number of red snapper that contained prey for each respective size class.

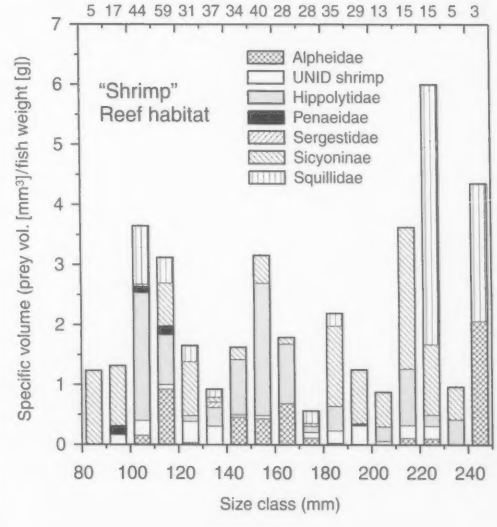

Figure 9

"Shrimp" prey from reef habitat. Stomach contents by specific volume over 10-mm size classes of red snapper (*Lutjanus campechanus*) from the northern Gulf of Mexico. Numbers on the upper axis are the number of red snapper that contained prey for each respective size class.

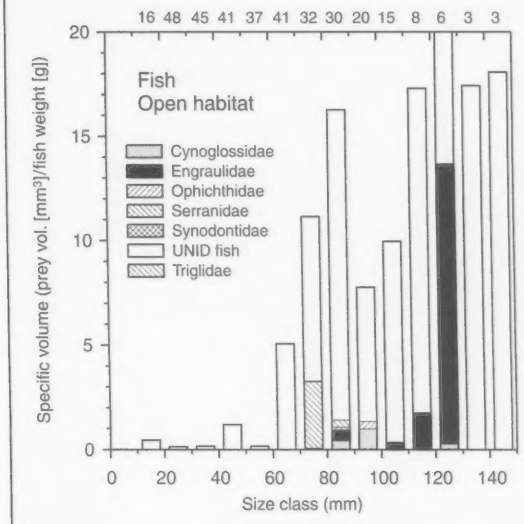

Figure 10

Fish prey from open habitat. Stomach contents by specific volume over 10-mm size classes of red snapper (*Lutjanus campechanus*) from the northern Gulf of Mexico. Numbers on the upper axis are the number of red snapper that contained prey for each respective size class.

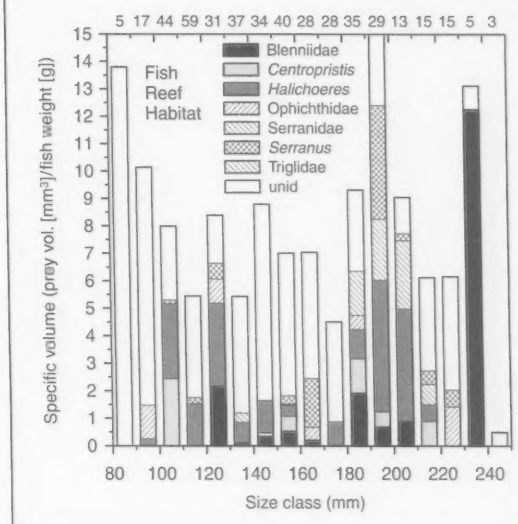

Figure 11

Fish prey from reef habitat. Stomach contents by specific volume over 10-mm size classes of red snapper (*Lutjanus campechanus*) from the northern Gulf of Mexico. Numbers on the upper axis are the number of red snapper that contained prey for each respective size class.

high percentage of stomachs with food (48%) compared to past studies. Rooker (1995) also showed a high percentage (69%; 312 out of 449 stomachs) of schoolmaster snapper (*Lutjanus apodus*) contained prey, when fish were collected from depths similar to those of the our study (1 to 27 m). The higher percentage of stomachs with prey found in our study compared to past studies of red snapper (Stearns, 1884; Camber,1955; Moseley, 1966) may be due to the shallower depths sampled (18 m; DeMartini et al., 1996).

Juvenile red snapper showed feeding patterns similar to many other marine fishes. After settlement, from approximately 20 to 60 mm SL, they showed a wide-ranging diet that included shrimp, copepods, chaetognaths, and squid. Prey fish were also found in the stomachs of the smallest red snapper collected (15–20 mm SL) but were not a dominant component. Sweatman (1993) reported similar results for the snapper *Lutjanus quinquelineatus*, ranging from 24 to 29 mm SL, i.e., piscivorous in the first few days after settlement. Above 60 mm SL, fish prey tended to dominate specific volume, but not by feeding less on shrimp because shrimp continued to be an important prey. Squid became another dominant component of red snapper diet at about 100 mm SL and also continued as an important prey up to 240 mm SL. Unfortunately, sample size was reduced above 230 mm SL, and it was difficult to estimate if squid and fish continued as dominant prey components above these size classes. Sedberry and Cuellar (1993) reported a similar shift in diets of reef-associated vermilion snapper (*Rhomboplites aurorubens*). This species shifted from small crustaceans to fishes and cephalopods over a size range similar to that of red snapper in the present study. Moseley (1966) reported a "slow transition from zooplankton to macro animals for red snapper sizes between 40 and 90 mm"—a transition that probably included fish prey that he did not specifically identify. Bradley and Bryan (1975), showed a shift in juvenile red snapper diets with size (25–325 mm FL). Their smallest red snapper keyed on invertebrates, then showed a sharp increase in dependency upon prey fish above 175 mm FL, when Batrachoididae (toadfish) became a dominant component. These shifts in diet are important in helping to identify fish habitat and are potentially key aspects of early survival.

Red snapper showed two major habitat shifts in their first year. Juvenile red snapper first settled from the plankton to benthic substrate near 20 mm SL (Szedlmayer and Conti, 1999). The present study showed a second shift from open habitat to reef habitat starting at about 70 mm SL (Fig. 3). No fish smaller than 70 mm were collected from the reefs, and smaller red snapper were rarely observed on these reefs from SCUBA visual surveys. No fish larger than 160 mm SL were caught from the open habitat but were present on the reefs. This finding suggested that red snapper had shifted to reef habitat by 160 mm SL but also may have avoided trawl gear as described earlier for age-0 red snapper (Bradley and Bryan, 1975) and age-0 summer flounder (*Paralichthys dentatus*) (Szedlmayer and Able, 1993). However, no large (150–300 mm) red

snapper were observed over open habitat by a SCUBA visual survey despite our observations that red snapper are attracted to SCUBA divers. Thus we suggest that a shift in habitat was more likely the cause of this absence than trawl avoidance.

The distinct diet shift as red snapper changed habitats was independent of increasing size and suggested that different benthic habitats play a critical role in the early life history of this species. This separation was completely independent of "a priori" knowledge of sample location and fish size. For example, the MDS analysis showed almost complete separation based on habitat rather then fish size (Fig. 5). These differences between open and reef habitat were readily apparent when prey taxa were separated into lower taxonomic categories. For example, fishes such as *Halichoeres* spp., *Serranus* spp., and *Centropristis* spp., were found only in the diets of reef-collected red snapper. These species are closely tied to reef structure (Nelson and Bortone, 1996). Prey shrimp also showed distinct differences in red snapper diets between habitats. Over open habitat, Mysidacea, Penaeidae, and Sergestidae were important components. After the shift to reef habitat, Mysidacea were absent and Penaeidae and Sergestidae were greatly reduced, and Sicyoninae, Hippolytidae, and Alpheidae became the dominant shrimp components. The latter are all families typically associated with reef habitats (Chance, 1970; Pequegnat and Heard, 1979). One exception was the increased feeding on Squillidae, an open habitat crustacean, at the largest size classes of this study (220–250 mm SL; Fig. 9). For crabs, the separation was not as clear, because of the dominance of Portunidae, which can be assigned to both open and reef habitats. However, increases in reef crabs were still apparent with habitat shift, i.e., Diogeninae, Porcellanidae, and Leucosiidae can all be considered reef prey. Although Bradley and Bryan (1975) pooled "juvenile" red snapper over open and reef habitats, they did show a marked increase in fish prey above 175 mm FL. This increase was almost exclusively due to Batrachoididae or toadfishes, which are typically found in reef habitat. We did not observe any toadfish prey in our juvenile red snapper collections, but its presence in this earlier study is consistent with present findings showing a shift to feeding on reef-habitat prey.

Red snapper diet shifted to greater percentages of reef-prey with movement to reef habitat, but with this shift they also continued feeding on other prey. This flexibility in feeding habits allows red snapper to take advantage of prey from wide-ranging habitats. Similar diet shifts related to habitat shifts have been shown in schoolmaster snapper, (*L. apodus*) (Rooker, 1995). The schoolmaster snapper shifted from nearshore mangroves to coral reef habitats near 70 mm SL; diets of fish ≤70.0 mm SL were dominated by crustaceans, particularly amphipods and crabs. Fish >70.0 mm SL fed on fishes and to a lesser extent crabs, shrimps, and stomatopods. Similar diet shifts were also shown for several fish species of Puget Sound. For example in pile perch (*Rhacochilus vacca*), striped seaperch (*Embiotoca lateralis*), and quillback rockfish (*Sebastes maliger*), the smallest juveniles preyed on open-habitat plankton and benthic fauna, and medium-size and larger fish (>121 mm) of all three species shifted their diets to include reef-associated prey (Hueckel and Stayton, 1982). However, at larger sizes these three species were not totally dependent on reef-associated prey.

We have examined red snapper diets based on specific volume of food. Although many other studies have used an index of relative importance (IRI; Pinkas et al., 1971; Cortes, 1997), we were specifically interested in the nutritional value of particular prey, and prey separation into open-habitat or reef-habitat. With IRIs these separations would be more difficult to define, e.g., pelagic prey with high numbers might be considered more important, but actually provide little nutritional value to red snapper diets (Macdonald and Green, 1983). Future studies on the effects of red snapper predation on prey distributions may be better suited for using IRIs.

In summary, red snapper diets from open habitat showed prey taxa associated with open sand-mud substrate and the planktonic environment. Open-habitat prey, such as chaetognaths, are known to be pelagic as well as benthic, as are sergestid shrimp, calanoid copepods, mysids, and stomatopods (Williams, 1968; Manning, 1969; Gosner, 1978; Stuck et al., 1979; Alldredge and King, 1985; Lindquist et al., 1994). Red snapper shifted diets to reef-associated prey with their habitat shift, and this diet shift was independent of fish size. These diet shifts were clearly apparent for both fish and shrimp prey but less so for crab prey. As shown with marine fish species from Puget sound, red snapper diets from reef habitat were not restricted to reef-associated prey. For example, squids were an important prey over both open and reef habitats in the present study and our findings agree with those of Bradley and Bryan (1975). The squids *Loligo* sp., and *Lolliguncula* sp. are both abundant in nearshore coastal waters and are not typically associated with reef structure (Gosner 1978; Laughlin and Livingston, 1982; Hopkins et al., 1987). Availability and ease in capture could be a key as to why squid are important for red snapper over size ranges of 40 to 240 mm SL. This flexibility in feeding habits allows red snapper to take advantage of prey from wide-ranging habitats, but clear shifts to additional reef prey supports the hypothesis that reef structure provides new prey resources.

Acknowledgments

We thank Joseph Conti, Kori M. Heaps, and Frank S. Rikard for help in field collections and invertebrate identification. This study was funded by NOAA, NMFS, MARFIN grant number USDC-NA47FF0018-0. This is a contribution of the Alabama Agricultural Station.

Literature cited

Alldredge, A. L., and J. M. King.
1985. The distance demersal zooplankton migrate above the benthos: implications for predation. Mar. Biol. 84:253–260.

Bradley, E., and C. E. Bryan.
1975. Life history and fishery of the red snapper (*Lutjanus campechanus*) in the northwestern Gulf of Mexico: 1970–1974. *In* Proceedings of the twenty-seventh Gulf and Caribbean Fisheries Institute, p. 77–106. Univ. Miami, Miami, FL.

Burke, J. S.
1995. Role of feeding and prey distribution of summer and southern flounder in selection of estuarine nursery habitats. J. Fish Biol. 47:355–366.

Camber, C. I.
1955. A survey of the red snapper fishery of the Gulf of Mexico, with special reference to the Campeche Banks. Florida State Board of Conservation Technical Series 12:1–64.

Chance, F. A., Jr.
1970. A new shrimp of the genus *Lysmata* (Decapoda: Hippolytidae) from the western Atlantic. Crustaceana 19:59–66.

Cortés, E.
1997. A critical review of methods of studying fish feeding based on analysis of stomach contents; application to elasmobranch fishes. Can. J. Fish. Aquat. Sci. 54:726–738.

DeMartini, E. E., F. A. Parrish, and D. M. Ellis.
1996. Barotrauma-associated regurgitation of food: implications for diet studies of Hawaiian pink snapper, *Pristipomoides filamentosus* (family Lutjanidae). Fish. Bull. 94:250–256.

Field, J. G., K. R. Clarke, and R. M. Warwick.
1982. A practical strategy for analyzing multispecies distribution patterns. Mar. Ecol. Prog. Ser. 8:37–52.

Gosner, K. L.
1978. A field guide to the Atlantic seashore, 329 p. Houghton Mifflin Company, Boston, MA.

Hellawell, J. M., and R. Able.
1971. A rapid volumetric method for the analysis of the food of fishes. J. Fish Biol. 3:29–37.

Hopkins, T. S., J. F. Valentine, and L. B. Lutz.
1987. An illustrated guide with key to selected benthic invertebrate fauna of the Northern Gulf of Mexico. Mississippi Alabama Sea Grant Publ. 087(10), Biloxi, MS.

Hueckel, G. S., and R. L. Stayton.
1982. Fish foraging on an artificial reef in Puget Sound, Washington. Mar. Fish. Rev. 44: 38–44.

Laughlin, R. A., and R. J. Livingston.
1982. Environmental and trophic determinants of the spatial/temporal distribution of the brief squid (*Lolliguncula brevis*) in the Apalachicola estuary (North Florida, USA). Bull. Mar. Sci. 32:489–497.

Lindquist, D. G., L. B. Cahoon, I. E. Clavijo, M. H. Posey, S. K. Bolden, L. A. Pike, S. W. Burk, and P. A. Cardullo.
1994. Reef fish stomach contents and prey abundance on a reef and sand substrata associated with adjacent artificial and natural reefs in Onslow Bay, North Carolina. Bull. Mar. Sci. 55:308–318.

Lowe, C. G., B. M. Wetherbee, G. L. Crow, and A. L. Tester.
1996. Ontogenetic dietary shifts and feeding behavior of the tiger shark, *Galeocerdo cuvier*, in Hawaiian waters. Environ. Biol. Fish. 47:203–211.

Macdonald, J. S., and R. H. Green.
1983. Redundancy of variables used to describe importance of prey species in fish diets. Can. J. Fish. Aquat. Sci. 40:635–637.

Manning, R. B.
1969. Stomatopod Crustacea of the Western Atlantic, 380 p. Univ. Miami Press, Miami, FL.

Moseley, F. N.
1966. Biology of the red snapper, *Lutjanus aya* Bloch, of the northwestern Gulf of Mexico. Publ. Inst. Mar. Sci. Univ. Texas 11:90–101.

Nelson, B. D., and S. A. Bortone.
1996. Feeding guilds among artificial-reef fishes in the northern Gulf of Mexico. Gulf Mex. Sci. 2:66–80.

Pequegnat, L. H., and R. W. Heard.
1979. *Synalpheus agelas*, new species of snapping shrimp from the Gulf of Mexico and Bahama Islands (Decapoda: Alpheidae). Bull. Mar. Sci. 29:110–116.

Pinkas, L., M. S. Oliphant, I. L. R. Iverson.
1971. Food habits of albacore, bluefin tuna, and bonito in California waters. Calif. Fish Game 152:1–105.

Rooker, J. R.
1995. Feeding ecology of the schoolmaster snapper, *Lutjanus apodus* (Walbum), from southwestern Puerto Rico. Bull. Mar. Sci. 56:881–894.

Schiffman, S. S., M. L. Reynolds, and F. W. Young.
1981. Introduction to multidimensional scaling, 413 p. Academic Press Inc., New York, NY.

Sedberry, G. R., and N. Cuellar.
1993. Planktonic and benthic feeding by the reef associated vermilion snapper, *Rhomboplites aurorubens* (Teleostei, Lutjanidae). Fish. Bull. 91:699–709.

Stearns, S.
1884. On the position and character of the fishing grounds of the Gulf of Mexico. Bull. U.S. Fish. Comm. 4:289–290.

Stuck, K. C., H. M. Perry, and R. W. Heard.
1979. An annotated key to the Mysidacea of the north central Gulf of Mexico. Gulf Res. Rep. 6: 225–238.

Sweatman, H. P. A.
1993. Tropical snapper (Lutjanidae) that is piscivorous at settlement. Copeia 1993:1137–1139.

Szedlmayer, S. T.
1997. Ultrasonic telemetry of red snapper, *Lutjanus campechanus*, at artificial reef sites in the northeast Gulf of Mexico. Copeia 1997:846–850.

Szedlmayer, S. T., and K. W. Able.
1993. Ultrasonic telemetry of age-0 summer flounder, *Paralichthys dentatus*, movements in a southern New Jersey estuary. Copeia 1993:728–736.

Szedlmayer, S. T., and J. Conti.
1999. Nursery habitats, growth rates, and seasonality of age-0 red snapper, *Lutjanus campechanus*, in the northeast Gulf of Mexico. Fish. Bull. 97:626–635.

Szedlmayer, S. T., and R. L. Shipp.
1994. Movement and growth of red snapper, *Lutjanus campechanus*, from an artificial reef area in the northeastern Gulf of Mexico. Bull. Mar. Sci. 55: 887–896.

Williams, A. B.
1968. Substrate as a factor in shrimp distribution. Limnol. Oceanog. 3:283–290.

Individual growth rates and movement of juvenile white shrimp (*Litopenaeus setiferus*) in a tidal marsh nursery*

Stacey Webb
Florida Department of Environmental Protection
Water Quality Standards and Special Projects Program
2600 Blair Stone Road, M.S. 3560
Tallahassee, Floida 32399
E-mail address: stacey.feken@dep.state.fl.us

Ronald T. Kneib
UGA Marine Institute
Sapelo Island, Georgia 31327

Abstract—We measured growth and movements of individually marked free-ranging juvenile white shrimp (*Litopenaeus setiferus*) in tidal creek subsystems of the Duplin River, Sapelo Island, Georgia. Over a period of two years, 15,974 juvenile shrimp (40–80 mm TL) were marked internally with uniquely coded microwire tags and released in the shallow upper reaches of four salt marsh tidal creeks. Subsequent samples were taken every 3–6 days from channel segments arranged at 200-m intervals along transects extending from the upper to lower reach of each tidal creek. These collections included 201,384 juvenile shrimp, of which 184 were marked recaptures. Recaptured shrimp were at large an average of 3–4 weeks (range: 2–99 days) and were recovered a mean distance of <0.4 km from where they were initially marked. Mean residence times in the creek subsystems ranged from 15.2 to 25.5 days and were estimated from exponential decay functions describing the proportions of marked individuals recaptured with increasing days at large. Residence time was not significantly correlated with creek length (Pearson=–0.316, P=0.684), but there was suggestive evidence of positive associations with either intertidal (Pearson r=0.867, P=0.133) or subtidal (Pearson r=0.946, P=0.054) drainage area. Daily mean specific growth rates averaged 0.009 to 0.013 among creeks; mean absolute growth rates ranged from 0.56–0.84 mm/d, and were lower than those previously reported for juvenile penaeids in estuaries of the southeastern United States. Mean individual growth rates were not significantly different between years (t-test, P>0.30) but varied significantly during the season, tending to be greater in July than November. Growth rates were size-dependent, and temporal changes in size distributions rather than temporal variation in physical environmental factors may have accounted for seasonal differences in growth. Growth rates differed between creeks in 1999 (t-test, P<0.015), but not in 1998 (t-test, P>0.5). We suggest that spatial variation in landscape structure associated with access to intertidal resources may have accounted for this apparent interannual difference in growth response.

Manuscript approved for publication 30 September 2003 by Scientific Editor.
Manuscript received 20 January 2004 at NMFS Scientific Publications Office.
Fish. Bull. 102:376–388 (2004).

In 2001, shrimp became the most popular seafood in the United States when per capita consumption (1.54 kg) surpassed that of canned tuna (1.32 kg) for the first time in recorded history (NOAA[1]). Although 77% of the catch is from the Gulf of Mexico, commercial fisheries in Atlantic coastal states of the southeastern United States also depend heavily on penaeid shrimp populations. Of the three most common estuarine-dependent penaeid species (*Litopenaeus setiferus, Farfantepenaeus aztecus,* and *F. duorarum*)[2] harvested in the South Atlantic Bight, white shrimp *Litopenaeus setiferus* dominate, comprising >70% of the catch in the region (North Carolina to the east coast of Florida) and 75–87% in South Carolina and Georgia (NMFS[3]).

Concerns over the possibility of depleting the resource as early as the 1930s led to intensive studies of the life cycle (Lindner and Anderson, 1956; Williams, 1984). The white shrimp has an annual life cycle that can be divided into offshore (oceanic) and inshore (estuarine) phases. Adults spawn in Atlantic waters in spring and the postlarvae migrate into estuaries, aided by flood tides and wind-generated currents (Lindner and Anderson, 1956; Wenner et al., 1998). Postlarvae penetrate into the shallow upper reaches of the nursery habitat where juveniles achieve a substantial portion of their adult body mass before moving into deeper creeks, rivers, and sounds where they approach maturity and emigrate seaward to spawning areas (Muncy, 1984; Williams, 1984).

Given the commercial importance and early interest in this species, surprisingly little research has focused on the juvenile stages within tidal marsh nursery habitats (Minello and Zimmerman, 1985; Zein-Eldin and Renaud, 1986; Knudsen et al., 1996; McTigue and Zimmerman, 1998). Seasonal migrations and ontogenetic movements of white shrimp between coastal ocean spawning grounds and estuarine nurseries are well known (Dall et al., 1990), as are the sometimes extensive migrations of adult shrimp along the Atlantic coast, primarily to the south during fall and early winter, and northward in late winter and early spring (Lindner and Anderson, 1956; Shipman, 1983). Within the estuary, juvenile white

*Contribution 921 of the Univerisity of Georgia Marine Institute, Sapelo Island, GA.

[1] NOAA (National Oceanic and Atmospheric Administration. 2002. Shrim p overtakes canned tuna as top U.S. seafood. Website: http://www.noaanews.noaa.gov/stories/s970.htm. [Accessed: 28 August 2002.]

[2] These species were all previously included in the genus *Penaeus*, but the subgenera were elevated to genera by Pérez-Farfante and Kensley (1997).

[3] NMFS (National Marine Fisheries Service). 2002. Unpubl. data. Website: http://www.st.nmfs.gov/st1/commercial/index.html. [Accessed 29 August 2002.]

shrimp, in contrast to other penaeid species, are found across a wider range of environmental conditions and habitats (Kutkuhn, 1966) and often make tidal excursions between subtidal and vegetated intertidal habitats to forage (Mayer, 1985; Kneib, 1995; 2000). However, relatively little is known about movements within subtidal creeks of the primary nursery areas, and the degree to which individuals exhibit fidelity to a particular tidal creek drainage system is unknown.

Direct measurement of juvenile shrimp growth rates within the nursery have also been rare. Most growth estimates for free-ranging juvenile shrimp are based on analyses of size-frequency data, which can be misleading (Loesch, 1965). Shrimp grow rapidly while in the estuarine nursery throughout the summer and early fall, and juveniles approach adult, or commercially harvestable size within 2–4 months after immigration to the estuary (Kutkuhn, 1966; Williams, 1984). Mean absolute growth rates of 0.7–1.1 mm/d are commonly reported for many penaeids (Dall et al., 1990). However, growth studies are difficult to compare because the rate of growth may vary between years and among seasons, as well as with size, age, and sex of individuals (Perez-Farfante, 1969). Growth estimates for *Litopenaeus setiferus* range widely, from 10 to 65 mm/month (Williams, 1984). Previous estimates were based on a variety of approaches including experimental studies in aquaria and ponds (Pearson, 1939; Johnson and Fielding, 1956), size distributions from tagging studies of adults (Lindner and Anderson, 1956), length-frequency distributions of juveniles in field samples (Gunter, 1950; Williams, 1955; Loesch, 1965; Harris, 1974; Mayer, 1985), mark-recapture of uniform size ranges of subadults and adults (Klima, 1974), and mark-recapture of shrimp in marsh ponds (Knudsen et al., 1996). Many estimates of growth for small (<80 mm TL) juvenile *L. setiferus* have been extrapolated from mark-recapture studies of larger (>100 mm TL) individuals (Lindner and Anderson, 1956; Harris, 1974; Klima, 1974). However, there is a paucity of empirical data on growth rates of small, free-ranging juvenile white shrimp within natural estuarine nursery habitats. The purpose of the present study was to provide reliable data on growth and movements of individual juvenile white shrimp within a natural estuarine nursery environment and to initiate an assessment of spatial variation in habitat quality in relation to tidal marsh landscape structure.

Recent innovations in tagging techniques have produced an effective way to obtain information on individual organisms through the use of sequentially numbered binary-coded microwire tags (Northwest Marine Technology, Inc. Shaw Island, WA). Microwire tags were first used in tagging experiments by Jefferts et al. (1963) and have since been used successfully to tag a variety of crustaceans including prawns (Prentice and Rensel, 1977), crayfish (Isely and Eversole, 1998), blue crabs (van Montfrans et al., 1986; Fitz and Weigert, 1991), and lobsters (Krouse and Nutting, 1990; Uglem and Grimsen, 1995). Results of these studies and others generally show that tag retention rates are high and tagging has little effect on the growth or survival of the fishes and crustaceans in which microwire tags have been used. In a laboratory study involving 240 juvenile white shrimp, Kneib and Huggler (2001) confirmed that tag retention was high (~98%), growth rates between tagged and control individuals were not significantly different, and the best location (based on tag retention and survival) for tag injection was in the muscle tissue of the abdomen. This type of tag allows for identification of individuals because each tag is etched with a unique number encoded in binary form. In addition, the tag is completely internal and inconspicuous, thus eliminating problems associated with external tags (e.g., streamer-type tags) that might interfere with molting or increase predation risk (Garcia and LeReste, 1981; van Montfrans et al., 1986; Isely and Eversole, 1998).

Materials and methods

Study area

All samples were collected from four tidal creek subsystems associated with the Duplin River on the west side of Sapelo Island, Georgia. The Duplin River tidal drainage (~11 km^2) includes almost 10 km^2 of tidal salt marsh that is inundated twice daily by unequal tides with a mean range of 2.1 m (Wadsworth, 1980). Smooth cordgrass (*Spartina alterniflora*) is the dominant vegetation in the intertidal marshes of this area. Seasonal water temperatures average between 10°C and 30°C, and salinity is characteristically polyhaline, ranging from 15 to 30 ppt (Kneib, 1995). Freshwater flow into the system is intermittent and originates largely from local upland runoff and indirect flows by several interconnected tidal channels from the Altamaha River about 8 km to the southwest (Ragotzkie and Bryson, 1955).

Tidal creeks included in this study were Post Office Creek (PO) and Stacey Creek (SC) in 1998, and the East and West forks (EF, WF, respectively) of the upper Duplin River in 1999 (Fig. 1). Logistical constraints precluded sampling shrimp populations from more than two creek systems within the same year, and different pairs of creeks were chosen in each of the two years to broaden the spatial coverage of the study. High-resolution black and white photographs (1:16000 scale) from an aerial survey of the region in December 1989 were used to measure broad-scale structural characteristics of the creek systems, including areal extent of the intertidal and subtidal portions of each drainage. The metrics and methods of extracting the information from the photographs are fully described elsewhere (see Webb and Kneib, 2002).

Field sampling

Shrimp were collected by cast net along the shallow (<1 m depth) edges of the subtidal portion of each creek system during low tide. Preliminary studies showed that 1.52-m diameter nets with ca. 1-cm mesh size collected the range of juvenile shrimp sizes (40–80 mm) targeted for marking in this study. All samples were collected within 2–3 hours of low tide to ensure that the shrimp popula-

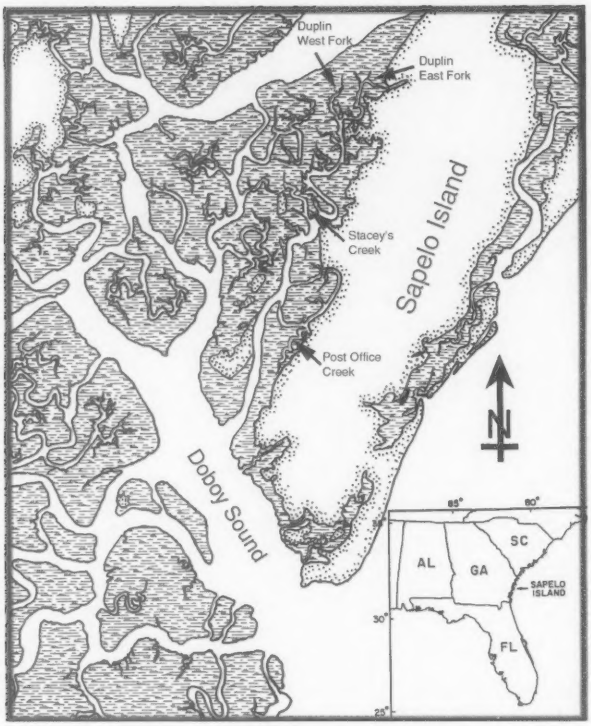

Figure 1

Map of the salt marsh estuary in the vicinity of Sapelo Island, Georgia, showing locations of the tidal creek subsystems within the tidal drainage of the Duplin River.

tion was restricted to the tidal creek channels and had no refuge in the intertidal vegetation. A series of stations, at intervals of approximately 200 m, was established along the length of the subtidal portion of each creek from the upper reaches to the mouth, so that the number of stations within a creek depended on the navigable length of the subtidal channel. There were 13 stations in PO, 11 in SC, 9 in EF, and 7 in WF. Salinity, water temperature, and dissolved oxygen were measured near the surface (<1 m depth) at the mouth of the tidal creek on each day of sampling by using a YSI model 85 meter (YSI, Inc. Yellow Springs, OH). Juvenile shrimp were marked with uniquely coded microwire tags (1.1 mm long×0.25-mm diameter, Northwest Marine Technology [NMT], Inc. Shaw Island, WA), which were injected into the muscle tissue of the first abdominal segment. We used a hand-held multishot injector (NMT) that was designed to cut, magnetize, and inject sequentially coded tags from a continuous stainless-steel wire spool. Each tag was etched with six lines of binary code that could be read under a microscope (25×) and translated into a set of numbered coordinates. Only three of the coded lines were required to identify a unique individual. A master line contained a distinguishing sequence code that was necessary to properly interpret codes on data lines designated D3 and D4. The numerical values associated with these coded lines were entered into a sequential tag conversion computer program (GR [Growth Rate], version 1.3, Northwest Marine Technology, Inc. Shaw Island, WA) that output the unique tag number corresponding to those coordinates.

A reference tag was archived for every shrimp marked in order that the code on either side of the tag injected into a shrimp was known with certainty. This was necessary to ensure positive identification of recaptured individuals because the injector was designed only to cut tags to a known length (1.1 mm) and did not distinguish between the beginning and end of sequential codes and often cut tags that included a portion of two adjacent codes. Prior to their release, marked shrimp were passed across a magnetometer (NMT) which signaled the presence of the ferromagnetic tag with an audible tone and flashing light. All shrimp collected after these marking sessions were scanned in the same manner and when a tag was detected, it was removed from the recaptured shrimp, cleaned and read under the microscope. The two reference tags bracketing the recovered tag were then located in the archive set to determine the date, location, and initial length at release of the marked shrimp. Thus the growth rate, time at large, and distance between points of release and recapture could be determined with certainty for individual shrimp.

Shrimp were marked and released only in the upper reaches of each tidal creek. During the marking process, small batches of shrimp (<50 individuals) were collected and held in insulated plastic coolers. Water in the coolers was exchanged each time a new batch of shrimp was collected. Only active individuals, 40–80 mm total length (TL, tip of the rostrum to end of the telson) and in apparently good condition, were candidates for marking. The marking process required a minimum field crew of two researchers. One measured shrimp and recorded data, while the other injected tags and released marked shrimp at the edge of the tidal creek.

We attempted to mark 1000 shrimp during a 3-day period in each tidal creek near the beginning of every month from July to November in both years. It was not possible to tag shrimp in both creeks simultaneously; therefore shrimp were marked and released in week 1 during the first week of the month, then in creek 2 during the second week of the month. The remainder of the month was spent collecting marked shrimp (Fig. 2). Inclement weather and mechanical problems with the tagging equipment sometimes prevented us from achieving the goal of tagging 1000 shrimp per creek within the first week of each month. In August 1998, the tag injector malfunctioned on the first day of tagging in SC and was unavailable for several weeks while it was being refurbished. Consequently, sampling was suspended in SC during that time. Although the same problem occurred while we attempted to mark shrimp from the EF in September 1999, we continued sampling in an attempt to recapture shrimp tagged in previous months.

A total of 6 sampling events after marking were planned in each creek per month (Fig. 2). A sample consisted of the combined contents of 10 haphazard casts of the net along the edge of the tidal creek within each station per sampling date. Shrimp populations were usually sampled at 3-day intervals for 21 days beginning from the midpoint of the marking period. A consistent exception was the second sample in the series, which occurred at a 6-day interval to accommodate the marking effort in the second creek and to keep the sampling effort consistent in all creeks. Inclement weather interrupted the sampling schedule on occasion and when unfavorable conditions persisted for more than 3 days, some of the planned sampling events after marking were cancelled; some months were represented by fewer than 6 sampling events. Sampling was terminated when, as a result of normal seasonal emigration from the nursery areas, shrimp densities declined to the point that they could no longer be consistently collected from the tidal creeks by cast net (19 November 1998 and 21 November 1999).

Catches of marked shrimp from each station were retained in separate plastic bags, placed on ice, and transported to the laboratory. A subsample of shrimp from each station (every tenth individual) was measured (TL, mm) to construct size distributions. If a sample included fewer than 100 shrimp, all were measured. Sex was not determined. All individuals were scanned for the presence of tags and when a marked shrimp was detected, it was measured (TL, mm) before the tag was removed and stored in a plastic vial for reading at a later date. For each recapture, we recorded date, creek, station of recapture (i.e., distance from original release site) and size of fish.

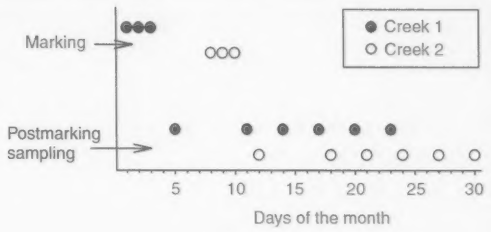

Figure 2

Schedule for monthly marking and postmarking field schedule for the juvenile white shrimp study.

Daily instantaneous (specific) growth rates (mm/[mm/d]) were calculated as

$$[(\ln L_2 - \ln L_1)/t],$$

where L_2 = total length (mm) of an individual on the date of recapture;
L_1 = initial total length (mm) on the date of tagging; and
t = number of days at large.

Daily absolute growth rates (mm/d) also were calculated (L_2-L_1/t) to facilitate comparison with estimates from previous studies. Displacement (distance moved) was determined by comparing the location of recapture with the original location at marking. Residence time within a tidal creek was determined from a plot of the proportion of recaptured individuals against time-at-large for each creek system. First, using the Regression Wizard in the computer program SigmaPlot® (version 8.0, SPSS, Inc. Chicago, IL), we fitted the data to an exponential decay function:

$$(y=a \times e^{-bt}),$$

where y = the proportion of total recaptures;
t = time at large; and
a and b = the estimated parameters.

Constraints imposed on the fit were a=1 (because the proportion of total recaptures could not exceed 1) and b>0 (because this was an exponential decay function). Mean residence time for shrimp in each creek was then estimated from the area below the fitted curves describing the proportion of recaptures with time at large. This was calculated with the macro function "area below curves" included in the "Toolbox" menu selection of SigmaPlot® (vers. 8.0, SPSS, Inc. Chicago, IL) which uses the trapezoidal rule to estimate the area under curves.

Statistical analyses

Most of the data analyses used statistical procedures in version 8.0 of the computer software package Systat®

(SPSS, Inc. Chicago, IL). When parametric tests were performed, residuals were analyzed to determine whether the data met the required assumptions (Sokal and Rohlf, 1995). Levene's test was used to evaluate conformity to the assumption of variance homogeneity among groups. When this assumption was violated, the data were transformed and retested. If the assumptions were still not met, then an appropriate nonparametric test was applied (e.g., Kruskal-Wallis one-way analysis of variance). Two sample *t*-tests were used to compare spatial and temporal variation in water temperature, salinity, and dissolved oxygen between creeks within a year and between years. August was omitted in comparisons of data between creeks in 1998, and between years because sampling in SC was suspended during August 1998. Regression analyses were performed to determine whether there were significant linear relationships between initial shrimp length and growth rates within each tidal creek. One-way ANOVA (controlling for the covariate initial length) was used to test for differences in growth rates between creeks within each year. A similar approach (controlling for initial size) was used to test for monthly (seasonal) differences in growth rate within years. If growth rates did not differ significantly between creeks, the data were pooled within year, otherwise creeks were treated separately. Only individuals at large for a month or less (to ensure that growth was representative of individual months) were included in the analyses.

Shrimp at large for fewer than 3 days were excluded from the statistical analyses to reduce certain anticipated biases associated with estimating growth rates. These included 1) measurement error (assumed to be at least 1 mm), which would likely represent a substantial proportion of the growth rate estimate when absolute change in size was small; 2) increments of growth associated with molting (Dall et al., 1990), which could either underestimate growth for shrimp that had been at large for a short time or had not molted since they were tagged or overestimate growth if shrimp were recaptured shortly after the first molt following marking; and 3) size-specific growth, where shrimp marked at a relatively small size and smaller shrimp exhibit a higher relative growth, so that early recaptures could represent larger than average growth rates.

Results

Physical parameters

Average water temperature, salinity, and dissolved oxygen (measured at the mouth of each tidal creek) were similar between creeks within years (see Table 1 in Webb and Kneib, 2002). In 1998, temperature ranged from 18.9 to 33.4°C, salinity from 18.2 to 28.0 ppt, and dissolved oxygen from 1.4 to 11.3 mg/L. In 1999, temperature ranged from 15.0 to 33.4°C, salinity from 23.9 to 32.5 ppt, and dissolved oxygen from 0.8 to 7.1 mg/L. Temperature followed expected seasonal patterns each year; mean values were highest in summer and declined toward autumn. Results of *t*-tests with separate variance estimates showed no significant differences between years in either mean temperature ($=0.14$, df=134.0, $P=0.80$) or dissolved oxygen ($t=1.82$, df=115.9, $P=0.07$) but mean salinity was significantly ($t=11.63$, df=122.7, $P<0.01$) higher in 1999 (28.1 ppt) than in 1998 (24.8 ppt). Cumulative rainfall was 83.9 cm/yr in 1998 and 82.9 cm/yr in 1999 (Garbisch[4]). These values were indicative of drought conditions because they were well below the long-term mean annual precipitation value of ca. 132 cm/yr reported for Sapelo Island between May 1957 and March 2003 (Southeast Regional Climate Center[5]).

Growth

Shrimp collections during recapture efforts ranged from 20,077 to 78,724 individuals, but the proportion of marked individuals recaptured was low in both years, averaging just over 1% (Table 1). However, the recaptures included 184 individuals for which growth rates and net movements within the nursery were known precisely.

Daily absolute growth rates of individuals, which ranged from 0.25 to 2.5 mm, averaged 0.86, 0.78, 0.84, and 0.61 mm at PO, SC, WF and EF, respectively. The mean values are on the low end of the range reported in previous studies of juvenile *Litopenaeus setiferus* with other methods and conducted in different locations (Table 2). Daily specific growth rates were size-dependent in both years. Negative linear relationships between growth rate and initial size (i.e., smaller shrimp grew relatively faster) was the prevalent trend in all creeks (Fig. 3). No significant difference ($t=1.19$, df=74, $P=0.237$) in growth was detected between PO and SC, where mean (±SD) specific (instantaneous) daily growth rates were 0.014 ±0.006 and 0.012 ±0.007, respectively. In 1999, shrimp exhibited significantly ($t=2.12$, df=56, $P=0.038$) higher mean specific growth rates in the WF (0.014 ±0.008) compared to the EF (0.010 ±0.006) of the Duplin River. The physical environment was similar at these sites (Webb and Kneib, 2002), and there was no significant difference ($t=1.43$, df=81, $P=0.156$) in the mean final sizes of shrimp recaptured from these sites. However, the mean (±SD) initial size of marked shrimp at EF (61.3 ±8.3) was significantly ($t=2.20$, df=81, $P=0.031$) larger than at WF (56.0 ±10.9); therefore a lower specific growth rate was to be expected at EF.

On a finer temporal scale, seasonal variation in growth rates occurred in both years, more rapid growth early in the season, and a general increase in the mean size of individuals as the season progressed were evident (Fig. 4). The earlier observation that specific growth rate declined with size (Fig. 3) opens the possibility that seasonal variation in growth rates could be explained simply by

[4] Garbisch, J. Unpubl. data. Univ. Georgia Marine Institute Flume Dock Monitoring Station, NOAA, Sapelo Island National Estuarine Research Reserve. Univ. Georgia Marine Institute, Sapelo Island, GA 31327.

[5] Southeast Regional Climate Center. Unpubl. data. Website: http://water.dnr.state.sc.us/water/climate/sercc/climateinfo/historical/historical_ga.html. [Accessed 21 November 2003].

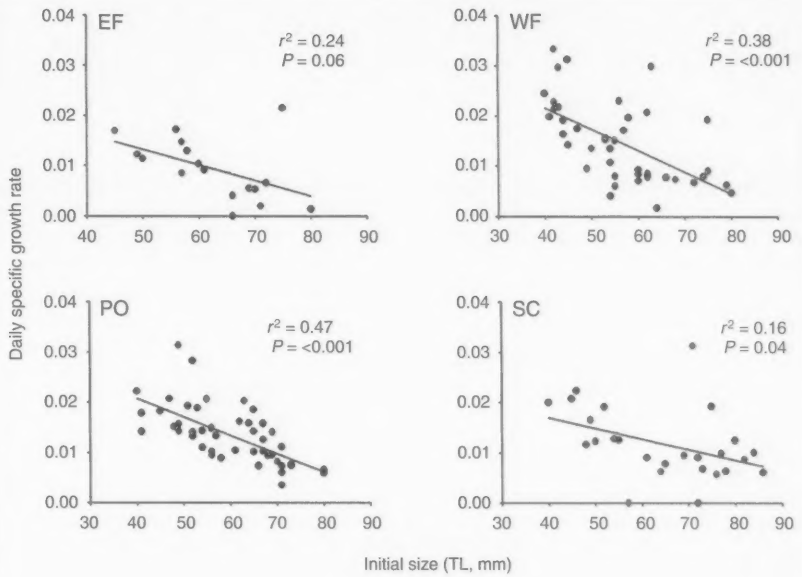

Figure 3

Scatter plots and linear regression results for the relationships between individual specific growth rates and initial sizes of recaptured juvenile shrimp in each tidal creek subsystem: EF = East Fork of Duplin River, WF = West Fork of Duplin River, PO = Post Office Creek, SC = Stacey Creek.

Table 1

Monthly summary of the number of shrimp tagged, number collected in subsequent sampling, and the number of tagged shrimp recaptured in each tidal creek.

Collection site and sampling process	July	August	September	October	November	Total
Post Office Creek						
Number tagged and released	1004	1077	1025	1000	779	4885
Number collected after tagging	7477	13,851	4730	8384	1298	35,740
Number of tags recaptured	13	16	16	22	1	68
Stacey Creek						
Number tagged and released	719	91	804	862	623	3099
Number collected after tagging	5877	0	5466	6376	2358	20,077
Number of tags recaptured	2	0	12	16	3	33
East Fork of Duplin River						
Number tagged and released	812	1000	0	1024	1003	3839
Number collected after tagging	23,080	14,490	11,020	14,804	3449	66,843
Number of tags recaptured	7	11	0	4	4	26
West Fork of Duplin River						
Number tagged and released	1008	1000	447	696	1000	4151
Number collected after tagging	32,130	17,926	10,954	10,600	7114	78,724
Number of tags recaptured	27	16	3	4	7	57

Table 2

Summary of estimated mean daily absolute growth rates for juvenile *Litopenaeus setiferus*. Growth rates were converted to mm/d if reported in other units.

Reference	Location	Growth rate (mm/d)	Method and notes
Gunter, 1950	Gulf of Mexico, Texas	0.8–1.3	Size frequency in field samples, juveniles 28–100 mm
Williams, 1955	coastal North Carolina	1.2	Size frequency in field samples, progression of maximum sizes of juveniles, 32–117 mm
Johnson and Fielding, 1956	Florida	1.3	Pond culture, juveniles
Lindner and Anderson, 1956	South Atlantic Bight and Gulf of Mexico	1.0–1.3	Extrapolated for juveniles 40–80 mm from Walford plot results using field mark-recapture (disc tags) data for individuals 70–205 mm
Loesch, 1965	Mobile Bay, Alabama	0.6–1.0	Size frequency from spring and summer field samples; progression of maximum sizes of juveniles 50–135 mm
		2.2	juveniles 15–70 mm
Klima, 1974	Galveston Bay, Texas	1.4–1.8	Extrapolated for juveniles 40–80 mm from Walford plot results determined from field mark-recaptured (stain-injected) subadults (117 mm)
	coastal Louisiana	1.0–1.3	Extrapolated for juveniles 40–80 mm from Walford plot results determined from field mark-recaptured (stain-injected) subadults (120 mm)
Mayer, 1985[1]	Sapelo Island, Georgia	0.9–1.5	Estimated from modal size-frequency data for juveniles 20–120 mm
Knudson et al., 1996	coastal Louisiana	0.3–0.7	Mark-recapture (injected pigments) of juveniles 45–58 mm (initial size) from coastal marsh ponds
This study	Sapelo Island, Georgia	0.6–0.9	Monthly mark-recapture (coded ferromagnetic tags) of juveniles 40–80 mm (initial size) from subtidal creeks

[1] Mean growth rates reported in Table 3 of Mayer (1985) were inconsistent with cohort data in Figure 8 of that thesis; rates reported here were derived directly from the data points shown in Figure 8 of Mayer's thesis.

changes in the average size of shrimp within the nursery over time.

We tested this hypothesis by comparing mean growth rates among months after controlling for initial length as a covariate. For these analyses, the 1998 data from PO and SC were pooled because there was no evidence of a difference in growth rates between these two creeks; the 1999 data from EF and WF were analyzed separately because mean growth rates differed between these two systems. After removing the effect of initial size, there was no significant difference among months in 1998, nor in 1999 at EF, but significant differences in mean growth remained detectable among months at WF (Table 3). The findings from WF also were unusual in that the covariate (initial length) was not a significant factor in the analysis. *Post hoc* multiple comparisons (Bonferroni, experiment-wise α=0.05) of mean growth rates among months (without accounting for the covariate) indicated that the specific growth rate in July (0.021) was significantly greater than that in the other months (0.007 to 0.011). This was the only statistically significant evidence of seasonal variation in growth apparently not associated with shrimp size distributions.

With respect to spatial variation in growth rates of juvenile shrimp, the most notable observation in this study was the relatively low mean growth rate observed at EF compared to the other sites. This difference could have resulted from the larger mean initial size of individuals tagged at EF (61.3 mm) compared with those at WF (56.0) in 1999. However, a similar difference in mean initial sizes of marked shrimp between tidal creek subsystems (SC, 64.2 mm; PO, 59.6 mm) in the previous year did not result in a significant difference in growth rates. When we considered the structural characteristics of each tidal creek at a landscape level, the EF subsystem had the largest tidal drainage area (119.5 ha.) compared to the other sites (58.6 to 104.9 ha.), but proportionally less of that area was intertidal drainage. There was a stronger correlation between mean growth rate (pooled across all individuals within a creek) and the proportion of the drainage area that was

Table 3

Summary of ANOVA results for the effects of month on specific growth rate of *Litopenaeus setiferus* after controlling for the covariate initial length. Only individuals at large between 3 and 32 days were included in the analyses. PO = Post Office Creek; SC = Stacey Creek; EF = East Fork of Duplin River; and WF = West Fork of Duplin River. Prob. = probability.

	1998 (PO and SC)			EF			WF		
Source	df	*F*-value	Prob.	df	*F*-value	Prob.	df	*F*-value	Prob.
Covariate (initial size)	1	30.77	<0.01	1	1.42	0.26	1	1.42	0.24
Month	4	1.25	0.30	3	0.74	0.55	4	4.32	<0.01
Error	70			11			36		

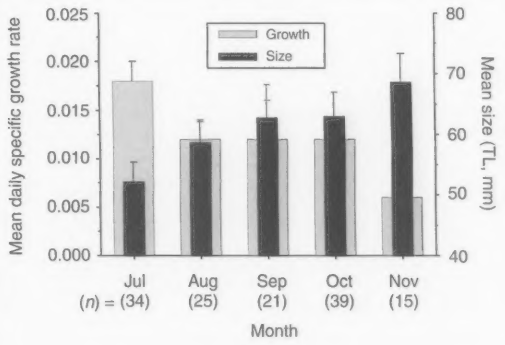

Figure 4

Mean daily specific growth rates and mean initial size of marked and recaptured juvenile white shrimp by month. Only individuals at large for 3 to 32 days were included. Error bars are 2 SEs and the number of observations are given in parentheses below each month.

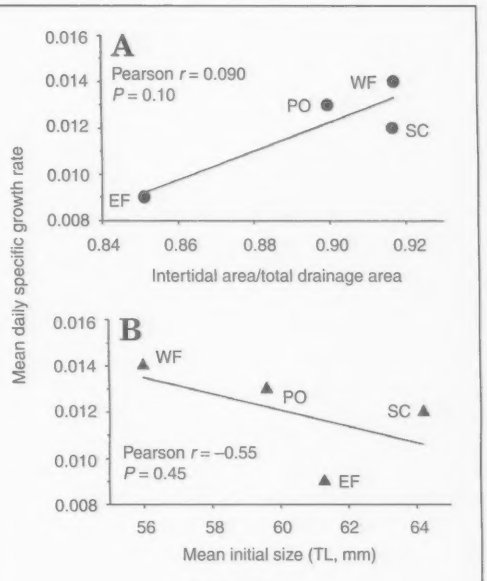

Figure 5

Correlations between mean daily specific growth rate in each tidal creek (PO=Post Office, SC=Stacey Creek, EF=East Fork of Duplin River, WF=West Fork of Duplin River). (**A**) The proportion of the tidal drainage area that is intertidal; (**B**) mean initial size of marked shrimp.

intertidal (Fig. 5A) than there was between growth and mean initial size (Fig. 5B) at the landscape level. There was almost no correlation between proportion of drainage area that was intertidal and initial mean size of marked shrimp (Pearson r=–0.18, P=1.0).

Residence time and movement of marked shrimp

Recaptured shrimp were at large for up to 99 days, but mean residence time for individuals marked in all four tidal creeks was between 15 and 26 days (Fig. 6). Mean residence time was greatest at EF and least at SC. During their time-at-large, net displacement (distance between mark and recapture sites) of the marked individuals ranged from 0 to 3000 m , but averaged 258–373 m in all creeks. There was no evidence of a significant relationship between time-at-large and mean net displacement (linear regression F=1.48; df=1,45; P=0.23), but movement was slightly related to shrimp size, and larger individuals showed greater displacement (Fig. 7). Variation in residence time among creek subsystems was not significantly correlated with length of the creek mainstem (Pearson r=–0.32, P=0.684), but there was evidence of positive associations with the amount of intertidal (Pearson r=0.87, P=0.133) and subtidal (Pearson r=0.95, P=0.054) drainage areas within each subsystem.

Most shrimp (93%) were recaptured in the same tidal creek subsystem in which they were originally marked, but there was some evidence of movement among creeks and between the subtidal and intertidal components of the shrimp nursery within creeks. The marked individual at large for the longest time (99 days) was recaptured at the same station where it was originally marked (net

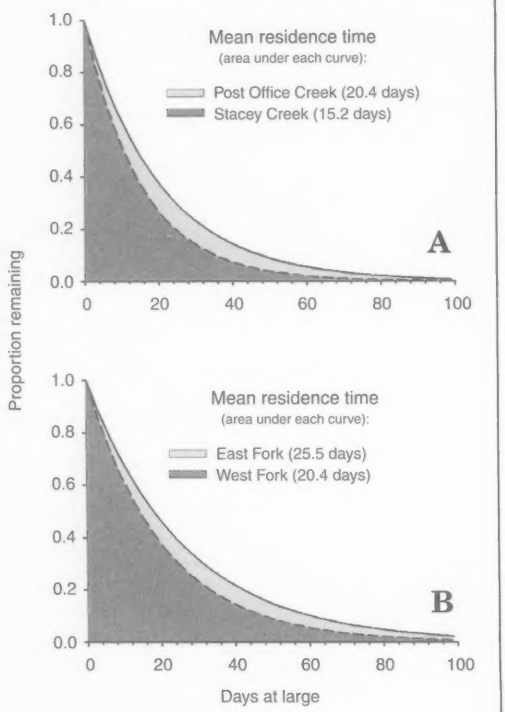

Figure 6

Estimates of mean residence times of marked shrimp in (**A**) tidal creeks sampled in 1998 and (**B**) creeks sampled in 1999. Estimates are based on the area under the curves describing the proportion of recaptured marked shrimp in each creek system that still remained to be captured after the indicated number of days-at-large.

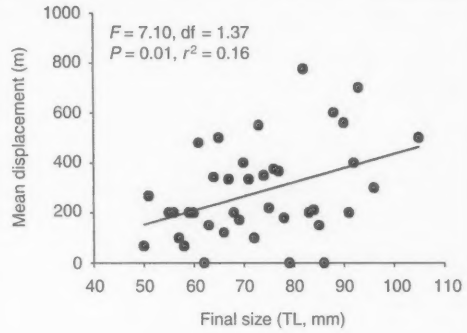

Figure 7

The effect of shrimp size at recapture on mean distance between mark and recapture locations (displacement). Summary results from the linear regression ANOVA performed on the data are shown. Values of mean displacement were based on data from 2–11 individuals within each size.

displacement=0 m). In contrast, one shrimp marked at PO demonstrated a net displacement of 3 km when it was recaptured at SC after 61 days at large. Nine shrimp (at large from 18 to 49 days) marked at WF were recaptured at EF, and two (at large 19 and 45 days) tagged at EF were recaptured at WF. It was not possible to determine precisely when these shrimp moved out of the creek in which they were tagged or how long they were present in the creek subsystem where they were ultimately recaptured. For the growth rate analyses, it was assumed that most growth occurred while the shrimp were in the creek and where individuals were marked. The mean (±SD) final size (mm, TL) of individuals that moved between creek subsystems was significantly (separate variance estimate t=2.62, df=16.9, P=0.018) larger (78.9 ±7.4) than that of the group tagged and recaptured in the same subsystem (71.3 ±13.1); the initial mean size of the two groups was nearly identical (57.5 ±10.8 and 57.7 ±10.4, respectively). Two shrimp (at large 7 and 17 days) tagged at EF were recaptured at high tide in flume weirs located 25 m into the interior of the intertidal marsh drained by that tidal creek subsystem. The flume weir samples were part of an ongoing study (Kneib, unpubl. data) to determine nekton use of the intertidal marsh surface (see Kneib, 1991, 1997; Kneib and Wagner, 1994).

Discussion

Growth

Mean growth rates of juvenile white shrimp measured in this study (0.6–0.9 mm/d) were near the lower end of the range of estimates previously reported for juvenile white shrimp along the U.S. Atlantic and Gulf coasts (Table 2). The principal difference between the present and previous studies is that the values presented in this study were based on direct measurements of free-ranging individual juvenile shrimp rather than on extrapolations from batch mark-recaptures of larger individuals or changes in modal size frequencies. The open nature of estuarine ecosystems, prolonged seasonal recruitment to the nursery, and ontogenetic differences in mortality and movement all may confound the interpretation of size-frequency data (Haywood and Staples, 1993). Given that our growth values were based on actual changes in the size of individuals rather than estimated from the apparent growth trajectories of cohorts, we are confident that the mean growth rates reported here accurately reflect those of free-ranging juvenile white shrimp (40–80 mm TL) in the polyhaline portion of the tidal marsh nursery habitat of coastal Georgia.

Temporal differences in observed growth rates in this study may have resulted from either variation in environmental conditions or spatial variation in habitat quality.

Penaeids are most abundant in tidal marsh nurseries when physical conditions (eg., temperature and salinity) appear optimal for their growth and survival (Zein-Eldin and Renaud, 1986), but environmental variability is characteristic of most estuaries and therefore is an obvious starting point for explaining observed differences in shrimp growth among sites or times. Salinity was the only environmental factor we measured that showed a significant difference between years but could not be associated with any interannual difference in mean growth rates.

Temperature may affect the growth and estuarine distribution of juvenile penaeids more than salinity (Vetter, 1983), and interactions between salinity and temperature may have even greater effects than variation in either factor alone (Zein-Eldin and Renaud, 1986). Mean temperatures throughout our study period (with the exception of November) in both years were largely within the optimum range for growth of white shrimp which, in the laboratory, was reported to be between 25° and 32.5°C (Zein-Eldin and Griffith, 1969). Higher temperatures generally contribute to faster growth in young penaeids (Perez-Farfante, 1969; Muncy, 1984), and therefore it seems reasonable to expect seasonal variation in temperature to be reflected in growth rates. However, this interpretation is confounded by the fact that growth rates also are size dependent (Fig. 3, Table 3) and that increases in mean size of juvenile white shrimp (Fig. 4) occurred while temperature in the nursery habitat was decreasing from the July maxima. It seems likely that growth rates of juvenile white shrimp were robust over the relatively narrow range of seasonal variation in temperature and salinity observed in the present study.

Alternatively, differences in growth between certain sites could be the result of spatial variation in habitat quality. This variation need not be a function of water quality, but rather a function of some structural aspect of the nursery habitat. There was a strong correlation between mean growth rates and the proportion of tidal creek drainage area that was intertidal. Only four creek subsystems were examined in ours study, and we recognize that this is an insufficient sample size to justify anything more than a suggestive hypothesis. However, evidence of relationships between the amount of intertidal habitat and penaeid shrimp production (Turner, 1977, 1992), as well as the amount of intertidal creek edge and juvenile shrimp abundance in adjacent subtidal creeks (Webb and Kneib, 2002), supports the contention that intertidal accessibility is an important component of nursery habitat quality for juvenile white shrimp. We propose that the ratio between intertidal and shallow subtidal habitat may be a key feature of white shrimp nursery habitat quality. When tidally inundated, the intertidal portion of marsh creek drainage systems is used extensively by juvenile white shrimp (Kneib, 1995, 2000), most likely as a rich foraging area (Kneib, 1997), and the shallow subtidal portion functions as a low tide refuge and corridor for the seasonal migration of postlarvae and subadults between the open estuary and coastal ocean spawning grounds and the juvenile nursery (Kneib, 1997, 2000).

Movement and residence time

Understanding the causes of broad-scale migration of penaeids has obvious implications for predicting commercial catches and therefore these causes have been the focus of research on shrimp movements for decades (Perez-Farfante, 1969; Muncy, 1984). However, finer-scale movements, which may affect growth and survival of juvenile shrimp within the estuary, are not as well known. Emigration of white shrimp from estuaries is determined by size, maturity, and environmental conditions (Muncy, 1984), and size plays a principal role (Dall et al., 1990). In the South Atlantic Bight, larger white shrimp (>100 mm TL) begin emigrating from the nursery to commercial fishing areas in the nearshore coastal ocean in August (Lindner and Anderson 1956, Shipman, 1983). We collected few shrimp >100 mm in the tidal marsh creeks, which is consistent with previous observations of ontogenetic migration to deeper waters. According to growth rates measured in this study, a shrimp of 40 mm TL would become large enough to emigrate from the estuary to the coastal ocean in 2–3 months (i.e., a shrimp tagged at 40 mm TL could reach 85–108 mm TL in 2.5 months).

The presence of high densities of small juvenile white shrimp in the upper reaches of Georgia's tidal marsh creeks (Harris, 1974; Hackney and Burbanck, 1976; Webb and Kneib, 2002) has supported the contention advanced by Weinstein (1979) that these areas are primary nurseries for juvenile fish and shellfish. However, it has been unclear whether these aggregations represent stable resident populations or are composed of tidal transients that constantly migrate among creek subsystems within the broader estuarine nursery. Young shrimp are known to move short distances to avoid unfavorable physiochemical conditions (Hackney and Burbanck, 1976; Dall et al., 1990) and routinely make tidally mediated excursions between subtidal and intertidal portions of the nursery to forage or escape predators (Kneib, 1995, 1997). Our findings showed that juvenile white shrimp also tended to remain resident in the upper reaches of tidal creeks where they were originally tagged until attaining a size (80–100 mm) at which they normally begin to emigrate from the nursery (Perez-Farfante, 1969).

Although there was some movement between tidal creek subsystems, the high level of site fidelity demonstrated by juvenile white shrimp was remarkable given the openness and degree of tidal flux in the Duplin River system (mean tide range=2.1 m). Data from the chemical analysis of shrimp tissue composition also suggest limited movements of juvenile penaeids within estuarine nurseries. Using the stable isotopes of carbon and nitrogen from muscle tissues of pink shrimp (*Farfantepenaeus duorarum*), Fry et al. (1999) traced shrimp movements within and between seagrass and mangrove habitats of southwestern Florida. They found distinct differences among individuals sampled from similar inshore habitat types separated by small (3–5 km) open water distances, indicating that individuals remained "resident" in specific portions of the estuary at least for several weeks. Noting a similar study in coastal Louisiana, Fry et al. (2003) suggested that

small juvenile brown shrimp (*Farfantepenaeus aztecus*) are more transient in suboptimal habitat (open bays and deeper channels) and exhibit less movement upon reaching optimal habitat (ponds and shallow channels).

The only study with which we can directly compare our findings on residence time and movements was conducted by Knudsen et al. (1996) near Calcasieu Lake, Louisiana, where tidal flux was considerably lower (mean tide range <0.6 m) and the system (marsh impoundments) was less open than that in the present study. Knudsen et al. (1996) marked batches of juvenile white shrimp (45–69 mm TL) by injection of colored pigments and released them into a pair of 35-ha. impoundments, each connected to the open estuary through a narrow channel that was fitted with screen deflectors and traps designed to collect all emigrating nekton. The mean time from release to emigration of juvenile white shrimp ranged from 30.2 to 59.9 days. Our estimates of tidal creek residence time for juvenile shrimp in Georgia tidal creeks was about half that reported for impoundments in Louisiana and may be explained by the differences in tidal flux and openness between the two systems. However, the values we observed were likely underestimates of the actual residence period of survivors within the creeks because they included losses due to mortality as well as emigration.

It seems clear from the studies conducted thus far that juvenile penaeids, once having entered the estuarine nursery, tend to remain within a limited spatial range where they are exposed to local conditions for several weeks. Our findings also provide evidence of spatial variation for both residence time and growth rate of juvenile white shrimp that is possibly attributable to structural differences in tidal creek subsystems. We suggest there may be an optimal value for the ratio of subtidal to intertidal drainage area within marsh creek systems that can achieve a favorable balance between suitable habitat (space) at low tide, which tends to enhance residence time and density of juvenile shrimp, while providing sufficient intertidal foraging habitat and predator refugia at high tide to promote high rates of juvenile shrimp growth and survival. Spatially explicit information on growth rates and the extent to which individual shrimp move within their estuarine nurseries are necessary initial steps toward meeting the challenge of maintaining quality nursery habitat for a sustainable shrimp fishery and satisfying other demands associated with human development in and around estuarine watersheds.

Acknowledgments

Several individuals provided field and laboratory assistance for this project, but we especially thank K. Feeley, J. Kneib, and J. Spicer for helping on a regular basis. The primary source of funding was a National Estuarine Research Reserve System Graduate Research Fellowship to S. Webb (NA870R0284) (Estuarine Reserves Division, Office of Ocean and Coastal Resource Management, NOS, NOAA), and matching funds provided by the University of Georgia Marine Institute. The Georgia Sea Grant College Program contributed funds for the purchase of an additional tag injector unit, which substantially improved the effectiveness of the mark-recapture program. The conceptual basis for this project was derived from research conducted under a grant from the National Science Foundation (DEB-9629621), which also contributed supplemental student support.

Literature cited

Dall, W., B. J. Hill, P. C. Rothlisberg, and D. J. Staples.
1990. The biology of the Penaeidae. *In* Advances in marine biology, vol. 27 (J. H. S. Blaxter and A. J. Southward, eds.), 489 p. Academic Press, London.

Fitz, H. C., and R. G. Weigert.
1991. Tagging juvenile blue crabs, *Callinectes sapidus*, with microwire tags: retention, survival, and growth through multiple molts. J. Crust. Biol. 11(2):229–235.

Fry, B., D. M. Baltz, M. C. Benfield, J. W. Fleeger, A. Gace, H. L. Haas, and Z. J.Quinones-Rivera.
2003. Stable isotope indicators of movement and residency for brown shrimp (*Farfantepenaeus aztecus*) in coastal Louisiana marshscapes. Estuaries 26:82–97.

Fry, B., P. L. Mumford, and M. B. Robblee.
1999. Stable isotope studies of pink shrimp (*Farfantepenaeus duorarum* Burkenroad) migrations on the southwestern Florida shelf. Bull. Mar. Sci. 65(2):419–430.

Garcia, S., and L. Le Reste.
1981. Life cycles, dynamics, exploitation and management of coastal penaeid shrimp stocks. FAO Fish. Tech. Paper 203, 215 p. FAO, Rome.

Gunter, G.
1950. Seasonal population changes and distributions as related to salinity, of certain invertebrates of the Texas coast, including the commercial shrimp. Publ. Inst. Mar. Sci., Univ. Texas 1:7–31.

Hackney, C. T., and W. D. Burbanck.
1976. Some observations on the movement and location of juvenile shrimp in coastal waters of Georgia. Bull. GA Acad. Sci. 34:129–136.

Harris, C. D.
1974. Observations on the white shrimp (*Penaeus setiferus*) in Georgia. Georgia Dep. Nat. Res. Contr. Ser. 27:1–47.

Haywood, M. D. E., and D. J. Staples.
1993. Field estimates of growth and mortality of juvenile banana prawn (*Penaeus merguiensis*). Mar. Biol. 116: 407–416.

Isely, J .J., and A. G. Eversole.
1998. Tag retention, growth, and survival of red swamp crayfish *Procambarus clarkii* marked with coded wire tags. Trans. Am. Fish. Soc. 127:658–660.

Jefferts, K. B., P. K. Bergmann, and H. F. Fiscusest.
1963. A coded wire identification system for macro-organisms. Nature 198:460–462.

Johnson, M. C., and J. R. Fielding.
1956. Propagation of the white shrimp, *Penaeus setiferus* (Linn.), in captivity. Tul. Stud. Zool. 2:49–56.

Klima, E. F.
1974. A white shrimp mark-recapture study. Trans. Am. Fish. Soc. 103(1):107–113.

Kneib, R. T.
1991. Flume weir for quantitative collection of nekton from vegetated intertidal habitats. Mar. Ecol. Prog. Ser. 75:29–38.

1995. Behaviour separates potential and realized effects of decapod crustaceans in salt marsh communities. J. Exp. Mar. Biol. Ecol. 193:239–256.
1997. The role of tidal marshes in the ecology of estuarine nekton. Oceanogr. Mar. Biol. Ann. Rev. 35:163–220.
2000. Salt marsh ecoscapes and production transfers by estuarine nekton in the southeastern United States. *In* Concepts and controversies in tidal marsh ecology (M. P. Weinstein and D. A. Kreeger, eds.), p. 267–291. Kluwer Academic Publishers, Dordrecht, The Netherlands.

Kneib, R. T., and M. C. Huggler.
2001. Tag placement, mark retention, survival and growth of juvenile white shrimp (*Litopenaeus setiferus* Pérez-Farfante, 1969) injected with coded wire tags. J. Exp. Mar. Biol. Ecol. 266:109–120.

Kneib, R. T., and S. L. Wagner.
1994. Nekton use of vegetated marsh habitats at different stages of tidal inundation. Mar. Ecol. Prog. Ser. 106:227–238.

Knudsen, E. E., B. D. Rogers, R. F. Paille, W. H. Herke, and J. P. Geaghan.
1996. Juvenile white shrimp growth, mortality, and emigration in weired and unweired Lousiana marsh ponds. North Am. J. Fish. Manag. 16:640–652.

Krouse, J. S., and G. E. Nutting.
1990. Evaluation of coded microwire tags inserted in legs of small juvenile American lobsters. *In* Fish-marking techniques (N. C. Parker, et al., eds.), p. 304–310. Am. Fish. Soc. Symp. 7, Bethesda, MD.

Kutkuhn, J. H.
1966. The role of estuaries in the development and perpetuation of commercial shrimp resources. Am. Fish. Soc. Spec. Publ. 3:16–36.

Lindner, M. J., and W. W. Anderson.
1956. Growth, migrations, spawning and size distribution of shrimp, *Penaeus setiferus*. Fish. Bull. 56:555–645.

Loesch, H.
1965. Distribution and growth of penaeid shrimp in Mobile Bay, Alabama. Publ. Inst. Mar. Sci., Univ. Texas 10:41–58.

Mayer, M. A.
1985. Ecology of juvenile white shrimp, *Penaeus setiferus* Linnaeus, in the Salt Marsh Habitat. M.S. thesis, 62 p. Georgia Inst. Technology, Atlanta, GA.

McTigue, T. A., and R. J. Zimmerman.
1998. The use of infauna by juvenile *Penaeus aztecus* Ives and *Penaeus setiferus* (Linnaeus). Estuaries 21:160–175.

Minello, T. J, and R. J. Zimmerman.
1985. Differential selection for vegetative structure between juvenile brown shrimp (*Penaeus aztecus*) and white shrimp (*Penaeus setiferus*), and implications in predator-prey relationships. Estuar. Coastal Shelf Sci. 20:707–716.

Muncy, R. J.
1984. Species profiles: life histories and environmental requirements of coastal fishes and invertebrates (South Atlantic)—white shrimp. U.S. Fish and Wildlife Service FWS/OBS-82/11.27, 19 p. U.S. Army Corps of Engineers TR EL-82-4, 19 p.

Pearson, J. C.
1939. The early life history of some American Penaeidae, chiefly the commercial shrimp *Penaeus setiferus* (Linn.). Fish. Bull. 30:1–73.

Perez-Farfante, I.
1969. Western Atlantic shrimps of the genus *Penaeus*. Fish. Bull. 67:461–591.

Perez-Farfante, I., and B. F. Kensley.
1997. Penaeoid and sergestoid shrimps and prawns of the world: keys and diagnoses for the families and genera. Memoires du Muséum National d'Historie Naturelle 175: 1–233.

Prentice, E. F., and J. E. Rensel.
1977. Tag retention of the spot prawn, *Pandalus platyceros*, injected with coded wire tags. J. Fish. Res. Board Can. 34:2199–2203.

Ragotzkie, R. A., and R. A. Bryson.
1955. Hydrography of the Duplin River, Sapelo Island, Georgia. Bull. Mar. Sci. Gulf Caribb. 5:297–314.

Shipman, S.
1983. Mark-recapture studies of penaeid shrimp in Georgia, 1978–1981. *In* Studies and assessment of Georgia's marine fisheries resources, 1977–1981 (S. Shipman, V. Baisden, and H. Ashley, eds.), p. 1–176. Georgia Dep. Nat. Res. Contr. Ser. 35.

Sokal, R. R., and F. J. Rohlf.
1995. Biometry: the principles and practice of statistics in biological research, 3rd ed., 887 p. W.H. Freeman and Co., New York, NY.

Turner, R. E.
1977. Intertidal vegetation and commercial yields of penaeid shrimp. Trans. Am. Fish. Soc. 106:411–416.
1992. Coastal wetlands and penaeid shrimp habitat. *In* Stemming the tide of coastal fish habitat loss (R. H. Stroud, ed.), p. 97–104. National Coalition for Marine Conservation, Savannah, GA.

Uglem, I., and S. Grimsen.
1995. Tag retention and survival of juvenile lobsters, *Hommarus gammarus*, marked with coded wire tags. Aquacult. Res. 26:837–841.

van Montfrans, J., J. Capelli, R. J. Orth, and C. H. Ryer.
1986. Use of microwire tags for tagging juvenile blue crabs (*Callinectes sapidus*). J. Crust. Biol. 6:370–376.

Vetter, E. A.
1983. The ecology of *Penaeus setiferus*: habitat selection, carbon and nitrogen metabolism, and simulation modeling. Ph.D. diss., 151 p. Univ. Georgia. Athens, GA.

Wadsworth, J. R.
1980. Geomorphic characteristics of tidal drainage networks in the Duplin River system, Sapelo Island, Georgia. Ph.D. diss., 247 p. Univ. Georgia, Athens, GA.

Webb, S. R., and R. T. Kneib.
2002. Abundance and distribution of juvenile white shrimp *Litopenaeus setiferus* within a tidal marsh landscape. Mar. Ecol. Prog. Ser. 232:213–223.

Weinstein, M. P.
1979. Shallow marsh habitats as primary nurseries for fishes and shellfish, Cape Fear River, North Carolina. Fish. Bull. 77:339–357.

Wenner, E. L., D. Knott, J. O. Blanton, C. Barans, and J. Amft.
1998. Roles of tidal and wind-generated currents in transporting white shrimp (*Penaeus setiferus*) postlarvae through a South Carolina (USA) inlet. J. Plank. Res. 20(12):2333–2356.

Williams, A. B.
1955. Contribution to the life histories of commercial shrimp (Penaeidae) in North Carolina. Bull. Mar. Sci. Gulf Caribb. 5:116–146.
1984. Shrimps, lobsters, and crabs of the Atlantic coast of the eastern United States, Maine to Florida, 550 p. Smithsonian Institution Press, Washington, D.C.

Zein-Eldin, Z. P., and G. W. Griffith.
1969. An appraisal of the effects of salinity and temperature on growth and survival of postlarval penaeids. FAO Fish. Rep. 57(3):1015–1026.

Zein-Eldin, Z. P., and M. L. Renaud.
1986. Inshore environmental effects on brown shrimp, *Penaeus aztecus*, and white shrimp, *P. setiferus*, populations in coastal waters, particularly of Texas. Mar. Fish. Rev. 48(3):9–19.

Does the California market squid (*Loligo opalescens*) spawn naturally during the day or at night? A note on the successful use of ROVs to obtain basic fisheries biology data

John Forsythe

National Resource Center for Cephalopods
University of Texas Medical Branch at Galveston
301 University Blvd
Galveston, Texas 77555-1163
E-mail address: john.forsythe@utmb.edu

Nuutti Kangas

Roger T. Hanlon

Marine Resources Center
Marine Biological Laboratory
Woods Hole, Massachusetts 02543

The California market squid (*Loligo opalescens* Berry), also known as the opalescent inshore squid (FAO), plays a central role in the nearshore ecological communities of the west coast of the United States (Morejohn et al., 1978; Hixon, 1983) and it is also a prime focus of California fisheries, ranking first in dollar value and tons landed in recent years (Vojkovich, 1998). The life span of this species is only 7–10 months after hatching, as ascertained by aging statoliths (Butler et al., 1999; Jackson, 1994; Jackson and Domier, 2003) and mariculture trials (Yang, et al., 1986). Thus, annual recruitment is required to sustain the population. The spawning season ranges from April to November and spawning peaks from May to June. In some years there can be a smaller second peak in November. In Monterey Bay, the squids are fished directly on the egg beds, and the consequences of this practice for conservation and fisheries management are unknown but of some concern (Hanlon, 1998). Beginning in April 2000, we began a study of the *in situ* spawning behavior of *L. opalescens* in the southern Monterey Bay fishing area.

The prevailing thought is that the majority of spawning activity takes place at night because fishermen have observed these squids mating under their bright lights (which are used to attract and capture squids) and because television documentaries have revealed mating and spawning activity in large aggregations at night. The scientific literature on reproductive behavior is sparse. There are some cursory observations of actively spawning *L. opalescens* during diver surveys of egg beds (McGowan, 1954; Fields, 1965; Hobson, 1965; Hurley, 1977). Some daytime spawning has been seen both in southern and northern California but Fields (1965) and Hixon (1983) suggested indirectly that most spawning occurs at night. Shimek et al. (1984) also suggested night spawning by *L. opalescens* in Canada. Other loliginid squids whose natural behavior has been studied in the field were found to be daytime spawners (e.g., *L. pealeii*, *L. vulgaris reynaudii*, *Sepioteuthis sepioidea*; summarized in Hanlon and Messenger, 1996).

To help resolve this issue, we conducted three field expeditions (28 April–8 May 2000, 10–17 September 2000, and 16–21 August 2001) using remotely operated vehicles (ROVs) deployed either from the RV *John Martin* (Moss Landing Marine Laboratory) or the commercial squid FV *Lady J*. The ROVs were tethered vehicles with onboard video cameras and lights. Live video signals were transmitted by the tether to shipboard VCRs where observational data were viewed and recorded. For the first field trip, a large S4 Phantom ROV was used; it was outfitted with a video camera and zoom lens with tilt capability, and the video was recorded on Hi8 format video decks. For the second and third trips, a smaller S2 inspection-class Phantom ROV on loan from the NOAA Sustainable Seas Expeditions was used; this ROV had a customized fiber-optic tether and the video data were recorded on mini-digital video cassettes. Our goal was to make ROV dives each day from approximately dawn to dusk and to make a few comparable all-night surveys. A combination of adverse weather conditions and technical problems with the ROVs rarely allowed continuous video observations. During dives, if squids were encountered, we used video to conduct focal animal samples on females (which were paired) for as long as squids were present, or as long as we could keep track of the same individuals. Unless absolutely necessary to see the squids (for instance at night or at depths greater than 30 m in turbid daytime conditions), lights were not used for video taping in an effort to minimize their impact on the mating squids. Squids acclimated within minutes to the ROVs. After the expeditions, the videotapes were studied and the behavioral and biological data were quantified on a multimotion playback VCR.

By "mating" we refer to the peculiar mating behavior of this species that is unique among loliginid squids. The male firmly grasps the female from her ventral side and holds her for minutes or hours in a "copulatory embrace" in a nearly vertical position. Both copulation (i.e., transfer of spermatophores) and deposition of egg capsules occur in this posture. For example, as the female exudes a new egg capsule, the male and female lower themselves in unison to the egg bed where the female deposits the egg capsule in the sand. We have reported elsewhere on egg-

Manuscript approved for publication
20 January 2004 by Scientific Editor.
Manuscript received 25 January 2004
at NMFS Scientific Publications Office.
Fish. Bull. 102:389–392 (2004).

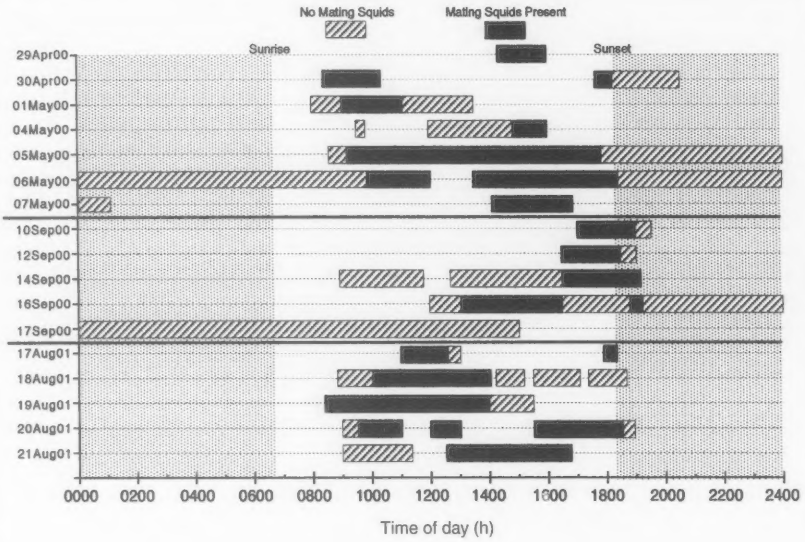

Figure 1

A summary of 154 spawning groups of *Loligo opalescens* showing the daily presence or absence of mating squids on egg beds in Monterey Bay, California. The horizontal bars represent the time periods when a ROV was on the bottom searching for mating squids during three different expeditions. Note three occasions in which operations were conducted continuously through the day and night, and also that spawning ceased at dusk.

laying frequency (Hanlon et al., in press). Only very rarely did we observe females laying eggs while unattended by a male; in these cases the female was moribund and laying her last few egg strands.

Results and discussion

We examined 28 hours of videotape recorded during 50 ROV dives over 18 days (divided into three expeditions). Figure 1 illustrates the relative presence or absence of mating *Loligo opalescens* throughout 24-hour periods. The large gaps in the daytime observation record were due to ROV problems. Although observation times varied daily, it is clear that normal mating and egg-laying behaviors were exclusively observed during daylight hours (ca. 0800–1800 hours but with some seasonal variation) and concluded near dusk. In all instances in Figure 1 where egg-laying extended into the early evening, these mating assemblages had formed during daylight hours and persisted slightly past sunset and the number of participating squids constantly decreased as sunset approached and passed. Observations were made throughout the night on three nights. Not only were no mating squids ever encountered around the egg beds at night, but generally no squids were encountered at all near the seabed, despite large aggregations that were present higher in the water column. Thus the 200–400 watt lights on the ROVs never induced any artificial spawning behavior because there were no squids present.

Figure 2 provides some quantification of Figure 1. This graph is based on 154 spawning groups that were videotaped and includes all three trips as well as the three "all night observations" illustrated in Figure 1. We were studying discrete groups of squids to examine mating dynamics and thus were sometimes biased to smaller groups of squids that could be kept in view. Overall, we observed that squids were present in greatest numbers in mid to late afternoon and absent during the night.

Our findings strongly indicate that the extensive egg beds produced at depths of 20–60 m in southern Monterey Bay (just beyond the kelp beds) are the result of daytime aggregations of mating *Loligo opalescens*. These benthic aggregations begin forming in the early morning hours and tend to be larger in the afternoon. Reproductive activity begins to wane toward sunset and comes to a near halt at sunset. We could find no evidence that egg laying occurs naturally during the night. All observations that we are aware of (mainly television documentaries) have occurred in the presence of artificial light sources near the surface provided either by fishermen or cinematographers. In the absence of artificial lighting, *L. opalescens* in South Monterey Bay does not aggregate into mating and spawning groups at night. Thus, we conclude that all significant egg deposition in the Monterey Bay fishery is the result of daytime aggregations of squids.

Two other ascribed characteristics of *L. opalescens* spawning are mass aggregations at the sea floor and subsequent die-offs after squids have spawned. Mass aggregations can be detected by standard fathometers used by commercial fishermen, who report that mass aggregations on the sea floor are rare in Monterey Bay. During our ROV operations we encountered only one large aggregation, which occurred on 21 August 2001. We estimated from our video recordings that there were approximately 3000–4000 squid in a 50-m^2 area on the sea floor and that intermittent egg laying was occurring over an area of ca. 2000 m^2 during a period of about 3 hours. Collectively, then, we recorded 154 very small spawning groups and one large spawning group. There was no mass die-off during or after this large spawning aggregation. Instead, we consistently observed in all spawning groups that females actively broke the embrace of the paired male and jetted strongly upwards away from the spawning groups and rejoined large schools in the upper water column. Thus, squids that dispersed from the egg beds were consistently in excellent condition—certainly not senescent or moribund. These observations corroborate the results of other studies on loliginid squids that spawn intermittently (Moltschaniwskyj, 1995; Maxwell and Hanlon, 2000). Twice we encountered large numbers of dead squids on the sea floor in the early morning, but in both instances the squid fishing fleet had been working in the same area the night before and it appeared as though these mortalities were associated with the purse-seine fishery; there were few eggs in those localities. McGowan (1954), Hobson (1965), and Cousteau and Diole (1973) reported that squids died after spawning in S. California. Various *Loligo* spp. are noted for flexible reproductive strategies (*cf.* Hanlon and Messenger, 1996) so it should not be surprising if *L. opalescens* occasionally engaged in large reproductive events. Our data suggest that small groups of squids (20–200 individuals) generally descend during the day and lay eggs for several hours before rejoining squids in the water column. We encourage other researchers to use ROVs or SCUBA without lights and with stealthy approaches to determine the natural diurnal spawning of *L. opalescens* throughout its range. Given our findings that active sexual selection processes are occurring during the day and that there is vertical migration between the large schools of squid in the water column and the small spawning groups at the substrate, it would be prudent, at the very least, to restrict daytime fishing directly over egg beds or to create protected spawning areas in southern Monterey Bay. This strategy would allow the complex mating system of *L. opalescens* to be played out without direct disruption by fishing activity. In such a short-lived species, annual recruitment to the population is necessary; thus sufficient eggs must be laid for each new generation to ensure a viable living resource.

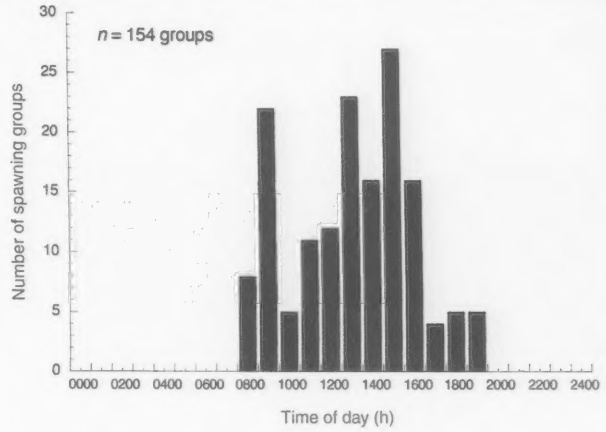

Figure 2

The number of squid spawning groups at the egg beds at different times of day (data pooled from three expeditions over 2 years; n=154 groups). A group is defined as a group of two or more mating pairs. These data correspond hour by hour with data in Figure 1.

Acknowledgments

We are most grateful for funding on NOAA grant UAF 98 0037 from the National Undersea Research Center (West Coast). Additional funding was provided by the David and Lucile Packard Foundation and the Sholley Foundation. J. Forsythe gratefully acknowledges financial support for travel from the National Institutes of Health, National Center for Research Resources (grant P40 RR0102423-23), and the Marine Medicine General Budget account of the Marine Biomedical Institute. N. Kangas gratefully acknowledges financial support from the Academy of Finland. We thank Sylvia Earle for loan of the Sustainable Seas ROV and we appreciate the professional efforts of Deep Ocean Exploration and Research (DOER) who supported the ROV operations. We especially thank John Rummel who helped begin this project, and Brett Hobson who kept it going at a critical juncture. We are thankful for expert shipboard assistance from the captains and crew of the RV *John Martin* and the FV *Lady J* (especially Captain Tom Noto). We benefitted from discussions with Bob Leos, Bill Gilly, Annette Henry, John Butler, Teirney Thies, and Sue Houghton.

Literature cited

Butler, J., D. Fuller, and M. Yaremko.
1999. Age and growth of market squid (*Loligo opalescens*) off California during1998. CalCOFI Rep. 40:191–195.

Cousteau J.-Y., and P. Diole.
1973. Octopus and squid: the soft intelligence, 304 p. Cassell, London.

Fields, W. G.
1965. The structure, development, food relations, reproduction, and life history of the squid *Loligo opalescens* Berry. Fish. Bull. 131:1–108.
Hanlon, R. T.
1998. Mating systems and sexual selection in the squid *Loligo*: How might commercial fishing on spawning squids affect them? CalCOFI Rep. 39:92–100.
Hanlon, R.T., N. Kangas, and J. W. Forsythe.
In press. Rate of egg capsule deposition, changing OSR and associated reproductive behavior of the squid *Loligo opalescens* on spawning grounds. Mar. Biol.
Hanlon, R. T., and J. B. Messenger.
1996. Cephalopod behaviour, 232 p. Cambridge Univ. Press, Cambridge.
Hixon, R. F.
1983. *Loligo opalescens*. *In* Cephalopod life cycles, vol. I, species accounts, 475 p. Academic Press, London.
Hobson, E. S.
1965. Spawning in the Pacific Coast squid. *Loligo opalescens*. Underwater Naturalist 3:20–21.
Hurley, A. C.
1977. Mating behavior of the squid *Loligo opalescens*. Mar. Behav. Physiol. 4:195–203.
Jackson, G. D.
1994. Statolith age estimates of the loliginid squid *Loligo opalescens*: corroboration with culture data. Bull. Mar. Sci. 54:554–557.
Jackson, G. D., and M. L. Domeier.
2003. The effects of an extraordinary El Nino/La Nina event on the size and growth of the squid *Loligo opalescens* off Southern California. Mar. Biol. 142:925–935.
Maxwell, M. R., and R. T. Hanlon.
2000. Female reproductive output in the squid *Loligo pealeii*: multiple egg clutches and implications for a spawning strategy. Mar. Ecol. Prog. Ser. 199:159–170.
McGowan, J. A.
1954. Observations on the sexual behavior and spawning of the squid, *Loligo opalescens*, at LaJolla, CA. Cal. Fish Game 40:47–54.
Moltschaniwskyj, N. A.
1995. Multiple spawning in the tropical squid *Photololigo* sp.: what is the cost in somatic growth? Mar. Biol. 124:127–135.
Morejohn, G. V., J. T. Harvey, and L. T.Krasnow.
1978. The importance of *Loligo opalescens* in the food web of marine vertebrates in Monterey Bay, California. *In* Biological, oceanographic, and acoustic aspects of the market squid, *Loligo opalescens* Berry (C. W. Recksiek and H. W . Frey, eds.), p. 67–98. Calif. Dep. Fish Game Fish Bull. 169.
Shimek, R. L., D. Fyfe, L. Ramsey, A. Bergey, J. Elliott, and S. Guy.
1984. A note on spawning of the Pacific market squid, *Loligo opalescens* (Berry, 1911), in the Barkley sound region, Vancouver Island, Canada. Fish. Bull. 82:445–446.
Vojkovich, M.
1998. The California fishery for market squid (*Loligo opalescens*). CalCOFI Rep. 39:55–60.
Yang, W. T., R. F. Hixon, P. E. Turk, M. E. Krejci, W. H. Hulet, and R. T. Hanlon.
1986. Growth, behavior, and sexual maturation of the market squid, *Loligo opalescens*, cultured through the life cycle. Fish. Bull. 84:771–798.

Incidental capture of loggerhead (*Caretta caretta*) and leatherback (*Dermochelys coriacea*) sea turtles by the pelagic longline fishery off southern Brazil

Jorge E. Kotas
IBAMA/Acordo Projeto TAMAR-
Instituto de Pesca/CPPM
Programa REVIZEE-SCORE SUL
Rodovia Osvaldo Reis 345 apt. 22 C
Itajaí-SC 88306-001, Brazil

Sílvio dos Santos
DTI-CNPq
Programa REVIZEE-SCORE SUL
Rua Ezio Testini 320
Santos-SP 11089-210, Brazil

Venâncio G. de Azevedo
DTI-CNPq
Programa REVIZEE-SCORE SUL
Av. Pavão 164
Caraguatatuba-SP 11676-520, Brazil

Berenice M. G. Gallo
Fundação Pró-TAMAR
Rua Antonio Athanásio 273
Ubatuba-SP 11680-000, Brazil

Paulo C. R. Barata
Fundação Oswaldo Cruz
Rua Leopoldo Bulhões 1480 - 8A
Rio de Janeiro - RJ 21041-210, Brazil
E-mail address (for P. C. R. Barata, contact author):
pbarata@alternex.com.br

Incidental capture of loggerhead and leatherback sea turtles by the surface longline fishery operating off the southern coast of Brazil, within Brazil's 200 mile exclusive economic zone (EEZ) and in international waters, and present catch-per-unit-of-effort (CPUE) data and estimates of average probability of death at capture for these species. Preliminary results of incidental captures of sea turtles by longliners during one longline trip in this area were presented by Barata et al.[2] In the present study we provide more detailed data from additional trips, including information concerning leatherback sea turtles, as well as analyses of these data. To our knowledge, this is the first detailed report about the incidental capture of sea turtles by the Brazilian commercial longline fleet.

Incidental capture in fishing gear is one of the main sources of injury and mortality of juvenile and adult sea turtles (NRC, 1990; Lutcavage et al., 1997; Oravetz, 1999). Six out of the seven extant species of sea turtles—the leatherback (*Dermochelys coriacea*), the green turtle (*Chelonia mydas*), the loggerhead (*Caretta caretta*), the hawksbill (*Eretmochelys imbricata*), the olive ridley (*Lepidochelys olivacea*), and the Kemp's ridley (*Lepidochelys kempii*)—are currently classified as endangered or critically endangered by the World Conservation Union (IUCN, formerly the International Union for Conservation of Nature and Natural Resources), which makes the assessment and reduction of incidental capture and mortality of these species in fisheries priority conservation issues (IUCN/Species Survival Commission, 1995).

Several studies have examined sea turtle bycatch by pelagic longline fisheries, especially in the North Atlantic and Pacific oceans (NRC, 1990; Nishemura and Nakahigashi, 1990; Tobias, 1991; Bolten et al., 1996; Williams et al., 1996; Lutcavage et al., 1997), but little is known about sea turtle bycatch in the South Atlantic. One of the most detailed reports on longline incidental captures in that area is that by Achaval et al. (2000), which documents the incidental capture of loggerhead and leatherback sea turtles in the southwestern Atlantic by longliners targeting swordfish (*Xiphias gladius*), tuna (*Thunnus obesus*), and other related species. Additional references, sometimes with scant detail, can be found in Weidner and Arocha (1999), Fallabrino et al. (2000), and Domingo et al.[1]

In this study, we report the incidental capture of loggerhead and leatherback sea turtles by the surface longline fishery operating off the southern coast of Brazil, within Brazil's 200 mile exclusive economic zone (EEZ) and in international waters, and present catch-per-unit-of-effort (CPUE) data and estimates of average probability of death at capture for these species. Preliminary results of incidental captures of sea turtles by longliners during one longline trip in this area were presented by Barata et al.[2] In the present study we provide more detailed data from additional trips, including information concerning leatherback sea turtles, as well as analyses of these data. To our knowledge, this is the first detailed report about the incidental capture of sea turtles by the Brazilian commercial longline fleet.

Materials and methods

Observations were carried out by three of the authors (JEK, SS, and VGA) during three trips aboard Brazil-flagged commercial longline vessels based in Itajaí, State of Santa Catarina, southern Brazil (Fig. 1). The trips occurred in 1998, the first (10 sets) between 13 March and 12 April (summer–fall), the second (13 sets) between 15 June and 5 July (fall–winter), and the third (11 sets) between 28 September and 13 October (spring), and took place between latitudes 27°30′S and 34°30′S and longitudes 36°00′W and 52°00′W (Fig. 1). The

[1] Domingo, A., A. Fallabrino, R. Forselledo, and V. Quirici. 2002. Incidental capture of loggerhead (*Caretta caretta*) and leatherback (*Dermochelys coriacea*) sea turtles in the Uruguayan long-line fishery in Southwest Atlantic. Presented at the 22nd Annual Symposium on Sea Turtle Biology and Conservation, Miami, USA, 4–7 April 2002. [Available from A. Domingo: Dirección Nacional de Recursos Acuáticos, Constituyente 1497, C.P. 11.200, Montevideo, Uruguay.]

[2] Barata, P. C. R., B. M. G. Gallo, S. dos Santos, V. G. Azevedo, and J. E. Kotas. 1998. Captura acidental da tartaruga marinha *Caretta caretta* (Linnaeus, 1758) na pesca de espinhel de superfície na ZEE brasileira e em águas internacionais. *In* Resumos Expandidos da XI Semana Nacional de Oceanografia, Rio Grande, RS, outubro de 1998, p. 579–581. Editora Universitária-UFPel, Pelotas, RS, Brazil. [Available from FURG, Oceanologia, Av. Itália, km 8, Campus Carreiros, C.P 474, Rio Grande, RS 96201-900, Brazil.]

Manuscript approved for publication
22 December 2003 by Scientific Editor.
Manuscript received 20 January 2004
at NMFS Scientific Publications Office.
Fish. Bull. 102:393–399 (2004).

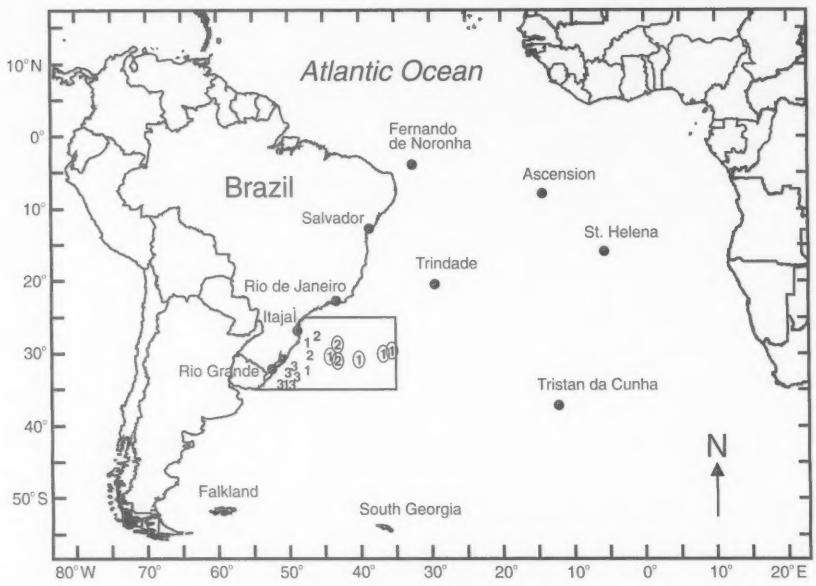

Figure 1

Fishing locations. Numbers 1, 2, and 3 indicate locations of the first, second, and third longline trips respectively; for each location, one or more sets were performed. Circled numbers indicate international waters outside the 200-mile Brazilian exclusive economic zone. The rectangular ocean area is limited by latitudes 25°S and 35°S and longitude 35°W. The fishing location farthest to the east is about 1320 km (713 nautical miles) from Itajaí, State of Santa Catarina, Brazil, the home port of the fishing vessels.

seabed in this area ranged from the continental shelf border to abyssal plains, including submarine elevations (e.g., Rio Grande). Operation depths, ranging from 170 to 4000 m, were obtained from nautical charts.

The first and second trips were aboard the *Yamaya III*, a 20.7-m, 325-hp engine, 30-t hold capacity, 10-crew longliner, and the third trip was aboard the *Basco*, a 24.4-m, 330-hp engine, 70-t hold capacity, 11-crew longliner. The vessels targeted swordfishes, sharks (mainly blue sharks, *Prionace glauca*) and tunas (*Thunnus albacares*, *T. alalunga* and *T. obesus*). Their fishing gear was the U.S.-style monofilament nylon longline, with 200–300 m sections between buoys, and each section contained four to five gangions set 40–60 m apart. Buoy dropper length ranged between 10 and 20 m, and gangion length ranged between 13 and 20 m. Each non-offset "J" hook (Swordfish 9/0) was baited with Argentine shortfin squid (*Illex argentinus*) and had a yellow chemical light stick hung over it. The average number of hooks per set was 1030, 992, and 950 on the first, second, and third trips, respectively.

On the first and second trips, the mainline was set off the stern by means of a line shooter so that a marked catenary was formed between buoys, allowing the hooks to operate at a greater depth. In this case, the maximum hook depth may have reached more than 40 m. On the third trip, the vessel *Basco* did not use a line shooter, and thus the hook depth for that trip may have been shallower. The longline gear was set around 5:30 PM, and was retrieved early in the morning. The average soak time was 7 h 30 min. For each set, the date, time, geographical position, number of hooks, and sea surface temperature were recorded. The species and condition (i.e., if the animal was alive or dead) of captured turtles were recorded; specimens with no apparent movement were considered dead.

Incidentally captured loggerhead turtles were taken aboard and hooks and lines were then removed. Whenever possible curved carapace length (CCL) and width were measured, and the turtles were double tagged (inconel tags style 681, National Band and Tag Co., Newport, KY), according to Projeto TAMAR's (Projeto Tartaruga Marinha, the Brazilian sea turtle conservation program) standard methods (Marcovaldi and Laurent, 1996). In some cases, it was not possible to bring loggerhead sea turtles on board the fishing vessel and, because of their great size, no leatherback sea turtles were brought on board. On these occasions, the turtles were pulled close to the boat and the gangions were then cut to free the turtles with the hooks still attached to them; however the length of the line remaining on the turtle was not recorded. None of these turtles was measured or tagged, although some of the leatherback sea turtles were filmed on video. No additional data and measurements, other than those presented in this study, were obtained.

Table 1

Data referring to fishing practices, sea surface temperature (°C), and capture of loggerhead and leatherback sea turtles, by trip. CPUE = catch-per-unit-of-effort (number of captured turtles/1000 hooks).

					Loggerheads				Leatherbacks			
Trip	Date	No. of sets	Average hooks/set	Average sea surface temperature	Alive (tagged)	Dead	Condition not recorded	CPUE	Alive	Dead	Condition not recorded	CPUE
1	13 Mar 98–12 Apr 98	10	1030	13.6	84 (17)	15	9	10.49	1	—	—	0.10
2	15 Jun 98–5 Jul 98	13	992	21.4	28 (12)	4	—	2.48	13	1	—	1.09
3	28 Sep 98–13 Oct 98	11	950	18.9	5 (5)	—	—	0.48	5	—	—	0.48
Total		34	990		117 (34)	19	9	4.31	19	1	—	0.59

CPUE (number of captured turtles/1000 hooks) was calculated separately for each species. Straight carapace lengths in published data were converted to CCL by using the formula in Teas (1993) to compare the CCL of captured loggerhead sea turtles to carapace length data found in the literature. To assess the significance of the difference in the proportion of dead loggerhead or leatherback sea turtles among trips, exact tests were applied, because ordinary chi-square tests are not reliable when expected cell frequencies are too small. The test statistics were $\chi^2 = \Sigma[(Observed - Expected)^2/Expected]$, and exact probabilities were computed for all tables with marginal frequencies fixed at the observed values (Lindgren, 1993, p. 376). These probability calculations were performed by a Turbo Pascal vers. 7 program (Borland International, Scotts Valley, CA). The confidence interval for overall probability of death at capture was calculated by the method in Zar (1996, p. 524). Ordinary chi-square tests and analysis of variance (ANOVA) tests followed Zar (1996) and were carried out with the software Systat vers. 9 (SPSS Inc., Chicago, IL). In the statistical tests, type-I error α was equal to 0.05. In the construction of Figure 2, to avoid overlapping of data points, the temperatures (but not the CPUEs) were jittered, that is, a small amount of uniform random noise was added to the temperature measurements (Cleveland, 1993).

Results

From a total of 34 sets and 33,650 hooks, 145 loggerhead (CPUE=4.31/1000 hooks) and 20 leatherback (CPUE=0.59/1000 hooks) sea turtles were captured. There was a significant difference in loggerhead CPUE among the trips (chi-square test, χ^2=137.3, P<0.001), but the proportion of dead loggerhead sea turtles was not significantly different among the trips (exact test, P=0.656). The average probability of death at capture for loggerhead sea turtles for the three trips was 0.140 (95% confidence interval=[0.086, 0.210]). For leatherback sea turtles, the difference in CPUE among the trips was significant (chi-square test, χ^2=9.76, P<0.01), and the proportion of dead leatherback sea turtles was not significantly different among the trips (exact test, P=1.000). The average probability of death at capture for leatherback sea turtles for the three trips was 0.050 (95% confidence interval=[0.001, 0.249]).

Table 2

Curved carapace length (CCL, cm) for loggerhead sea turtles, by trip.

Trip	Sample size	Average CCL	Standard deviation	Minimum	Maximum
1	19	56.9	7.3	46.0	70.0
2	30	57.2	7.5	46.0	68.0
3	5	67.0	5.9	58.0	73.0
Total	54	58.0	7.7	46.0	73.0

The average sea surface temperature (Table 1) was significantly different among the trips (ANOVA, n=34, F=55.37, P<0.001). The average temperature on the first trip was significantly lower than those on the second and third trips, and the average temperature on the second trip was significantly higher than that on the third trip (Tukey's *post hoc* test). For loggerhead sea turtles, CPUEs were generally higher on the first trip, which had the lowest average temperature (Fig. 2). For leatherback sea turtles, on the contrary, the lowest CPUEs were found on the first trip, on which only one leatherback sea turtle was captured (Table 1).

CCLs of captured loggerheads were in the range of 46–73 cm. Detailed loggerhead CCL data are presented in Table 2. There was a significant difference in average loggerhead CCL among the trips (Table 2); the average CCL on the third trip was greater than those on the first and second trips (ANOVA, n=54, F=4.209, P=0.020, Tukey's

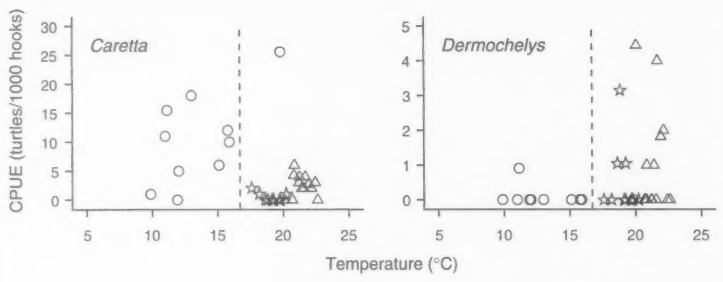

Figure 2

CPUE (number of captured turtles/1000 hooks) by sea surface temperature (°C) in each set, by species. Circles = first trip, triangles = second trip, stars = third trip. In each graph, the dashed vertical line, arbitrarily placed at 16.7 °C, marks a separation between the temperatures in the first trip and those in the second and third trips (except for one set in the first trip). Note that the two graphs have different vertical scales, and that, in the construction of this figure, temperature measurements (but not the CPUEs) have been jittered (see "Materials and methods" section).

post hoc test). Although leatherback sea turtles could not be hauled aboard for measurements, on board observations and video recordings indicated that they were subadult or adult animals.

Most of the loggerhead turtles were hooked through their mouths or esophagus, but a small number were hooked through their flippers or were found to be simply entangled in the lines. Loggerhead sea turtles taken aboard had their hooks removed, sometimes in a careless way that caused severe injury, and they were then returned to the sea. Leatherback sea turtles were found entangled in the lines or hooked either through the flippers or carapace or through the mouth. Because no leatherback sea turtle was hauled aboard, we could not tell if any were hooked in the esophagus.

Discussion

Achaval et al. (2000) reported data obtained from nine trips aboard two different longline vessels operating within the Uruguayan EEZ and in international waters in the South Atlantic in different seasons of the year, and employing different longline methods. Those authors reported that 28 loggerhead and 28 leatherback sea turtles were captured in 86 sets with 75,033 hooks in zones I and II, that correspond approximately to the fishing area covered in this study, yielding a CPUE of 0.37/1000 hooks for both loggerhead and leatherback sea turtles. For loggerhead sea turtles, there was a significant difference between our CPUE (Table 1) and that of Achaval et al. (chi-square test, χ^2=226.4, P<0.001); whereas for leatherback sea turtles no significant difference was found (chi-square test, χ^2=1.97, P=0.161).

Although the variations in CPUE observed in our study could be explained by differences in temperatures (Fig. 2), other physical, spatial, or temporal factors (or a combination of these factors) could be involved. The trips were carried out at different times of the year (Table 1); the third trip was more to the south and closer to the coast, and the first trip had sets more to the east (Fig. 1).

Our estimates of sea turtle mortality at capture may be lower than the actual mortality rates from longlines because our estimates do not consider postrelease deaths derived from 1) wounds caused by hooks removed from turtles on board, 2) embedded hooks and lines, and 3) stress caused by capture itself. Other researchers have also recognized that, because of factors such as these, there is great uncertainty in the estimates of mortality levels for sea turtles captured in longline gear (Balazs and Pooley, 1994; Eckert, 1994).

Captured loggerhead sea turtles were smaller (Table 2) than loggerhead sea turtles nesting in Brazil (minimum CCL=83.0 cm, average CCL= 103.0 cm, nesting season 1982–83 through nesting season 1999–2000; Projeto TAMAR[3]) and in several places in the North Atlantic and the Caribbean (minimum CCL=75.4 cm, average CCL in the range of 94.0–105.1 cm; Dodd, 1988). However, loggerhead sea turtles nesting in Cape Verde, in the northeastern Atlantic, are smaller than those nesting in those other places: minimum CCL=68.0 cm, average CCL=82.9 cm, data from 1998 (Cejudo et al., 2000). There is an overlap between the observed CCL range and that of adult Cape Verde loggerhead sea turtles (seven loggerhead turtles out of 54 observed, or 13.0%, had a CCL equal or greater than the minimum Cape Verde CCL), but the average CCL of the captured loggerhead sea turtles (Table 2) was well below that of loggerhead sea turtles nesting in Cape Verde. We estimate that the captured loggerhead sea turtles were generally juveniles, although a small number of them could have been adult turtles. However, size is

[3] Projeto TAMAR. 2000. Unpubl. data. Caixa Postal 2219, Salvador, BA 40210-970, Brazil.

not a reliable indicator of maturity or breeding status for sea turtles (Miller, 1997).

Along the southern coast of Brazil (between latitudes 23°S and 33°S), loggerhead sea turtles stranded or incidentally captured in fishing gear with CCLs as small as 32.5 cm have been observed (Projeto TAMAR[4]), but usually loggerhead sea turtles found in that region have CCLs greater than 50 cm, most commonly in the range of 60–90 cm (Pinedo et al., 1998; Bugoni et al., 2001; Projeto TAMAR[4]). Loggerhead sea turtles have also been found in Uruguay and Argentina (Frazier, 1984; Fallabrino et al., 2000). Their CCLs in those countries have been reported to be in the approximate range of 50–115 cm (Frazier, 1984). The loggerhead sea turtles reported here have an average CCL smaller than that usually observed for loggerhead sea turtles stranded or captured in southern Brazil, Uruguay, and Argentina, although most of the turtles (45 out of 54, or 83%) had CCLs equal to or greater than 50 cm, that is, they were within the size range for that region.

Cumulative evidence obtained from genetic and size-distribution data around oceanic basins, as well as tag returns, shows that the ontogenetic development of loggerhead sea turtles involves a pelagic juvenile stage (Carr, 1987; Musick and Limpus, 1997; Bolten et al., 1998). Transoceanic developmental migrations establishing a link between juveniles in feeding grounds and hatchlings from nesting beaches on opposite sides of the ocean basin have been demonstrated through genetic analysis for the North Atlantic and North Pacific (Bowen et al., 1995; Bolten et al., 1998). It has been suggested that a similar pattern may be expected for the South Atlantic (Bolten et al., 1998), where loggerhead sea turtles nest in Brazil and possibly in Africa (Marcovaldi and Laurent, 1996; Fretey, 2001). The incidental captures reported in our study, indicating the use of the pelagic environment by juvenile loggerhead sea turtles in the South Atlantic, support the hypothesis of transoceanic developmental migrations for those turtles in that ocean. Future genetic analysis of turtles incidentally captured in the South Atlantic would help to clarify their natal origin.

For leatherback sea turtles, there are important nesting grounds in the Atlantic, mainly in French Guiana and Suriname in South America, and Gabon and Congo in Africa (Spotila et al., 1996; Fretey, 2001). Leatherback sea turtles are known to travel long distances from their nesting beaches into pelagic waters (Goff et al., 1994; Morreale et al., 1996; Eckert and Sarti, 1997; Eckert, 1998). Satellite telemetry data indicate that leatherback sea turtles nesting in eastern South Africa can enter the South Atlantic (Hughes et al., 1998; Hughes[5]). In the southwestern Atlantic, leatherback sea turtles have been observed or captured in Brazil, Uruguay, and Argentina (Frazier, 1984; Pinedo et al., 1998; Achaval et al., 2000; Fallabrino et al., 2000; Bugoni et al., 2001).

Some measure of the significance of the three trips reported in the present study in terms of the potential for turtle capture and mortality in the South Atlantic longline fishery can be obtained by looking at information concerning the total fishing effort in the study area. In 1999, the Brazilian longline fleet consisted of 70 longliners (42 Brazilian and 28 leased foreign vessels); among them, 33 vessels were operating out of ports in southern Brazil, in the states of São Paulo, Santa Catarina, and Rio Grande do Sul. In that year, the total number of hooks of that longline fleet (both Brazilian and leased vessels) amounted to 13,598,260 hooks (ICCAT[6]). However, the southwestern Atlantic is fished not only by Brazil-based longliners, but also by longliners from Uruguay, Chile, Japan, Taiwan, and Spain (Folsom, 1997; Weidner and Arocha, 1999; Weidner et al., 1999). According to ICCAT's (International Commission for the Conservation of Atlantic Tunas) CATDIS data set (ICCAT)[7] longliners operating during 1995–97 in the area delineated by the present study (latitudes 25°S and 35°S and longitude 35°W, or eight ICCAT 5×5° statistical blocks, Fig. 1) had an average annual catch of tunas and swordfishes of 6885 metric tons (t) (the total hold capacity of the vessels on the three trips reported in this study was 130 t). However, due to unreported landings by vessels flying flags of convenience (FAO, 2001; FAO[8]) and other sources, the estimate obtained from ICCAT data should be considered a minimum estimate of the total annual tuna and swordfish catch (ICCAT[9]). Furthermore, because North Atlantic stocks of swordfishes and some species of tuna are considered overfished (NMFS[10]), quota or closure regulations (or both) in the North Atlantic may be driving longline fleets to the South Atlantic, increasing the risk of incidental capture of sea turtles there.

In Brazil, sea turtle capture is prohibited by federal legislation (Marcovaldi and Marcovaldi, 1999), and measures have been taken to address the problem of incidental capture by longlines and other kinds of fishing

[4] Projeto TAMAR. 2000. Unpubl. data. Rua Antonio Athanásio 273, Ubatuba, SP 11680-000, Brazil.

[5] Hughes, G. R. 2002. Personal commun. Ezemvelo KZN Wildlife, P O Box 13053, Cascades 3202, South Africa.

[6] ICCAT (International Commission for the Conservation of Atlantic Tunas). 2001. National report of Brazil. Report for biennial period, 2000–2001, part I (2000), vol. 1, English version, p. 312–315. Calle Corazón de María, 8, 28002 Madrid, Spain.

[7] ICCAT (International Commission for the Conservation of Atlantic Tunas). 2002. CATDIS dataset. Calle Corazón de María, 8, 28002 Madrid, Spain. [Available from http://www.iccat.org.]

[8] FAO (Food and Agriculture Organization of the United Nations). 2001. International plan of action to prevent, deter and eliminate illegal, unreported and unregulated fishing, 24 p. FAO, Rome. [Available from http://www.fao.org/docrep/003/y1224e/y1224e00.htm.]

[9] ICCAT (International Commission for the Conservation of Atlantic Tunas). 1999. Detailed report for swordfish, ICCAT SCRS swordfish stock assessment session (Madrid, Spain, September 27 to October 4, 1999), 176 p. Calle Corazón de María, 8, 28002 Madrid, Spain.

[10] NMFS (National Marine Fisheries Service). 2000. 2000 stock assessment and fishery evaluation for Atlantic highly migratory species, 150 p. U.S. Dep. Commer., NOAA, NMFS, Highly Migratory Species Management Division, 1315 East-West Highway, Silver Spring, MD 20910.

gear. Since 2001, Projeto TAMAR has been developing and implementing (through partnerships with other institutions) an action plan whose main objective is to reduce incidental sea turtle capture, including captures occurring in the open sea (Marcovaldi et al., 2002). The action plan includes, among other things, an assessment of fishery-related sea turtle mortality, the development of mitigation methods, and a proposal of adequate conservation and enforcement policies (Marcovaldi et al., 2002). However, because the longline fleet is composed of vessels from many nations, the reduction of incidental capture in the open sea calls for international cooperation (Eckert and Sarti, 1997; Trono and Salm, 1999; Crowder, 2000).

The observations reported in this study and the presence of a sizable longline fleet operating in the southwestern Atlantic indicate 1) the need for research to clarify habitat use by sea turtles in that part of the ocean (Eckert and Sarti, 1997; Bolten et al., 1998), 2) the need for continued research to quantify the impact of longline fishing on sea turtles in the pelagic realm of that ocean (Balazs and Pooley, 1994; Eckert, 1994), and 3) the implementation of conservation measures for sea turtles in that environment. We suggest the implementation of an International Observers Program on board longliners operating throughout the South Atlantic ocean.

Acknowledgments

This note is the result of observations made possible through an agreement between the REVIZEE Program (National Program for the Assessment of the Sustainable Fishing Potential of the Exclusive Economic Zone Live Resources, a Brazilian Government program) and Projeto TAMAR's station at Ubatuba, State of São Paulo. We would like to thank José Kowalsky of the Kowalsky fishing company and Marcelino Talavera (Itajaí, State of Santa Catarina), owners of the vessels *Yamaya III* and *Basco,* respectively, for kindly allowing access to the fishing vessels, and the crew of the two longliners, and also the fishing research center Centro de Pesquisa e Extensão Pesqueira do Sudeste-Sul–CEPSUL/IBAMA (Itajaí, State of Santa Catarina), and particularly Jorge Almeida de Albuquerque, for making this research possible. We also thank Larisa Avens and Matthew Godfrey for their generous reviews of the paper, and the two anonymous referees, whose suggestions helped to improve our work. Projeto TAMAR is affiliated with IBAMA (the Brazilian Institute for the Environment and Renewable Natural Resources), is co-managed by Fundação Pró-TAMAR, and officially sponsored by Petrobras. In Ubatuba, TAMAR is supported by Ubatuba's municipal government (Prefeitura Municipal de Ubatuba). S.S. and V.G.A. were supported by CNPq (Brazilian National Research Council).

Literature cited

Achaval, F., Y. H. Marin, and L. C. Barea.
2000. Captura incidental de tortugas con palangre pelágico oceánico en el Atlántico sudoccidental. *In* Captura de grandes peces pelágicos (pez espada y atunes) en el Atlántico Sudoccidental, y su interacción con otras poblaciones (G. Arena and M Rey, eds.), p. 83–88. Instituto Nacional de Pesca, Programa de las Naciones Unidas para el Desarrollo, Montevideo, Uruguay.

Balazs, G. H., and S. G. Pooley (comps.).
1994. Research plan to assess marine turtle hooking mortality: results of an expert workshop held in Honolulu, Hawaii, November 16–18, 1993. NOAA Tech. Memo. NOAA-TM-NMFS-SWFSC-201, 166 p.

Bolten, A. B., K. A. Bjorndal, H. R. Martins, T. Dellinger, M. J. Biscoito, S. E. Encalada, and B. W. Bowen.
1998. Transatlantic developmental migrations of loggerhead sea turtles demonstrated by mtDNA sequence analysis. Ecol. Appl. 8:1–7.

Bolten, A. B., J. A. Wetherall, G. H. Balazs, and S. G. Pooley (comps.).
1996. Status of marine turtles in the Pacific Ocean relevant to incidental take in the Hawaii-based pelagic longline fishery. NOAA Tech. Memo. NOAA-TM-NMFS-SWFSC-230, 167 p.

Bowen, B. W., F. A. Abreu-Grobois, G. H. Balazs, N. Kamezaki, C. J. Limpus, and R. J. Ferl.
1995. Trans-Pacific migrations of the loggerhead turtle (*Caretta caretta*) demonstrated with mitochondrial DNA markers. Proc. Natl. Acad. Sci. USA 92: 3731–3734.

Bugoni, L., L. Krause, and M. V. Petry.
2001. Marine debris and human impacts on sea turtles in southern Brazil. Mar. Pollut. Bull. 42:1330–1334.

Carr, A.
1987. New perspectives on the pelagic stage of sea turtle development. Conserv. Biol. 1: 103–121.

Cejudo, D., I. Cabrera, L. F. López-Jurado, C. Évora, and P. Alfama.
2000. The reproductive biology of *Caretta caretta* on the Island of Boavista (Republic of Cabo Verde, Western Africa). NOAA Tech. Memo. NMFS-SEFSC-443:244–245.

Cleveland, W. S.
1993. Visualizing data, 360 p. Hobart Press, Summit, NJ.

Crowder, L.
2000. Leatherback's survival will depend on an international effort. Nature 405:881.

Dodd, C. K., Jr.
1988. Synopsis of the biological data on the loggerhead sea turtle *Caretta caretta* (Linnaeus 1758). U.S. Fish Wildl. Serv. Biol. Rep. 88, 110 p.

Eckert, S. A.
1994. Evaluating the post-release mortality of sea turtles incidentally caught in pelagic longline fisheries. NOAA Tech. Memo. NMFS-SWFSC-201:106–110.
1998. Perspectives on the use of satellite telemetry and other electronic technologies for the study of marine turtles, with reference to the first year long tracking of leatherback sea turtles. NOAA Tech. Memo. NMFS-SEFSC-415:44–46.

Eckert, S. A., and M. L. Sarti.
1997. Distant fisheries implicated in the loss of the world's largest leatherback nesting population. Mar. Turtle Newsl. 78:2–7.

Fallabrino, A., A. Bager, A. Estrades, and F. Achaval.
2000. Current status of marine turtles in Uruguay. Mar. Turtle Newsl. 87:4–5.

FAO (Food and Agriculture Organization of the United Nations).
2001. Report of the second technical consultation on illegal,

unreported and unregulated fishing. Rome, 22–23 February 2001. FAO Fisheries Rep. 646, 38 p. FAO, Rome.

Folsom, W. B.
1997. World swordfish fisheries: an analysis of swordfish fisheries, market trends and trade patterns, vol. VI: Western Europe. NOAA Tech. Memo. NMFS-F/SPO-29, 324 p.

Frazier, J.
1984. Las tortugas marinas en el Atlántico sur occidental. *In* Serie divulgación no. 2, p. 2–21. Associacion Herpetologica Argentina, La Plata, Argentina.

Fretey, J.
2001. Biogeography and conservation of marine turtles of the Atlantic coast of Africa. CMS Technical Series Publ. no. 6, 429 p. UNEP/CMS Secretariat, Bonn, Germany.

Goff, G. P., J. Lien, G. B. Stenson, and J. Fretey.
1994. The migration of a tagged leatherback turtle, *Dermochelys coriacea*, from French Guiana, South America, to Newfoundland, Canada, in 128 days. Can. Field Nat. 108:72–73.

Hughes, G. R., P. Luschi, R. Mencacci, and F. Papi.
1998. The 7000 km oceanic journey of a leatherback turtle tracked by satellite. J. Exp. Mar. Biol. Ecol. 229: 209–217.

IUCN (International Union for Conservation of Nature and Natural Resources) Species Survival Commission.
1995. A global strategy for the conservation of marine turtles, 25 p. IUCN, Gland, Switzerland.

Lindgren, B. W.
1993. Statistical theory, 4th ed., 633 p. Chapman & Hall, New York, NY.

Lutcavage, M. E., P. Plotkin, B. Witherington, and P. L. Lutz.
1997. Human impacts on sea turtle survival. *In* The biology of sea turtles (P. L. Lutz and J. A. Musick, eds.), p. 387–409. CRC Press, Boca Raton, FL.

Marcovaldi, M. A., and A. Laurent.
1996. A six season study of marine turtle nesting at Praia do Forte, Bahia, Brazil, with implications for conservation and management. Chelonian Conserv. Biol. 2:55–59.

Marcovaldi, M. A., and G. G. dei Marcovaldi.
1999. Marine turtles of Brazil: the history and structure of Projeto TAMAR-IBAMA. Biol. Conserv. 91:35–41.

Marcovaldi, M. A., J. C. Thomé, G. Sales, A. C. Coelho, B. Gallo, and C. Bellini.
2002. Brazilian plan for reduction of incidental sea turtle capture in fisheries: Mar. Turtle Newsl. 96:24–25.

Miller, J. D.
1997. Reproduction in sea turtles. *In* The biology of sea turtles (P. L. Lutz and J. A. Musick, eds.), p. 51–81. CRC Press, Boca Raton, FL.

Morreale, S. J., E. A. Standora, J. R. Spotila, and F. V. Paladino.
1996. Migration corridor for sea turtles. Nature 384: 319–320.

Musick, J. A., and C. J. Limpus.
1997. Habitat utilization and migration in juvenile sea turtles. *In* The biology of sea turtles (P. L. Lutz and J. A. Musick, eds.), p. 137–163. CRC Press, Boca Raton, FL.

NRC (National Research Council).
1990. Decline of the sea turtles: causes and prevention, 259 p. National Academy Press, Washington, D.C.

Nishemura, W., and S. Nakahigashi.
1990. Incidental capture of sea turtles by Japanese research and training vessels: results of a questionaire. Mar. Turtle Newsl. 51:1–4.

Oravetz, C. A.
1999. Reducing incidental catch in fisheries. *In* Research and management techniques for the conservation of sea turtles (K. L. Eckert, K. A. Bjorndal, F. A. Abreu-Grobois, and M. Donnelly, eds.), p. 189–193. IUCN SSC Marine Turtle Specialist Group publication no. 4.

Pinedo, M. C., R. Capitoli, A. S. Barreto, and A. L. V. Andrade.
1998. Occurrence and feeding of sea turtles in southern Brazil. NOAA Tech. Memo. NMFS-SEFSC-412:117–118.

Spotila, J. R., A. E. Dunham, A. J. Leslie, A. C. Steyermark, P. T. Plotkin, and F.V. Paladino.
1996. Worldwide decline of *Dermochelys coriacea*: are leatherback turtles going extinct? Chelonian Conserv. Biol. 2:209–222.

Teas, W. G.
1993. Species composition and size class distribution of marine turtle strandings on the Gulf of Mexico and southeast United States coasts, 1985–1991. NOAA Tech. Memo. NMFS-SEFSC-315, 43 p.

Tobias, W.
1991. Turtles caught in Caribbean swordfish net fishery. Mar. Turtle Newsl. 53:10–12.

Trono, R. B., and R V. Salm.
1999. Regional collaboration. *In* Research and management techniques for the conservation of sea turtles (K. L. Eckert, K. A. Bjorndal, F. A. Abreu-Grobois, and M. Donnelly, eds.), p. 224–227. IUCN SSC Marine Turtle Specialist Group publication no. 4.

Weidner, D. M., and F. Arocha.
1999. World swordfish fisheries: an analysis of swordfish fisheries, market trends and trade patterns. Vol. IV, Part A2b: Brazil. NOAA Tech. Memo. NMFS-F/SPO-35:237–628.

Weidner, D. M., F. J. Fontes, and J. Serrano.
1999. World swordfish fisheries: an analysis of swordfish fisheries, market trends and trade patterns. Vol. IV, part A2c: Uruguay, Paraguay and Argentina. NOAA Tech. Memo. NMFS-F/SPO-36:631–916.

Williams, P., P. J. Anninos, P. T. Plotkin, and K. L. Salvini (comps.).
1996. Pelagic longline fishery—sea turtle interactions. Proceedings of an industry, academic and government experts, and stakeholders workshop held in Silver Spring, Maryland, 24–25 May 1994. NOAA Tech. Memo. NMFS-OPR-7, 77 p.

Zar, J. H.
1996. Biostatistical analysis, 3rd ed., 662 p. Prentice Hall, Upper Saddle River, NJ.

Diet changes of Pacific cod (*Gadus macrocephalus*) in Pavlof Bay associated with climate changes in the Gulf of Alaska between 1980 and 1995

Mei-Sun Yang

Alaska Fisheries Science Center
National Marine Fisheries Service, NOAA
7600 Sand Point Way NE
Seattle, Washington 98115
E-mail address: mei-sun.yang@noaa.gov

The diet of Pacific cod (*Gadus macrocephalus*) in the area of Pavlof Bay, Alaska, was studied in the early 1980s by Albers and Anderson (1985). They found that the dominant prey species were forage species like pandalid shrimp, capelin (*Mallotus villosus*), and walleye pollock (*Theragra chalcogramma*). The shrimp fishery in Pavlof Bay began in 1968 and closed in 1980 because of low shrimp abundance (Ruccio and Worton[1]). Survey data indicate that, during the period between 1972 and 1997, the abundance of forage species such as pandalid shrimp and capelin declined and higher trophic-level groundfish such as Pacific cod increased. There is a general recognition that a long-term ocean climate shift in the Gulf of Alaska has been partially responsible for the observed reorganization of the community structure (Anderson and Piatt, 1999).

Because there has been an apparent shift in the abundance of both predators and prey in Pavlof Bay, it is important to understand how trophic relationships may also have changed. In order to partially address this question, stomach samples of Pacific cod and other groundfishes were taken in 1995. By performing a comparison of the diet of Pacific cod right after the climate shift with Pacific cod and other groundfishes well after the shift, this analysis may demonstrate how the relative abundance of prey in the Gulf of Alaska may have changed.

Methods

Stomachs of Pacific cod, walleye pollock, and arrowtooth flounder (*Atheresthes stomias*) were collected by National Marine Fisheries Service (NMFS) scientists on board the chartered vessel FV *Arcturus* conducting a trawl survey in Pavlof Bay, Alaska, (Fig. 1) from 5 August to 7 August 1995. The survey targeted shrimp and used a high-opening net with small mesh (32-mm stretched mesh). Each tow was about 1.2 km in length. The average depth of the 13 hauls where stomachs were collected was 108.9 (±9.5) m with a range from 90 to 123 m. When a sampled stomach was retained, it was put in a cloth stomach bag. A field tag with the species name, fork length (FL in cm) of the fish, and haul data (vessel, cruise, haul number, specimen number) was also put in the bag. All the samples collected were then preserved in buckets containing a 10% formalin solution. When the samples arrived at the laboratory, they were transferred into 70% ethanol before the stomach contents were analyzed. In the laboratory, the stomach was cut open, the contents were removed and blotted with a paper towel. Wet weight was then recorded to the nearest 0.1 g. After obtaining the total weight for a stomach's contents, the contents were placed in a Petri dish and examined under a microscope. Each prey item was classified to the lowest practical taxonomic level. Prey weights and numbers of commercially important fish were recorded. Standard lengths of prey fish and carapace width of crabs were also recorded. The diet of Pacific cod was summarized to show the percent frequency of occurrence, the percentage by number, and the percentage of the total weight of each prey item found in the stomachs. Stomach contents of walleye pollock and arrowtooth flounder were analyzed for comparisons.

Results

Of 130 Pacific cod stomachs analyzed, 129 contained food. Pacific cod sizes ranged from 40 to 80 cm FL (fork length); a mean size was 55.4 (SD ±7.2) cm.

Polychaetes, crangonid shrimp, pea crab, and clams were the most frequently found prey items in Pacific cod stomachs (Table 1). However, in terms of weight, eelpouts (zoarcids), Tanner crab (*Chionoecetes bairdi*), crangonid shrimp, hermit crab, and polychaetes were the most important prey of Pacific cod. Pandalid shrimp, spinyhead sculpin (*Dasycottus setiger*), pricklebacks (stichaeid), Pacific sandlance (*Ammodytes hexapterus*), arrowtooth flounder (*Atheresthes stomias*), and flathead sole (*Hippoglossoides elassodon*) were minor prey.

Invertebrates (mainly crangonid shrimp, polychaetes, and crabs) were the principal prey of Pacific cod smaller than 60 cm (Fig. 2). There were nine prey categories as shown in Figure 2. The miscellaneous prey included Sipuncula, Echiura, fish offal (processed

[1] Ruccio, M. P., and C. L. Worton. 1999. Annual management report for the shellfish fisheries of the Alaska peninsula area, 1998. *In* Annual management report for the shellfish fisheries of the westward region, 1998. Regional Information Report 4K99-49, 312 p. Alaska Department of Fish and Game, Division of Commercial Fisheries, 211 Mission Road, Kodiak, Alaska 99615.

Manuscript approved for publication 24 December 2003 by Scientific Editor.
Manuscript received 20 January 2004 at NMFS Scientific Publications Office.
Fish. Bull. 102:400–405 (2004).

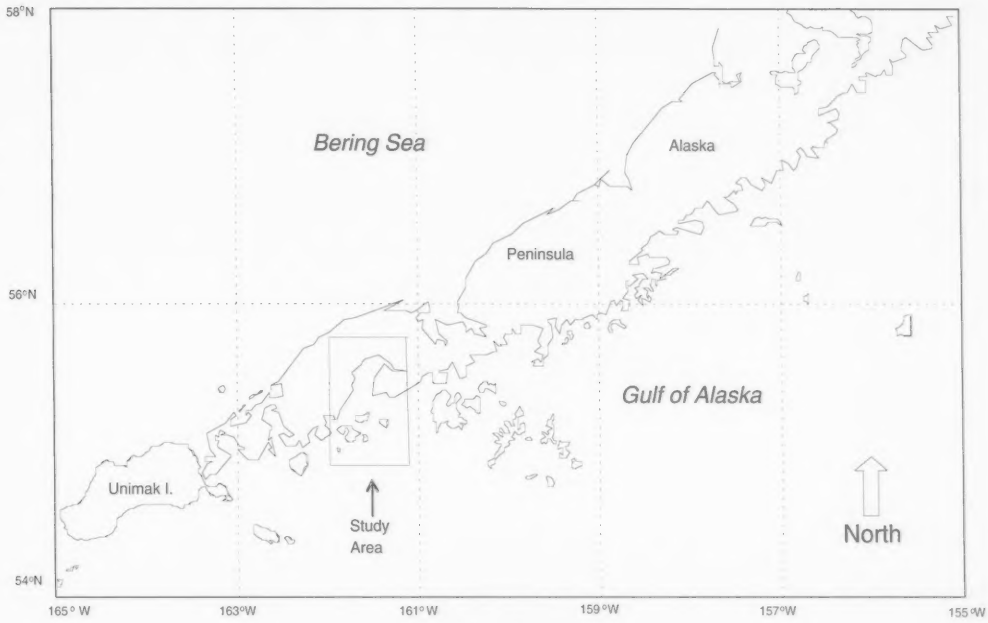

Figure 1

Location of study area in 1980, 1981, and 1995.

fish parts like head, tail, pyloric caeca, etc.), and all other prey organisms not included in the other eight prey categories. The importance of fish in the diet of Pacific cod increased after 60 cm FL. Walleye pollock were consumed only by Pacific cod ≥60 cm FL.

In general, Pacific cod ate prey of small individual size (Table 2). Tanner crabs (*Chionoecetes bairdi*) ranged from 4.5 to 42.3 mm carapace width. Eelpouts ranged in length from 36.2 to 256.6 mm standard length. Other fish prey ranged in length from 32.7 to 81.5 mm. Walleye pollock were consumed by Pacific cod but were not measurable.

In 1995, when Pacific cod stomachs were collected in Pavlof Bay, 218 walleye pollock and 80 arrowtooth flounder stomachs were also collected. Similar to the results for Pacific cod, pandalid shrimp and capelin were not important food of walleye pollock and arrowtooth flounder either (Fig. 3). These prey each comprised less than 3% of the total stomach content weight of walleye pollock and arrowtooth flounder. Instead, eelpouts, pricklebacks, euphausiids, and walleye pollock were important food of arrowtooth flounder, and euphausiids (83% by weight) were the main food of walleye pollock.

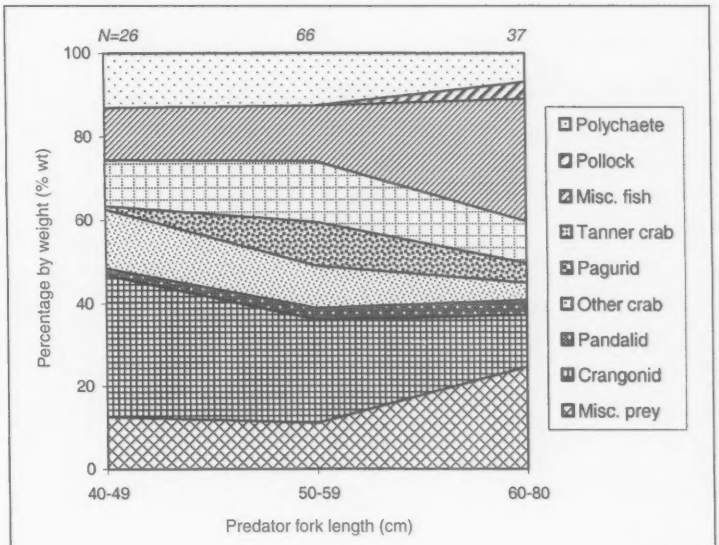

Figure 2

Variations in the main food items of Pacific cod, by predator size, in Pavlof Bay in 1995. *n*=sample size.

Discussion

This study shows that eelpouts, Tanner crabs, crangonids, hermit crabs, polychaetes, and echiuroids were the princi-

Table 1

Percent frequency of occurrence (*%F*), percentage by number (*%N*), and percentage by weight (*%W*) of prey items of Pacific cod collected in Pavlof Bay, Alaska, 1995.

Prey name	*%F*	*%N*	*%W*
Polychaeta (worm)	79.8	11.4	9.2
Gastropoda (snail)	14.0	0.8	0.4
Bivalvia (clam)	55.0	6.1	2.1
Cephalopoda (squid and octopus)	10.1	0.5	2.1
Copepoda	0.8	0.0	0.0
Peracarida Mysidacea (mysid)	31.8	11.5	0.2
Cumacea (cumacean)	13.2	0.9	0.0
Amphipoda (amphipod)	17.1	1.2	0.0
Euphausiacea (euphausiid)	15.5	10.0	0.7
Natantia (unidentified shrimp)	12.4	0.7	0.1
Caridea (shrimp)	12.4	1.2	1.2
Hippolytidae (shrimp)	17.8	1.2	0.2
Pandalidae (shrimp)	41.1	5.7	2.3
Crangonidae (shrimp)	76.0	18.9	13.3
Reptantia (unidentified crab)	11.6	0.5	1.9
Paguridae (hermit crab)	22.5	1.3	9.5
Decapoda Brachyura (crab)	0.8	0.0	0.1
Hyas sp. (lyre crab)	0.8	0.0	0.9
Hyas lyratus (lyre crab)	1.6	0.1	0.6
Chionoecetes sp. (snow and Tanner crab)	40.3	3.5	13.9
Pinnotheridae (pea crab)	1.6	0.1	0.1
Pinnixa sp. (pea crab)	68.2	8.4	3.2
Sipuncula (marine worm)	0.8	0.0	0.6
Echiura (marine worm)	24.0	1.4	6.6
Ophiuroidea (basket and brittle star)	9.3	0.7	0.1
Chaetognatha (arrow worm)	1.6	0.2	0.0
Rajidae (skate)	2.3	0.1	0.4
Osteichthyes Teleostei (fish)	12.4	1.1	0.6
Nongadoid fish remains	47.3	6.5	2.3
Gadidae (unidentified)	1.6	0.1	0.4
Theragra chalcogramma (walleye pollock)	2.3	0.1	1.4
Zoarcidae (eelpout)	16.3	0.9	14.0
Cottoidei (Sculpin)	2.3	0.1	0.2
Dasycottus setiger (spinyhead sculpin)	0.8	0.0	0.2
Stichaeidae (prickleback)	8.5	1.5	0.6
Lumpenus sp. (prickleback)	0.8	0.0	0.0
Ammodytes hexapterus (Pacific sand lance)	0.8	0.0	0.0
Pleuronectidae (flatfish)	2.3	0.2	0.2
Atheresthes stomias (arrowtooth flounder)	1.6	0.1	0.0
Hippoglossoides elassodon (flathead sole)	3.9	0.2	0.5
Unidentified organic material	10.1	0.5	0.6
Unidentified worm-like organism	5.4	0.3	0.5
Fish offal (processed fish parts, e.g., head, tail)	0.8	0.0	8.1
Total prey weight	2715 g		
Total stomachs	130		
Total empty stomachs	1		

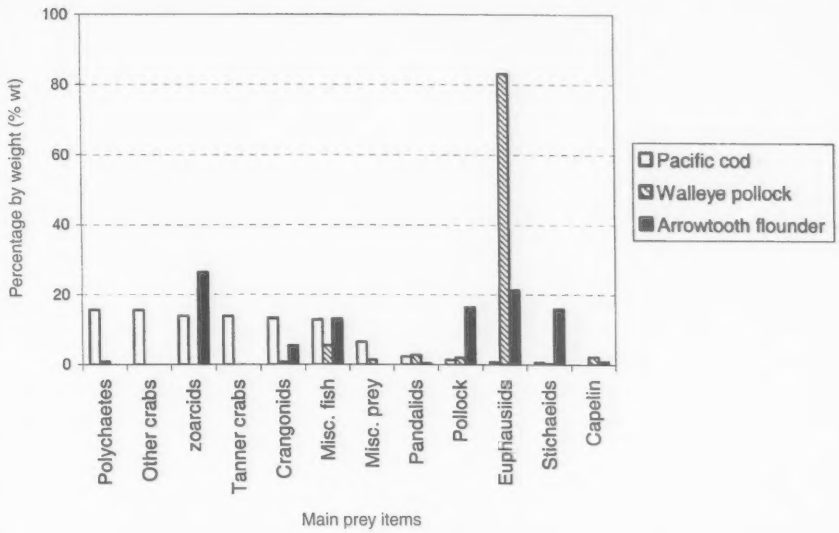

Figure 3

Percentage by weight of the main prey in the diet of Pacific cod (n=129), walleye pollock (n=216), and arrowtooth flounder (n=43) collected in Pavlof Bay in 1995.

pal prey of Pacific cod collected in Pavlof Bay in 1995. This is a large change in diet composition compared with that observed 15 years earlier (Albers and Anderson, 1985). In Albers and Anderson's (1985) study, pandalid shrimp, capelin, and walleye pollock were the main prey of Pacific cod (Fig. 4). The change in main prey from pelagic prey in the 1980s to benthic prey in 1995 corresponds to changes in species abundance trends in nearshore small-mesh trawl surveys observed by Anderson and Piatt (1999). In that study, they described that the community reorganization in the Gulf of Alaska was triggered by a shift in ocean climate during the late 1970s. They showed that the abundance of species such as pandalid shrimp and capelin declined while the abundance of predators such as Pacific cod, walleye pollock, and flatfish increased between 1972 and 1997.

The mean weight of pandalid shrimp consumed by Pacific cod in 1995 was only 0.5 g/cod. In contrast, the mean weights of undigested pink shrimp in Pacific cod stomachs ranged between 4.5 g/cod and 24.4 g/cod during 1980 and 1981. This finding corroborates those of Anderson (2000) and show that pandalid shrimp abundance continued to decrease in the late 1990s and Pacific cod abundance continued to increase during that same period.

The diet of Pacific cod in the present study was also compared with the diet of Pacific cod in the broader Gulf of Alaska shelf area (Fig. 5) (Yang and Nelson, 2000). The values of the percentage by weight of capelin in Pacific cod stomachs in the Gulf of Alaska in 1990, 1993, and 1996 were similar (all were less than 3%) to that in Pavlof Bay in 1995. However, pandalid shrimp were an important food item of Pacific cod throughout the Gulf of Alaska, comprising from 11% to 15% by weight of the total stomach contents of Pacific cod in the Gulf of Alaska in 3 years (1990, 1993, and 1996) (Yang and Nelson, 2000). These values are higher than that in Pavlof Bay (2% by weight). By comparing the depths of the sampling locations of the Pacific cod, high percentages of pandalid shrimp were found in the cod diet in deeper offshore areas of the Gulf of Alaska in 1990, 1993, and 1996, whereas low percentages of pandalid shrimp were found in cod diet in much

Table 2

Mean standard length (or carapace width), standard deviation, and the size range of prey consumed by Pacific cod in Pavlof Bay 1995.

Prey name	Mean (mm)	SD (mm)	Range (mm)	No. of individuals
Tanner crab	22.1	10.5	4.5–42.3	70
Zoarcid	86.4	73.5	36.2–256.6	15
Cottid	48.2	9.4	41.8–59	3
Stichaeid	46.9	19.6	32.7–81.5	5
Pacific sand lance	44.8	0.0	44.8–44.8	1
Arrowtooth flounder	39.1	7.4	33.8–44.3	2
Flathead sole	58.2	14.4	47.5–80.4	4

shallower areas in the Pavlof Bay area (Fig. 6). From the shrimp survey data, Anderson (2000) showed that pandalid shrimp occupying inshore and shallower water (e.g., Pavlof Bay area) declined to near extinction (<0.1 kg/km) from 1978 to 1982, while offshore and deepwater pandalid shrimp species maintained low population levels (>0.1 kg/km). The data from this study corroborates Anderson's (2000) results.

Anderson (2000) also reported that during the period of the decline of pandalid shrimp in inshore waters of the Gulf of Alaska, the abundance of some pleuronectids, Pacific cod, and walleye pollock increased. These species are predators of pandalid shrimp (Yang and Nelson, 2000). One hypothesis is that predators keep pandalid shrimp populations low. Albers and Anderson (1985) suggested that cod predation was one reason for the failure of the pink shrimp stock to rebuild in Pavlof Bay. In the Northwest Atlantic, Lilly et al. (2000) showed that the large increase in shrimp biomass seen in the 1990s was related to the collapse of cod (*Gadus morhua*) populations during the late 1980s and 1990s in the northeast Newfoundland shelf. The impact of cod on Barents Sea shrimp (*P. borealis*) was also reported by Berenboim et al. (2000). They found that when cod biomass is high, the shrimp frequency of occurrence in cod stomachs declines; there is a significant inverse correlation between the abundance of cod and shrimp.

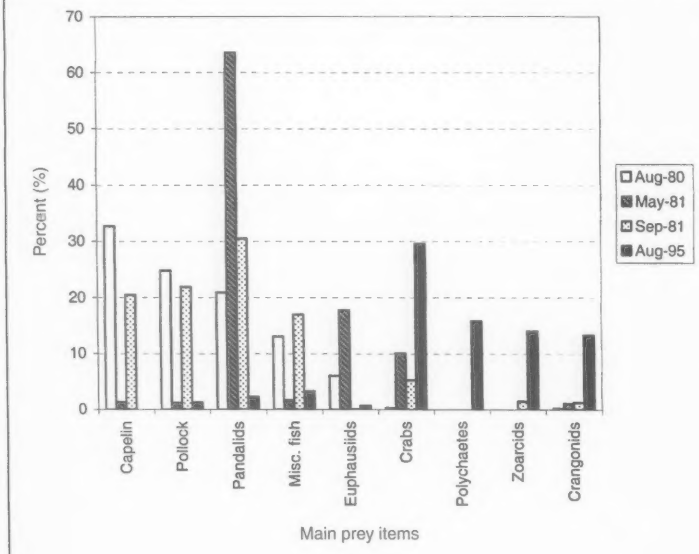

Figure 4

Percentage by volume (for the values in 1980s) and the percentage by weight (for the values in 1995) of the main prey items of Pacific cod collected in Pavlof Bay, Alaska.

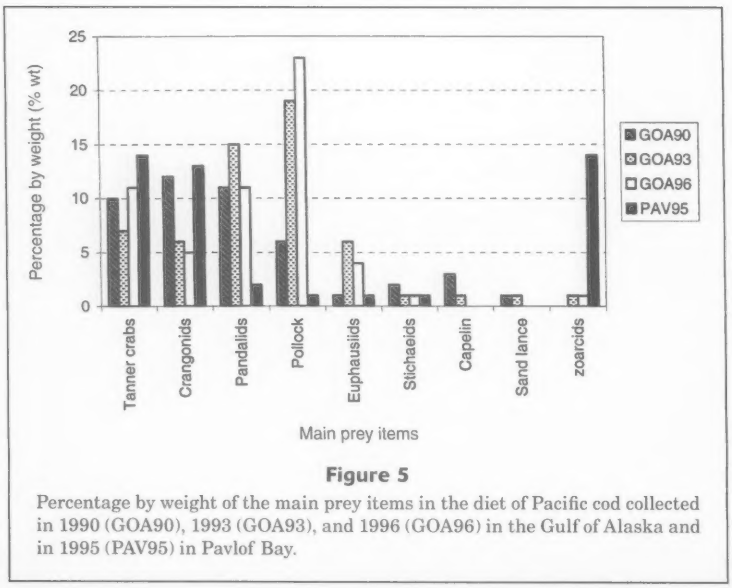

Figure 5

Percentage by weight of the main prey items in the diet of Pacific cod collected in 1990 (GOA90), 1993 (GOA93), and 1996 (GOA96) in the Gulf of Alaska and in 1995 (PAV95) in Pavlof Bay.

Tanner crabs consumed by Pacific cod in this study ranged from 5 to 42 mm carapace width (CW). In general, the size of Tanner crabs consumed increases as Pacific cod size increases. The size range of Tanner crabs consumed by Pacific cod in this study is similar to that (5–45 mm) found in Pacific cod stomachs in Albers and Anderson's (1985) study and is also similar to that (1–40 mm) found in Hunter's (1979) study near Kodiak Island.

Jewett's (1978) Pacific cod diet study around Kodiak Island from 1973 to 1976 showed that Tanner crabs were the most frequent (37%) prey of Pacific cod; pandalid shrimp occurred in 8–10% of the stomachs examined from 1973 to 1975; and walleye pollock were found in 4% of the stomachs examined. The importance of Tanner crabs as food of Pacific cod in Jewett's (1978) study is coincident with our study.

This study suggests that there were substantial differences between the diets of Pacific cod in Pavlof Bay between the early 1980s and 1995. In the 1980s, pandalid shrimp and capelin were the main food of Pacific cod, whereas benthic species (polychaetes,

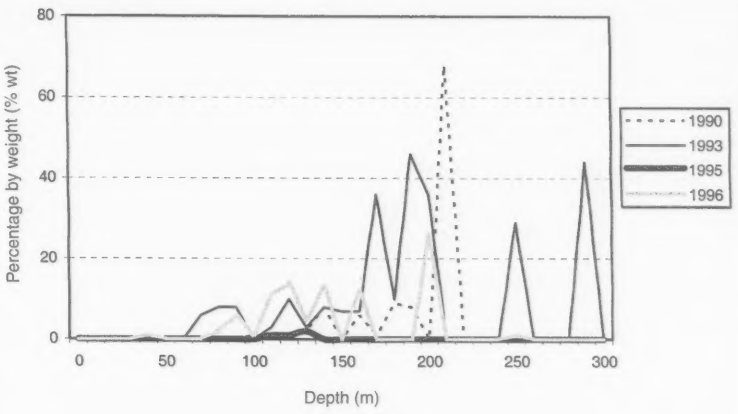

Figure 6

Pandalid shrimp consumed by Pacific cod sampled at different bottom depths (m) in Pavlof Bay in 1995, and in the Gulf of Alaska in 1990, 1993, and 1996.

hermit crabs, Tanner crabs, and eelpouts) were the dominant food in 1995. This change was probably due to the climate shift from cold to warm in the Gulf of Alaska.

Acknowledgments

I would like to thank Paul Anderson, Troy Buckley, and Patricia Livingston for reviewing the manuscript and for their very helpful suggestions. I also want to thank the two anonymous reviewers for their comments and suggestions.

Literature cited

Albers W. D., and P. J. Anderson.
1985. Diet of the Pacific cod. *Gadus macrocephalus*, and predation on the northern pink shrimp, *Pandalus borealis*, in Pavlof Bay, Alaska. Fish. Bull. 83:601–610.

Anderson, P. J .
2000. Pandalid shrimp as indicators of ecosystem regime shift. J. Northw. Atl. Fish. Sci. 27:1–10.

Anderson, P. J., and J. F. Piatt.
1999. Community reorganization in the Gulf of Alaska following ocean climate regime shift. Mar. Ecol. Prog. Ser. 189:117–123.

Berenboim, B. I., A. V. Dolgov, V. A. Korzhev, and N. A. Yaragina.
2000. The impact of cod on the dynamics of Barents Sea shrimp (*Pandalus borealis*) as determined by multispecies models. J. Northw. Atl. Fish. Sci. 27:69–75.

Hunter, M. A.
1979. Food resource partitioning among demersal fishes in the vicinity of Kodiak Island, Alaska. M.S. thesis, 120 p. Univ. Washington, Seattle, WA.

Jewett, S. C.
1978. Summer food of the Pacific cod, *Gadus macrocephalus*, near Kodiak Island, Alaska. Fish. Bull. 76:700–706.

Lilly, G. R., D. G. Parsons, and D. W. Kulka.
2000. Was the increase in shrimp biomass on the Northeast Newfoundland shelf a consequence of a release in predation pressure from cod? J. Northw. Atl. Fish. Sci. 27:45–61.

Yang, M-S., and M. W. Nelson.
2000. Food habits of the commercially important groundfishes in the Gulf of Alaska in 1990, 1993, and 1996. NOAA Tech. Memo. NMFS-AFSC-112, 174 p.

Superintendent of Documents **Publications** Order Form

*5178

☐ YES, please send me the following publications:

____ Subscriptions to *Fishery Bulletin*
for $55.00 per year ($68.75 foreign)

The total cost of my order is $ _____ . Prices include regular domestic postage and handling and are subject to change.

_____
(Company or Personal Name) (Please type or print)

_____
(Additional address/attention line)

_____
(Street address)

_____
(City, State, ZIP Code)

_____
(Daytime phone including area code)

_____
(Purchase Order No.)

Charge your order. IT'S EASY!

VISA

MasterCard

Please Choose Method of Payment:

☐ Check Payable to the Superintendent of Documents

☐ GPO Deposit Account ☐☐☐☐☐☐–☐

☐ VISA or MasterCard Account

☐☐☐☐☐☐☐☐☐☐☐☐☐☐☐☐

☐☐☐☐ (Credit card expiration date)

To fax your orders (202) 512-2250

_____
(Authorizing Signature)

Mail To: Superintendent of Documents
P.O. Box 371954, Pittsburgh, PA 15250-7954

Thank you for your order!

Fishery Bulletin

Guidelines for contributors

Content of papers

Articles

Articles are reports of 10 to 30 pages (double spaced) that describe original research in one or a combination of the following fields of marine science: taxonomy, biology, genetics, mathematics (including modeling), statistics, engineering, economics, and ecology.

Notes

Notes are reports of 5 to 10 pages without an abstract that describe methods and results not supported by a large body of data. Although all contributions are subject to peer review, responsibility for the contents of articles and notes rests upon the authors and not upon the editor or the publisher. It is therefore important that authors consider the contents of their manuscripts carefully. Submission of an article is un-derstood to imply that the article is original and is not being considered for publication elsewhere. Manuscripts must be written in English. Authors whose native language is not English are strongly advised to have their manuscripts checked for fluency by English-speaking colleagues prior to submission.

Preparation of papers

Text

Title page should include authors' full names and mailing addresses (street address required) and the senior author's telephone, fax number, e-mail address, as well as a list of key words to describe the contents of the manuscript. **Abstract** must be less than one typed page (double spaced) and must not contain any citations. It should state the main scope of the research but emphasize the author's conclusions and relevant findings. Because abstracts are circulated by abstracting agencies, it is important that they represent the research clearly and concisely. **General text** must be typed in double-spaced format. A brief introduction should state the broad significance of the paper; the remainder of the paper should be divided into the following sections: Materials and methods, Results, Discussion (or Conclusions), and Acknowledgments. Headings within each section must be short, reflect a logical sequence, and follow the rules of multiple subdivision (i.e. there can be no subdivision without at least two subheadings). The entire text should be intelligible to interdisciplinary readers; therefore, all acronyms and abbreviations should be written out and all lesser-known technical terms should be defined the first time they are mentioned. The scientific names of species must be written out the first time they are mentioned; subsequent mention of scientific names may be abbreviated. Follow *Scientific style and format: CBE manual for authors, editors, and publishers* (6th ed.) for editorial style and the most current issue of the *American Fisheries Society's common and scientific names of fishes from the United States and Canada* for fish nomenclature. Dates should be written as follows: 11 November 1991. Measurements should be expressed in metric units, e.g. metric tons (t). The numeral one (1) should be typed as a one, not as a lower-case el (l).

Footnotes

Use footnotes to add editorial comments regarding claims made in the text and to document unpublished works or works with local circulation. Footnotes should be numbered with Arabic numerals and inserted in 10-point font at the bottom of the first page on which they are cited. Footnotes should be formatted in the same manner as citations. If a manuscript is unpublished, in the process of review, or if the information provided in the footnote has been conveyed verbally, please state this information as "unpubl. data," "manuscript in review," and "personal commun.," respectively. Authors are advised wherever possible to avoid references to nonstandard literature (unpublished literature that is difficult to obtain, such as internal reports, processed reports, administrative reports, ICES council minutes, IWC minutes or working papers, any "research" or "working" documents, laboratory reports, contract reports, and manuscripts in review). If these references are used, please indicate whether they are available from NTIS (National Technical Information Service) or from some other public depository. Footnote format: author (last name, followed by first-name initials); year; title of report or manuscript; type of report and its administrative or serial number; name and address of agency or institution where the report is filed.

Literature cited

The literature cited section comprises works that have been published and those accepted for publication (works in press) in peer-reviewed journals and books. Follow the name and year system for citation format. In the text, write "Smith and Jones (1977) reported" but if the citation takes the form of parenthetical matter, write "(Smith and Jones, 1977)." In the literature cited section, list citations alphabetically by last name of senior author: For example, Alston, 1952; Mannly, 1988; Smith, 1932; Smith, 1947; Stalinsky and Jones, 1985. Abbreviations of journals should conform to the abbreviations given in the *Serial sources for the BIOSIS previews database*. Authors are responsible for the accuracy and completeness of all citations. Literature citation format: author (last name, followed by first-name initials); year; title of report or article; abbreviated title of the journal in which the article was published, volume number, page numbers. For books, please provide publisher, city, and state.

Tables

Tables should not be excessive in size and must be cited in numerical order in the text. Headings in tables should be short but ample enough to allow the table to be intelligible on its own. All unusual symbols must be explained in the table legend. Other incidental comments may be footnoted (use italic arabic numerals for footnote markers). Use asterisks only to indicate probability in statistical data. Place table legends on the same page as the table data. We accept tables saved in most spreadsheet software programs (e.g. Microsoft Excel). Please note the following:

- Use a comma in numbers of five digits or more (e.g. 13,000 but 3000).
- Use zeros before all decimal points for values less than one (e.g. 0.31).

Figures

Figures include line illustrations, computer-generated line graphs, and photographs (or slides). They must be cited in numerical order in the text. Line illustrations are best submitted as original drawings. Computer-generated line graphs should be printed on laser-quality paper. Photographs should be submitted on glossy paper with good contrast. All figures are to be labeled with senior author's name and the number of the figure (e.g. Smith, Fig. 4). Use Helvetica or Arial font to label anatomical parts (line drawings) or variables (graphs) within figures; use Times Roman bold font to label the different sections of a figure (e.g. **A**, **B**, **C**). Figure legends should explain all symbols and abbreviations seen within the figure and should be typed in double-spaced format on a separate page at the end of the manuscript. We advise authors to peruse a recent issue of *Fishery Bulletin* for standard formats. Please note the following:

- Capitalize the first letter of the first word of axis labels.
- Do not use overly large font sizes to label axes or parts within figures.
- Do not use boldface fonts within figures.
- Do not create outline rules around graphs.
- Do not use horizontal lines through graphs.
- Do not use large font sizes to label degrees of longitude and latitude on maps.
- Indicate direction of degrees longitude and latitude on maps (e.g. 170°E).
- Avoid placing labels on a vertical plane (except on *y* axis).
- Avoid odd (nonstandard) patterns to mark sections of bar graphs and pie charts.

Copyright law

Fishery Bulletin, a U.S. government publication, is not subject to copyright law. If an author wishes to reproduce any part of *Fishery Bulletin* in his or her work, he or she is obliged, however, to acknowledge the source of the extracted literature.

Submission of papers

Send four printed copies (one original plus three copies)—clipped, *not stapled*—to the Scientific Editor, at the address shown below. Send photocopies of figures with initial submission of manuscript. Original figures will be requested later when the manuscript has been accepted for publication. Do not send your manuscript on diskette until requested to do so.

Dr. Norman Bartoo
National Marine Fisheries Service, NOAA
8604 La Jolla Shores Drive
La Jolla, CA 92037

Once the manuscript has been accepted for publication, you will be asked to submit a software copy of your manuscript. The software copy should be submitted in WordPerfect or Word format (in Word, save as Rich Text Format). Please note that we do not accept ASCII text files.

Reprints
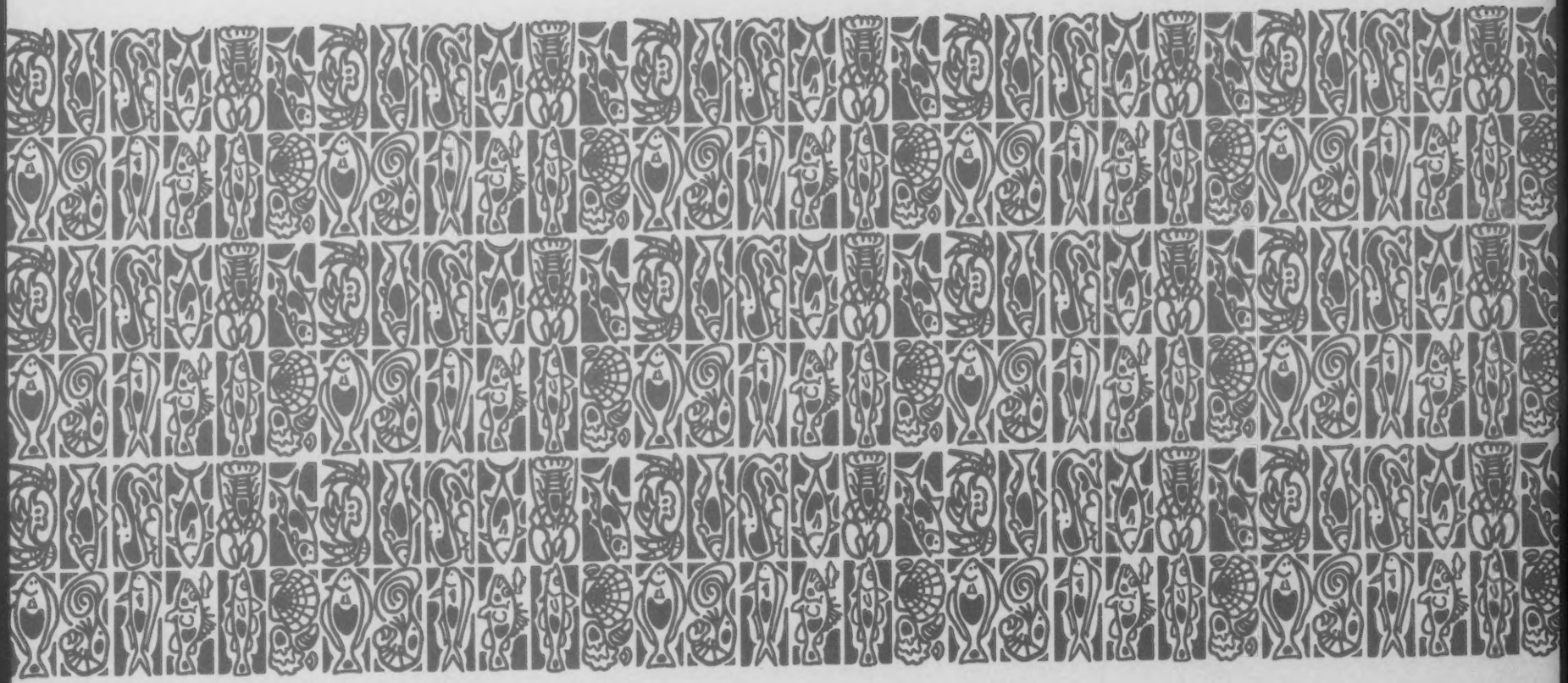
Copies of published articles and notes are available free of charge to the senior author (50 copies) and to his or her laboratory (50 copies). Additional copies may be purchased in lots of 100 when the author receives page proofs.